GLUCOSE TRANSPORTER 4 CONTENT AND LOCALISATION IN SKELETAL MUSCLE: THE EFFECT OF GLUCOSE AND INSULIN ADMINISTRATION, ACUTE EXERCISE AND EXERCISE TRAINING

HELEN ELIZABETH BRADLEY

A thesis submitted to the

University of Birmingham

for the degree of

DOCTOR OF PHILOSOPHY

School of Sport and Exercise Sciences

College of Life and Environmental Sciences

University of Birmingham

August 2013

GENERAL ABSTRACT

Glucose transporter 4 (GLUT4) in skeletal muscle plays a vital role in the maintenance of glucose homeostasis. Chapter 2 of this thesis develops an immunofluorescence microscopy method to generate novel information in human skeletal muscle on the effect of physiological stimuli on GLUT4 localisation, translocation to the plasma membrane and total protein content. Chapter 3 shows that training-induced increases in total GLUT4 protein content are driven by increases in the number of large and size of smaller intracellular GLUT4 storage clusters in human skeletal muscle. In chapter 4 the method successfully demonstrates GLUT4 translocation 30 min following glucose ingestion and 30 min after the start of moderate intensity cycling exercise in humans. GLUT4 translocation after glucose ingestion is transient and modest in comparison to the exercise response. Chapters 5 and 6 report no changes in GLUT4 translocation following an 80 min hyperinsulinaemic-isoglycaemic clamp in rats and a 2 h hyperglycaemic clamp in humans despite elevated rates of whole body glucose disposal in both experiments. This immunofluorescence method will be a valuable analytical tool in future studies investigating the mechanisms behind changes in muscle glucose uptake in response to obesity, age-related chronic diseases and therapeutic interventions including diet and exercise.

ACKNOWLEDGEMENTS

There are many people whom I need to thank for their support during the completion of this PhD thesis.

Firstly, I would like to thank my supervisors, Professor Anton Wagenmakers, Dr Chris Shaw and Dr Gareth Wallis, for their help and support over the course of this PhD. In particular, I thank Chris and Anton for their continued support towards the later stages despite no longer being in Birmingham and I thank Gareth for subsequently being willing to take up the mantle. Your knowledge and encouragement over the course of this PhD has been invaluable and I am very grateful for the opportunities with which I have been presented.

I also want to thank a number of collaborators who have been instrumental in the completion of this PhD. Colleagues at AstraZeneca have offered a great deal of expertise and guidance. I also thank Dr Matt Cocks, Dr Sam Shepherd, Dr Annie Stride and Dr Thomas Solomon for allowing samples they have worked so hard to collect to be used as part of this thesis. I also thank members of the histology lab in Birmingham, Jules, Ollie, Sam, Matt and Dan, for their help and advice. I am also extremely grateful to the study participants for offering their time so willingly, as without them this research would not have been possible.

Outside of the lab, I would like to thank the many friends and colleagues in Birmingham, in particular inhabitants of office number 125 and Kenilworth Court, who have helped make the completion of this PhD a thoroughly enjoyable experience. Finally I want to thank all of my friends and family for their love, help and support over the course of this PhD and beyond.

CONTENTS LISTING

LIST OF CONFERENCE COMMUNICATIONS

During the period of postgraduate study at the University of Birmingham, data from the current thesis resulted in the following conference communications:

Bradley, H., Shepherd, S.O., Cocks, M., Shaw, C.S. and Wagenmakers, A.J.M. GLUT4 protein expression and localisation in human skeletal muscle following endurance and high intensity interval training. 17th Congress of the European College of Sport Science, Bruges, 2012.

Bradley, H., Wilson, O.J., Shaw, C.S. and Wagenmakers, A.J.M. Imaging of contraction mediated GLUT4 translocation in human skeletal muscle fibres. 15th International Biochemistry of Exercise Conference, Stockholm, 2012.

Bradley, H., Wilson, O.J., Shaw, C.S. and Wagenmakers, A.J.M. Imaging of contraction mediated GLUT4 translocation in human skeletal muscle fibres. 1st International Symposium on Advances in Human Metabolism Research, Warwick, 2011.

Bradley, H., Shaw, C.S. and Wagenmakers, A.J.M. Visualisation of GLUT4 localisation in human skeletal muscle with immunofluorescence microscopy. 16th Congress of the European College of Sport Science, Liverpool, 2011.

Bradley, H., Shaw, C.S. and Wagenmakers, A.J.M. Visualisation of GLUT4 and AS160 in fasted human skeletal muscle. Physiology, Manchester, 2010.

LIST OF ABBREVIATIONS

AS160	Akt substrate of 160 kDa
DAPI	4,6'-diamidino-2-phenylindole
DHPR	Dihydropyridine receptor
EM	Electron microscopy
eNOS	Endothelial nitric oxide synthase
ERC	Endosomal recycling compartments
ET	Endurance training
FA	Fatty acid
GLUT	Glucose transporter
GSV	GLUT4 storage vesicle
IGT	Impaired glucose tolerance
IMTG	Intramuscular triacylglycerol
IR	Insulin receptor
IRS	Insulin receptor substrate
LCFA-CoA	Long-chain fatty acyl-CoA
LD	Lipid droplet
LZR	Lean Zucker rat
MBV	Microvascular blood volume
MHC	Myosin heavy chain
NGT	Normal glucose tolerance
NO	Nitric oxide
OGTT	Oral glucose tolerance test
OZR	Obese Zucker rat
PI3K	Phosphatidylinositol 3-kinase
PM	Plasma membrane
PSA	Permeability surface area
ROS	Reactive oxygen species
SIT	Sprint interval training
SNAP23	Synaptosomal-associated protein of 23 kDa
SNARE	Soluble *N*-ethylmaleimide-sensitive factor attachment protein receptor

T2D	Type 2 Diabetes
TA	*Tibialis anterior* muscle
TAG	Triacylglycerol
TGN	Trans-Golgi network
TIRF	Total internal reflection fluorescence
t-SNARE	Target SNARE
VAMP2	Vesicle-associated membrane protein 2
v-SNARE	Vesicle SNARE
WGA	Wheat germ agglutinin

AUTHOR'S DECLARATION

I carried out the development of the GLUT4 immunofluorescence and analysis method detailed in chapter 2. Technical support was received from Dr Samantha Peel during antibody validation experiments in L6 GLUT4-myc cells completed onsite at Astra Zeneca.

The training study detailed in chapter 3 was run by Dr Sam Shepherd and Dr Matthew Cocks as part of their PhD. I was present during testing sessions to assist with muscle biopsy collection. I completed all GLUT4 immunofluorescence and Western blot analysis of muscle.

The studies detailed in chapter 4 were run by myself, with the assistance of Oliver Wilson in the case of experiment 1. I conducted all participant recruitment, VO_2 max testing and study testing (together with the biopsy taker). I completed all GLUT4 immunofluorescence analysis.

In chapters 5 and 6, I completed all stages of GLUT4 immunofluorescence muscle analysis. The studies performed prior to muscle collection were completed by Dr Annie Stride and Dr Thomas Solomon for chapters 5 and 6, respectively.

TABLE OF CONTENTS

LIST OF FIGURES

LIST OF TABLES

CHAPTER 1

GENERAL INTRODUCTION

1.1. Glucose homeostasis

Blood glucose concentration must be maintained within a tight range (70 – 90 mg.dL^{-1} ~ 3.9 – 5.0 mM) in order to meet the physiological demands of the human body (Abdul-Ghani et al., 2006, Wasserman, 2009). Glucose is a major fuel used in humans and is the sole fuel source for the brain in the fed, post-absorptive and overnight fasted state (Abdul-Ghani et al., 2006). In the post-absorptive state the brain accounts for 50 % of glucose disposal (Defronzo, 2009). Severe reductions in blood glucose to concentrations as low as 2 mM (hypoglycemia) are deleterious to brain function (Wasserman, 2009). Conversely prolonged recurrent increases in blood glucose concentration (hyperglycaemia) as occurs in type 2 diabetes lead to function loss and damage in all tissues (Manley, 2003). Therefore, tight control mechanisms exist in healthy individuals to prevent substantial perturbations in blood glucose concentration (Abdul-Ghani et al., 2006). The main control mechanisms are outlined below.

1.1.1. Mechanisms to ensure tight control of blood glucose concentration

Feeding and exercise challenge the glucose homeostasis mechanisms. In the postprandial state, elevations in blood glucose concentrations are sensed by the beta cells of the pancreas, resulting in insulin secretion (Fridlyand and Phillipson, 2011). In order to counter the rise in glucose appearance in the circulation, increased insulin production by the beta cells of the pancreas leads to an increase in plasma insulin concentration and suppression of the hepatic glucose production (Abdul-Ghani et al., 2006). Postprandial increases in plasma insulin concentration also stimulate glucose uptake into insulin-sensitive peripheral tissues such as muscle (Katz et al., 1983) and adipose tissue (Coppack et al., 1990) and also the liver (Ferrannini et al., 1980). The rise in plasma insulin also stimulates glycogen synthesis in liver and muscle (Wasserman, 2009). Conversely, in the post-absorptive state decreases in blood glucose concentration are sensed by the alpha cells of the pancreas which secrete the hormone

glucagon (Abdul-Ghani et al., 2006). Glucagon stimulates endogenous glucose output from the liver and to a lesser extent the kidneys in order to maintain blood glucose concentration sufficient for normal brain function (Gerich et al., 2001). Liver glucose output occurs via increased rates of glycogenolysis (glycogen breakdown) and gluconeogenesis (glucose synthesis) (Wasserman, 2009). During the initial stages of moderate to high intensity exercise (> 50 % VO_{2max}), increased rates of muscle glycogen breakdown and glucose uptake from the circulation provide the glucose moieties that are required to generate the ATP that is needed to support continued muscle contraction, while an acute increase in liver glycogen breakdown generates the glucose that is required to prevent reductions in plasma glucose concentration (Coggan, 1991). In the case of longer duration exercise (3-4 h), gradual increases in whole body lipolysis generates glycerol (Coggan, 1991), while acceleration of the glucose-alanine cycle increases net alanine release from the muscle (Felig et al., 1970, Van Hall et al., 1999). Glycerol and alanine, in addition to lactate, are substrates that can be used for hepatic gluconeogenesis (Felig et al., 1970, Bergman et al., 2000, Emhoff et al., 2013). As a result hepatic gluconeogenesis becomes the more dominant source of glucose production compared to liver glycogen breakdown and serves to prevent decreases in plasma glucose concentration during prolonged exercise.

1.1.2. Impaired glucose homeostasis

Insulin resistance is a phenomenon whereby normally insulin sensitive tissues do not respond adequately to insulin (Shulman, 2000). The development of insulin resistance can be associated with obesity and is an early step in the pathogenesis of type 2 diabetes (T2D), occurring many years before the onset of the disease. It is important to note that metabolic abnormalities such as insulin resistance and a predisposition to T2D can also be present in normal weight individuals, driven, for example, by inflammation (Ruderman et al., 1998,

Karelis et al., 2004). Blood glucose concentration is not as tightly regulated and large excursions in blood glucose can occur following glucose ingestion due to a reduction in insulin-mediated glucose uptake in peripheral tissues (primarily skeletal muscle) and a failure in insulin-mediated suppression of hepatic glucose production (Abdul-Ghani et al., 2006). Initially, insulin secretion is elevated in the postprandial state to compensate for the reduction in insulin-mediated glucose disposal (Abdul-Ghani et al., 2006). However over time the increased demand exerted on the pancreatic beta cells leads to beta cell apoptosis (Costes et al., 2013). As a result insulin secretion in response to excursions in plasma glucose is reduced and can no longer compensate for reduced insulin-mediated glucose disposal. Therefore plasma glucose concentration becomes chronically elevated (Abdul-Ghani et al., 2006) and overt T2D has developed. Chronically high plasma glucose concentrations (hyperglycaemia) can lead to the secondary complications of T2D such as cardiovascular disease, microvascular damage, retinopathy and neuropathy (Crawford et al., 2009, Stirban and Tschoepe, 2008, Park et al., 2004, Khan and Chakrabarti, 2006).

The oral glucose tolerance test (OGTT) is a method used to assess whole body glucose tolerance, at the start of which glucose is ingested and blood samples are taken every 30 min to measure blood glucose and insulin concentrations (Matsuda and DeFronzo, 1999). It reflects the efficiency of the body to return plasma glucose concentration to baseline following an oral glucose load. The OGTT is not a direct measure of whole body insulin sensitivity as many factors apart from sensitivity to insulin affect the removal of glucose from the blood (Muniyappa et al., 2008). For example, individuals with a higher body mass, and in particular a higher muscle mass, will have a higher capacity to dispose of an oral glucose load. However the OGTT is a simple and practical, low cost tool to use in the lab and importantly, the Matsuda insulin sensitivity index derived from OGTT plasma insulin and

glucose concentrations has been shown to have a high correlation ($r = 0.73$, $P < 0.0001$) with the rate of whole body glucose disposal during the gold standard assessment of insulin sensitivity, the hyperinsulinaemic-euglycaemic clamp (Matsuda and Defronzo, 1999). In some of the studies in this PhD thesis the aim will be to relate skeletal muscle insulin sensitivity to GLUT4 translocation from intracellular stores to the muscle plasma membrane. It should be noted that both the OGTT and the hyperinsulinaemic-euglycaemic clamp have the limitation that multiple tissues (liver, adipose tissue and skeletal muscle) contribute to whole body glucose uptake.

According to the clinical definitions an individual is regarded to have normal glucose tolerance (NGT) if the fasting plasma glucose remains between 3.9 – 5.0 mM (Gagliardino, 2005) and if plasma glucose concentrations return to baseline by 2 h after the start of an OGTT (Matsuda and DeFronzo, 1999, Zhou et al., 2006). T2D is diagnosed if fasting plasma glucose is greater than 7 mM or if plasma glucose 2 h after glucose ingestion is greater than 11.1 mM (Genuth et al., 2003). T2D develops over time and intermediate states of insulin resistance have been diagnosed before overt T2D (Abdul-Ghani et al., 2006). Fasting plasma glucose concentration of 5.6 – 6.9 mM has been suggested to point at hepatic insulin resistance, while 2 h plasma glucose of 7.8 – 11 mM has been suggested to point at impaired glucose tolerance (IGT) and reduced peripheral tissue insulin sensitivity (Genuth et al., 2003).

1.1.3. Epidemiology of obesity and type 2 diabetes

Increases in the availability of food and changing eating habits towards convenience food with low nutritional value and often a high fat content combined with reduced physical activity has caused alarming increases in the prevalence of obesity throughout the globe (Kelly et al., 2008). According to the World Health Organisation (WHO) fact sheet No 311 in 2008 approximately 500 million adults were classed as obese (body mass index > 30 $kg.m^{-2}$)

and this figure is predicted to further increase to 1.12 billion by 2030 (Kelly et al., 2008). In addition to the increasing prevalence of obesity, in 2008 347 million adults worldwide were classed as T2D (Danaei et al., 2011). Importantly T2D has a significant impact on mortality. In 2004, 3.4 million deaths were attributed to the consequences of high fasting blood glucose (World Health Organisation, 2009). The cost to the NHS in Great Britain in 2010-2011 of treatment of the secondary complications of T2D has been estimated at £8.8 billion (Hex et al., 2012) and approximately 10 % of the total NHS budget (Department for Health, 2006). This is estimated to rise to £15.1 billion by 2035-2036 (Hex et al., 2012). These figures highlight the need for research into the mechanisms behind the development of T2D to guide strategies for the prevention and treatment of T2D.

1.1.4. Central role of skeletal muscle in glucose homeostasis

Skeletal muscle is the primary site of postprandial glucose uptake (Katz et al., 1983, Ferrannini et al., 1985). Leg glucose uptake was elevated four-fold 30 min after oral glucose ingestion in healthy young individuals and remained significantly elevated above baseline for 4 h with maximal leg glucose uptake occurring between 30 min and 120 min (Katz et al., 1983). Furthermore peripheral tissues such as skeletal muscle have been shown to be the most significant site of insulin resistance with leg glucose uptake being reduced by 45 % in patients with T2D compared to healthy control (DeFronzo et al., 1985). In addition, the contribution of plasma glucose to ATP production in the working muscle during endurance exercise demonstrates the importance of glucose uptake into skeletal muscle during exercise (Katz et al., 1991, Kjaer et al., 1991, van Loon et al., 2001). Skeletal muscle glucose uptake is central to the maintenance of glucose homeostasis both following feeding and during exercise and is also a major site of insulin resistance. Therefore this thesis will concentrate solely on glucose uptake mechanisms in skeletal muscle. Skeletal muscle glucose uptake requires three distinct

stages; delivery of glucose to the muscle fibre, glucose transport across the plasma membrane (PM) and phosphorylation of glucose by hexokinase to make the process irreversible and trap glucose inside the muscle fibre (Wasserman and Ayala, 2005). Glucose transport is believed to be the main barrier to skeletal muscle glucose uptake (Wasserman and Ayala, 2005). As glucose transporter 4 (GLUT4) is the main glucose transporter protein isoform expressed in skeletal muscle (Mueckler, 1994, Bell et al., 1993) this thesis investigates the role of GLUT4 in insulin- and contraction-mediated glucose uptake in human skeletal muscle. Substrate delivery to muscle cells will be discussed in section 1.2 and glucose phosphorylation will be returned to in the general discussion in section 7.4.

1.2. Substrate delivery to muscle cells

Insulin delivery to the skeletal muscle is proposed to be a rate-limiting step in insulin-stimulated skeletal muscle glucose uptake (Barrett et al., 2009). Insulin acts on the microvasculature to increase its own delivery and the delivery of glucose to the skeletal muscle. This occurs through two key mechanisms which will be outlined in subsequent sections; firstly the dilatation of skeletal muscle terminal arterioles to increase blood delivery to capillaries supplying muscle fibres and secondly by increasing the trans-endothelial transport of insulin from the blood into the muscle interstitium (Barrett et al., 2009). Insulin-mediated increases in total limb blood flow start to occur after about 90 min and do not correspond temporally to the insulin-mediated increases in skeletal muscle glucose uptake which start to occur after 15-30 min (Barrett et al., 2009). Rather it is insulin action on the microvasculature that is key to increasing insulin and glucose delivery to the skeletal muscle (Barrett et al., 2009).

1.2.1 Microvascular recruitment

Insulin has been shown to increase microvascular blood volume (MBV, for review see Barrett *et al.* 2009). The mechanism involves insulin-induced dilation of terminal arterioles, which leads to recruitment of previously unperfused skeletal muscle capillaries, thereby increasing the endothelial surface area available for insulin and glucose transport and, therefore, increasing glucose and insulin delivery to the skeletal muscle fibres. Microvascular recruitment occurs before insulin-mediated increases in total limb blood flow (Barrett et al., 2009). In rats increases in microvascular blood volume are seen as early as 5-10 min into a hyperinsulinaemic-euglycaemic clamp and these increases precede the activation of the insulin signalling cascade and increases in glucose uptake in skeletal muscle fibres (Vincent and Barrett, 2002, Vincent et al., 2004). Gudbjornsdottir *et al.* (2003) have shown that there is a marked increase in the capillary permeability surface area (PSA) product for glucose in humans, which is proportional to the increase in glucose uptake during an OGTT and also proportional to the larger increase seen during a hyperinsulinaemic-euglycaemic clamp leading to physiological increases in insulin concentrations (Gudbjornsdottir et al., 2003).

Insulin has been shown to act on vascular endothelial cells via the insulin receptor resulting in the activation of phosphatidylinositol 3-kinase (PI3K), Akt and ultimately, via serine^{1177} phosphorylation, activation of endothelial nitric oxide synthase (eNOS) (Liu et al., 2009b). The active form of eNOS synthesises nitric oxide (NO) and it is NO that causes relaxation of the surrounding vascular smooth muscle and is responsible for the dilatation of the terminal arterioles (Steinberg et al., 1994, Vincent et al., 2003, Barrett et al., 2009). Treatment of rats with the NOS inhibitor L-NAME prevented both the insulin-mediated increases in MBV and skeletal muscle glucose uptake, demonstrating that MBV increases are vital for insulin-mediated glucose uptake (Vincent et al., 2003).

Increases in microvascular recruitment have been shown to occur following insulin stimulation (Rattigan et al., 1997, Coggins et al., 2001, Vincent et al., 2004, Zhang et al., 2004), feeding (Vincent et al., 2006) and exercise (Honig et al., 1982, Dawson et al., 2002, Wheatley et al., 2004, Vincent et al., 2006).

1.2.2. Trans-endothelial insulin transport

Insulin concentration in the muscle interstitium is 40-60 % of that in the plasma indicating that there is a barrier to movement of insulin across the endothelial cell layer of the capillaries (Barrett et al., 2009). The mechanism by which insulin traverses the endothelial cell barrier is somewhat controversial (Barrett et al., 2009), however studies in human forearm using increasing physiological insulin concentrations suggest the movement of insulin out of the capillaries relies on a saturable transport process and points to a mechanism whereby endothelial cell insulin receptors mediate a transport mechanism in which insulin is transported through the endothelial cells from the luminal to the interstitial side, thus allowing insulin entry into the muscle interstitium (Eggleston et al., 2007).

It is important to state at this point that the microvascular effects of insulin are vital for insulin and glucose to be transported into the interstitial fluid of skeletal muscle fibres and activate the insulin signalling cascade. However, the focus of this thesis is on the regulation of glucose uptake in the skeletal muscle fibres and particularly the role played by increases and decreases in GLUT4 translocation in mediating skeletal muscle glucose uptake and as a cause of skeletal muscle insulin resistance, respectively. It is however acknowledged that insulin must first exert its effects on the microvasculature before skeletal muscle insulin signalling and GLUT4 translocation can occur. It is recognised that impairments in the microvascular effect

of insulin most likely also contribute to skeletal muscle insulin resistance in T2D and pre-diabetic states.

1.3. Glucose transporters in skeletal muscle

Glucose is lipophobic and also too large to traverse muscle cell membranes via diffusion, therefore transmembrane transporter proteins are required to facilitate glucose movement into the cell (Stuart et al., 2006). Glucose transporters (GLUTs) are passive carriers that do not require energy as they transport their substrate down a concentration gradient (Mueckler, 1994). All tissues in the human body express a GLUT isoform to allow glucose uptake into the cell (Uldry and Thorens, 2004). There are 14 members of the SLC2A/GLUT family of facilitative hexose transporters, of which the mRNAs for GLUT4, GLUT5, GLUT12, GLUT8, GLUT11, GLUT3 and GLUT1 have all been detected in human skeletal muscle, listed in the order of greatest abundance (Stuart et al., 2006). In the same study Western blotting and immunohistochemistry demonstrated strong expression of GLUT4, GLUT5 and GLUT12 in skeletal muscle. Furthermore despite its low mRNA expression, GLUT1 demonstrated a strong immunohistochemical signal in the endothelial cells of capillaries between muscle fibres (Stuart et al., 2006). All GLUT isoforms are composed of 12 transmembrane domains, with the amino- and carboxyl-termini on the cytoplasmic side of the membrane (Uldry and Thorens, 2004). GLUT4 is the primary glucose transporter isoform expressed in skeletal muscle and is largely responsible for insulin- and contraction mediated glucose uptake (Mueckler, 1994). GLUT1 is widely believed to be responsible for basal glucose uptake (Mueckler, 1994, Bell et al., 1993). In the coming paragraphs the expression and role of GLUT4, GLUT1, GLUT12 and GLUT5 will be reviewed.

1.3.1. GLUT4

GLUT4 is predominantly expressed in the insulin responsive tissues skeletal and cardiac muscle and adipose tissue (Mueckler, 1994) and is commonly reported to have a higher expression in type I oxidative skeletal muscle fibres compared to type II muscle fibres (Houmard et al., 1991, Gaster et al., 2000, Daugaard et al., 2000, Daugaard and Richter, 2004, Stuart et al., 2006). However other groups have shown no relationship between GLUT4 content and fibre type (Hughes et al., 1993, Andersen et al., 1993, Hardin et al., 1995), while one group has observed higher GLUT4 expression in type II muscle fibres (Borghouts et al., 2000).

Transgenic mice that express high levels of GLUT4 exhibit increased insulin- and contraction-mediated glucose disposal (Marshall and Mueckler, 1994, Hansen et al., 1995, Ren et al., 1995), increased basal glucose disposal (Liu et al., 1993, Hansen et al., 1995) and reduced basal plasma glucose concentrations (Liu et al., 1993, Ren et al., 1995). GLUT4 overexpression has a greater effect on insulin- and contraction-mediated glucose uptake compared to basal glucose uptake which is consistent with GLUT4 being responsible for insulin and contraction stimulated glucose uptake, though suggests a minor role for GLUT4 in basal glucose uptake (Hansen et al., 1995). Basal glucose uptake is primarily mediated by a different glucose transporter, thought to be GLUT1 (Mueckler, 1994, Bell et al., 1993). Further detail is given on GLUT1 in section 1.3.2 below.

Male GLUT4 knockout mice display elevated fed state plasma glucose concentration compared to wild type (Katz et al., 1995) and exhibit a reduced glucose uptake response to insulin (Stenbit et al., 1996). Interestingly, basal glucose uptake into the soleus muscle of male GLUT4 knockout mice was increased (Stenbit et al., 1996). In female GLUT4 knockout

mice there was no change in fed state glycaemia (Katz et al., 1995) or in insulin induced increases in glucose disposal compared to wild type (Stenbit et al., 1996). Therefore it seems that alternative glucose transporters are able to compensate for the lack of GLUT4 in GLUT4 knockout mice to increase basal glucose uptake in male mice and to maintain insulin-stimulated glucose uptake in female mice; these glucose transporters are proposed as GLUT1 and GLUT12, respectively (Stuart et al., 2009, Stenbit et al., 1996).

GLUT4 translocation in human skeletal muscle has been demonstrated through increased GLUT4 in PM cellular subfractions 60 min following glucose ingestion (Goodyear et al., 1996), following 30 – 40 min hyperinsulinaemic-euglycaemic clamp (Guma et al., 1995) and following 45 – 60 min exercise (Kennedy et al., 1999). In addition membrane fractionation studies using human skeletal muscle have demonstrated the effects of insulin and exercise on GLUT4 PM content are additive (Thorell et al., 1999). Additionally studies in rodents have shown GLUT4 translocation to the PM and T tubule membranes following insulin injection (Ploug et al., 1998, Lauritzen et al., 2006) and electrical stimulation of muscle (Ploug et al., 1998, Lauritzen et al., 2010) using confocal IF microscopy techniques.

As skeletal muscle is responsible for the majority of postprandial glucose uptake (Katz et al., 1983, Ferrannini et al., 1985) and takes up plasma glucose during endurance exercise for ATP production in the working muscle (Katz et al., 1991, Kjaer et al., 1991, van Loon et al., 2001) the role of GLUT4 in skeletal muscle is vital for the maintenance of glucose homeostasis; therefore supporting the attention of this thesis on the role of GLUT4 in insulin- and contraction-mediated skeletal muscle glucose uptake. Previously published literature in human skeletal muscle which measured the GLUT4 content of muscle PM fractions assumes a driving role for GLUT4 translocation in insulin and contraction-mediated increases in glucose uptake (Goodyear et al., 1996, Kennedy et al., 1999). This thesis will further

investigate the role of GLUT4 translocation in insulin and contraction mediated increases in glucose uptake using immunofluorescence microscopy methods in human skeletal muscle. The importance of using immunofluorescence microscopy methods to make estimates of GLUT4 localisation in the PM is discussed in section 1.4.1.

1.3.2. GLUT1

Glucose transporter 1 (GLUT1) is widely expressed and found in almost every tissue (Uldry and Thorens, 2004, Mueckler, 1994). GLUT1 overexpression studies have shown decreased fasting and fed plasma glucose concentrations and increased rates of basal glucose disposal (Ren et al., 1993, Marshall et al., 1993, Gulve et al., 1994, Hansen et al., 1998b) supporting its role as the primary glucose transporter isoform responsible for glucose uptake in the basal state. Consistent with its role in basal state glucose uptake, GLUT1 is constitutively localised at the PM (Gulve et al., 1994, Wang et al., 1996, Hansen et al., 1998b). Immunohistochemical studies of GLUT1 localisation in human skeletal muscle have shown high GLUT1 expression in the endothelial cells of capillaries between muscle fibres. Low intracellular GLUT1 signal was observed in type I muscle fibres (Stuart et al., 2006). In transgenic mice overexpressing GLUT1, the transporter was observed at the PM in the basal state and to a lesser extent the T tubule membranes (Wang et al., 1996). Intraperitoneal injection of insulin did not alter the localisation of GLUT1 in these mice (Wang et al., 1996).

1.3.3. GLUT12

Glucose transporter 12 (GLUT12) was first characterised in 2002 in MCF7 cells and the 50 kDa protein was subsequently shown to be expressed in skeletal muscle, adipose tissue cells and small intestine tissues with a substrate selectivity for D-glucose (Rogers et al., 2002, Rogers et al., 2003). Importantly the proportion of muscle cell GLUT12 localised to the PM

increased following 3 h hyperinsulinaemic-euglycaemic infusion in non-obese healthy individuals (Stuart et al., 2009). In L6 myoblasts inhibition of insulin signalling at the level of PI3K inhibits the insulin-mediated increase in GLUT12 at the PM (Stuart et al., 2009). Transgenic mice that overexpress GLUT12 exhibit improved glucose tolerance and insulin sensitivity and increased insulin stimulated glucose disposal into peripheral tissues, with no change in basal glucose disposal (Purcell et al., 2011). As stated previously, GLUT4 knockout mice do not lose their ability to increase glucose uptake in response to insulin (Katz et al., 1995, Stenbit et al., 1996). GLUT12 is therefore a good candidate for a second insulin regulatable glucose transporter that compensates for the lack of GLUT4 in GLUT4 null mice. In support of this, immunohistochemical staining has shown higher GLUT12 signal in type I compared to type II fibres (Stuart et al., 2006), consistent with its potential role in compensating for reduced GLUT4 expression in red muscle type (Stenbit et al., 1996). GLUT12 protein content has been shown to account for 12% of insulin-responsive glucose transporter (GLUT4 and GLUT12) protein content in human *vastus lateralis* muscle (Stuart et al., 2009).

1.3.4. GLUT5

Glucose transporter 5 (GLUT5) mRNA and protein have been shown to be present in human skeletal muscle at relatively high levels (Hundal et al., 1998, Stuart et al., 2006). However GLUT5 does not transport glucose; it is solely a fructose transporter and as such is expressed at much higher levels in the small intestine (Douard and Ferraris, 2008). GLUT5 expression appears to be higher in type IIb muscle fibres and its intracellular localisation is unaffected by insulin or contraction (Hundal et al., 1998, Stuart et al., 2006).

1.4. GLUT4 in skeletal muscle cells

GLUT4 is predominantly located in intracellular storage clusters with a small amount contained within the PM of muscle cells in the basal state. These intracellular storage clusters are mainly located at the fibre periphery, with some areas of intense intracellular staining (Ploug et al., 1998, Lauritzen et al., 2006). Large and smaller clusters of GLUT4 staining have been observed with a particularly high density in the perinuclear region (Ploug et al., 1998, Lauritzen et al., 2008). Studies combining confocal immunofluorescence microscopy techniques with immunogold labelling electron microscopy (EM) applied to whole single fibres of rat soleus muscle demonstrate a high concentration of GLUT4 in membranes associated with the trans-Golgi network (TGN) region as well as in smaller endosomal membrane stores. Tubulovesicular storage structures, which are still smaller, were also seen and were assumed to be the GLUT4 storage vesicles (GSVs) (Ploug et al., 1998). GSVs are formed by budding away from endosomal and TGN-associated membranes (Bogan and Kandror, 2010, Bogan, 2012) and following insulin and contraction stimulation GSVs translocate and dock and fuse with the PM and T-tubule membranes to allow increased glucose uptake (Foley et al., 2011). Fig.1.1 outlines the spatial distribution of these GLUT4 stores in skeletal muscle.

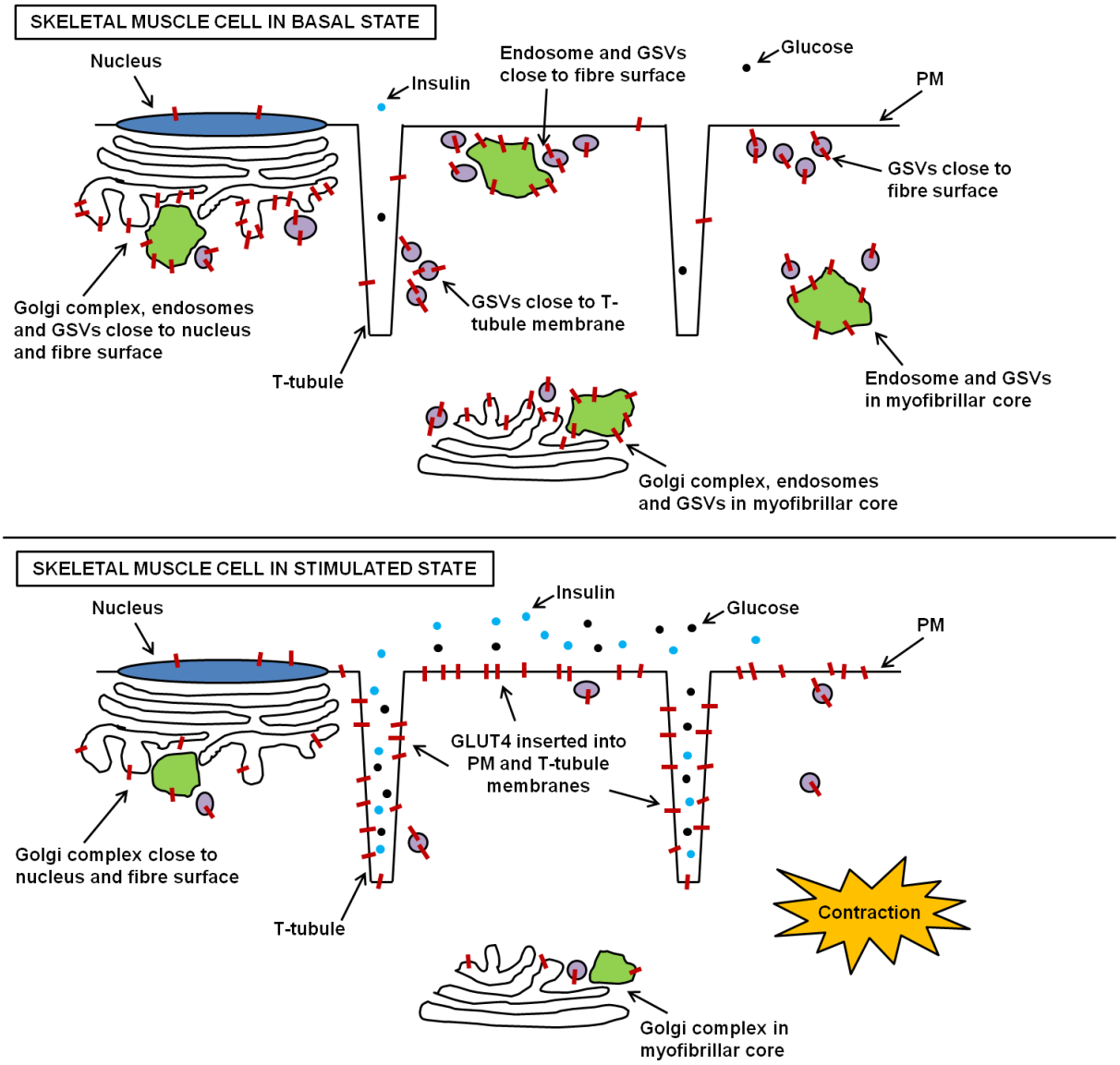

Fig. 1.1. *Representation of GLUT4 storage and trafficking in skeletal muscle cells in basal and stimulated states. During resting conditions and with low interstitial glucose and insulin concentrations GLUT4 is stored intracellularly associated with the membranes of the trans-Golgi complex and in endosomes and GSVs which are predominantly located at the fibre periphery, but also in deeper regions. A small amount of GLUT4 is located in the PM and T-tubule membranes. Following contraction or increasing interstitial insulin concentrations GSVs fuse with the outer membrane and GLUT4 becomes inserted into the PM and T-tubule membranes to enable increased rates of glucose uptake. TGN stores (large GLUT4 clusters)*

of GLUT4 reduce in size while endosomal stores reduce in number. The information in this figure is based on information provided by the following references all obtained from information generated in rat and mouse skeletal muscle (Ploug et al., 1998, Lauritzen et al., 2006, Lauritzen et al., 2008, Lauritzen et al., 2010).

1.4.1. Methods to investigate GLUT4 localisation and trafficking

The structure of skeletal muscle is complex with the contractile proteins actin and myosin comprising approximately 80 % of muscle protein (Jones, 1990) and the T-tubule membrane network of PM invaginations running deep into the fibre interior (Peachey and Eisenberg, 1978). The primary role of the T-tubule membranes is to rapidly conduct action potentials from the cell surface to the fibre interior, thereby inducing calcium release from the sarcoplasmic reticulum and subsequently activating myofibril contraction (Peachey and Eisenberg, 1978). T-tubule membranes run around the myofibrils either side of the Z line at the A-I band junctions of the sarcomere and adjacent to the sarcoplasmic reticulum (Jones, 1990). In immunofluorescence images of longitudinally-oriented skeletal muscle fibres T-tubule membranes are visualised as cross striations that run perpendicular to the fibre axis (Wilson et al., 2012, Murphy et al., 2009). As well as their role in action potential conduction, T-tubule membranes are well characterised as a site of insulin signalling and insulin- and contraction-mediated GLUT4 translocation (Ploug et al., 1998, Lauritzen et al., 2006, Lauritzen et al., 2010). T-tubule membrane surface area is proposed to be two- to three-fold higher than that of the sarcolemma (Lauritzen et al., 2006), with suggestions it may even be nine times higher and contribute 94 % of GLUT4-mediated glucose uptake (Wang et al., 1996).

The complex structure of a muscle fibre and the importance of the T-tubule membranes in insulin- and contraction-mediated glucose uptake elicit specific methodological requirements in the analysis of GLUT4 localisation and translocation. Contributing to these requirements are the heterogeneous intracellular GLUT4 storage pools which, to date, have undergone limited characterisation in skeletal muscle.

A wide range of techniques have been employed in the study of GLUT4 localisation and trafficking; each with their own advantages and disadvantages. In earlier studies GLUT4 translocation was primarily investigated using subcellular fractionation techniques in both rodent (Klip et al., 1987, Douen et al., 1990a, Marette et al., 1992) and human skeletal muscle (Goodyear et al., 1996, Kennedy et al., 1999) through quantitation of GLUT4 content in PM fractions. Firstly subcellular fractionation requires large muscle samples. For example previous studies investigating GLUT4 localisation through subcellular fractionation collected approximately 1g of muscle using an open biopsy method (Goodyear et al., 1996, Kennedy et al., 1999). While subcellular fractionation can be completed on smaller muscle samples (~100mg), this is the higher end of the yields obtainable with the Bergstrom percutaneous needle biopsy technique (Bergstrom, 1975) and is significantly more than what is needed to carry out immunofluorescence microscopy analysis which can be performed on as little as 20-30mg muscle, provided the sample is not damaged. Additional limitations include contamination of the isolated PM fractions with myofibrillar proteins and with other intracellular membrane fractions with a high GLUT4 content (Fazakerley et al., 2009b). A further limitation is the inability to discriminate between GLUT4 just adjacent to the PM and GLUT4 fully incorporated into the PM after docking and fusion of GSV's and, therefore, able to transport glucose (Schertzer et al., 2009). Therefore, repeated suggestions have been made in the literature that data generated with the PM fractionation method do not provide reliable

estimates of the amount of GLUT4 present in the PM (Fazakerley et al., 2009b, Schertzer et al., 2009, Lauritzen and Schertzer, 2010).

Immunofluorescence studies in rodent skeletal muscle have clearly shown translocation of GLUT4 to PM and T tubule membrane regions (Ploug et al., 1998, Wang et al., 1996). However as no PM marker was used in these studies GLUT4 was assessed in a region assumed to represent the PM rather than know to be the PM. The same is true for GLUT4 translocation to the T-tubule membranes.

Temporal information regarding GLUT4 translocation in response to insulin and contraction in rodent skeletal muscle *in vivo* has been generated using highly elegant experiments utilising GFP-tagged GLUT4 (Lauritzen et al., 2006, Lauritzen et al., 2010), however this is still limited by the aforementioned lack of PM marker therefore leaving uncertainty about the exact location of GLUT4 docking in PM and T-tubule membranes. *In vitro* experiments in non-permeabilised L6 skeletal muscle cells expressing GLUT4 with HA or myc tags on the first exofacial loop resolved this problem as the tag was only detectable when GLUT4 was fully inserted into the PM (Fazakerley et al., 2009a). However cultured muscle cells are missing key features of mature skeletal muscle such as the T tubule membrane system and, therefore, in vivo model systems were developed in which mice express GLUT4-myc or GLUT4-HA for confirmation of GLUT4 insertion into the PM in vivo (Schertzer et al., 2009, Fazakerley et al., 2009b). However in human skeletal muscle *in vivo* transient or chronic expression of tagged-GLUT4 for experimental purposes is not technologically possible.

Electron microscopy (EM) methods using immuno-gold labelling of GLUT4 have been utilised to generate high resolution images of GLUT4 at the PM, T-tubule membranes and in intracellular stores (Ploug et al., 1998). Immuno-gold EM, however, also has limitations. The

most important of which is the negative effect tissue dehydration and embedding can have on the preservation of GLUT4 antigenicity through GLUT4 denaturation (Hayat, 1989, Hyatt, 1991). Furthermore dehydration and embedding can also effect the penetration of the antibody to the target (Hayat, 1989). Finally the addition of colloidal gold particles to an antibody can alter the protein conformation of that antibody, thereby affecting its binding affinity to the target (Hayat, 1989). Taken together these limitations could all reduce the sensitivity of GLUT4 detection using immuno-gold EM.

To summarise, there are limitations associated with many of the methods used to investigate GLUT4 localisation and trafficking. Therefore, new methods, beyond PM fractionation and immuno-EM, must be developed to enable further investigation of GLUT4 localisation and trafficking in human skeletal muscle. As expression of tagged GLUT4 is not technologically possible in human skeletal muscle, confocal immunofluorescence microscopy, despite its resolution limitations, could generate novel information on GLUT4 localisation and trafficking in human skeletal muscle. The novel approach chosen in this PhD project will be to measure the colocalisation of GLUT4 with the PM marker dystrophin as a measure of GLUT4 present in the PM using traditional immunofluorescence microscopy methods. This approach has not been used in previous research investigating translocation of GLUT4 to the PM.

1.4.2. GSV components

GSVs (GLUT4 storage vesicles) are lipid bilayer bound structures that have been shown to contain between 1 and 25 GLUT4 molecules (Ploug et al., 1998). GSVs are characterised biochemically by the presence of the SNARE protein VAMP2 and insulin-regulated amino peptidase (IRAP) (Foley et al., 2011). As a SNARE protein VAMP2, in combination with other SNARE proteins, is responsible for the docking and fusion of GSVs at the PM

(Kristiansen et al., 1996, Randhawa et al., 2000). IRAP may be involved in GSV intracellular retention in the basal state (Foley et al., 2011). Also involved in GSV intracellular retention and present in the GSV is a protein called 'tether containing a UBX domain for GLUT4' (TUG) (Foley et al., 2011). In the basal state Akt substrate of 160 kDa (AS160) is also associated with the GSVs, potentially via interaction with the N terminal of IRAP (Larance et al., 2005, Eguez et al., 2005, Thong et al., 2007). Sortillin is another protein identified on the GSV and is thought to play a role in GSV biogenesis at the TGN (Foley et al., 2011). GSVs contain no endosomal or TGN proteins (Stockli et al., 2011).

1.4.3. Other intracellular GLUT4 stores

GLUT4 continually cycles between intracellular membranes and the surface membranes of cells (Fazakerley et al., 2009a, Stockli et al., 2011, Foley et al., 2011). Studies on GLUT4 intracellular trafficking have been carried out predominantly in cultures of rodent adipocyte cells and to a lesser degree in cultured L6 skeletal muscle cells (Stockli et al., 2011, Foley et al., 2011). While there are specific differences in GLUT4 trafficking between adipose tissue cells and skeletal muscle cells the fundamental mechanisms are comparable (Foley et al., 2011). GLUT4 internalisation from the PM occurs via clathrin-mediated endocytosis and cholesterol-dependent endocytosis (Handberg et al., 1990). Following internalisation, GLUT4-containing regions of the PM form early endosomes, which in turn accumulate into endosomal recycling compartments (ERC) for cycling of GLUT4-containing membranes back to the PM (~10 %) or sorting into GSVs or subcompartments of the TGN. In the absence of stimulation GLUT4 is retained in this slow cycling state between the ERC and the PM or the ERC, GSVs and the TGN (Bryant et al., 2002, Adachi et al., 2007, Foley et al., 2011, Stockli et al., 2011).

Immunofluorescence analysis of rat skeletal muscle fibres showed GLUT4 staining as large and smaller clusters which are located predominantly in perinuclear regions and at the fibre periphery (68 % within 3 µm of the PM), though staining was also present in deeper regions (Ralston and Ploug, 1996, Ploug et al., 1998). In rodent skeletal muscle TGN GLUT4 stores have been estimated as > 1 µm in diameter (Lauritzen et al., 2008). The size of endosomal stores and GSVs in skeletal muscle is less conclusively reported. Adipose cell studies have revealed that GLUT4 is stored in 50 – 70 nm GSVs (Larance et al., 2008, Bogan and Kandror, 2010, Stockli et al., 2011, Bogan, 2012) and approximately 200 nm endosomal stores (Bogan, 2012). Based on EM images and their scale bars endosomes appear to be 200 – 300 nm in rodent skeletal muscle with GSVs smaller still (Ploug et al., 1998). TGN markers partially overlapped with large clusters of GLUT4 only, while the endosomal marker (transferrin receptor) overlapped with both large and smaller clusters of GLUT4, but there were additional smaller clusters that did not overlap with the endosomal marker. These are likely to be GSVs (Ploug et al., 1998). *In vivo* studies in mice transiently transfected with green fluorescent protein (GFP)-tagged GLUT4 also confirmed the presence of GLUT4 in large and small clusters; again the large clusters were located predominantly in perinuclear regions (Lauritzen et al., 2006). A limited amount of non-continuous GLUT4 staining was present in the PM region in the basal state, while a weak and irregular staining of cross striations was seen, which demonstrates limited presence of GLUT4 in T-tubule membranes in the basal unstimulated state (Ploug et al., 1998, Lauritzen et al., 2006). In addition studies in transgenic mouse muscle fibres using labelling of exofacially *myc*-tagged GLUT4 demonstrate a substantial GLUT4 fusion with the PM in the basal state, with externalised *myc* labelling under basal conditions approximately 50 % of that after insulin stimulation (Schertzer et al., 2009). In contrast EM immunogold labelling studies suggest that GLUT4 is completely

excluded from the PM in the basal state (Ploug et al., 1998). This discrepancy may be due to the effects of tissue fixation and embedding on GLUT4 antigenicity which as discussed previously may reduce the sensitivity of immuno-gold EM methods (Hayat, 1989, Hyatt, 1991). Previous attempts of immunohistochemical studies of GLUT4 in human skeletal muscle in the basal state have shown a high punctuate staining intensity in the perinuclear region, a granular staining pattern in the PM region and a small amount of a diffuse intracellular staining with higher intensity in type I muscle fibres (Gaster et al., 2000, Stuart et al., 2006).

1.4.4. GLUT4 trafficking following insulin stimulation and muscle contraction

Following insulin stimulation and muscle contraction the slow cycling of GLUT4 between the PM and intracellular storage membranes is interrupted, which is assumed to lead to increased presence of GLUT4 at the PM through increases in the exocytosis of GSVs and reductions in the endocytosis of GLUT4 containing PM sections (Foley et al., 2011, Kampmann et al., 2011). Studies in L6 muscle cells have demonstrated increases in GLUT4 at the surface membrane following stimulation with insulin or AMPK agonists (Fazakerley et al., 2009a). In these studies the GLUT4 internalisation rate constant was reduced by 50 % following insulin or AICAR stimulation. In comparison the externalisation rate constant was increased only slightly following insulin stimulation and even decreased slightly following AICAR stimulation (Fazakerley et al., 2009a). This study highlights the importance of a decrease in GLUT4 endocytosis following insulin stimulation and muscle contraction to increase GLUT4 availability at the PM (Fazakerley et al., 2009a).

Insulin injection and electrical muscle stimulation led to a redistribution of GLUT4 from intracellular clusters to the PM and T-tubule membranes in *in vivo* studies of mice transiently transfected with GFP-tagged GLUT4 (Lauritzen et al., 2006, Lauritzen et al., 2010). Increased

GLUT4 staining in the PM region was observed 10 min after insulin stimulation, reached maximum values by 20 min after insulin injection (Lauritzen et al., 2006) and was maintained for 150 min (Lauritzen et al., 2008). Following insulin injection a 10 minute delay was observed between maximal GLUT4 translocation to the PM and to the T-tubule membranes, with T-tubule GLUT4 staining reaching maximum values 30 min after insulin stimulation (Lauritzen et al., 2006). The authors suggest that this delay is the result of reductions in insulin diffusion rate into the T-tubular lumen (Lauritzen et al., 2006). In contrast contraction-induced GLUT4 translocation to the PM and T-tubule membranes occurred simultaneously and continued to increase throughout three 5 min bouts of high voltage electrical stimulation and three 10 min bouts of lower voltage electrical stimulation (Lauritzen et al., 2010). Immuno-gold particle electron microscopy studies have demonstrated that the effects of insulin and contraction on GLUT4 redistribution to the PM and T-tubule membranes are additive in rat skeletal muscle with 14-fold increases in immunogold particle density in the PM in comparison to the unstimulated state. Following insulin and exercise alone increases were 7-fold and 9-fold, respectively (Ploug et al., 1998). It must be emphasised that the insulin boluses given to the animals in the experiments described above were very large and elicited very high plasma insulin concentrations (peak 200 000 $\mu IU.mL^{-1}$ in Lauritzen *et al.* (2008)). In addition contraction was induced through electrical stimulation consisting of two 5 min periods of tetanic contractions (one 200ms train of 100 Hz pulses each second) with electrodes inserted in the feet and through the skin in the posterior hip region close to the sciatic nerve (Ploug et al., 1998). This is a stronger stimulus than dynamic exercise. Therefore the strong insulin and contraction stimuli described above may explain why the magnitude of insulin and contraction induced increases in GLUT4 immunogold labelling at the PM are larger in this EM study than those that can be expected in human skeletal muscle under

normal physiolological conditions (OGTT and moderate intensity exercise; chapter 4 of this thesis). A reduced sensitivity of immunogold labeling of GLUT4 at the PM under basal conditions may also exaggerate the increase seen under stimulated conditions using EM immunogold labelling (Hayat, 1989, Hyatt, 1991).

During the 4 h period following glucose feeding leg glucose uptake increased threefold (Katz et al., 1983), during a hyperinsulinaemic-euglycaemic clamp leg glucose uptake increased fivefold (DeFronzo et al., 1985) and during submaximal exercise leg glucose uptake increased approximately fifteen-fold (Katz et al., 1986, Martin et al., 1995). While there are limitations associated with subcellular fractionation methods, the increases in GLUT4 content of PM fractions in response to physiological increases in plasma insulin concentration (27 % increase in PM GLUT4) and cycling exercise (71 % increase in PM GLUT4) (Goodyear et al., 1996, Kennedy et al., 1999) in human skeletal muscle only partly explain these large increases in leg glucose uptake. Therefore, while this thesis focuses on GLUT4 translocation to the PM as it has been suggested to be the primary mechanism to increase skeletal muscle glucose uptake under stimulated conditions, there seem to be other mechanisms that contribute to the insulin- and contraction-mediated increases in skeletal muscle glucose uptake as well.

Previous research in rats suggested that both exercise and insulin appeared to recruit GLUT4 from large and small clusters with reductions seen in the size of the large clusters and in the number of the small clusters (Ploug et al., 1998). The additive nature of GLUT4 translocation in response to insulin and contraction stimulation has led to the suggestion that insulin and contraction recruit GLUT4 from different pools. Consistent with this suggestion density gradient centrifugation studies using rodent skeletal muscle have shown insulin and contraction deplete GLUT4 from different intracellular membrane fractions (Douen et al., 1990b, Coderre et al., 1995). The endosomal marker, transferrin receptor, was subsequently

used to define the insulin- and contraction-responsive intracellular GLUT4 pools using subcellular fractionation techniques (Lemieux et al., 2000). Insulin only recruited GLUT4 from transferrin receptor negative, non-endosomal pools, while contraction recruited GLUT4 from both transferrin receptor positive and negative pools (Lemieux et al., 2000). Similarly Ploug *et al.* (1998) used immunofluorescence microscopy to show GLUT4 depletion primarily from small transferrin receptor negative (non-endosomal) stores in response to insulin, while contraction recruited GLUT4 primarily from transferrin receptor positive endosomal storage sites (Ploug et al., 1998).

During the first 30 min of insulin stimulation large (>1 μm) GLUT4 clusters did not move as a whole, rather they were stationary in their original position at the PM or T-tubules and were locally depleted of GLUT4 by budding off of smaller vesicles (Lauritzen et al., 2008). Photobleaching experiments revealed that smaller vesicles (<1 μM) moved from perinuclear GLUT4 clusters out along the PM upon insulin stimulation (Lauritzen et al., 2008).

To summarise the above section insulin-mediated increases in GLUT4 PM content appear to occur as a result of reduced endocytosis and increased exocytosis, while contraction-mediated increases in GLUT4 PM content occur predominantly through reductions in endocytosis (Fazakerley et al., 2009a). Insulin depletes GLUT4 from small, non-endosomal stores which are likely to be GSVs, while contraction is reported to deplete GLUT4 predominantly from endosomal stores (Ploug et al., 1998).

1.4.5. The role of the cytoskeleton

Insulin-mediated cortical actin polymerisation and remodelling has been demonstrated in L6 skeletal muscle myoblasts and myotubes (He et al., 1995). Furthermore disruption of insulin-mediated actin remodelling via inhibition of actin polymerisation prevented GLUT4

translocation and glucose uptake in L6 myotubes (He et al., 1995, Tsakiridis et al., 1995, Khayat et al., 2000) and rat skeletal muscle (Brozinick et al., 2004). The Rho-GTPase Rac1 is thought to be responsible for the stimulation of cortical actin remodelling in skeletal muscle in response to insulin (Chiu et al., 2011) and contraction (Sylow et al., 2013b). A Rac1-dependent insulin signalling pathway occurs in parallel to the commonly-described Akt-dependent pathway (Chiu et al., 2011). Downstream of $PI(4,5)P_2$ conversion to $PI(3,4,5)P_3$ by PI3K, Rac1 is GTP-bound and activated leading to p21-activated kinase (PAK) autophosphorylation at Thr423 and cortical actin remodelling (Chiu et al., 2011, JeBailey et al., 2004). Downstream of Rac1 and PAK, nucleating factors such as N-WASp bind and activate the Arp2/3 complex, which then directly binds actin filaments and catalyses the formation of branches of actin filaments (Chiu et al., 2011). Silencing of the individual subunits of the Arp2/3 complex in L6 muscle cells prevented insulin-mediated cortical actin remodelling (Chiu et al., 2010). The functional role of cortical actin remodelling in GLUT4 translocation and glucose uptake remains unclear. However possible suggestions include; tethering of GLUT4 or other insulin signalling molecules to the remodelled actin filaments to bring them into close proximity to the PM and the provision of tracks along which GSV movement over short distances can occur (Chiu et al., 2011). The myosin motor proteins Myo1c and Myo5 have been proposed to mediate this process as they are associated with GSVs and the actin filaments (Chiu et al., 2011, Stockli et al., 2011). In particular Myo5 was found to associate with actin following insulin stimulation and silencing Myo5 reduced insulin-mediated GLUT4 translocation (Yoshizaki et al., 2007).

1.5. Insulin stimulated GLUT4 translocation

Insulin stimulates GLUT4 translocation from intracellular stores to the muscle fibre surface via a relatively well characterised, though in parts still incomplete, signalling pathway. This pathway will be outlined in the subsequent sections and is broken down into proximal signalling from the insulin receptor and distal signalling regulating GLUT4 docking and fusion at the PM. A representation of insulin and contraction signalling pathways leading to GLUT4 translocation is shown in Fig. 1.2.

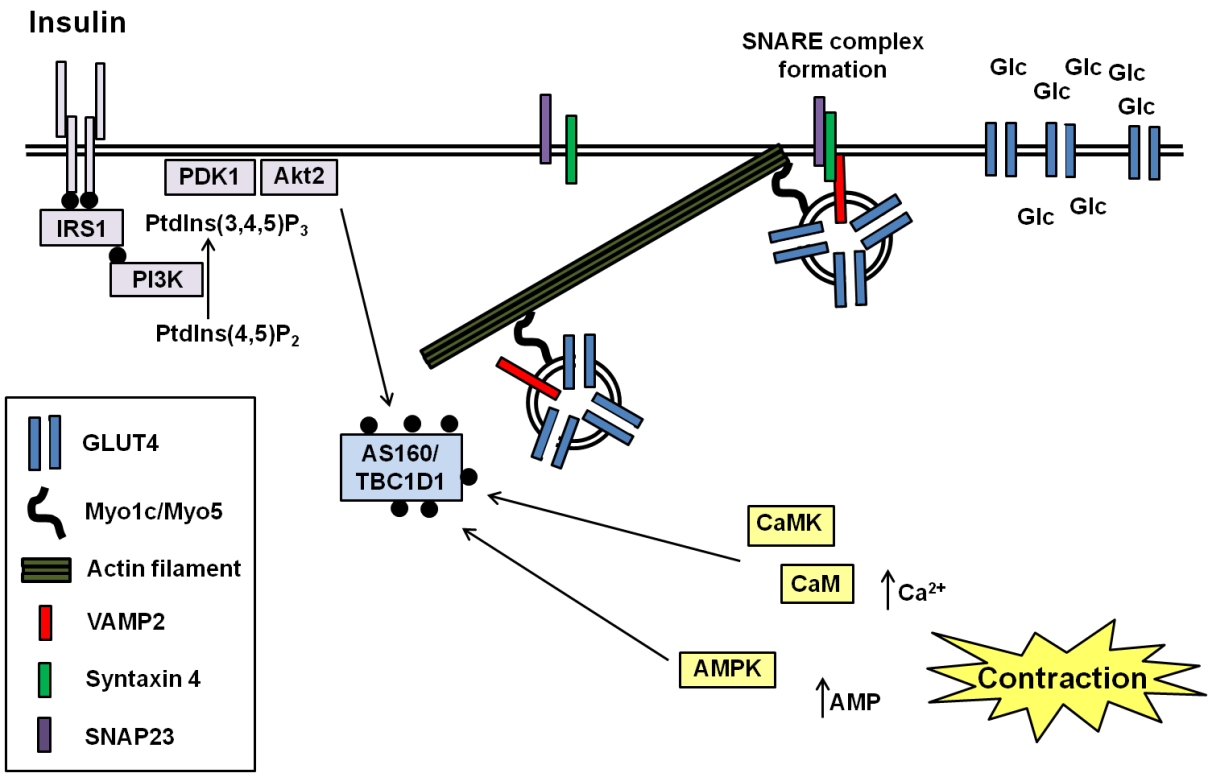

Fig. 1.2. *Representation of insulin and contraction signalling cascades leading to GLUT4 translocation in skeletal muscle. Insulin- and contraction-mediated signals converge at AS160 and TBC1D1 releasing GSVs for translocation to the PM along actin filaments. At the PM SNARE complex formation mediates GSV fusion and GLUT4 insertion into the PM to allow insulin- or contraction-mediated increases in glucose uptake. For references see sections 1.5 and 1.6.*

1.5.1. Proximal insulin signalling

Many cells in the body express insulin receptor (IR) proteins which are localised in the cell PM and insulin elicits a range of responses in different cell types (Saltiel and Kahn, 2001, Minokoshi et al., 2003). In skeletal muscle cells, IR is found on the PM and the deep membrane invaginations of the T-tubule membranes (Burdett et al., 1987, Lauritzen et al.,

2006). The IR is a heterotetramer with two extracellular insulin binding α subunits and two membrane-spanning β subunits with tyrosine kinase activity. When insulin binds the IR, the tyrosine kinase activity of the β subunits is activated and the β subunits are transphosphorylated (Watson et al., 2004, Chang et al., 2004). Phosphorylated tyrosine residues on the IR β subunits provide docking sites for insulin receptor substrate (IRS) proteins with a phosphotyrosine binding (PTB) domain; of which there are 4 isoforms (Watson et al., 2004, Chang et al., 2004, Karlsson and Zierath, 2007). IRS1 appears to be the main isoform involved in insulin signalling in skeletal muscle (Krook et al., 2004). IRS1 global knockout mouse models display reduced glucose tolerance and reduced insulin stimulated glucose uptake (Tamemoto et al., 1994, Araki et al., 1994). Similarly gene silencing of IRS1 in L6 myotubes reduced glucose uptake and GLUT4 translocation (Huang et al., 2005). IRS1 is itself tyrosine phosphorylated by IR (Karlsson and Zierath, 2007) to provide docking sites for recruitment of downstream signalling proteins containing src-homology 2 (SH2) domains. Phosphatidylinositol 3-kinase (PI3K) is an important insulin signalling intermediate that is recruited to IRS1 (Krook et al., 2004). PI3K is formed of two subunits; the p85 regulatory subunit of PI3K contains an SH2 domain which docks at IRS1 and allosterically activates the p110 catalytic subunit recruiting it to the PM (Watson et al., 2004). The activated p110 subunit of PI3K phosphorylates the 3' –OH moiety of the PM inositol phospholipid phosphatidylinositol-4,5-bisphosphate ($PI(4,5)P_2$) to generate phosphatidylinositol-3,4,5-triphosphate ($PI(3,4,5)P_3$) (Karlsson and Zierath, 2007). PI3K is necessary for insulin stimulated glucose uptake (Krook et al., 2004, Chang et al., 2004). In L6 skeletal muscle cells inhibition of PI3K by wortmannin reduced insulin stimulated glucose uptake (Tsakiridis et al., 1995). Furthermore overexpression of a dominant negative form of PI3K in 3T3-L1 adipocytes that prevents the IRS1/PI3K interaction reduces GLUT4

translocation and glucose uptake (Sharma et al., 1998), while overexpression of a constitutively active form of PI3K in 3T3-L1 adipocytes results in GLUT4 translocation (Martin et al., 1996). PI(3,4,5)P_3 binds proteins containing pleckstrin homology (PH) domains, such as phosphoinositide-dependent kinase (PDK) and protein kinase B (PKB), otherwise known as Akt, to localise these proteins to the PM (Chang et al., 2004). Furthermore PI(3,4,5)P_3 allosterically activates PDK (Krook et al., 2004). Akt is phosphorylated by the mammalian target of rapamycin (mTor) and Rictor protein complex on Ser 473 and subsequently by PDK on Thr 308, to achieve full Akt activation (Chang et al., 2004, Watson et al., 2004). There are three known isoforms of Akt, with Akt2 the main isoform in skeletal muscle and adipose (Karlsson and Zierath, 2007). Akt2 is vital for normal glucose homeostasis. In global Akt2 knockout mice insulin sensitivity and glucose tolerance are reduced (Cho et al., 2001).

Akt substrate of 160 kDa (AS160, also known as TBC1D4) was identified in 2002 in 3T3-L1 adipocytes as an Akt substrate (Kane et al., 2002). Following insulin stimulation in adipocytes AS160 is phosphorylated on residues Ser318, Ser570, Ser588, Thr642 and Ser751 (Sano et al., 2003). As these residues lie within Akt consensus sequences it is likely that Akt is the kinase responsible for their phosphorylation (Sano et al., 2003). GLUT4 translocation is inhibited in the AS160-4P mutant in which Ser318, Ser588, Thr642 and Ser751 phosphorylation sites are mutated to alanine residues, demonstrating the need for AS160 phosphorylation in GLUT4 translocation (Sano et al., 2003). Importantly studies have also confirmed AS160 expression in skeletal muscle and insulin-stimulated phosphorylation of AS160 by Akt in skeletal muscle (Bruss et al., 2005). AS160 contains a Rab GTPase activating protein (GAP) domain which is active in the basal state promoting GTP hydrolysis to GDP and maintaining associated Rab proteins in the GDP-loaded inactive form (Kane et

al., 2002, Chen et al., 2011). In support of the inhibitory effect of AS160 activity on GLUT4 translocation, AS160 RNA interference in adipocytes resulted in GLUT4 translocation to the cell surface without insulin stimulation (Eguez et al., 2005). Rabs are small G proteins required for membrane trafficking (Zerial and McBride, 2001) and in the inactive GDP-bound state GSV-associated Rabs retain GSVs inside the cell (Chen et al., 2011). Upon insulin stimulation phosphorylation of AS160 inhibits AS160 RabGAP activity and GSV-associated Rab proteins remain in a GTP-loaded active form to allow GSV translocation to the PM (Chen et al., 2008). Interestingly in the basal state AS160 is found associated with GSVs, but upon insulin stimulation this association is reduced (Larance et al., 2005). Interaction of a single 14-3-3 protein dimer with phosphorylated residues pT642 and pS341 either side of a PTB domain of AS160 has been shown to be important in insulin mediated GLUT4 translocation and indicates that 14-3-3 binding may regulate the RabGAP activity of AS160 (Ramm et al., 2006, Geraghty et al., 2007, Chen et al., 2008).

1.5.2. Distal insulin signalling

The GSV-associated Rab proteins appear to differ between muscle and adipose cells (Sun et al., 2010). In adipose cells the AS160 GAP domain has been shown to be active against Rabs 2A, 10 and 14 (Larance et al., 2005, Miinea et al., 2005). However, in L6 muscle cells Rab10 is not activated by insulin (Sun et al., 2010). Instead Rabs 8A and 13 are GTP loaded following insulin stimulation in L6 muscle cells (Sun et al., 2010). Furthermore in L6 muscle cells Rab8A and Rab13 overexpression rescue the reduced GLUT4 translocation observed in AS160-4P mutant cells and siRNA knockdown of either Rab reduces GLUT4 translocation (Ishikura et al., 2007, Ishikura and Klip, 2008, Sun et al., 2010). Rab protein signalling is thought to impact on the initial docking stages of GSVs at the PM (Krook et al., 2004).

For insulin mediated glucose uptake to occur GSVs containing 1 to 25 GLUT4 molecules must be inserted into the muscle cell surface membrane following the formation of specific SNARE protein complexes (Chen and Scheller, 2001). Vesicle and target membrane fusion events are controlled by vesicle (v)- and target (t)-SNARE proteins that interact via coiled-coil domains to form a 4 helix bundle (Watson et al., 2004) in a SNARE complex which brings the two membranes into close proximity and is able to overcome the energy barrier of membrane fusion (Weber et al., 1998). t-SNARES are located on target membranes, while v-SNARES are located in the donor membrane; in the case of insulin mediated GLUT4 translocation this equates to the PM and the GSV membrane, respectively (Watson et al., 2004). Studies have identified SNAP23 and syntaxin 4 as the t-SNAREs involved in insulin-mediated GSV docking and fusion (Kawaguchi et al., 2010). In line with this, SNAP23 and syntaxin 4 are localised at the PM (Bostrom et al., 2010, Khan et al., 2001). The identity of the v-SNARE responsible for insulin-mediated GLUT4 fusion is less certain (Bryant and Gould, 2011). VAMP2, VAMP3, VAMP5 and VAMP7 are enriched in GSVs in mature rat skeletal muscle (Rose et al., 2009). Addition of VAMP2, but not VAMP3, to L6 skeletal muscle cells in which endogenous VAMP2 and VAMP3 had been proteolytically cleaved by tetanus toxin rescued inhibition of GLUT4 translocation (Randhawa et al., 2000). In addition siRNA knockdown of VAMP2 and VAMP5 but not VAMP3 or VAMP7 inhibited insulin-mediated GLUT4 translocation in cultured cardiomyocytes (Schwenk et al., 2010). In the basal state syntaxin 4 binds the Sec1/Munc18 (SM) family member Munc18c preventing VAMP2 binding to form the SNARE complex (Tellam et al., 1995, Tellam et al., 1997). Insulin stimulation reduces the Munc18c-Syntaxin 4 interaction, indicating that GSV docking and fusion is inhibited by Munc18c in the basal state and that insulin stimulation removes this inhibition (Pessin et al., 1999). In addition overexpression of Munc18c reduces GLUT4

translocation, consistent with an inhibitory role for Munc18c (Khan et al., 2001). Tyrosine phosphorylation of Munc18c has been demonstrated at Tyr521 in adipocytes prior to dissociation from syntaxin 4 (Oh and Thurmond, 2006, Umahara et al., 2008). Furthermore Munc18c phosphorylation of Tyr219 and Tyr521 has been shown to be necessary for GSV exocytosis (Jewell et al., 2011). Interestingly IR tyrosine kinase activity was found to be responsible for the phosphorylation of Munc18c at Tyr521 in both adipocytes and skeletal muscle cells linking the insulin proximal insulin signalling pathway with stimulation of GSV docking and fusion (Jewell et al., 2011).

1.6. Contraction stimulated GLUT4 translocation

Glucose uptake into skeletal muscle increases in response to muscle contraction (Katz et al., 1986, Martin et al., 1995, Rose and Richter, 2005). Whole body or muscle-specific GLUT4 knockout abolishes contraction-stimulated glucose uptake demonstrating the crucial importance of GLUT4 in contraction stimulated glucose uptake (Ryder et al., 1999, Zisman et al., 2000). Subcellular fractionation has been used to demonstrate a 71 % increase in GLUT4 in the PM regions in response to 45-60 min of cycling exercise in human skeletal muscle (Kennedy et al., 1999). The mechanisms controlling contraction stimulated GLUT4 translocation and glucose uptake are distinct from insulin mediated glucose uptake, though interplay does occur (Rose and Richter, 2005, Wojtaszewski and Richter, 2006, Richter and Hargreaves, 2013).

1.6.1. Calcium signalling

Skeletal muscle fibre surface membrane depolarisation leads to Ca^{2+} release from the sarcoplasmic reticulum into the cytosol to induce muscle fibre contraction (Jones, 1990). Increases in cytosolic Ca^{2+} concentration that occur during muscle contraction are associated

with increased glucose transport (Holloszy and Narahara, 1967). Furthermore pharmacological methods to increase intracellular Ca^{2+} concentration also induce increases in glucose transport (Youn et al., 1991, Terada et al., 2003). Ca^{2+}/Calmodulin (CaM) dependent protein kinase II (CaMKII) is activated by Ca^{2+}-bound CaM during exercise in human skeletal muscle (Rose and Hargreaves, 2003, Rose and Richter, 2005). Inhibition of CaMKII reduces contraction-stimulated glucose transport in rat muscle demonstrating that CAMKII activation plays a role in contraction-mediated glucose transport (Wright et al., 2004, Wright et al., 2005). Conventional protein kinase C (cPKC) isoforms are activated in response to elevated intracellular Ca^{2+} concentration (Nishizuka, 1995), exercise and contraction in rat muscle (Richter et al., 1987, Cleland et al., 1989), but not in human muscle (Rose et al., 2004). Downregulation or inhibition of novel (nPKC) and cPKC isoforms reduces contraction mediated glucose transport (Cleland et al., 1990, Ihlemann et al., 1999). Therefore PKC may be involved in contraction signalling leading to increases in muscle glucose uptake, however further studies are required for more conclusive evidence (Rose and Richter, 2005).

1.6.2. Sensing cellular energy status

AMP-activated protein kinase (AMPK) is a serine/threonine protein kinase that senses the energy status of the muscle cell based on the AMP:ATP and creatine:phosphocreatine ratios (Hardie et al., 1998). As would therefore be expected muscle AMPK activity has been shown consistently to increase during muscle contraction and exercise (Rose and Richter, 2005, Jorgensen et al., 2006). Furthermore pharmacological activation of AMPK through the AMP analogue AICAR has been shown to increase muscle glucose transport (Jorgensen et al., 2006). Therefore it seems logical for AMPK to have a role in contraction mediated GLUT4 translocation. However studies investigating the role of AMPK in contraction-mediated glucose uptake via AMPK knockout, inhibition and overexpression of dominant negative

forms have proved inconclusive (Rose and Richter, 2005). In incubated mouse muscle, knockout, over-expression of a dominant-negative isoform or inhibition of α1 or α2 catalytic or γ3 regulatory subunits of AMPK does not reduce contraction-mediated glucose uptake following electrical stimulation in comparison to wild-type mice (Barnes et al., 2004, Jorgensen et al., 2004, Merry et al., 2010). In addition, in vivo glucose uptake during electrically-stimulated contraction in mice expressing inactive α1 and α2 AMPK subunits was not different to wild-type mice (Fujii et al., 2004). In contrast Mu *et al.* (2001) demonstrated a 30 – 40 % reduction in contraction-mediated glucose transport in fast and slow twitch muscles of mice overexpressing a dominant negative form of AMPK (Mu et al., 2001). Subsequently however it was suggested that the reduction in glucose transport was attributable to impaired force development in these mice (Mu et al., 2003). AMPK may have a different role in different fibre types as dissociation between AMPK activity and glucose uptake has been observed in slow twitch, but not fast twitch muscle groups (Derave et al., 2000). In summary, AMPK is activated during muscle contraction, however a consensus has not been reached on the importance of AMPK activation in GLUT4 translocation and glucose uptake. Certainly alternative mechanisms appear able to maintain contraction-mediated glucose uptake in the absence of AMPK activity.

1.6.3. Role of ATP

Skeletal muscle releases ATP during contractile activity (Li et al., 2003). Incubation of primary myotubes in ATP resulted in increases in glucose uptake and GLUT4 translocation to the cell surface (Osorio-Fuentealba et al., 2013). Data suggest that ATP-induced increases in glucose uptake occur through purinergic receptor signalling to Akt, PI3K and ultimately AS160 phosphorylation to induce GLUT4 translocation (Osorio-Fuentealba et al., 2013). Incubation of primary myotubes in ATP led to Akt and AS160 phosphorylation and

furthermore inhibition of PI3K or Akt reduced the ATP-mediated increases in glucose uptake (Osorio-Fuentealba et al., 2013). Rab8A is likely to be involved as Rab8A knockdown in primary myotubes reduced ATP-mediated GLUT4 translocation (Osorio-Fuentealba et al., 2013).

1.6.4. Role of NO

As well as its role in endothelial cells, NO is produced in muscle fibres by nNOS (McConell et al., 2012). nNOS activity increases during exercise in humans (Linden et al., 2011). Inhibition of nNOS via infusion of the nNOS inhibitor N^G-monomethyl-$_L$-arginine ($_L$-NMMA) into the femoral artery during exercise in humans reduced the exercise-induced increases in glucose uptake by approximately 30% with no effect on blood flow (Bradley et al., 1999). This supports a role for NO in the signalling behind contraction-mediated increases in glucose uptake. Potential mechanisms include signalling via increased cGMP production and protein kinase G (PKG) activation and NO-induced posttranslational modification of signalling proteins such as Akt (McConell et al., 2012)

1.6.5. Intracellular signalling to GLUT4 plasma membrane insertion

As with insulin-mediated glucose uptake, there must be mechanisms to link intracellular contraction signalling pathways with GLUT4 insertion into the PM to allow contraction-mediated glucose uptake. TBC1D1 is a protein similar to AS160 with a RabGAP domain that is inhibited following stimulation to promote GTP loading of Rab proteins and GLUT4 translocation to the cell surface (Roach et al., 2007). Phosphorylated Ser237 and Thr590 are 14-3-3 binding sites on TBC1D1, which is confirmed through lack of 14-3-3 binding on the TBC1D1 double mutant (Chen et al., 2008). Stimulation of L6 cells with insulin alone induced Thr590 phosphorylation, but 14-3-3 binding did not occur. In contrast activation of

AMPK with phenformin induced Ser237 phosphorylation and 14-3-3 binding (Chen et al., 2008). In human skeletal muscle 30 s – 20 min 'all out' exercise induced 70 – 230 % increases in TBC1D1 Ser237 phosphorylation and concomitant 60 – 250 % increases in 14-3-3 binding capacity (Frosig et al., 2010). In rat epitrochlearis muscle inhibition of PI3K with wortmannin prevented contraction-stimulated phosphorylation of AS160 while TBC1D1 phosphorylation and glucose uptake were unaffected. In contrast AMPK inhibition reduced TBC1D1 phosphorylation and glucose uptake, while AS160 phosphorylation was unaffected (Funai and Cartee, 2009). Furthermore mutation of TBC1D1 phosphorylation sites in mouse skeletal muscle impairs contraction stimulated glucose transport but does not affect insulin stimulated glucose transport (An et al., 2010). These data implicate phosphorylation of TBC1D1, potentially by AMPK, in the regulation of contraction-mediated skeletal muscle glucose uptake.

Both insulin- and contraction-mediated glucose uptake into skeletal muscle require GLUT4 insertion into the PM therefore there may be convergence of the signalling pathways at this distal step in GLUT4 translocation. Proximal insulin signalling mechanisms, from IR to PI3K, are not involved in contraction mediated glucose uptake (Treadway et al., 1989, Goodyear et al., 1995, Wojtaszewski et al., 1999, Rose and Richter, 2005). Most, but not all, studies have shown increased Akt activity during contraction (Rose and Richter, 2005). Akt phosphorylation of AS160 increases during contraction in rodent skeletal muscle, but this is unlikely to be linked directly to contraction-mediated glucose uptake (Bruss et al., 2005). Interestingly AMPK has also been shown to phosphorylate AS160 in response to AICAR and contraction in mouse skeletal muscle (Kramer et al., 2006a) and more recently a novel AMPK phosphorylation site, Serine 711, has been identified on AS160 (Treebak et al., 2010). Furthermore in the AS160-4P mutant contraction- as well as insulin-mediated glucose uptake

is inhibited (Kramer et al., 2006b). In addition, mutation of the calmodulin binding domain of AS160 inhibits contraction- but not insulin-mediated glucose uptake (Kramer et al., 2007). Taken together these data suggest that AS160 may act as a point of convergence in both the insulin and contraction signalling pathways to glucose uptake (Rockl et al., 2008).

In 3T3-L1 adipocytes AS160 and TBC1D1 appear to have identical Rab protein specificity (Roach et al., 2007), however as stated previously the Rab proteins involved in AS160 regulation of glucose uptake in adipocytes and skeletal muscle are different (Sun et al., 2010) therefore in skeletal muscle it is not known which Rab proteins are targeted by TBC1D1. In skeletal muscle AS160 has specificity for RAB8A and Rab13 (Sun et al., 2010) and potentially Rab14 (Ishikura et al., 2007, Ishikura and Klip, 2008), therefore TBC1D1 specificity in skeletal muscle may be the same.

SNARE proteins are also required for GLUT4 docking and fusion at the PM in contraction-mediated GLUT4 translocation (Rose et al., 2009). The t SNAREs syntaxin 4 and SNAP23 located at the PM are likely to be required for contraction-, as well as insulin-mediated GLUT4 docking and fusion (Schwenk et al., 2010). There is no consensus regarding which v SNARE is responsible for contraction-mediated GSV fusion at the PM (Richter and Hargreaves, 2013). VAMP2 is the isoform more commonly reported to be responsible for insulin-mediated GSV fusion (Bryant et al., 2002). VAMP2, VAMP5 and VAMP7, but not VAMP3, have been shown to translocate to the PM in rat skeletal muscle in response to contraction (Rose et al., 2009). In addition VAMP3 null mice display normal contraction-mediated glucose uptake (Yang et al., 2001). However contrasting evidence suggests VAMP3 is involved in contraction-mediated GLUT4 translocation based on the observation that VAMP3 knockdown abolished glucose uptake increases induced by AMPK activation

(Schwenk et al., 2010). Further research is required to confirm the identity of the v-SNARE responsible for contraction mediated GLUT4 PM fusion.

1.7. Defects in obesity, insulin resistance and type 2 diabetes

Skeletal muscle insulin resistance is associated with obesity and precedes the development of type 2 diabetes. Using the hyperinsulinaemic-euglycaemic clamp technique it has been shown that whole body insulin-stimulated glucose metabolism is reduced by 38 % in T2D patients (DeFronzo et al., 1985). Furthermore insulin-stimulated leg glucose uptake was reduced by 45 % demonstrating that the peripheral tissues, and more specifically skeletal muscle, are the main sites of insulin resistance (DeFronzo et al., 1985). Interestingly contraction-mediated glucose uptake is unaffected in insulin resistant muscle, with evidence even demonstrating higher contraction-mediated leg glucose uptake in T2D patients compared to controls (Minuk et al., 1981, Martin et al., 1995). The higher glucose uptake rates may be the result of the higher basal plasma glucose levels (DeFronzo et al., 1989).

Western blot studies have shown that total GLUT4 protein content in skeletal muscle is unchanged in obesity and the early stages of T2D (Handberg et al., 1990, Pedersen et al., 1990), while GLUT4 protein content is reduced in later stages of T2D that require insulin treatment (Kampmann et al., 2011). As muscle GLUT4 protein content does not change in the early stages of T2D decreases in this variable do not appear to contribute to the initial development of insulin resistance. GLUT4 translocation, on the other hand, is reduced following hyperinsulinaemic-euglycaemic clamp in skeletal muscle from T2D patients compared to normal glucose tolerant controls (Zierath et al., 1996, Garvey et al., 1998). Interestingly contraction-mediated GLUT4 translocation, following 45-60 min cycling

exercise, measured with the PM fractionation method is preserved in obesity and T2D (Kennedy et al., 1999).

Regular exercise has long been recommended as a method to improve glycaemic control in T2D patients (American Diabetes Association, 1990) and the role of exercise in improving insulin sensitivity will be discussed in section 1.8 of this chapter. In the current section the main molecular mechanisms proposed to contribute to the development of insulin resistance and T2D will be considered. A representation of the main mechanisms that contribute to the development of insulin resistance and T2D is given in Fig. 1.3.

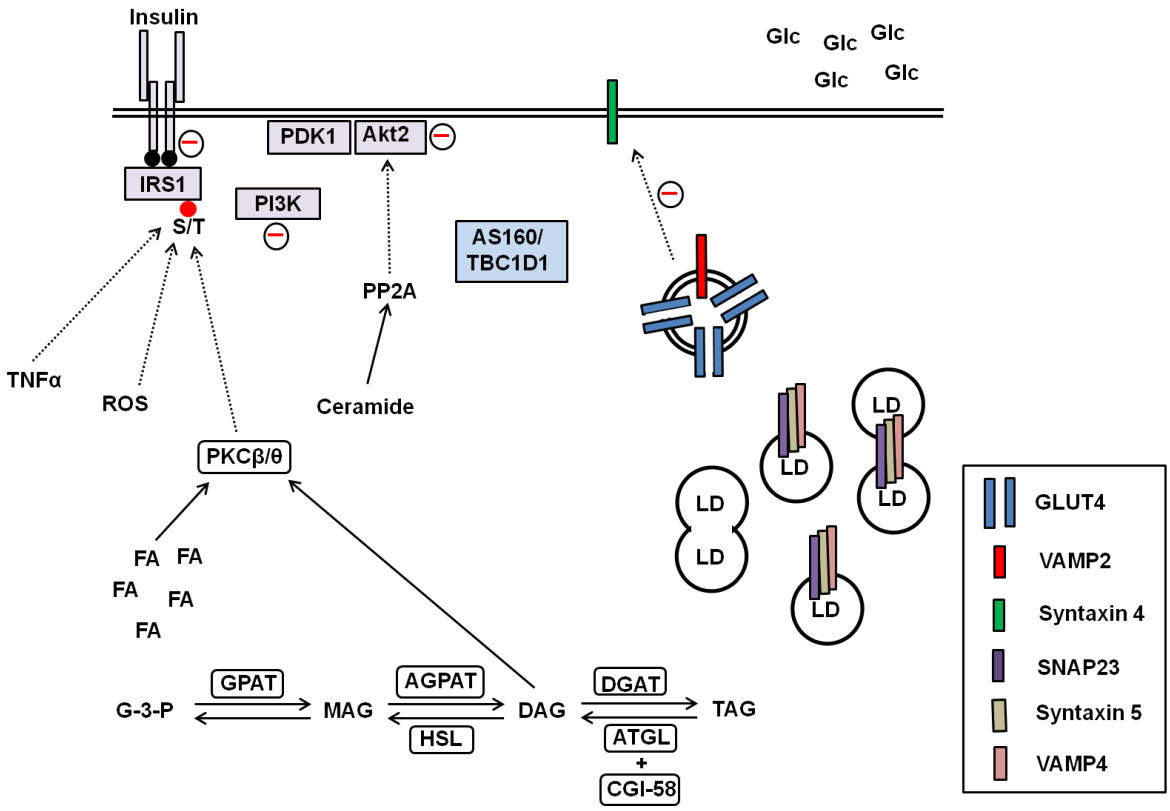

Fig. 1.3. *Mechanisms of skeletal muscle insulin resistance. The high abundance of fatty acids in skeletal muscle of obese individuals cannot be compensated for by TAG synthesis and or β-oxidation and therefore leads to the accumulation of FA metabolites, such as LCA-CoAs, DAGs and ceramides. These FA metabolites have been proposed to inhibit the proximal insulin signalling cascade resulting in reduced translocation of GLUT4 to the PM. Furthermore accumulation of LDs increases the demand for SNAP23 in LD fusion, therefore reducing SNAP23 availability at the PM for GSV fusion. As a result glucose uptake in response to insulin is reduced in insulin resistant individuals. This figure is based on the following references (Shulman, 2000, Shaw et al., 2010, Sollner, 2007).*

1.7.1. Altered lipid handling

Studies infusing intralipid/heparin into healthy individuals to increase the concentration of plasma fatty acids (FA) have demonstrated lipid-induced impairments in glucose uptake and insulin resistance in previously insulin sensitive individuals (Boden et al., 1994, Boden et al., 1991, Roden et al., 1999, Roden et al., 1996).

Fat is stored in the body as triacylglycerol (TAG) which is composed of a glycerol-3-phosphate backbone and three esterified long chain fatty acid side chains (Coleman and Lee, 2004). TAG is stored in lipid droplets (LDs); with the majority of TAG in the human body found in subcutaneous or visceral adipose tissue cells. Smaller TAG depots, also contained in smaller LDs, are found in most tissues. In muscle fibres these are known as intramuscular triacylglycerol (IMTG) (Shaw et al., 2010). Type I muscle fibres have a higher IMTG content than type II muscle fibres (Malenfant et al., 2001, van Loon et al., 2003, van Loon, 2004a, Shaw et al., 2009, Shepherd et al., 2013). IMTG provides a FA source that can be utilised during periods of high energy demand, such as during exercise in physically active individuals (Shaw et al., 2009). An increased IMTG content is seen in obese individuals and in patients with T2D (Phillips et al., 1996a, Goodpaster et al., 2001). In these groups there is a strong inverse association between IMTG content of skeletal muscle and insulin sensitivity (Phillips et al., 1996a, Pan et al., 1997). It, therefore, was initially postulated that elevated IMTG concentrations were mechanistically linked to the development of insulin resistance. However, a paradox has emerged whereby highly trained and highly insulin sensitive athletes have at least equal, if not higher IMTG content as obese and T2D individuals (Goodpaster et al., 2001, van Loon et al., 2004). This has led to the theory that the high concentration of intracellular FA metabolites, such as long-chain fatty acyl-CoAs (LCFA-CoAs), diacylglycerols (DAGs) and ceramides, that are seen in muscle fibres of obese and T2D

individuals lead to insulin resistance rather than the total IMTG content per se (Shaw et al., 2010). Increased LCFA-CoAs, DAGs and ceramide have been reported in skeletal muscle of obese and T2D humans (Pan et al., 1997, Goodpaster et al., 2001, Bandyopadhyay et al., 2006). More recent work, however, has shown that a similar paradox also applies to the total skeletal muscle DAG content with twofold higher DAG concentrations in endurance trained athletes compared to obese sedentary individuals (Amati et al., 2011). Amati *et al.* (2011) further showed that DAG species containing two saturated or only one unsaturated FA had a higher content in endurance trained compared to obese sedentary individuals, while DAG species that contain two unsaturated FAs had a higher content in the obese individuals (Amati et al., 2011). This led to the suggestion that FA composition of DAG is different between obese and endurance trained athletes, therefore suggesting that different DAG species impact insulin sensitivity differently (Amati et al., 2011). In addition Amati *et al.* (2011) showed that ceramide content was higher in obese individuals compared to endurance trained athletes (Amati et al., 2011).

The balance between IMTG synthesis, lipolysis and fatty acid oxidation determines not only the IMTG content, but also the concentration of FA metabolites (Shaw et al., 2010). Suggestions have also been made that high turnover rates of the IMTG pool are mechanistically linked to reductions in the intracellular concentration of FA metabolites (van Loon, 2004b, Moro et al., 2008). In trained individuals up to 70 % reductions in IMTG content in type I muscle fibres are observed during an endurance exercise bout of 2 – 3 h duration, in order to provide fatty acids for β-oxidation (van Loon et al., 2003, De Bock et al., 2007, Stellingwerff et al., 2007a, Stellingwerff et al., 2007b). In contrast fatty acid oxidation during exercise is low in lean sedentary, obese and obese T2D individuals (Blaak et al., 2000,

Schrauwen et al., 2002), therefore leading to increased levels of FA metabolites and insulin resistance.

The balance between the activity and content of the enzymes involved in IMTG breakdown and synthesis has a great impact on the intracellular concentration of FA metabolites and therefore on insulin sensitivity (Shaw et al., 2010). The initial step in IMTG hydrolysis is the liberation of the first FACoA by the enzyme adipose triglyceride lipase (ATGL) and its coactivator CGI-58. This generates DAG, which in turn is broken down to monoacylglycerol (MAG) and FACoA by the enzyme hormone sensitive lipase (HSL) (Haemmerle et al., 2002). Endurance training has been shown to increase ATGL content, but not HSL content therefore indicating that there may be differences in ATGL, but not HSL, between trained and untrained individuals (Alsted et al., 2009, Shaw et al., 2010). However in the muscle of obese insulin resistant individuals, reduced HSL content has been reported (Blaak et al., 2004). Therefore reductions in ATGL and HSL may explain the reduced utilisation of fatty acids during exercise in T2D (van Loon et al., 2005). Furthermore a high TAG/DAG hydrolysis ratio has been observed in obesity which would lead to DAG accumulation, potential inhibition of the insulin signalling cascade, and reductions in insulin sensitivity (Moro et al., 2009).

Alternatively, incorporation of intracellular fatty acids into inert IMTG stored within LDs appears to be a mechanism to protect muscle insulin sensitivity. The sequential addition of 3 fatty acids to the glycerol backbone is catalysed by 3 distinct enzymes. The addition of the first fatty acid to the glycerol-3-phosphate backbone is catalysed by glycerol-3-phosphate acyltransferase (GPAT), the second fatty acid is added by the enzyme acylglycerol-3-phosphate acyltransferase (AGPAT) and the final fatty acid by the enzyme diacylglycerol acyltransferase (DGAT) (Takeuchi and Reue, 2009). Overexpression of DGAT1 in rats has

been shown to increase TAG synthesis and protects insulin sensitivity even in the presence of increased levels of plasma fatty acids (Liu et al., 2009a, Roorda et al., 2005, Timmers et al., 2011). Schenk and Horowitz (2007) demonstrated the protective effect of a single bout of endurance exercise against FA-induced insulin resistance and showed concomitant increases in DGAT1 and mitochondrial GPAT expression (Schenk and Horowitz, 2007). Expression of the FA transporter (FAT/CD36) is increased in skeletal muscle in obesity and T2D (Bonen et al., 2004) and has been shown to be increased in the PM fraction of muscle in obese compared to non-obese women (Li et al., 2011). Therefore it has been suggested that increased fatty acid uptake into muscle cells in obesity is not compensated for by increased IMTG synthesis, therefore leading to accumulation of intracellular lipid metabolites which impact on insulin sensitivity (Bonen et al., 2004). This is supported by data showing there are no differences in skeletal muscle content of triglyceride synthesis enzymes between lean and obese women (Thrush et al., 2009, Li et al., 2011). Furthermore IMTG fractional synthetic rate is reduced in pre-diabetic men, compared to those with normal glucose tolerance (Perreault et al., 2010), which may also contribute to the accumulation of lipid metabolites, rather than storage as IMTG, in skeletal muscle of insulin resistant individuals.

1.7.2. Proximal insulin signalling defects.

Intracellular FA metabolites such as LCA-CoAs, DAGs and ceramides have been shown to interfere with proximal insulin signalling pathway events (Hulver and Dohm, 2004). IR autophorylation, IR tyrosine kinase activity, IRS1 tyrosine phosphorylation and PI3K and Akt activation have all been shown to be reduced in human skeletal muscle in obesity and insulin resistance (Caro et al., 1987, Itani et al., 2000, Goodyear et al., 1995). Serine or threonine, as opposed to tyrosine, phosphorylation is proposed to be responsible for these reductions (Hulver and Dohm, 2004). Protein kinase C (PKC) is a serine kinase which is activated by

LCFA-CoA and DAG (Shulman, 2000). Lipid/heparin infusion in rats resulted in reduced insulin-stimulated IRS1 tyrosine phosphorylation, which was associated with increased PKCθ activation (Griffin et al., 1999). PKCθ phosphorylates serine 312, 636 and 1101 on IRS1, thereby preventing IRS1 tyrosine phosphorylation and the propagation of downstream insulin signalling events, which ultimately reduces GLUT4 translocation and glucose uptake (Schenk and Horowitz, 2007). In addition the PKCβ isoform has been shown to phosphorylate and inactivate the IR (Bossenmaier et al., 1997). In support of this the IR from insulin resistant muscle cells has been shown to exhibit increased serine/threonine phosphorylation compared to insulin sensitive muscle cells (Hulver and Dohm, 2004). Ceramides also activate protein phosphatase 2A (PP2A) which dephosphorylates Akt, thereby preventing downstream signalling events and again reducing GLUT4 translocation and glucose uptake (Hulver and Dohm, 2004). AS160 protein content is not altered in T2D (Vind et al., 2011), while insulin-stimulated phosphorylation of AS160 at S318, S588 and S751 is impaired in T2D patients compared to controls (Vind et al., 2011). In contrast lipid infusion does not alter insulin-mediated AS160 phosphorylation (Hoeg et al., 2011, Storgaard et al., 2004).

1.7.3. The role of inflammation

Chronic low levels of inflammation have been associated with the development of skeletal muscle insulin resistance (Wei et al., 2008). Increased inflammatory cells and circulating levels of inflammatory cytokines such as TNFα, IL-1 and IL-6 are associated with insulin resistance in skeletal muscle in patients with T2D (Wei et al., 2008). TNFα activates JNK, NFkB and MAPK pathways and reduces insulin signal transduction by reducing IRS1 tyrosine phosphorylation (del Aguila et al., 1999) and increasing serine phosphorylation (Bouzakri and Zierath, 2007) and diminishing Akt activation (de Alvaro et al., 2004).

1.7.4. The role of oxidative stress and mitochondrial function

Reactive oxygen species (ROS) play important physiological roles, however excess ROS production in muscle mitochondria of obese individuals leads to oxidative stress (Samocha-Bonet et al., 2012). ROS are elevated in obesity and T2D and levels are inversely correlated with measures of insulin sensitivity in patients with T2D (Nourooz-Zadeh et al., 1997). Furthermore antioxidant treatment of insulin resistant animals improves insulin sensitivity (Blendea et al., 2005, Henriksen, 2006). ROS activate intracellular signalling pathways such as those involving MAPK, JAK/STAT and JNK activation which may subsequently interfere with the insulin signalling pathway (Wei et al., 2008). In addition ROS lead to increased expression of inflammatory cytokines such as TNFα which further exacerbates inflammation-induced insulin resistance (Nathan, 2003).

Lowell and Shulman (2005) proposed the hypothesis that skeletal muscle insulin resistance occurs as a consequence of mitochondrial dysfunction; including a reduction in ATP turnover and capacity to oxidise fatty acids (Lowell and Shulman, 2005). This hypothesis was supported by two publications from the Shulman group (Petersen et al., 2004 and Petersen et al., 2005), which used ^{31}P-magnetic resonance spectroscopy (MRS) methodology to show that both basal and insulin-stimulated ATP turnover rates in human skeletal muscle *in vivo* were lower in the muscle of insulin-resistant offspring of patients with type 2 diabetes compared to a control group with parents that did not have type 2 diabetes. It was therefore suggested that in individuals with a predisposition to the development of type 2 diabetes a reduction in mitochondrial ATP production was an early event in the development of insulin resistance (Petersen et al., 2004). This mitochondrial dysfunction was also proposed to reduce the rate of β-oxidation, therefore explaining the intramuscular accumulation of fatty acid metabolites

(fatty acyl CoA and diacylglyerol) that disrupt insulin signalling (Lowell and Shulman, 2005), as described in section 1.7.2 of this thesis.

However, the existence of mitochondrial dysfunction has since been disputed (Wagenmakers, 2005, Dela and Helge, 2013). In an editorial comment on the Petersen et al. (2005) publication, Wagenmakers (2005) questioned the evidence of a mitochondrial impairment based on alternative explanations for the observed reduction in ATP turnover in skeletal muscle both in the basal and insulin stimulated state (Wagenmakers, 2005). In addition, later studies measuring mitochondrial function concluded that there are no intrinsic defects in mitochondria in insulin resistant states (Boushel et al., 2007, Larsen et al., 2009, Rabol et al., 2009, Gnaiger et al., 2009, Ara et al., 2011). The O_2 flux capacity, measured by high-resolution respirometry in saponin-permeabilised muscle fibres from the quadriceps, was lower in T2D patients compared to age-matched controls. However when normalised for mitochondrial content or citrate synthase activity there were no differences in oxidative phosphorylation or electron transport capacity between the groups (Boushel et al., 2007). This suggests that lower ATP production rate is due to a decrease in the content of mitochondria, rather than a functional impairment. The reduction in mitochondrial content is likely a result of a sedentary lifestyle which is adopted by individuals that can go on to develop insulin resistance and type 2 diabetes later in life (Wagenmakers, 2005). Accordingly, as discussed by Goodpaster (2013) and Holloszy (2013), there is currently no consensus on whether there is simply an association between mitochondrial content and insulin resistance (Hollozsy, 2013) or whether the relationship is causal (Goodpaster, 2013).

1.7.5. Distal insulin signalling defects

As described above there is much evidence that implicates proximal insulin signalling defects in the development of insulin resistance. However there are also studies in which 2-6 h of

intralipid infusion in rats and lean and obese humans did not affect IRS1 tyrosine phorphorylation, PI3K activity, Akt or AS160 phosphorylation (Hoy et al., 2009, Hoy et al., 2007, Tsintzas et al., 2007, Storgaard et al., 2004, Hoeg et al., 2011). This suggests that proximal insulin signalling defects may not be responsible for reduced insulin-mediated glucose uptake in insulin resistance and, therefore, the more distal stages of the insulin signalling pathway such as in the GLUT4 translocation machinery and GLUT4 docking and fusion at the PM should also be considered as sites where insulin resistance may occur.

A recently suggested distal candidate for defects in the development of insulin resistance is Rac1. Rac1 muscle-specific knockout leads to decreased insulin-stimulated glucose transport in ex vivo mouse muscles (Sylow et al., 2013a). Mice fed a high fat diet, humans undergoing intralipid infusion and obese and T2D human patients display reduced insulin-mediated PAK phosphorylation, suggesting an impairment in the Rac1signal to PAK, which was associated with reduced insulin-mediated glucose uptake (Sylow et al., 2013a). As the Rac1-PAK pathway is thought to lead to cortical actin remodelling (JeBailey et al., 2004), Sylow *et al.* (2013) suggest that impairments in Rac1/PAK signalling in obesity and T2D limit insulin-mediated glucose uptake through impaired cortical actin remodelling therefore preventing GLUT4 translocation (Sylow et al., 2013a).

SNAP23, one of the t-SNAREs required for GSV fusion with the PM, is also required for lipid droplet fusion (Bostrom et al., 2007). One theory, known as the SNARE highjacking hypothesis, proposes that in muscle with a high concentration of IMTGs there is an increased requirement for SNAP23 in lipid droplet fusion, which may reduce the availability of SNAP23 at the PM for GSV fusion (Sollner, 2007). This SNAP23 highjacking hypothesis provides an alternative explanation for reduced insulin-mediated GLUT4 translocation and

glucose uptake in obesity and T2D. In support of the highjacking hypothesis, treatment of cardiomyocytes with oleic acid caused cellular lipid droplet expansion and insulin resistance and led to redistribution of SNAP23 from the PM to intracellular regions as well as increased SNAP23 association with LD (Bostrom et al., 2007). Furthermore SNAP23 was redistributed away from the PM to cytosolic membrane compartments in human skeletal muscle from patients with T2D in which lipid accumulation was apparent (Bostrom et al., 2010). In addition, the total SNAP23 protein content was shown to be increased in skeletal muscle from T2D patients compared to healthy insulin-sensitive controls (Bostrom et al., 2010).

More research will be required to further investigate the role of Rac1 and SNARE highjacking in lipid induced insulin resistance and their relative contribution to insulin resistance in comparison to the previously proposed proximal defects in the insulin signalling cascade. However, these alternative mechanisms will not be investigated in this thesis.

1.7.6. Impaired substrate delivery

Glucose and insulin delivery to skeletal muscle is vital to insulin-mediated glucose uptake but is also a key impairment in obesity and type 2 diabetes which may underlie insulin resistance in these conditions. Studies in obese Zucker rats (OZR) have shown that increases in skeletal muscle microvascular blood volume (MBV), which occur early in a hyperinsulinaemic-euglycaemic clamp in lean Zucker rats (Steinberg et al., 1994), may be defective. Furthermore capillary PSA available for insulin and glucose delivery is reduced in OZR due to reductions in insulin-mediated recruitment of the microvasculature (Gudbjornsdottir et al., 2003, Gudbjornsdottir et al., 2005). Additionally obesity and T2D have been associated with reduced NO production and reduced capillary density, which are suggested to contribute to skeletal muscle insulin resistance (Wagenmakers et al., 2006, Barrett et al., 2009, Barrett et

al., 2011). Furthermore insulin-mediated skeletal muscle microvascular recruitment has been shown to be reduced in obese compared to lean humans (Clerk et al., 2002, Clerk et al., 2006, Keske et al., 2009). These impairments in microvascular recruitment are likely to contribute to insulin resistance, as the surface area available for insulin and glucose delivery to the skeletal muscle will be reduced, thereby reducing insulin-mediated glucose uptake, but are beyond the scope of this thesis.

1.8. Exercise as a tool to improve insulin sensitivity

Exercise has long been recommended as a tool to improve glycaemic control and to prevent or delay the onset of T2D and insulin resistance (American Diabetes Association, 1990). Broadly speaking there are two aspects to the benefits of exercise on glucose homeostasis; firstly the effect of an acute bout of exercise to enhance glucose uptake and improve post exercise insulin sensitivity, and secondly the molecular adaptation to include changes in enzyme content and activities that is the result of chronic exercise training which coincide with a greater muscle insulin sensitivity (Rockl et al., 2008).

1.8.1. Effect of an acute exercise bout on glucose homeostasis

As mentioned previously contraction-mediated glucose uptake and GLUT4 translocation are maintained in obese and T2D patients with glucose uptake in fact higher in T2D patients compared to controls (Minuk et al., 1981, Martin et al., 1995, Kennedy et al., 1999), which provides a mechanism to reduce plasma glucose concentrations in such conditions. In support of this, 45 min of exercise at 70 % of maximum workload normalised plasma glucose concentration in T2D patients (Musi et al., 2001). An acute exercise bout can improve insulin sensitivity for up to 48 h, making acute exercise an effective treatment to improve insulin

sensitivity in insulin resistant and T2D individuals (Wojtaszewski and Richter, 2006). One hour cycling exercise increased insulin-mediated glucose uptake during a hyperinsulinaemic-euglcyaemic clamp in healthy, untrained humans immediately after and 48 h after exercise (Mikines et al., 1988). In addition 1 h one legged knee extensor exercise increased insulin-mediated glucose uptake during hyperinsulinaemic-euglycaemic clamp 4 h after exercise in healthy humans (Richter et al., 1989). GLUT4 mRNA concentration in skeletal muscle increases within 3 h after a single exercise bout in human muscle (Neufer and Dohm, 1993, Ren et al., 1994) and increases in GLUT4 protein content can be seen in as little as 16-24 h (Kraniou et al., 2006, Ren et al., 1994). Improved insulin sensitivity after an acute exercise bout has been proposed to be important in the repletion of skeletal muscle glycogen stores post exercise with studies showing an association between the amount of glycogen depletion and the observed increase in insulin sensitivity (Bogardus et al., 1983). Muscle insulin-mediated glucose uptake 4 h after an exercise bout is also primarily directed to glycogen synthesis (Richter et al., 1989) with a large activation of glycogen synthase occurring in the exercised and therefore glycogen depleted leg (Wojtaszewski et al., 2000). Insulin-stimulated GLUT4 translocation was shown to be increased 3.5 h after an exercise bout compared to after a rest period (Hansen et al., 1998a). The increased GLUT4 translocation does not appear to result from increases in proximal insulin signalling from IR-Akt (Wojtaszewski et al., 1997, Wojtaszewski et al., 2000). Research is currently investigating whether intracellular contraction-induced signals converge with the insulin signalling pathway at AS160 to mediate post exercise improvements in insulin sensitivity. Studies in rat and human muscle have shown increased AS160 phosphorylation post exercise which is maintained for 3-4 h in association with post exercise increases in insulin sensitivity (Arias et al., 2007, Howlett et al., 2008, Funai and Cartee, 2009, Treebak et al., 2009, Treebak et al., 2010). Furthermore

following insulin stimulation with hyperinsulinaemic-euglycaemic clamp AS160 phosphorylation at residues S318, S341 and S751 has been shown to be higher 3-4 h following a prior bout of exercise compared to a resting control (Arias et al., 2007, Treebak et al., 2009). This is not thought to be due to increased sensitivity of AS160 to insulin but rather a higher AS160 phosphorylation at baseline due to exercise-induced AS160 phosphorylation on these sites (Arias et al., 2007). Therefore part of the improved glycaemic control achieved through exercise may be due to the cumulative effects of acute exercise bouts which firstly reduce plasma glucose concentration through contraction-mediated glucose uptake and secondly improve insulin sensitivity of the working muscle up to 48 h after the exercise bout (Schneider et al., 1990).

1.8.2. Exercise training adaptations to improve insulin sensitivity

Endurance exercise training (ET) is known to increase whole body insulin sensitivity in young and old (Hughes et al., 1993, Dela et al., 1996, Cox et al., 1999), trained and sedentary (Houmard et al., 1991, Houmard et al., 1993), and obese diabetic and non-diabetic subjects (Vind et al., 2011). Similarly sprint interval training (SIT), a time efficient mode of exercise, has also been shown to increase whole body insulin sensitivity in young sedentary subjects (Babraj et al., 2009, Richards et al., 2010, Shepherd et al., 2013). Furthermore increased insulin-stimulated skeletal muscle glucose uptake has been demonstrated following ET in healthy, T2D and aging participant groups (Dela et al., 1992, Dela et al., 1995, Dela et al., 1996, Frosig et al., 2007).

Exercise can improve the content and fatty acid composition of intramuscular lipids (Bergman et al., 2010, Schenk and Horowitz, 2007). A single bout of endurance exercise has been shown to prevent FA acid induced insulin resistance during a lipid infusion on the following day (Schenk and Horowitz, 2007). This was accompanied by increased IMTG content,

increased expression of enzymes involved in triglyceride synthesis and reduced accumulation of FA metabolites in comparison to no prior exercise bout (Schenk and Horowitz, 2007). This is likely due to the high IMTG breakdown that occurs during exercise in athletes (van Loon et al., 2003, De Bock et al., 2007, Stellingwerff et al., 2007a, Stellingwerff et al., 2007b) allowing rapid repletion of the IMTG stores in conditions of high FA, therefore keeping the concentration of plasma TG and muscle FA metabolites low and insulin sensitivity high. A study comparing highly endurance trained athletes to sedentary controls has demonstrated endurance trained athletes have a higher IMTG fractional synthetic rate (Bergman et al., 2010). The increased capacity to store FA as IMTG may serve as a training adaptation in athletes (van Loon, 2004a, van Loon and Goodpaster, 2006). As expected the muscle cells of athletes contained more IMTG, while perhaps more surprisingly there were no differences in DAG content between the two groups (Bergman et al., 2010). Percentage DAG saturation was however lower in endurance trained athletes, and furthermore percentage DAG saturation correlated significantly with insulin sensitivity (Bergman et al., 2010). However this data conflicts with that of Amati *et al.* (2011) who showed that DAG containing two unsaturated FAs was increased in obese sedentary compared to endurance trained athletes (Amati et al., 2011). Taken together, the above data demonstrate that training status can influence lipid synthesis and lipid type and FA-composition in skeletal muscle ultimately providing multiple mechanisms to manipulate lipid induced insulin resistance.

The reported adaptations in the insulin signalling pathway intermediates that result from endurance training among others involve increases in Akt protein content but no change in protein content of IR, IRS1 or the p85 subunit of PI3K (Frosig et al., 2007). There was also no change in syntaxin 4, SNAP23 or Munc18c protein content (Frosig et al., 2007). Insulin-stimulated Akt phosphorylation and IRS1-associated PI3K activity were not affected by

training (Frosig et al., 2007). AS160 phosphorylation by Akt was increased following training, both in the basal and insulin-stimulated states (Frosig et al., 2007). Another study demonstrated increased AS160 protein content following training in T2D patients (Vind et al., 2011). Training also increased insulin-stimulated phosphorylation of AS160 at S341 and T642 in T2D patients. Before training insulin-stimulated increases in AS160 phosphorylation at S318, S588 and S751 were lower in T2D compared to controls. This difference was normalised by endurance training (Vind et al., 2011).

Increased mitochondrial oxidative capacity, in part through increases in mitochondrial protein content, is a major training adaptation which improves lipid and glucose fuel handling (Holloszy, 1967, Oscai and Holloszy, 1971, Rockl et al., 2008). Six weeks ET in mice increases mitochondrial protein content and enzyme activity (Rockl et al., 2008). Both ET and SIT increase mitochondrial enzyme content and activity over 2-6 week training periods (Gibala et al., 2006, Little et al., 2010, Hood et al., 2011, Shepherd et al., 2013). Increased mitochondrial protein content can improve glucose and lipid metabolism and reduce the ROS production that occurs as a result of mitochondrial dysfuction in insulin resistance, thereby reducing intracellular FA metabolites and improving insulin sensitivity (Kim et al., 2008).

Increased muscle GLUT4 content is associated with improved insulin action, as demonstrated in animal models overexpressing GLUT4 in skeletal muscle (Ren et al., 1995, Hansen et al., 1995, Leturque et al., 1996). Western blot analysis has also shown that GLUT4 protein content of muscle cells is increased robustly following both traditional ET (Houmard et al., 1991, Houmard et al., 1993, Hughes et al., 1993, Houmard et al., 1995, Dela et al., 1996, Phillips et al., 1996b, Cox et al., 1999, Daugaard et al., 2000, Vind et al., 2011) and SIT (Burgomaster et al., 2007, Little et al., 2010, Hood et al., 2011). Daugaard *et al.* (2000) reported that increases in total GLUT4 protein content following endurance exercise were

driven by increased GLUT4 content in type I muscle (Daugaard et al., 2000), whereas following more strength based exercise (more similar to SIT) Stuart *et al.* (2010) reported that increases in GLUT4 content occurred only in type II muscle fibres (Stuart et al., 2010).

Consecutive bouts of exercise increase GLUT4 content until a steady state is reached which is maintained for the duration of training (Ojuka et al., 2012). GLUT4 gene transcription is controlled by the transcription factors myocyte enhancer factor (MEF) 2, which binds the GLUT4 promoter as a heterodimer MEF2A/D and GLUT4 enhancer factor (GEF), an as yet unidentified histone acetyltransferase (HAT), and the histone deacetylase HDAC5 (Ojuka et al., 2012). A single bout of exercise increases MEF2A/D and GEF interaction with the GLUT4 gene in human skeletal muscle (McGee et al., 2006). Acetylation of histones associated with the GLUT4 gene is required for GLUT4 gene transcription, therefore HDAC5 must be inhibited (Ojuka et al., 2012). This is thought to be achieved through the phosphorylation of HDAC5 by AMPK (McGee et al., 2008) and CAMKII (Ojuka et al., 2012). Increases in the protein content of the transcriptional coactivator PGC1α are seen following ET and SIT (Burgomaster et al., 2008) and are thought to be involved in the upregulation of GLUT4 gene expression through MEF2 binding and in turn promoting histone acetylation (Rockl et al., 2008, Ojuka et al., 2012).

Increases in GLUT4 protein content resulting from training will enhance glucose uptake capacity of skeletal muscle, and therefore are likely to contribute to the improvement in insulin sensitivity that is observed with an OGTT or hyperinsulinaemic-euglcyaemic clamp following training (Goodyear and Kahn, 1998). Further research should investigate the mechanisms by which increases in GLUT4 content can improve insulin sensitivity measured in this way. One possibility is that following training GLUT4 content of insulin responsive

stores in particular is increased therefore increasing the GLUT4 available for translocation in response to a given insulin stimulus (Ivy, 2004).

1.9. Overview and aims of thesis

As described in this introductory chapter skeletal muscle is the major site of glucose uptake (Katz et al., 1983, Ferrannini et al., 1985) and GLUT4, as the main glucose transporter isoform expressed in skeletal muscle (Mueckler, 1994, Bell et al., 1993), has a significant role to play in the successful, or unsuccessful, maintenance of glucose homeostasis. Previously published literature, which observed an increased GLUT4 content using Western blots in isolated PM fractions following glucose feeding (Goodyear et al., 1996) and exercise (Kennedy et al., 1999), has implicitly assumed that this increase in PM GLUT4 content is the primary mechanism behind the increase in skeletal muscle glucose uptake that is seen in response to insulin and exercise. Furthermore it has been assumed that failure to achieve this increase in GLUT4 PM content is a major cause of insulin resistance in the muscle of individuals with obesity and metabolic syndrome (Zierath et al., 1996). As results obtained in these PM fractionation methods have been criticised (section 1.4.1), an overriding aim of this thesis is to develop an immunofluorescence microscopy method to visualise GLUT4 in human skeletal muscle and to subsequently investigate the above assumptions. Current literature relating to the subcellular distribution and storage of GLUT4 and the time profile of GLUT4 translocation following glucose ingestion, during a hyperinsulinaemic-euglycaemic clamp and after exercise in human skeletal muscle in particular is fragmented. Therefore the immunofluorescence microscopy method developed in this thesis, will be used to investigate GLUT4 intracellular storage sites and colocalisation of GLUT4 with the PM marker dystrophin in human skeletal muscle as a measure of GLUT4 translocation to the PM. This PhD project was part of a collaborative project between Eindhoven University of Technology,

AstraZeneca and the University of Birmingham and as such aimed to generate information on the time profiles of insulin- and contraction-mediated GLUT4 translocation in human skeletal muscle.

Chapter 2 of this thesis describes the development and validation of an immunofluorescence method to visualise GLUT4 in human skeletal muscle and has for the first time used a PM marker to assess colocalisation of GLUT4 with the PM marker as a measure of GLUT4 present in PM regions in human skeletal muscle. The method is used in chapter 3 to investigate the effect of training on GLUT4 content and spatial distribution to include colocalisation with the PM marker dystrophin in the basal state in type I and type II muscle fibres. Furthermore chapter 3 aims to add to the understanding of whether endurance and sprint interval training-induced improvements in glucose homeostasis and insulin sensitivity that are seen during an OGTT are driven by increases in GLUT4 content in specific subcellular locations.

Chapter 4 aims to visualise and quantify the redistribution of GLUT4 to the PM in human skeletal muscle following glucose feeding and exercise. In particular GLUT4 PM localisation was investigated 30, 60 and 90 min after glucose feeding to determine the time profiles and kinetics of GLUT4 translocation in human skeletal muscle. GLUT4 PM localisation is also investigated immediately after 30 min cycling exercise. In addition chapter 4 aims to quantity GLUT4 PM localisation following a combination of glucose feeding and exercise.

Chapter 5 uses the novel method developed to investigate GLUT4 PM localisation in the skeletal muscle of the obese Zucker rat model of obesity and compares GLUT4 PM localisation before and after an 80 min hyperinsulinaemic-isoglycaemic clamp in both lean and obese Zucker rats. The a priori hypothesis was that there would be an increased GLUT4

PM localisation following hyperinsulinaemic-isoglycaemic clamp in the LZR, which would not occur in the OZR because of insulin resistance.

Chapter 6 aims to characterise the effect of prolonged hyperglycaemia on GLUT4 PM localisation in human skeletal muscle. Glucose disposal and GLUT4 PM localisation are assessed during a hyperglycaemic glucose clamp (5.4 mM above the overnight fasted level) in normal glucose tolerance (NGT) after 2 and 24 of hyperglycaemia and in patients with type 2 diabetes (T2D) after 2 h only. It is hypothesised that glucose disposal and GLUT4 PM localisation following 2 h hyperglycaemia would be higher in NGT compared to T2D. We further hypothesized that insulin-mediated glucose disposal and GLUT4 PM localisation would be reduced in response to 24 h hyperglycaemia in NGT due to hyperglycaemia-induced insulin resistance.

1.10. References

ABDUL-GHANI, M. A., TRIPATHY, D. & DEFRONZO, R. A. 2006. Contributions of beta-cell dysfunction and insulin resistance to the pathogenesis of impaired glucose tolerance and impaired fasting glucose. *Diabetes Care,* 29**,** 1130-9.

ADACHI, T., KIKUCHI, N., YASUDA, K., ANAHARA, R., GU, N., MATSUNAGA, T., YAMAMURA, T., MORI, C., TSUJIMOTO, G., TSUDA, K. & ISHIHARA, A. 2007. Fibre type distribution and gene expression levels of both succinate dehydrogenase and peroxisome proliferator-activated receptor-gamma coactivator-1alpha of fibres in the soleus muscle of Zucker diabetic fatty rats. *Exp Physiol,* 92**,** 449-55.

ALSTED, T. J., NYBO, L., SCHWEIGER, M., FLEDELIUS, C., JACOBSEN, P., ZIMMERMANN, R., ZECHNER, R. & KIENS, B. 2009. Adipose triglyceride lipase in human skeletal muscle is upregulated by exercise training. *Am J Physiol Endocrinol Metab,* 296**,** E445-53.

AMATI, F., DUBE, J. J., ALVAREZ-CARNERO, E., EDREIRA, M. M., CHOMENTOWSKI, P., COEN, P. M., SWITZER, G. E., BICKEL, P. E., STEFANOVIC-RACIC, M., TOLEDO, F. G. & GOODPASTER, B. H. 2011. Skeletal muscle triglycerides, diacylglycerols, and ceramides in insulin resistance: another paradox in endurance-trained athletes? *Diabetes,* 60**,** 2588-97.

AMERICAN DIABETES ASSOCIATION. 1990. Diabetes mellitus and exercise. *Diabetes Care,* 13**,** 804-5.

AN, D., TOYODA, T., TAYLOR, E. B., YU, H., FUJII, N., HIRSHMAN, M. F. & GOODYEAR, L. J. 2010. TBC1D1 regulates insulin- and contraction-induced glucose transport in mouse skeletal muscle. *Diabetes,* 59**,** 1358-65.

ANDERSEN, P. H., LUND, S., SCHMITZ, O., JUNKER, S., KAHN, B. B. & PEDERSEN, O. 1993. Increased insulin-stimulated glucose uptake in athletes: the importance of GLUT4 mRNA, GLUT4 protein and fibre type composition of skeletal muscle. *Acta Physiol Scand,* 149**,** 393-404.

ARA, I., LARSEN, S., STALLKNECHT, B., GUERRA, B., MORALES-ALAMO, D., ANDERSEN, J.L., PONCE-GONZALEZ, J.G., GUADALUPE-GRAU, A., GALBO, H., CALBET, J.A. & HELGE, J.W. 2011. Normal mitochondrial function and increased fat oxidation capacity in leg and arm muscles in obese humans. *Int J Obes,* 35, 99-108.

ARAKI, E., LIPES, M. A., PATTI, M. E., BRUNING, J. C., HAAG, B., 3RD, JOHNSON, R. S. & KAHN, C. R. 1994. Alternative pathway of insulin signalling in mice with targeted disruption of the IRS-1 gene. *Nature,* 372**,** 186-90.

ARIAS, E. B., KIM, J., FUNAI, K. & CARTEE, G. D. 2007. Prior exercise increases phosphorylation of Akt substrate of 160 kDa (AS160) in rat skeletal muscle. *Am J Physiol Endocrinol Metab,* 292**,** E1191-200.

BABRAJ, J. A., VOLLAARD, N. B., KEAST, C., GUPPY, F. M., COTTRELL, G. & TIMMONS, J. A. 2009. Extremely short duration high intensity interval training substantially improves insulin action in young healthy males. *BMC Endocr Disord,* 9**,** 3.

BANDYOPADHYAY, G. K., YU, J. G., OFRECIO, J. & OLEFSKY, J. M. 2006. Increased malonyl-CoA levels in muscle from obese and type 2 diabetic subjects lead to decreased fatty acid oxidation and increased lipogenesis; thiazolidinedione treatment reverses these defects. *Diabetes,* 55**,** 2277-85.

BARNES, B. R., MARKLUND, S., STEILER, T. L., WALTER, M., HJALM, G., AMARGER, V., MAHLAPUU, M., LENG, Y., JOHANSSON, C., GALUSKA, D., LINDGREN, K., ABRINK, M., STAPLETON, D., ZIERATH, J. R. & ANDERSSON, L. 2004. The 5'-AMP-activated protein kinase gamma3 isoform has a key role in carbohydrate and lipid metabolism in glycolytic skeletal muscle. *J Biol Chem,* 279**,** 38441-7.

BARRETT, E. J., EGGLESTON, E. M., INYARD, A. C., WANG, H., LI, G., CHAI, W. & LIU, Z. 2009. The vascular actions of insulin control its delivery to muscle and regulate the rate-limiting step in skeletal muscle insulin action. *Diabetologia,* 52**,** 752-64.

BARRETT, E. J., WANG, H., UPCHURCH, C. T. & LIU, Z. 2011. Insulin regulates its own delivery to skeletal muscle by feed-forward actions on the vasculature. *Am J Physiol Endocrinol Metab,* 301**,** E252-63.

BELL, G. I., BURANT, C. F., TAKEDA, J. & GOULD, G. W. 1993. Structure and function of mammalian facilitative sugar transporters. *J Biol Chem,* 268**,** 19161-4.

BERGMAN, B. C., HORNING, M. A., CASAZZA, G. A., WOLFEL, E. E., BUTTERFIELD, G. E. & BROOKS, G. A. 2000. Endurance training increases gluconeogenesis during rest and exercise in men. *Am J Physiol Endocrinol Metab,* 278**,** E244-51.

BERGMAN, B. C., PERREAULT, L., HUNERDOSSE, D. M., KOEHLER, M. C., SAMEK, A. M. & ECKEL, R. H. 2010. Increased intramuscular lipid synthesis and low saturation relate to insulin sensitivity in endurance-trained athletes. *J Appl Physiol,* 108**,** 1134-41.

BERGSTROM, J. 1975. Percutaneous needle biopsy of skeletal muscle in physiological and clinical research. *Scand J Clin Lab Invest,* 35**,** 609-16.

BLAAK, E. E., SCHIFFELERS, S. L., SARIS, W. H., MENSINK, M. & KOOI, M. E. 2004. Impaired beta-adrenergically mediated lipolysis in skeletal muscle of obese subjects. *Diabetologia,* 47**,** 1462-8.

BLAAK, E. E., VAN AGGEL-LEIJSSEN, D. P., WAGENMAKERS, A. J., SARIS, W. H. & VAN BAAK, M. A. 2000. Impaired oxidation of plasma-derived fatty acids in type 2 diabetic subjects during moderate-intensity exercise. *Diabetes,* 49**,** 2102-7.

BLENDEA, M. C., JACOBS, D., STUMP, C. S., MCFARLANE, S. I., OGRIN, C., BAHTYIAR, G., STAS, S., KUMAR, P., SHA, Q., FERRARIO, C. M. & SOWERS, J. R. 2005. Abrogation of oxidative stress improves insulin sensitivity in the Ren-2 rat model of tissue angiotensin II overexpression. *Am J Physiol Endocrinol Metab,* 288**,** E353-9.

BODEN, G., CHEN, X., RUIZ, J., WHITE, J. V. & ROSSETTI, L. 1994. Mechanisms of fatty acid-induced inhibition of glucose uptake. *J Clin Invest,* 93**,** 2438-46.

BODEN, G., JADALI, F., WHITE, J., LIANG, Y., MOZZOLI, M., CHEN, X., COLEMAN, E. & SMITH, C. 1991. Effects of fat on insulin-stimulated carbohydrate metabolism in normal men. *J Clin Invest,* 88**,** 960-6.

BOGAN, J. S. 2012. Regulation of glucose transporter translocation in health and diabetes. *Annu Rev Biochem,* 81**,** 507-32.

BOGAN, J. S. & KANDROR, K. V. 2010. Biogenesis and regulation of insulin-responsive vesicles containing GLUT4. *Curr Opin Cell Biol,* 22**,** 506-12.

BOGARDUS, C., THUILLEZ, P., RAVUSSIN, E., VASQUEZ, B., NARIMIGA, M. & AZHAR, S. 1983. Effect of muscle glycogen depletion on in vivo insulin action in man. *J Clin Invest,* 72**,** 1605-10.

BONEN, A., PAROLIN, M. L., STEINBERG, G. R., CALLES-ESCANDON, J., TANDON, N. N., GLATZ, J. F., LUIKEN, J. J., HEIGENHAUSER, G. J. & DYCK, D. J. 2004. Triacylglycerol accumulation in human obesity and type 2 diabetes is associated with increased rates of skeletal muscle fatty acid transport and increased sarcolemmal FAT/CD36. *FASEB J,* 18**,** 1144-6.

BORGHOUTS, L. B., SCHAART, G., HESSELINK, M. K. & KEIZER, H. A. 2000. GLUT-4 expression is not consistently higher in type-1 than in type-2 fibres of rat and human vastus lateralis muscles; an immunohistochemical study. *Pflugers Arch,* 441**,** 351-8.

BOSSENMAIER, B., MOSTHAF, L., MISCHAK, H., ULLRICH, A. & HARING, H. U. 1997. Protein kinase C isoforms beta 1 and beta 2 inhibit the tyrosine kinase activity of the insulin receptor. *Diabetologia,* 40**,** 863-6.

BOSTROM, P., ANDERSSON, L., RUTBERG, M., PERMAN, J., LIDBERG, U., JOHANSSON, B. R., FERNANDEZ-RODRIGUEZ, J., ERICSON, J., NILSSON, T., BOREN, J. & OLOFSSON, S. O. 2007. SNARE proteins mediate fusion between cytosolic lipid droplets and are implicated in insulin sensitivity. *Nat Cell Biol,* 9**,** 1286-93.

BOSTROM, P., ANDERSSON, L., VIND, B., HAVERSEN, L., RUTBERG, M., WICKSTROM, Y., LARSSON, E., JANSSON, P. A., SVENSSON, M. K., BRANEMARK, R., LING, C., BECK-NIELSEN, H., BOREN, J., HOJLUND, K. & OLOFSSON, S. O. 2010. The SNARE protein SNAP23 and the SNARE-interacting protein Munc18c in human skeletal muscle are implicated in insulin resistance/type 2 diabetes. *Diabetes,* 59**,** 1870-8.

BOUSHEL, R., GNAIGER, E., SCHJERLING, P., SKOVBRO, M., KRAUNSOE, R. & DELA, F. 2007. Patients with type 2 diabetes have normal mitochondrial function in skeletal muscle. *Diabetologia,* 50, 790–6.

BOUZAKRI, K. & ZIERATH, J. R. 2007. MAP4K4 gene silencing in human skeletal muscle prevents tumor necrosis factor-alpha-induced insulin resistance. *J Biol Chem,* 282**,** 7783-9.

BRADLEY, S. J., KINGWELL, B. A. & MCCONELL, G. K. 1999. Nitric oxide synthase inhibition reduces leg glucose uptake but not blood flow during dynamic exercise in humans. *Diabetes,* 48**,** 1815-21.

BROZINICK, J. T., JR., HAWKINS, E. D., STRAWBRIDGE, A. B. & ELMENDORF, J. S. 2004. Disruption of cortical actin in skeletal muscle demonstrates an essential role of the cytoskeleton in glucose transporter 4 translocation in insulin-sensitive tissues. *J Biol Chem,* 279**,** 40699-706.

BRUSS, M. D., ARIAS, E. B., LIENHARD, G. E. & CARTEE, G. D. 2005. Increased phosphorylation of Akt substrate of 160 kDa (AS160) in rat skeletal muscle in response to insulin or contractile activity. *Diabetes,* 54**,** 41-50.

BRYANT, N. J. & GOULD, G. W. 2011. SNARE proteins underpin insulin-regulated GLUT4 traffic. *Traffic,* 12**,** 657-64.

BRYANT, N. J., GOVERS, R. & JAMES, D. E. 2002. Regulated transport of the glucose transporter GLUT4. *Nat Rev Mol Cell Biol,* 3**,** 267-77.

BURDETT, E., BEELER, T. & KLIP, A. 1987. Distribution of glucose transporters and insulin receptors in the plasma membrane and transverse tubules of skeletal muscle. *Arch Biochem Biophys,* 253**,** 279-86.

BURGOMASTER, K. A., CERMAK, N. M., PHILLIPS, S. M., BENTON, C. R., BONEN, A. & GIBALA, M. J. 2007. Divergent response of metabolite transport proteins in human skeletal muscle after sprint interval training and detraining. *Am J Physiol Regul Integr Comp Physiol,* 292**,** R1970-6.

BURGOMASTER, K. A., HOWARTH, K. R., PHILLIPS, S. M., RAKOBOWCHUK, M., MACDONALD, M. J., MCGEE, S. L. & GIBALA, M. J. 2008. Similar metabolic adaptations during exercise after low volume sprint interval and traditional endurance training in humans. *J Physiol,* 586**,** 151-60.

CARO, J. F., SINHA, M. K., RAJU, S. M., ITTOOP, O., PORIES, W. J., FLICKINGER, E. G., MEELHEIM, D. & DOHM, G. L. 1987. Insulin receptor kinase in human skeletal muscle from obese subjects with and without noninsulin dependent diabetes. *J Clin Invest,* 79**,** 1330-7.

CHANG, L., CHIANG, S. H. & SALTIEL, A. R. 2004. Insulin signaling and the regulation of glucose transport. *Mol Med,* 10**,** 65-71.

CHEN, S., MURPHY, J., TOTH, R., CAMPBELL, D. G., MORRICE, N. A. & MACKINTOSH, C. 2008. Complementary regulation of TBC1D1 and AS160 by growth factors, insulin and AMPK activators. *Biochem J,* 409**,** 449-59.

CHEN, S., WASSERMAN, D. H., MACKINTOSH, C. & SAKAMOTO, K. 2011. Mice with AS160/TBC1D4-Thr649Ala knockin mutation are glucose intolerant with reduced insulin sensitivity and altered GLUT4 trafficking. *Cell Metab,* 13**,** 68-79.

CHEN, Y. A. & SCHELLER, R. H. 2001. SNARE-mediated membrane fusion. *Nat Rev Mol Cell Biol,* 2**,** 98-106.

CHIU, T. T., JENSEN, T. E., SYLOW, L., RICHTER, E. A. & KLIP, A. 2011. Rac1 signalling towards GLUT4/glucose uptake in skeletal muscle. *Cell Signal,* 23**,** 1546-54.

CHIU, T. T., PATEL, N., SHAW, A. E., BAMBURG, J. R. & KLIP, A. 2010. Arp2/3- and cofilin-coordinated actin dynamics is required for insulin-mediated GLUT4 translocation to the surface of muscle cells. *Mol Biol Cell,* 21**,** 3529-39.

CHO, H., MU, J., KIM, J. K., THORVALDSEN, J. L., CHU, Q., CRENSHAW, E. B., 3RD, KAESTNER, K. H., BARTOLOMEI, M. S., SHULMAN, G. I. & BIRNBAUM, M. J. 2001. Insulin resistance and a diabetes mellitus-like syndrome in mice lacking the protein kinase Akt2 (PKB beta). *Science,* 292**,** 1728-31.

CLELAND, P. J., ABEL, K. C., RATTIGAN, S. & CLARK, M. G. 1990. Long-term treatment of isolated rat soleus muscle with phorbol ester leads to loss of contraction-induced glucose transport. *Biochem J,* 267**,** 659-63.

CLELAND, P. J., APPLEBY, G. J., RATTIGAN, S. & CLARK, M. G. 1989. Exercise-induced translocation of protein kinase C and production of diacylglycerol and phosphatidic acid in rat skeletal muscle in vivo. Relationship to changes in glucose transport. *J Biol Chem,* 264**,** 17704-11.

CLERK, L. H., RATTIGAN, S. & CLARK, M. G. 2002. Lipid infusion impairs physiologic insulin-mediated capillary recruitment and muscle glucose uptake in vivo. *Diabetes,* 51**,** 1138-45.

CLERK, L. H., VINCENT, M. A., JAHN, L. A., LIU, Z., LINDNER, J. R. & BARRETT, E. J. 2006. Obesity blunts insulin-mediated microvascular recruitment in human forearm muscle. *Diabetes,* 55**,** 1436-42.

CODERRE, L., KANDROR, K. V., VALLEGA, G. & PILCH, P. F. 1995. Identification and characterization of an exercise-sensitive pool of glucose transporters in skeletal muscle. *J Biol Chem,* 270**,** 27584-8.

COGGAN, A. R. 1991. Plasma glucose metabolism during exercise in humans. *Sports Med,* 11**,** 102-24.

COGGINS, M., LINDNER, J., RATTIGAN, S., JAHN, L., FASY, E., KAUL, S. & BARRETT, E. 2001. Physiologic hyperinsulinemia enhances human skeletal muscle perfusion by capillary recruitment. *Diabetes,* 50**,** 2682-90.

COLEMAN, R. A. & LEE, D. P. 2004. Enzymes of triacylglycerol synthesis and their regulation. *Prog Lipid Res,* 43**,** 134-76.

COPPACK, S. W., FISHER, R. M., GIBBONS, G. F., HUMPHREYS, S. M., MCDONOUGH, M. J., POTTS, J. L. & FRAYN, K. N. 1990. Postprandial substrate deposition in human forearm and adipose tissues in vivo. *Clin Sci (Lond),* 79**,** 339-48.

COSTES, S., LANGEN, R., GURLO, T., MATVEYENKO, A. V. & BUTLER, P. C. 2013. beta-Cell failure in type 2 diabetes: a case of asking too much of too few? *Diabetes,* 62**,** 327-35.

COX, J. H., CORTRIGHT, R. N., DOHM, G. L. & HOUMARD, J. A. 1999. Effect of aging on response to exercise training in humans: skeletal muscle GLUT-4 and insulin sensitivity. *J Appl Physiol,* 86**,** 2019-25.

CRAWFORD, T. N., ALFARO, D. V., 3RD, KERRISON, J. B. & JABLON, E. P. 2009. Diabetic retinopathy and angiogenesis. *Curr Diabetes Rev,* 5**,** 8-13.

DANAEI, G., FINUCANE, M. M., LU, Y., SINGH, G. M., COWAN, M. J., PACIOREK, C. J., LIN, J. K., FARZADFAR, F., KHANG, Y. H., STEVENS, G. A., RAO, M., ALI, M. K., RILEY, L. M., ROBINSON, C. A., EZZATI, M. & GLOBAL BURDEN OF METABOLIC RISK FACTORS OF CHRONIC DISEASES COLLABORATING, G. 2011. National, regional, and global trends in fasting plasma glucose and diabetes prevalence since 1980: systematic analysis of health examination surveys and epidemiological studies with 370 country-years and 2.7 million participants. *Lancet,* 378**,** 31-40.

DAUGAARD, J. R., NIELSEN, J. N., KRISTIANSEN, S., ANDERSEN, J. L., HARGREAVES, M. & RICHTER, E. A. 2000. Fiber type-specific expression of GLUT4 in human skeletal muscle: influence of exercise training. *Diabetes,* 49**,** 1092-5.

DAUGAARD, J. R. & RICHTER, E. A. 2004. Muscle- and fibre type-specific expression of glucose transporter 4, glycogen synthase and glycogen phosphorylase proteins in human skeletal muscle. *Pflugers Arch,* 447**,** 452-6.

DAWSON, D., VINCENT, M. A., BARRETT, E. J., KAUL, S., CLARK, A., LEONG-POI, H. & LINDNER, J. R. 2002. Vascular recruitment in skeletal muscle during exercise and hyperinsulinemia assessed by contrast ultrasound. *Am J Physiol Endocrinol Metab,* 282**,** E714-20.

DE ALVARO, C., TERUEL, T., HERNANDEZ, R. & LORENZO, M. 2004. Tumor necrosis factor alpha produces insulin resistance in skeletal muscle by activation of inhibitor kappaB kinase in a p38 MAPK-dependent manner. *J Biol Chem,* 279**,** 17070-8.

DE BOCK, K., DRESSELAERS, T., KIENS, B., RICHTER, E. A., VAN HECKE, P. & HESPEL, P. 2007. Evaluation of intramyocellular lipid breakdown during exercise by biochemical assay, NMR spectroscopy, and Oil Red O staining. *Am J Physiol Endocrinol Metab,* 293**,** E428-34.

DEFRONZO, R. A. 2009. Banting Lecture. From the triumvirate to the ominous octet: a new paradigm for the treatment of type 2 diabetes mellitus. *Diabetes,* 58**,** 773-95.

DEFRONZO, R. A., FERRANNINI, E. & SIMONSON, D. C. 1989. Fasting hyperglycemia in non-insulin-dependent diabetes mellitus: contributions of excessive hepatic glucose production and impaired tissue glucose uptake. *Metabolism,* 38**,** 387-95.

DEFRONZO, R. A., GUNNARSSON, R., BJORKMAN, O., OLSSON, M. & WAHREN, J. 1985. Effects of insulin on peripheral and splanchnic glucose metabolism in noninsulin-dependent (type II) diabetes mellitus. *J Clin Invest,* 76**,** 149-55.

DEL AGUILA, L. F., CLAFFEY, K. P. & KIRWAN, J. P. 1999. TNF-alpha impairs insulin signaling and insulin stimulation of glucose uptake in C2C12 muscle cells. *Am J Physiol,* 276**,** E849-55.

DELA, F. & HELGE, J.W. 2013. Insulin resistance and mitochondrial function in skeletal muscle. *Int J Biochem Cell B,* 45, 11-15.

DELA, F., LARSEN, J. J., MIKINES, K. J., PLOUG, T., PETERSEN, L. N. & GALBO, H. 1995. Insulin-stimulated muscle glucose clearance in patients with NIDDM. Effects of one-legged physical training. *Diabetes,* 44**,** 1010-20.

DELA, F., MIKINES, K. J., LARSEN, J. J. & GALBO, H. 1996. Training-induced enhancement of insulin action in human skeletal muscle: the influence of aging. *J Gerontol A Biol Sci Med Sci,* 51**,** B247-52.

DELA, F., MIKINES, K. J., VON LINSTOW, M., SECHER, N. H. & GALBO, H. 1992. Effect of training on insulin-mediated glucose uptake in human muscle. *Am J Physiol,* 263**,** E1134-43.

DEPARTMENT FOR HEALTH. 2006. Turning the Corner: Improving Diabetes Care. London, United Kingdom.

DERAVE, W., AI, H., IHLEMANN, J., WITTERS, L. A., KRISTIANSEN, S., RICHTER, E. A. & PLOUG, T. 2000. Dissociation of AMP-activated protein kinase activation and glucose transport in contracting slow-twitch muscle. *Diabetes,* 49**,** 1281-7.

DOUARD, V. & FERRARIS, R. P. 2008. Regulation of the fructose transporter GLUT5 in health and disease. *Am J Physiol Endocrinol Metab,* 295**,** E227-37.

DOUEN, A. G., RAMLAL, T., CARTEE, G. D. & KLIP, A. 1990a. Exercise modulates the insulin-induced translocation of glucose transporters in rat skeletal muscle. *FEBS Lett,* 261**,** 256-60.

DOUEN, A. G., RAMLAL, T., RASTOGI, S., BILAN, P. J., CARTEE, G. D., VRANIC, M., HOLLOSZY, J. O. & KLIP, A. 1990b. Exercise induces recruitment of the "insulin-responsive glucose transporter". Evidence for distinct intracellular insulin- and exercise-recruitable transporter pools in skeletal muscle. *J Biol Chem,* 265**,** 13427-30.

EGGLESTON, E. M., JAHN, L. A. & BARRETT, E. J. 2007. Hyperinsulinemia rapidly increases human muscle microvascular perfusion but fails to increase muscle insulin clearance: evidence that a saturable process mediates muscle insulin uptake. *Diabetes,* 56**,** 2958-63.

EGUEZ, L., LEE, A., CHAVEZ, J. A., MIINEA, C. P., KANE, S., LIENHARD, G. E. & MCGRAW, T. E. 2005. Full intracellular retention of GLUT4 requires AS160 Rab GTPase activating protein. *Cell Metab,* 2**,** 263-72.

EMHOFF, C. A., MESSONNIER, L. A., HORNING, M. A., FATTOR, J. A., CARLSON, T. J. & BROOKS, G. A. 2013. Gluconeogenesis and hepatic glycogenolysis during exercise at the lactate threshold. *J Appl Physiol,* 114**,** 297-306.

FAZAKERLEY, D. J., HOLMAN, G. D., MARLEY, A., JAMES, D. E., STOCKLI, J. & COSTER, A. C. 2009a. Kinetic evidence for unique regulation of GLUT4 trafficking by insulin and AMP-activated protein kinase activators in L6 myotubes. *J Biol Chem,* 285**,** 1653-60.

FAZAKERLEY, D. J., LAWRENCE, S. P., LIZUNOV, V. A., CUSHMAN, S. W. & HOLMAN, G. D. 2009b. A common trafficking route for GLUT4 in cardiomyocytes in response to insulin, contraction and energy-status signalling. *J Cell Sci,* 122**,** 727-34.

FELIG, P., POZEFSKY, T., MARLISS, E. & CAHILL, G. F., JR. 1970. Alanine: key role in gluconeogenesis. *Science,* 167**,** 1003-4.

FERRANNINI, E., BJORKMAN, O., REICHARD, G. A., JR., PILO, A., OLSSON, M., WAHREN, J. & DEFRONZO, R. A. 1985. The disposal of an oral glucose load in healthy subjects. A quantitative study. *Diabetes,* 34**,** 580-8.

FERRANNINI, E., WAHREN, J., FELIG, P. & DEFRONZO, R. A. 1980. The role of fractional glucose extraction in the regulation of splanchnic glucose metabolism in normal and diabetic man. *Metabolism,* 29**,** 28-35.

FOLEY, K., BOGUSLAVSKY, S. & KLIP, A. 2011. Endocytosis, recycling, and regulated exocytosis of glucose transporter 4. *Biochemistry,* 50**,** 3048-61.

FRIDLYAND, L. E. & PHILLIPSON, L. H. 2011. Mechanisms of glucose sensing in the pancreatic beta-cell: A computational systems-based analysis. *Islets,* 3**,** 224-30.

FROSIG, C., PEHMOLLER, C., BIRK, J. B., RICHTER, E. A. & WOJTASZEWSKI, J. F. 2010. Exercise-induced TBC1D1 Ser237 phosphorylation and 14-3-3 protein binding capacity in human skeletal muscle. *J Physiol,* 588**,** 4539-48.

FROSIG, C., ROSE, A. J., TREEBAK, J. T., KIENS, B., RICHTER, E. A. & WOJTASZEWSKI, J. F. 2007. Effects of endurance exercise training on insulin signaling in human skeletal muscle: interactions at the level of phosphatidylinositol 3-kinase, Akt, and AS160. *Diabetes,* 56**,** 2093-102.

FUJII, N., ASCHENBACH, W. G., MUSI, N., HIRSHMAN, M. F. & GOODYEAR, L. J. 2004. Regulation of glucose transport by the AMP-activated protein kinase. *Proc Nutr Soc,* 63**,** 205-10.

FUNAI, K. & CARTEE, G. D. 2009. Inhibition of contraction-stimulated AMP-activated protein kinase inhibits contraction-stimulated increases in PAS-TBC1D1 and glucose transport without altering PAS-AS160 in rat skeletal muscle. *Diabetes,* 58**,** 1096-104.

GAGLIARDINO, J. J. 2005. Physiological endocrine control of energy homeostasis and postprandial blood glucose levels. *Eur Rev Med Pharmacol Sci,* 9**,** 75-92.

GARVEY, W. T., MAIANU, L., ZHU, J. H., BRECHTEL-HOOK, G., WALLACE, P. & BARON, A. D. 1998. Evidence for defects in the trafficking and translocation of GLUT4 glucose transporters in skeletal muscle as a cause of human insulin resistance. *J Clin Invest,* 101**,** 2377-86.

GASTER, M., POULSEN, P., HANDBERG, A., SCHRODER, H. D. & BECK-NIELSEN, H. 2000. Direct evidence of fiber type-dependent GLUT-4 expression in human skeletal muscle. *Am J Physiol Endocrinol Metab,* 278**,** E910-6.

GENUTH, S., ALBERTI, K. G., BENNETT, P., BUSE, J., DEFRONZO, R., KAHN, R., KITZMILLER, J., KNOWLER, W. C., LEBOVITZ, H., LERNMARK, A., NATHAN, D., PALMER, J., RIZZA, R., SAUDEK, C., SHAW, J., STEFFES, M., STERN, M., TUOMILEHTO, J., ZIMMET, P., EXPERT COMMITTEE ON THE, D. & CLASSIFICATION OF DIABETES, M. 2003. Follow-up report on the diagnosis of diabetes mellitus. *Diabetes Care,* 26**,** 3160-7.

GERAGHTY, K. M., CHEN, S., HARTHILL, J. E., IBRAHIM, A. F., TOTH, R., MORRICE, N. A., VANDERMOERE, F., MOORHEAD, G. B., HARDIE, D. G. & MACKINTOSH, C. 2007. Regulation of multisite phosphorylation and 14-3-3 binding of AS160 in response to IGF-1, EGF, PMA and AICAR. *Biochem J,* 407**,** 231-41.

GERICH, J. E., MEYER, C., WOERLE, H. J. & STUMVOLL, M. 2001. Renal gluconeogenesis: its importance in human glucose homeostasis. *Diabetes Care,* 24**,** 382-91.

GIBALA, M. J., LITTLE, J. P., VAN ESSEN, M., WILKIN, G. P., BURGOMASTER, K. A., SAFDAR, A., RAHA, S. & TARNOPOLSKY, M. A. 2006. Short-term sprint interval versus traditional endurance training: similar initial adaptations in human skeletal muscle and exercise performance. *J Physiol,* 575**,** 901-11.

GNAIGER, E. 2009. Capacity of oxidative phosphorylation in human skeletal muscle; new perspectives of mitochondrial physiology. *Int J Biochem Cell B,* 41, 1837-1845.

GOODPASTER, B.H. 2013. Mitochondrial deficiency is associated with insulin resistance. *Diabetes,* 62, 1032-1035.

GOODPASTER, B. H., HE, J., WATKINS, S. & KELLEY, D. E. 2001. Skeletal muscle lipid content and insulin resistance: evidence for a paradox in endurance-trained athletes. *J Clin Endocrinol Metab,* 86**,** 5755-61.

GOODYEAR, L. J., GIORGINO, F., SHERMAN, L. A., CAREY, J., SMITH, R. J. & DOHM, G. L. 1995. Insulin receptor phosphorylation, insulin receptor substrate-1 phosphorylation, and phosphatidylinositol 3-kinase activity are decreased in intact skeletal muscle strips from obese subjects. *J Clin Invest,* 95**,** 2195-204.

GOODYEAR, L. J., HIRSHMAN, M. F., NAPOLI, R., CALLES, J., MARKUNS, J. F., LJUNGQVIST, O. & HORTON, E. S. 1996. Glucose ingestion causes GLUT4 translocation in human skeletal muscle. *Diabetes,* 45**,** 1051-6.

GOODYEAR, L. J. & KAHN, B. B. 1998. Exercise, glucose transport, and insulin sensitivity. *Annu Rev Med,* 49**,** 235-61.

GRIFFIN, M. E., MARCUCCI, M. J., CLINE, G. W., BELL, K., BARUCCI, N., LEE, D., GOODYEAR, L. J., KRAEGEN, E. W., WHITE, M. F. & SHULMAN, G. I. 1999. Free fatty acid-induced insulin resistance is associated with activation of protein kinase C theta and alterations in the insulin signaling cascade. *Diabetes,* 48**,** 1270-4.

GUDBJORNSDOTTIR, S., SJOSTRAND, M., STRINDBERG, L. & LONNROTH, P. 2005. Decreased muscle capillary permeability surface area in type 2 diabetic subjects. *J Clin Endocrinol Metab,* 90**,** 1078-82.

GUDBJORNSDOTTIR, S., SJOSTRAND, M., STRINDBERG, L., WAHREN, J. & LONNROTH, P. 2003. Direct measurements of the permeability surface area for insulin and glucose in human skeletal muscle. *J Clin Endocrinol Metab,* 88**,** 4559-64.

GULVE, E. A., REN, J. M., MARSHALL, B. A., GAO, J., HANSEN, P. A., HOLLOSZY, J. O. & MUECKLER, M. 1994. Glucose transport activity in skeletal muscles from transgenic mice overexpressing GLUT1. Increased basal transport is associated with a defective response to diverse stimuli that activate GLUT4. *J Biol Chem,* 269**,** 18366-70.

GUMA, A., ZIERATH, J. R., WALLBERG-HENRIKSSON, H. & KLIP, A. 1995. Insulin induces translocation of GLUT-4 glucose transporters in human skeletal muscle. *Am J Physiol,* 268**,** E613-22.

HAEMMERLE, G., ZIMMERMANN, R., HAYN, M., THEUSSL, C., WAEG, G., WAGNER, E., SATTLER, W., MAGIN, T. M., WAGNER, E. F. & ZECHNER, R. 2002. Hormone-sensitive lipase deficiency in mice causes diglyceride accumulation in adipose tissue, muscle, and testis. *J Biol Chem,* 277**,** 4806-15.

HANDBERG, A., VAAG, A., DAMSBO, P., BECK-NIELSEN, H. & VINTEN, J. 1990. Expression of insulin regulatable glucose transporters in skeletal muscle from type 2 (non-insulin-dependent) diabetic patients. *Diabetologia,* 33**,** 625-7.

HANSEN, P. A., GULVE, E. A., MARSHALL, B. A., GAO, J., PESSIN, J. E., HOLLOSZY, J. O. & MUECKLER, M. 1995. Skeletal muscle glucose transport and metabolism are enhanced in transgenic mice overexpressing the Glut4 glucose transporter. *J Biol Chem,* 270**,** 1679-84.

HANSEN, P. A., NOLTE, L. A., CHEN, M. M. & HOLLOSZY, J. O. 1998a. Increased GLUT-4 translocation mediates enhanced insulin sensitivity of muscle glucose transport after exercise. *J Appl Physiol,* 85**,** 1218-22.

HANSEN, P. A., WANG, W., MARSHALL, B. A., HOLLOSZY, J. O. & MUECKLER, M. 1998b. Dissociation of GLUT4 translocation and insulin-stimulated glucose transport in transgenic mice overexpressing GLUT1 in skeletal muscle. *J Biol Chem,* 273**,** 18173-9.

HARDIE, D. G., CARLING, D. & CARLSON, M. 1998. The AMP-activated/SNF1 protein kinase subfamily: metabolic sensors of the eukaryotic cell? *Annu Rev Biochem,* 67**,** 821-55.

HARDIN, D. S., AZZARELLI, B., EDWARDS, J., WIGGLESWORTH, J., MAIANU, L., BRECHTEL, G., JOHNSON, A., BARON, A. & GARVEY, W. T. 1995. Mechanisms of enhanced insulin sensitivity in endurance-trained athletes: effects on blood flow and differential expression of GLUT 4 in skeletal muscles. *J Clin Endocrinol Metab,* 80**,** 2437-46.

HAYAT, M. A. 1989. *Principles and Techniques of Electron Microscopy Third Edition,* London, The Macmillan Press Ltd.

HE, D., BOLSTAD, G., BRUBAKK, A. & MEDBO, J. I. 1995. Muscle fibre type and dimension in genetically obese and lean Zucker rats. *Acta Physiol Scand,* 155**,** 1-7.

HENRIKSEN, E. J. 2006. Exercise training and the antioxidant alpha-lipoic acid in the treatment of insulin resistance and type 2 diabetes. *Free Radic Biol Med,* 40**,** 3-12.

HEX, N., BARTLETT, C., WRIGHT, D., TAYLOR, M. & VARLEY, D. 2012. Estimating the current and future costs of Type 1 and Type 2 diabetes in the UK, including direct health costs and indirect societal and productivity costs. *Diabet Med,* 29**,** 855-62.

HOEG, L. D., SJOBERG, K. A., JEPPESEN, J., JENSEN, T. E., FROSIG, C., BIRK, J. B., BISIANI, B., HISCOCK, N., PILEGAARD, H., WOJTASZEWSKI, J. F., RICHTER, E. A. & KIENS, B. 2011. Lipid-induced insulin resistance affects women less than men and is not accompanied by inflammation or impaired proximal insulin signaling. *Diabetes,* 60**,** 64-73.

HOLLOSZY, J. O. 1967. Biochemical adaptations in muscle. Effects of exercise on mitochondrial oxygen uptake and respiratory enzyme activity in skeletal muscle. *J Biol Chem,* 242**,** 2278-82.

HOLLOSZY, J.O. 2013. "Deficiency" of mitochondria in muscle does not cause insulin resistance. *Diabetes,* 62, 1036-1042.

HOLLOSZY, J. O. & NARAHARA, H. T. 1967. Enhanced permeability to sugar associated with muscle contraction. Studies of the role of Ca++. *J Gen Physiol,* 50**,** 551-62.

HONIG, C. R., ODOROFF, C. L. & FRIERSON, J. L. 1982. Active and passive capillary control in red muscle at rest and in exercise. *Am J Physiol,* 243**,** H196-206.

HOOD, M. S., LITTLE, J. P., TARNOPOLSKY, M. A., MYSLIK, F. & GIBALA, M. J. 2011. Low-volume interval training improves muscle oxidative capacity in sedentary adults. *Med Sci Sports Exerc,* 43**,** 1849-56.

HOUMARD, J. A., EGAN, P. C., NEUFER, P. D., FRIEDMAN, J. E., WHEELER, W. S., ISRAEL, R. G. & DOHM, G. L. 1991. Elevated skeletal muscle glucose transporter levels in exercise-trained middle-aged men. *Am J Physiol,* 261**,** E437-43.

HOUMARD, J. A., HICKEY, M. S., TYNDALL, G. L., GAVIGAN, K. E. & DOHM, G. L. 1995. Seven days of exercise increase GLUT-4 protein content in human skeletal muscle. *J Appl Physiol,* 79**,** 1936-8.

HOUMARD, J. A., SHINEBARGER, M. H., DOLAN, P. L., LEGGETT-FRAZIER, N., BRUNER, R. K., MCCAMMON, M. R., ISRAEL, R. G. & DOHM, G. L. 1993. Exercise training increases GLUT-4 protein concentration in previously sedentary middle-aged men. *Am J Physiol,* 264**,** E896-901.

HOWLETT, K. F., MATHEWS, A., GARNHAM, A. & SAKAMOTO, K. 2008. The effect of exercise and insulin on AS160 phosphorylation and 14-3-3 binding capacity in human skeletal muscle. *Am J Physiol Endocrinol Metab,* 294**,** E401-7.

HOY, A. J., BRANDON, A. E., TURNER, N., WATT, M. J., BRUCE, C. R., COONEY, G. J. & KRAEGEN, E. W. 2009. Lipid and insulin infusion-induced skeletal muscle insulin resistance is likely due to metabolic feedback and not changes in IRS-1, Akt, or AS160 phosphorylation. *Am J Physiol Endocrinol Metab,* 297**,** E67-75.

HOY, A. J., BRUCE, C. R., CEDERBERG, A., TURNER, N., JAMES, D. E., COONEY, G. J. & KRAEGEN, E. W. 2007. Glucose infusion causes insulin resistance in skeletal muscle of rats without changes in Akt and AS160 phosphorylation. *Am J Physiol Endocrinol Metab,* 293**,** E1358-64.

HUANG, C., THIRONE, A. C., HUANG, X. & KLIP, A. 2005. Differential contribution of insulin receptor substrates 1 versus 2 to insulin signaling and glucose uptake in l6 myotubes. *J Biol Chem,* 280**,** 19426-35.

HUGHES, V. A., FIATARONE, M. A., FIELDING, R. A., KAHN, B. B., FERRARA, C. M., SHEPHERD, P., FISHER, E. C., WOLFE, R. R., ELAHI, D. & EVANS, W. J. 1993. Exercise increases muscle GLUT-4 levels and insulin action in subjects with impaired glucose tolerance. *Am J Physiol,* 264**,** E855-62.

HULVER, M. W. & DOHM, G. L. 2004. The molecular mechanism linking muscle fat accumulation to insulin resistance. *Proc Nutr Soc,* 63**,** 375-80.

HUNDAL, H. S., DARAKHSHAN, F., KRISTIANSEN, S., BLAKEMORE, S. J. & RICHTER, E. A. 1998. GLUT5 expression and fructose transport in human skeletal muscle. *Adv Exp Med Biol,* 441**,** 35-45.

HYATT, A. D. 1991. *Electron Microscopy in Biology,* New York, Oxford University Press.

IHLEMANN, J., GALBO, H. & PLOUG, T. 1999. Calphostin C is an inhibitor of contraction, but not insulin-stimulated glucose transport, in skeletal muscle. *Acta Physiol Scand,* 167**,** 69-75.

ISHIKURA, S., BILAN, P. J. & KLIP, A. 2007. Rabs 8A and 14 are targets of the insulin-regulated Rab-GAP AS160 regulating GLUT4 traffic in muscle cells. *Biochem Biophys Res Commun,* 353**,** 1074-9.

ISHIKURA, S. & KLIP, A. 2008. Muscle cells engage Rab8A and myosin Vb in insulin-dependent GLUT4 translocation. *Am J Physiol Cell Physiol,* 295**,** C1016-25.

ITANI, S. I., ZHOU, Q., PORIES, W. J., MACDONALD, K. G. & DOHM, G. L. 2000. Involvement of protein kinase C in human skeletal muscle insulin resistance and obesity. *Diabetes,* 49**,** 1353-8.

IVY, J. L. 2004. Muscle insulin resistance amended with exercise training: role of GLUT4 expression. *Med Sci Sports Exerc,* 36**,** 1207-11.

JEBAILEY, L., RUDICH, A., HUANG, X., DI CIANO-OLIVEIRA, C., KAPUS, A. & KLIP, A. 2004. Skeletal muscle cells and adipocytes differ in their reliance on TC10 and Rac for insulin-induced actin remodeling. *Mol Endocrinol,* 18**,** 359-72.

JEWELL, J. L., OH, E., RAMALINGAM, L., KALWAT, M. A., TAGLIABRACCI, V. S., TACKETT, L., ELMENDORF, J. S. & THURMOND, D. C. 2011. Munc18c phosphorylation by the insulin receptor links cell signaling directly to SNARE exocytosis. *J Cell Biol,* 193**,** 185-99.

JONES, D. A. 1990. *Skeletal muscle in health and disease: a textbook of muscle physiology,* Manchester University Press.

JORGENSEN, S. B., RICHTER, E. A. & WOJTASZEWSKI, J. F. 2006. Role of AMPK in skeletal muscle metabolic regulation and adaptation in relation to exercise. *J Physiol,* 574**,** 17-31.

JORGENSEN, S. B., VIOLLET, B., ANDREELLI, F., FROSIG, C., BIRK, J. B., SCHJERLING, P., VAULONT, S., RICHTER, E. A. & WOJTASZEWSKI, J. F. 2004. Knockout of the alpha2 but not alpha1 5'-AMP-activated protein kinase isoform abolishes 5-aminoimidazole-4-carboxamide-1-beta-4-ribofuranosidebut not contraction-induced glucose uptake in skeletal muscle. *J Biol Chem,* 279**,** 1070-9.

KAMPMANN, U., CHRISTENSEN, B., NIELSEN, T. S., PEDERSEN, S. B., ORSKOV, L., LUND, S., MOLLER, N. & JESSEN, N. 2011. GLUT4 and UBC9 protein expression

is reduced in muscle from type 2 diabetic patients with severe insulin resistance. *PLoS One,* 6**,** e27854.

KANE, S., SANO, H., LIU, S. C., ASARA, J. M., LANE, W. S., GARNER, C. C. & LIENHARD, G. E. 2002. A method to identify serine kinase substrates. Akt phosphorylates a novel adipocyte protein with a Rab GTPase-activating protein (GAP) domain. *J Biol Chem,* 277**,** 22115-8.

KARELIS, A.D., ST-PIERRE, D.H., CONUS, F., RABASA-LHORET, R. & POEHLMAN, E.T. 2004. Metabolic and body composition factors in subgroups of obesity: what do we know? *J. Clin. Endocrinol. Metab.*, 89, 2569-2575.

KARLSSON, H. K. & ZIERATH, J. R. 2007. Insulin signaling and glucose transport in insulin resistant human skeletal muscle. *Cell Biochem Biophys,* 48**,** 103-13.

KATZ, A., BROBERG, S., SAHLIN, K. & WAHREN, J. 1986. Leg glucose uptake during maximal dynamic exercise in humans. *Am J Physiol,* 251**,** E65-70.

KATZ, A., SAHLIN, K. & BROBERG, S. 1991. Regulation of glucose utilization in human skeletal muscle during moderate dynamic exercise. *Am J Physiol,* 260**,** E411-5.

KATZ, E. B., STENBIT, A. E., HATTON, K., DEPINHO, R. & CHARRON, M. J. 1995. Cardiac and adipose tissue abnormalities but not diabetes in mice deficient in GLUT4. *Nature,* 377**,** 151-5.

KATZ, L. D., GLICKMAN, M. G., RAPOPORT, S., FERRANNINI, E. & DEFRONZO, R. A. 1983. Splanchnic and peripheral disposal of oral glucose in man. *Diabetes,* 32**,** 675-9.

KAWAGUCHI, T., TAMORI, Y., KANDA, H., YOSHIKAWA, M., TATEYA, S., NISHINO, N. & KASUGA, M. 2010. The t-SNAREs syntaxin4 and SNAP23 but not v-SNARE VAMP2 are indispensable to tether GLUT4 vesicles at the plasma membrane in adipocyte. *Biochem Biophys Res Commun,* 391**,** 1336-41.

KELLEY, D. E., HE, J., MENSHIKOVA, E. V. & RITOV, V. B. 2002. Dysfunction of mitochondria in human skeletal muscle in type 2 diabetes. *Diabetes,* 51**,** 2944-50.

KELLY, T., YANG, W., CHEN, C. S., REYNOLDS, K. & HE, J. 2008. Global burden of obesity in 2005 and projections to 2030. *Int J Obes (Lond),* 32**,** 1431-7.

KENNEDY, J. W., HIRSHMAN, M. F., GERVINO, E. V., OCEL, J. V., FORSE, R. A., HOENIG, S. J., ARONSON, D., GOODYEAR, L. J. & HORTON, E. S. 1999. Acute exercise induces GLUT4 translocation in skeletal muscle of normal human subjects and subjects with type 2 diabetes. *Diabetes,* 48**,** 1192-7.

KESKE, M. A., CLERK, L. H., PRICE, W. J., JAHN, L. A. & BARRETT, E. J. 2009. Obesity blunts microvascular recruitment in human forearm muscle after a mixed meal. *Diabetes Care,* 32**,** 1672-7.

KHAN, A. H., THURMOND, D. C., YANG, C., CERESA, B. P., SIGMUND, C. D. & PESSIN, J. E. 2001. Munc18c regulates insulin-stimulated glut4 translocation to the transverse tubules in skeletal muscle. *J Biol Chem,* 276**,** 4063-9.

KHAN, Z. A. & CHAKRABARTI, S. 2006. Therapeutic targeting of endothelial dysfunction in chronic diabetic complications. *Recent Pat Cardiovasc Drug Discov,* 1**,** 167-75.

KHAYAT, Z. A., TONG, P., YAWORSKY, K., BLOCH, R. J. & KLIP, A. 2000. Insulin-induced actin filament remodeling colocalizes actin with phosphatidylinositol 3-kinase and GLUT4 in L6 myotubes. *J Cell Sci,* 113 Pt 2**,** 279-90.

KIM, J. A., WEI, Y. & SOWERS, J. R. 2008. Role of mitochondrial dysfunction in insulin resistance. *Circ Res,* 102**,** 401-14.

KJAER, M., KIENS, B., HARGREAVES, M. & RICHTER, E. A. 1991. Influence of active muscle mass on glucose homeostasis during exercise in humans. *J Appl Physiol,* 71**,** 552-7.

KLIP, A., RAMLAL, T., YOUNG, D. A. & HOLLOSZY, J. O. 1987. Insulin-induced translocation of glucose transporters in rat hindlimb muscles. *FEBS Lett,* 224**,** 224-30.

KRAMER, H. F., TAYLOR, E. B., WITCZAK, C. A., FUJII, N., HIRSHMAN, M. F. & GOODYEAR, L. J. 2007. Calmodulin-binding domain of AS160 regulates contraction- but not insulin-stimulated glucose uptake in skeletal muscle. *Diabetes,* 56**,** 2854-62.

KRAMER, H. F., WITCZAK, C. A., FUJII, N., JESSEN, N., TAYLOR, E. B., ARNOLDS, D. E., SAKAMOTO, K., HIRSHMAN, M. F. & GOODYEAR, L. J. 2006a. Distinct signals regulate AS160 phosphorylation in response to insulin, AICAR, and contraction in mouse skeletal muscle. *Diabetes,* 55**,** 2067-76.

KRAMER, H. F., WITCZAK, C. A., TAYLOR, E. B., FUJII, N., HIRSHMAN, M. F. & GOODYEAR, L. J. 2006b. AS160 regulates insulin- and contraction-stimulated glucose uptake in mouse skeletal muscle. *J Biol Chem,* 281**,** 31478-85.

KRANIOU, G. N., CAMERON-SMITH, D. & HARGREAVES, M. 2006. Acute exercise and GLUT4 expression in human skeletal muscle: influence of exercise intensity. *J Appl Physiol,* 101**,** 934-7.

KRISTIANSEN, S., HARGREAVES, M. & RICHTER, E. A. 1996. Exercise-induced increase in glucose transport, GLUT-4, and VAMP-2 in plasma membrane from human muscle. *Am J Physiol,* 270**,** E197-201.

KROOK, A., WALLBERG-HENRIKSSON, H. & ZIERATH, J. R. 2004. Sending the signal: molecular mechanisms regulating glucose uptake. *Med Sci Sports Exerc,* 36**,** 1212-7.

LARANCE, M., RAMM, G. & JAMES, D. E. 2008. The GLUT4 code. *Mol Endocrinol,* 22**,** 226-33.

LARANCE, M., RAMM, G., STOCKLI, J., VAN DAM, E. M., WINATA, S., WASINGER, V., SIMPSON, F., GRAHAM, M., JUNUTULA, J. R., GUILHAUS, M. & JAMES, D. E. 2005. Characterization of the role of the Rab GTPase-activating protein AS160 in insulin-regulated GLUT4 trafficking. *J Biol Chem,* 280**,** 37803-13.

LARSEN, S., ARA, I., RABOL, R., ANDERSEN, J.L., BOUSHEL, R., DELA, F. & HELGE, J.W. 2009. Are substrate use during exercise and mitochondrial respiratory capacity decreased in arm and leg muscle in type 2 diabetes? *Diabetologia, 52,* 1400-1408.

LAURITZEN, H. P., GALBO, H., BRANDAUER, J., GOODYEAR, L. J. & PLOUG, T. 2008. Large GLUT4 vesicles are stationary while locally and reversibly depleted during transient insulin stimulation of skeletal muscle of living mice: imaging analysis of GLUT4-enhanced green fluorescent protein vesicle dynamics. *Diabetes,* 57**,** 315-24.

LAURITZEN, H. P., GALBO, H., TOYODA, T. & GOODYEAR, L. J. 2010. Kinetics of contraction-induced GLUT4 translocation in skeletal muscle fibers from living mice. *Diabetes,* 59**,** 2134-44.

LAURITZEN, H. P., PLOUG, T., PRATS, C., TAVARE, J. M. & GALBO, H. 2006. Imaging of insulin signaling in skeletal muscle of living mice shows major role of T-tubules. *Diabetes,* 55**,** 1300-6.

LAURITZEN, H. P. & SCHERTZER, J. D. 2010. Measuring GLUT4 translocation in mature muscle fibers. *Am J Physiol Endocrinol Metab,* 299**,** E169-79.

LEMIEUX, K., HAN, X. X., DOMBROWSKI, L., BONEN, A. & MARETTE, A. 2000. The transferrin receptor defines two distinct contraction-responsive GLUT4 vesicle populations in skeletal muscle. *Diabetes,* 49**,** 183-9.

LETURQUE, A., LOIZEAU, M., VAULONT, S., SALMINEN, M. & GIRARD, J. 1996. Improvement of insulin action in diabetic transgenic mice selectively overexpressing GLUT4 in skeletal muscle. *Diabetes,* 45**,** 23-7.

LI, J., KING, N. C. & SINOWAY, L. I. 2003. ATP concentrations and muscle tension increase linearly with muscle contraction. *J Appl Physiol,* 95**,** 577-83.

LI, M., PARAN, C., WOLINS, N. E. & HOROWITZ, J. F. 2011. High muscle lipid content in obesity is not due to enhanced activation of key triglyceride esterification enzymes or the suppression of lipolytic proteins. *Am J Physiol Endocrinol Metab,* 300**,** E699-707.

LINDEN, K. C., WADLEY, G. D., GARNHAM, A. P. & MCCONELL, G. K. 2011. Effect of l-arginine infusion on glucose disposal during exercise in humans. *Med Sci Sports Exerc,* 43**,** 1626-34.

LITTLE, J. P., SAFDAR, A., WILKIN, G. P., TARNOPOLSKY, M. A. & GIBALA, M. J. 2010. A practical model of low-volume high-intensity interval training induces mitochondrial biogenesis in human skeletal muscle: potential mechanisms. *J Physiol,* 588**,** 1011-22.

LIU, L., SHI, X., CHOI, C. S., SHULMAN, G. I., KLAUS, K., NAIR, K. S., SCHWARTZ, G. J., ZHANG, Y., GOLDBERG, I. J. & YU, Y. H. 2009a. Paradoxical coupling of triglyceride synthesis and fatty acid oxidation in skeletal muscle overexpressing DGAT1. *Diabetes,* 58**,** 2516-24.

LIU, M. L., GIBBS, E. M., MCCOID, S. C., MILICI, A. J., STUKENBROK, H. A., MCPHERSON, R. K., TREADWAY, J. L. & PESSIN, J. E. 1993. Transgenic mice expressing the human GLUT4/muscle-fat facilitative glucose transporter protein exhibit efficient glycemic control. *Proc Natl Acad Sci U S A,* 90**,** 11346-50.

LIU, Z., LIU, J., JAHN, L. A., FOWLER, D. E. & BARRETT, E. J. 2009b. Infusing lipid raises plasma free fatty acids and induces insulin resistance in muscle microvasculature. *J Clin Endocrinol Metab,* 94**,** 3543-9.

LOWELL, B. B. & SHULMAN, G. I. 2005. Mitochondrial dysfunction and type 2 diabetes. *Science,* 307**,** 384-7.

MALENFANT, P., TREMBLAY, A., DOUCET, E., IMBEAULT, P., SIMONEAU, J. A. & JOANISSE, D. R. 2001. Elevated intramyocellular lipid concentration in obese subjects is not reduced after diet and exercise training. *Am J Physiol Endocrinol Metab,* 280**,** E632-9.

MANLEY, S. 2003. Haemoglobin A1c--a marker for complications of type 2 diabetes: the experience from the UK Prospective Diabetes Study (UKPDS). *Clin Chem Lab Med,* 41**,** 1182-90.

MARETTE, A., BURDETT, E., DOUEN, A., VRANIC, M. & KLIP, A. 1992. Insulin induces the translocation of GLUT4 from a unique intracellular organelle to transverse tubules in rat skeletal muscle. *Diabetes,* 41**,** 1562-9.

MARSHALL, B. A. & MUECKLER, M. M. 1994. Differential effects of GLUT-1 or GLUT-4 overexpression on insulin responsiveness in transgenic mice. *Am J Physiol,* 267**,** E738-44.

MARSHALL, B. A., REN, J. M., JOHNSON, D. W., GIBBS, E. M., LILLQUIST, J. S., SOELLER, W. C., HOLLOSZY, J. O. & MUECKLER, M. 1993. Germline manipulation of glucose homeostasis via alteration of glucose transporter levels in skeletal muscle. *J Biol Chem,* 268**,** 18442-5.

MARTIN, I. K., KATZ, A. & WAHREN, J. 1995. Splanchnic and muscle metabolism during exercise in NIDDM patients. *Am J Physiol,* 269**,** E583-90.

MARTIN, S. S., HARUTA, T., MORRIS, A. J., KLIPPEL, A., WILLIAMS, L. T. & OLEFSKY, J. M. 1996. Activated phosphatidylinositol 3-kinase is sufficient to mediate actin rearrangement and GLUT4 translocation in 3T3-L1 adipocytes. *J Biol Chem,* 271**,** 17605-8.

MATSUDA, M. & DEFRONZO, R. A. 1999. Insulin sensitivity indices obtained from oral glucose tolerance testing: comparison with the euglycemic insulin clamp. *Diabetes Care,* 22**,** 1462-70.

MCCONELL, G. K., RATTIGAN, S., LEE-YOUNG, R. S., WADLEY, G. D. & MERRY, T. L. 2012. Skeletal muscle nitric oxide signaling and exercise: a focus on glucose metabolism. *Am J Physiol Endocrinol Metab,* 303**,** E301-7.

MCGEE, S. L., SPARLING, D., OLSON, A. L. & HARGREAVES, M. 2006. Exercise increases MEF2- and GEF DNA-binding activity in human skeletal muscle. *FASEB J,* 20**,** 348-9.

MCGEE, S. L., VAN DENDEREN, B. J. W., HOWLETT, K. F., MOLLICA, J., SCHERTZER, J. D., KEMP, B. E. & HARGREAVES, M. 2008. AMP-Activated Protein Kinase Regulates GLUT4 Transcription by Phosphorylating Histone Deacetylase 5. *Diabetes,* 57**,** 860-867.

MERRY, T.L., STEINBERG, G.R., LYNCH, G.S. & MCCONNEL, G.K. 2010. Skeletal muscle glucose uptake during contraction is regulated by nitric oxide and ROS independently of AMPK. *Am J Physiol Endocrinol Metab*, 298, E577-E585.

MIINEA, C. P., SANO, H., KANE, S., SANO, E., FUKUDA, M., PERANEN, J., LANE, W. S. & LIENHARD, G. E. 2005. AS160, the Akt substrate regulating GLUT4 translocation, has a functional Rab GTPase-activating protein domain. *Biochem J,* 391**,** 87-93.

MIKINES, K. J., FARRELL, P. A., SONNE, B., TRONIER, B. & GALBO, H. 1988. Postexercise dose-response relationship between plasma glucose and insulin secretion. *J Appl Physiol,* 64**,** 988-99.

MINOKOSHI, Y., KAHN, C. R. & KAHN, B. B. 2003. Tissue-specific ablation of the GLUT4 glucose transporter or the insulin receptor challenges assumptions about insulin action and glucose homeostasis. *J Biol Chem,* 278**,** 33609-12.

MINUK, H. L., VRANIC, M., MARLISS, E. B., HANNA, A. K., ALBISSER, A. M. & ZINMAN, B. 1981. Glucoregulatory and metabolic response to exercise in obese noninsulin-dependent diabetes. *Am J Physiol,* 240**,** E458-64.

MORINO, K., PETERSEN, K. F. & SHULMAN, G. I. 2006. Molecular mechanisms of insulin resistance in humans and their potential links with mitochondrial dysfunction. *Diabetes,* 55 Suppl 2**,** S9-S15.

MORO, C., BAJPEYI, S. & SMITH, S. R. 2008. Determinants of intramyocellular triglyceride turnover: implications for insulin sensitivity. *Am J Physiol Endocrinol Metab,* 294**,** E203-13.

MORO, C., GALGANI, J. E., LUU, L., PASARICA, M., MAIRAL, A., BAJPEYI, S., SCHMITZ, G., LANGIN, D., LIEBISCH, G. & SMITH, S. R. 2009. Influence of gender, obesity, and muscle lipase activity on intramyocellular lipids in sedentary individuals. *J Clin Endocrinol Metab,* 94**,** 3440-7.

MU, J., BARTON, E. R. & BIRNBAUM, M. J. 2003. Selective suppression of AMP-activated protein kinase in skeletal muscle: update on 'lazy mice'. *Biochem Soc Trans,* 31**,** 236-41.

MU, J., BROZINICK, J. T., JR., VALLADARES, O., BUCAN, M. & BIRNBAUM, M. J. 2001. A role for AMP-activated protein kinase in contraction- and hypoxia-regulated glucose transport in skeletal muscle. *Mol Cell,* 7**,** 1085-94.

MUECKLER, M. 1994. Facilitative glucose transporters. *Eur J Biochem,* 219**,** 713-25.

MUNIYAPPA, R., LEE, S., CHEN, H. & QUON, M.J. 2008. Current approaches for assessing insulin sensitivity and resistance in vivo: advantages limitations and appropriate usage. *Am J Physiol Endocrinol Metab,* 294, E15-E26.

MURPHY, R. M., MOLLICA, J. P. & LAMB, G. D. 2009. Plasma membrane removal in rat skeletal muscle fibers reveals caveolin-3 hot-spots at the necks of transverse tubules. *Exp Cell Res,* 315**,** 1015-28.

MUSI, N., FUJII, N., HIRSHMAN, M. F., EKBERG, I., FROBERG, S., LJUNGQVIST, O., THORELL, A. & GOODYEAR, L. J. 2001. AMP-activated protein kinase (AMPK) is activated in muscle of subjects with type 2 diabetes during exercise. *Diabetes,* 50**,** 921-7.

NATHAN, C. 2003. Specificity of a third kind: reactive oxygen and nitrogen intermediates in cell signaling. *J Clin Invest,* 111**,** 769-78.

NEUFER, P. D. & DOHM, G. L. 1993. Exercise induces a transient increase in transcription of the GLUT-4 gene in skeletal muscle. *Am J Physiol,* 265**,** C1597-603.

NISHIZUKA, Y. 1995. Protein kinase C and lipid signaling for sustained cellular responses. *FASEB J,* 9**,** 484-96.

NOUROOZ-ZADEH, J., RAHIMI, A., TAJADDINI-SARMADI, J., TRITSCHLER, H., ROSEN, P., HALLIWELL, B. & BETTERIDGE, D. J. 1997. Relationships between

plasma measures of oxidative stress and metabolic control in NIDDM. *Diabetologia,* 40**,** 647-53.

OH, E. & THURMOND, D. C. 2006. The stimulus-induced tyrosine phosphorylation of Munc18c facilitates vesicle exocytosis. *J Biol Chem,* 281**,** 17624-34.

OJUKA, E. O., GOYARAM, V. & SMITH, J. A. 2012. The role of CaMKII in regulating GLUT4 expression in skeletal muscle. *Am J Physiol Endocrinol Metab,* 303**,** E322-31.

OSCAI, L. B. & HOLLOSZY, J. O. 1971. Biochemical adaptations in muscle. II. Response of mitochondrial adenosine triphosphatase, creatine phosphokinase, and adenylate kinase activities in skeletal muscle to exercise. *J Biol Chem,* 246**,** 6968-72.

OSORIO-FUENTEALBA, C., CONTRERAS-FERRAT, A. E., ALTAMIRANO, F., ESPINOSA, A., LI, Q., NIU, W., LAVANDERO, S., KLIP, A. & JAIMOVICH, E. 2013. Electrical Stimuli Release ATP to Increase GLUT4 Translocation and Glucose Uptake via PI3Kgamma-Akt-AS160 in Skeletal Muscle Cells. *Diabetes,* 62**,** 1519-26.

PAN, D. A., LILLIOJA, S., KRIKETOS, A. D., MILNER, M. R., BAUR, L. A., BOGARDUS, C., JENKINS, A. B. & STORLIEN, L. H. 1997. Skeletal muscle triglyceride levels are inversely related to insulin action. *Diabetes,* 46**,** 983-8.

PARK, T. S., PARK, J. H. & BAEK, H. S. 2004. Can diabetic neuropathy be prevented? *Diabetes Res Clin Pract,* 66 Suppl 1**,** S53-6.

PEACHEY, L. D. & EISENBERG, B. R. 1978. Helicoids in the T system and striations of frog skeletal muscle fibers seen by high voltage electron microscopy. *Biophys J,* 22**,** 145-54.

PEDERSEN, O., BAK, J. F., ANDERSEN, P. H., LUND, S., MOLLER, D. E., FLIER, J. S. & KAHN, B. B. 1990. Evidence against altered expression of GLUT1 or GLUT4 in skeletal muscle of patients with obesity or NIDDM. *Diabetes,* 39**,** 865-70.

PERREAULT, L., BERGMAN, B. C., HUNERDOSSE, D. M. & ECKEL, R. H. 2010. Altered intramuscular lipid metabolism relates to diminished insulin action in men, but not women, in progression to diabetes. *Obesity (Silver Spring),* 18**,** 2093-100.

PESSIN, J. E., THURMOND, D. C., ELMENDORF, J. S., COKER, K. J. & OKADA, S. 1999. Molecular basis of insulin-stimulated GLUT4 vesicle trafficking. Location! Location! Location! *J Biol Chem,* 274**,** 2593-6.

PETERSEN, K.F., DUFOUR, S., BEFROY, D., GARCIA, R. & SHULMAN, G.I. 2004. Impaired mitochondrial activity in the insulin-resistant offspring of patients with type 2 diabetes. *N Engl J Med,* 350, 664-671.

PETERSEN, K.F., DUFOUR, S. & SHULMAN, G.I. 2005. Decreased insulin-stimulated ATP synthesis and phosphate transport in muscle of insulin-resistant offspring of type 2 diabetic parents. *PLos Med,* 2, e233.

PHILLIPS, D. I., CADDY, S., ILIC, V., FIELDING, B. A., FRAYN, K. N., BORTHWICK, A. C. & TAYLOR, R. 1996a. Intramuscular triglyceride and muscle insulin sensitivity: evidence for a relationship in nondiabetic subjects. *Metabolism,* 45**,** 947-50.

PHILLIPS, S. M., HAN, X. X., GREEN, H. J. & BONEN, A. 1996b. Increments in skeletal muscle GLUT-1 and GLUT-4 after endurance training in humans. *Am J Physiol,* 270**,** E456-62.

PLOUG, T., VAN DEURS, B., AI, H., CUSHMAN, S. W. & RALSTON, E. 1998. Analysis of GLUT4 distribution in whole skeletal muscle fibers: identification of distinct storage compartments that are recruited by insulin and muscle contractions. *J Cell Biol,* 142**,** 1429-46.

PURCELL, S. H., AERNI-FLESSNER, L. B., WILLCOCKSON, A. R., DIGGS-ANDREWS, K. A., FISHER, S. J. & MOLEY, K. H. 2011. Improved insulin sensitivity by GLUT12 overexpression in mice. *Diabetes,* 60**,** 1478-82.

RABOL, R., HOJBERG, P.M., ALMDAL, T., BOUSHEL, R., HAUGAARD, S.B., MADSBAD, S. & DELA, F. 2009. Effect of hyperglycemia on mitochondrial respiration in type 2 diabetes. *J Clin Endocrinol Metab,* 94, 1372-1378.

RALSTON, E. & PLOUG, T. 1996. Pre-embedding staining of single muscle fibers for light and electron microscopy studies of subcellular organization. *Scanning Microsc Suppl,* 10**,** 249-59; discussion 259-60.

RAMM, G., LARANCE, M., GUILHAUS, M. & JAMES, D. E. 2006. A role for 14-3-3 in insulin-stimulated GLUT4 translocation through its interaction with the RabGAP AS160. *J Biol Chem,* 281**,** 29174-80.

RANDHAWA, V. K., BILAN, P. J., KHAYAT, Z. A., DANEMAN, N., LIU, Z., RAMLAL, T., VOLCHUK, A., PENG, X. R., COPPOLA, T., REGAZZI, R., TRIMBLE, W. S. & KLIP, A. 2000. VAMP2, but not VAMP3/cellubrevin, mediates insulin-dependent incorporation of GLUT4 into the plasma membrane of L6 myoblasts. *Mol Biol Cell,* 11**,** 2403-17.

RATTIGAN, S., CLARK, M. G. & BARRETT, E. J. 1997. Hemodynamic actions of insulin in rat skeletal muscle: evidence for capillary recruitment. *Diabetes,* 46**,** 1381-8.

REN, J. M., MARSHALL, B. A., GULVE, E. A., GAO, J., JOHNSON, D. W., HOLLOSZY, J. O. & MUECKLER, M. 1993. Evidence from transgenic mice that glucose transport is rate-limiting for glycogen deposition and glycolysis in skeletal muscle. *J Biol Chem,* 268**,** 16113-5.

REN, J. M., MARSHALL, B. A., MUECKLER, M. M., MCCALEB, M., AMATRUDA, J. M. & SHULMAN, G. I. 1995. Overexpression of Glut4 protein in muscle increases basal and insulin-stimulated whole body glucose disposal in conscious mice. *J Clin Invest,* 95**,** 429-32.

REN, J. M., SEMENKOVICH, C. F., GULVE, E. A., GAO, J. & HOLLOSZY, J. O. 1994. Exercise induces rapid increases in GLUT4 expression, glucose transport capacity, and insulin-stimulated glycogen storage in muscle. *J Biol Chem,* 269**,** 14396-401.

RICHARDS, J. C., JOHNSON, T. K., KUZMA, J. N., LONAC, M. C., SCHWEDER, M. M., VOYLES, W. F. & BELL, C. 2010. Short-term sprint interval training increases insulin sensitivity in healthy adults but does not affect the thermogenic response to beta-adrenergic stimulation. *J Physiol,* 588**,** 2961-72.

RICHTER, E. A., CLELAND, P. J., RATTIGAN, S. & CLARK, M. G. 1987. Contraction-associated translocation of protein kinase C in rat skeletal muscle. *FEBS Lett,* 217**,** 232-6.

RICHTER, E. A. & HARGREAVES, M. 2013. Exercise, GLUT4, and Skeletal Muscle Glucose Uptake. *Physiol Rev,* 93**,** 993-1017.

RICHTER, E. A., MIKINES, K. J., GALBO, H. & KIENS, B. 1989. Effect of exercise on insulin action in human skeletal muscle. *J Appl Physiol,* 66**,** 876-85.

RITOV, V.B., MENSHIKOVA, E.V., AZUMA, K., WOOD, R., TOLEDO, F.G., GOODPASTER, B.H., RUDERMAN, N.B. & KELLEY, D.E. 2010. Deficiency of electron transport chain in human skeletal muscle mitochondria in type 2 diabetes mellitus and obesity. *Am J Physiol Endocrinol Metab*, 298- E49-E58.

ROACH, W. G., CHAVEZ, J. A., MIINEA, C. P. & LIENHARD, G. E. 2007. Substrate specificity and effect on GLUT4 translocation of the Rab GTPase-activating protein Tbc1d1. *Biochem J,* 403**,** 353-8.

ROCKL, K. S., WITCZAK, C. A. & GOODYEAR, L. J. 2008. Signaling mechanisms in skeletal muscle: acute responses and chronic adaptations to exercise. *IUBMB Life,* 60**,** 145-53.

RODEN, M., KRSSAK, M., STINGL, H., GRUBER, S., HOFER, A., FURNSINN, C., MOSER, E. & WALDHAUSL, W. 1999. Rapid impairment of skeletal muscle glucose transport/phosphorylation by free fatty acids in humans. *Diabetes,* 48**,** 358-64.

RODEN, M., PRICE, T. B., PERSEGHIN, G., PETERSEN, K. F., ROTHMAN, D. L., CLINE, G. W. & SHULMAN, G. I. 1996. Mechanism of free fatty acid-induced insulin resistance in humans. *J Clin Invest,* 97**,** 2859-65.

ROGERS, S., CHANDLER, J. D., CLARKE, A. L., PETROU, S. & BEST, J. D. 2003. Glucose transporter GLUT12-functional characterization in Xenopus laevis oocytes. *Biochem Biophys Res Commun,* 308**,** 422-6.

ROGERS, S., MACHEDA, M. L., DOCHERTY, S. E., CARTY, M. D., HENDERSON, M. A., SOELLER, W. C., GIBBS, E. M., JAMES, D. E. & BEST, J. D. 2002.

Identification of a novel glucose transporter-like protein-GLUT-12. *Am J Physiol Endocrinol Metab,* 282**,** E733-8.

ROORDA, B. D., HESSELINK, M. K., SCHAART, G., MOONEN-KORNIPS, E., MARTINEZ-MARTINEZ, P., LOSEN, M., DE BAETS, M. H., MENSINK, R. P. & SCHRAUWEN, P. 2005. DGAT1 overexpression in muscle by in vivo DNA electroporation increases intramyocellular lipid content. *J Lipid Res,* 46**,** 230-6.

ROSE, A. J. & HARGREAVES, M. 2003. Exercise increases Ca2+-calmodulin-dependent protein kinase II activity in human skeletal muscle. *J Physiol,* 553**,** 303-9.

ROSE, A. J., JEPPESEN, J., KIENS, B. & RICHTER, E. A. 2009. Effects of contraction on localization of GLUT4 and v-SNARE isoforms in rat skeletal muscle. *Am J Physiol Regul Integr Comp Physiol,* 297**,** R1228-37.

ROSE, A. J., MICHELL, B. J., KEMP, B. E. & HARGREAVES, M. 2004. Effect of exercise on protein kinase C activity and localization in human skeletal muscle. *J Physiol,* 561**,** 861-70.

ROSE, A. J. & RICHTER, E. A. 2005. Skeletal muscle glucose uptake during exercise: how is it regulated? *Physiology (Bethesda),* 20**,** 260-70.

RUDERMAN, N., Chisholm, D., Pi-Sunyer, X. & Schneider, S. 1998. The metabolically obese, normal-weight individual revisited. *Diabetes,* 47, 699-713.

RYDER, J. W., KAWANO, Y., GALUSKA, D., FAHLMAN, R., WALLBERG-HENRIKSSON, H., CHARRON, M. J. & ZIERATH, J. R. 1999. Postexercise glucose uptake and glycogen synthesis in skeletal muscle from GLUT4-deficient mice. *FASEB J,* 13**,** 2246-56.

SALTIEL, A. R. & KAHN, C. R. 2001. Insulin signalling and the regulation of glucose and lipid metabolism. *Nature,* 414**,** 799-806.

SANO, H., KANE, S., SANO, E., MIINEA, C. P., ASARA, J. M., LANE, W. S., GARNER, C. W. & LIENHARD, G. E. 2003. Insulin-stimulated phosphorylation of a Rab GTPase-activating protein regulates GLUT4 translocation. *J Biol Chem,* 278**,** 14599-602.

SCHENK, S. & HOROWITZ, J. F. 2007. Acute exercise increases triglyceride synthesis in skeletal muscle and prevents fatty acid-induced insulin resistance. *J Clin Invest,* 117**,** 1690-8.

SCHERTZER, J. D., ANTONESCU, C. N., BILAN, P. J., JAIN, S., HUANG, X., LIU, Z., BONEN, A. & KLIP, A. 2009. A transgenic mouse model to study glucose transporter 4myc regulation in skeletal muscle. *Endocrinology,* 150**,** 1935-40.

SCHNEIDER, S. H., WOOD JOHNSON, R. & RUDERMAN, N. B. 1990. Exercise and NIDDM. *Diabetes Care,* 13**,** 785-9.

SCHRAUWEN, P., VAN AGGEL-LEIJSSEN, D. P., HUL, G., WAGENMAKERS, A. J., VIDAL, H., SARIS, W. H. & VAN BAAK, M. A. 2002. The effect of a 3-month low-intensity endurance training program on fat oxidation and acetyl-CoA carboxylase-2 expression. *Diabetes,* 51**,** 2220-6.

SCHWENK, R. W., DIRKX, E., COUMANS, W. A., BONEN, A., KLIP, A., GLATZ, J. F. & LUIKEN, J. J. 2010. Requirement for distinct vesicle-associated membrane proteins in insulin- and AMP-activated protein kinase (AMPK)-induced translocation of GLUT4 and CD36 in cultured cardiomyocytes. *Diabetologia,* 53**,** 2209-19.

SHARMA, P. M., EGAWA, K., HUANG, Y., MARTIN, J. L., HUVAR, I., BOSS, G. R. & OLEFSKY, J. M. 1998. Inhibition of phosphatidylinositol 3-kinase activity by adenovirus-mediated gene transfer and its effect on insulin action. *J Biol Chem,* 273**,** 18528-37.

SHAW, C. S., CLARK, J. & WAGENMAKERS, A. J. 2010. The effect of exercise and nutrition on intramuscular fat metabolism and insulin sensitivity. *Annu Rev Nutr,* 30**,** 13-34.

SHAW, C. S., SHERLOCK, M., STEWART, P. M. & WAGENMAKERS, A. J. 2009. Adipophilin distribution and colocalization with lipid droplets in skeletal muscle. *Histochem Cell Biol,* 131**,** 575-81.

SHEPHERD, S. O., COCKS, M., TIPTON, K. D., RANASINGHE, A. M., BARKER, T. A., BURNISTON, J. G., WAGENMAKERS, A. J. & SHAW, C. S. 2013. Sprint interval and traditional endurance training increase net intramuscular triglyceride breakdown and expression of perilipin 2 and 5. *J Physiol,* 591**,** 657-75.

SHULMAN, G. I. 2000. Cellular mechanisms of insulin resistance. *J Clin Invest,* 106**,** 171-6.

SOLLNER, T. H. 2007. Lipid droplets highjack SNAREs. *Nat Cell Biol,* 9**,** 1219-20.

STEINBERG, H. O., BRECHTEL, G., JOHNSON, A., FINEBERG, N. & BARON, A. D. 1994. Insulin-mediated skeletal muscle vasodilation is nitric oxide dependent. A novel action of insulin to increase nitric oxide release. *J Clin Invest,* 94**,** 1172-9.

STELLINGWERFF, T., BOON, H., GIJSEN, A. P., STEGEN, J. H., KUIPERS, H. & VAN LOON, L. J. 2007a. Carbohydrate supplementation during prolonged cycling exercise spares muscle glycogen but does not affect intramyocellular lipid use. *Pflugers Arch,* 454**,** 635-47.

STELLINGWERFF, T., BOON, H., JONKERS, R. A., SENDEN, J. M., SPRIET, L. L., KOOPMAN, R. & VAN LOON, L. J. 2007b. Significant intramyocellular lipid use during prolonged cycling in endurance-trained males as assessed by three different methodologies. *Am J Physiol Endocrinol Metab,* 292**,** E1715-23.

STENBIT, A. E., BURCELIN, R., KATZ, E. B., TSAO, T. S., GAUTIER, N., CHARRON, M. J. & LE MARCHAND-BRUSTEL, Y. 1996. Diverse effects of Glut 4 ablation on glucose uptake and glycogen synthesis in red and white skeletal muscle. *J Clin Invest,* 98**,** 629-34.

STIRBAN, A. O. & TSCHOEPE, D. 2008. Cardiovascular complications in diabetes: targets and interventions. *Diabetes Care,* 31 Suppl 2**,** S215-21.

STOCKLI, J., FAZAKERLEY, D. J. & JAMES, D. E. 2011. GLUT4 exocytosis. *J Cell Sci,* 124**,** 4147-59.

STORGAARD, H., JENSEN, C. B., BJORNHOLM, M., SONG, X. M., MADSBAD, S., ZIERATH, J. R. & VAAG, A. A. 2004. Dissociation between fat-induced in vivo insulin resistance and proximal insulin signaling in skeletal muscle in men at risk for type 2 diabetes. *J Clin Endocrinol Metab,* 89**,** 1301-11.

STUART, C. A., HOWELL, M. E., BAKER, J. D., DYKES, R. J., DUFFOURC, M. M., RAMSEY, M. W. & STONE, M. H. 2010. Cycle training increased GLUT4 and activation of mammalian target of rapamycin in fast twitch muscle fibers. *Med Sci Sports Exerc,* 42**,** 96-106.

STUART, C. A., HOWELL, M. E., ZHANG, Y. & YIN, D. 2009. Insulin-stimulated translocation of glucose transporter (GLUT) 12 parallels that of GLUT4 in normal muscle. *J Clin Endocrinol Metab,* 94**,** 3535-42.

STUART, C. A., YIN, D., HOWELL, M. E., DYKES, R. J., LAFFAN, J. J. & FERRANDO, A. A. 2006. Hexose transporter mRNAs for GLUT4, GLUT5, and GLUT12 predominate in human muscle. *Am J Physiol Endocrinol Metab,* 291**,** E1067-73.

SUN, Y., BILAN, P. J., LIU, Z. & KLIP, A. 2010. Rab8A and Rab13 are activated by insulin and regulate GLUT4 translocation in muscle cells. *Proc Natl Acad Sci U S A,* 107**,** 19909-14.

SYLOW, L., JENSEN, T. E., KLEINERT, M., HOJLUND, K., KIENS, B., WOJTASZEWSKI, J., PRATS, C., SCHJERLING, P. & RICHTER, E. A. 2013a. Rac1 Signaling Is Required for Insulin-Stimulated Glucose Uptake and Is Dysregulated in Insulin-Resistant Murine and Human Skeletal Muscle. *Diabetes,* 62**,** 1865-1875.

SYLOW, L., JENSEN, T. E., KLEINERT, M., MOUATT, J. R., MAARBJERG, S. J., JEPPESEN, J., PRATS, C., CHIU, T. T., BOGUSLAVSKY, S., KLIP, A., SCHJERLING, P. & RICHTER, E. A. 2013b. Rac1 is a novel regulator of contraction-stimulated glucose uptake in skeletal muscle. *Diabetes,* 62**,** 1139-51.

TAKEUCHI, K. & REUE, K. 2009. Biochemistry, physiology, and genetics of GPAT, AGPAT, and lipin enzymes in triglyceride synthesis. *Am J Physiol Endocrinol Metab,* 296**,** E1195-209.

TAMEMOTO, H., KADOWAKI, T., TOBE, K., YAGI, T., SAKURA, H., HAYAKAWA, T., TERAUCHI, Y., UEKI, K., KABURAGI, Y., SATOH, S. & ET AL. 1994. Insulin resistance and growth retardation in mice lacking insulin receptor substrate-1. *Nature,* 372**,** 182-6.

TELLAM, J. T., MACAULAY, S. L., MCINTOSH, S., HEWISH, D. R., WARD, C. W. & JAMES, D. E. 1997. Characterization of Munc-18c and syntaxin-4 in 3T3-L1 adipocytes. Putative role in insulin-dependent movement of GLUT-4. *J Biol Chem,* 272**,** 6179-86.

TELLAM, J. T., MCINTOSH, S. & JAMES, D. E. 1995. Molecular identification of two novel Munc-18 isoforms expressed in non-neuronal tissues. *J Biol Chem,* 270**,** 5857-63.

TERADA, S., MURAOKA, I. & TABATA, I. 2003. Changes in [Ca2+]i induced by several glucose transport-enhancing stimuli in rat epitrochlearis muscle. *J Appl Physiol,* 94**,** 1813-20.

THONG, F. S., BILAN, P. J. & KLIP, A. 2007. The Rab GTPase-activating protein AS160 integrates Akt, protein kinase C, and AMP-activated protein kinase signals regulating GLUT4 traffic. *Diabetes,* 56**,** 414-23.

THORELL, A., HIRSHMAN, M. F., NYGREN, J., JORFELDT, L., WOJTASZEWSKI, J. F., DUFRESNE, S. D., HORTON, E. S., LJUNGQVIST, O. & GOODYEAR, L. J. 1999. Exercise and insulin cause GLUT-4 translocation in human skeletal muscle. *Am J Physiol,* 277**,** E733-41.

THRUSH, A. B., BRINDLEY, D. N., CHABOWSKI, A., HEIGENHAUSER, G. J. & DYCK, D. J. 2009. Skeletal muscle lipogenic protein expression is not different between lean and obese individuals: a potential factor in ceramide accumulation. *J Clin Endocrinol Metab,* 94**,** 5053-61.

TIMMERS, S., DE VOGEL-VAN DEN BOSCH, J., HESSELINK, M. K., VAN BEURDEN, D., SCHAART, G., FERRAZ, M. J., LOSEN, M., MARTINEZ-MARTINEZ, P., DE BAETS, M. H., AERTS, J. M. & SCHRAUWEN, P. 2011. Paradoxical increase in TAG and DAG content parallel the insulin sensitizing effect of unilateral DGAT1 overexpression in rat skeletal muscle. *PLoS One,* 6**,** e14503.

TREADWAY, J. L., JAMES, D. E., BURCEL, E. & RUDERMAN, N. B. 1989. Effect of exercise on insulin receptor binding and kinase activity in skeletal muscle. *Am J Physiol,* 256**,** E138-44.

TREEBAK, J. T., FROSIG, C., PEHMOLLER, C., CHEN, S., MAARBJERG, S. J., BRANDT, N., MACKINTOSH, C., ZIERATH, J. R., HARDIE, D. G., KIENS, B., RICHTER, E. A., PILEGAARD, H. & WOJTASZEWSKI, J. F. 2009. Potential role of TBC1D4 in enhanced post-exercise insulin action in human skeletal muscle. *Diabetologia,* 52**,** 891-900.

TREEBAK, J. T., TAYLOR, E. B., WITCZAK, C. A., AN, D., TOYODA, T., KOH, H. J., XIE, J., FEENER, E. P., WOJTASZEWSKI, J. F., HIRSHMAN, M. F. & GOODYEAR, L. J. 2010. Identification of a novel phosphorylation site on TBC1D4 regulated by AMP-activated protein kinase in skeletal muscle. *Am J Physiol Cell Physiol,* 298**,** C377-85.

TSAKIRIDIS, T., MCDOWELL, H. E., WALKER, T., DOWNES, C. P., HUNDAL, H. S., VRANIC, M. & KLIP, A. 1995. Multiple roles of phosphatidylinositol 3-kinase in regulation of glucose transport, amino acid transport, and glucose transporters in L6 skeletal muscle cells. *Endocrinology,* 136**,** 4315-22.

TSINTZAS, K., CHOKKALINGAM, K., JEWELL, K., NORTON, L., MACDONALD, I. A. & CONSTANTIN-TEODOSIU, D. 2007. Elevated free fatty acids attenuate the insulin-induced suppression of PDK4 gene expression in human skeletal muscle: potential role of intramuscular long-chain acyl-coenzyme A. *J Clin Endocrinol Metab,* 92**,** 3967-72.

TURNER, N. & HEILBRONN, L. K. 2008. Is mitochondrial dysfunction a cause of insulin resistance? *Trends Endocrinol Metab,* 19**,** 324-30.

ULDRY, M. & THORENS, B. 2004. The SLC2 family of facilitated hexose and polyol transporters. *Pflugers Arch,* 447**,** 480-9.

UMAHARA, M., OKADA, S., YAMADA, E., SAITO, T., OHSHIMA, K., HASHIMOTO, K., YAMADA, M., SHIMIZU, H., PESSIN, J. E. & MORI, M. 2008. Tyrosine phosphorylation of Munc18c regulates platelet-derived growth factor-stimulated glucose transporter 4 translocation in 3T3L1 adipocytes. *Endocrinology,* 149**,** 40-9.

VAN HALL, G., SALTIN, B. & WAGENMAKERS, A. J. 1999. Muscle protein degradation and amino acid metabolism during prolonged knee-extensor exercise in humans. *Clin Sci (Lond),* 97**,** 557-67.

VAN LOON, L. J. 2004a. Intramyocellular triacylglycerol as a substrate source during exercise. *Proc Nutr Soc,* 63**,** 301-7.

VAN LOON, L. J. 2004b. Use of intramuscular triacylglycerol as a substrate source during exercise in humans. *J Appl Physiol,* 97**,** 1170-87.

VAN LOON, L. J. & GOODPASTER, B. H. 2006. Increased intramuscular lipid storage in the insulin-resistant and endurance-trained state. *Pflugers Arch,* 451**,** 606-16.

VAN LOON, L. J., GREENHAFF, P. L., CONSTANTIN-TEODOSIU, D., SARIS, W. H. & WAGENMAKERS, A. J. 2001. The effects of increasing exercise intensity on muscle fuel utilisation in humans. *J Physiol,* 536**,** 295-304.

VAN LOON, L. J., KOOPMAN, R., MANDERS, R., VAN DER WEEGEN, W., VAN KRANENBURG, G. P. & KEIZER, H. A. 2004. Intramyocellular lipid content in type

2 diabetes patients compared with overweight sedentary men and highly trained endurance athletes. *Am J Physiol Endocrinol Metab,* 287**,** E558-65.

VAN LOON, L. J., KOOPMAN, R., STEGEN, J. H., WAGENMAKERS, A. J., KEIZER, H. A. & SARIS, W. H. 2003. Intramyocellular lipids form an important substrate source during moderate intensity exercise in endurance-trained males in a fasted state. *J Physiol,* 553**,** 611-25.

VAN LOON, L. J., MANDERS, R. J., KOOPMAN, R., KAASTRA, B., STEGEN, J. H., GIJSEN, A. P., SARIS, W. H. & KEIZER, H. A. 2005. Inhibition of adipose tissue lipolysis increases intramuscular lipid use in type 2 diabetic patients. *Diabetologia,* 48**,** 2097-107.

VINCENT, M. A. & BARRETT, E. J. 2002. Insulin-induced capillary recruitment precedes changes in skeletal muscle glucose uptake. *Diabetes,* 51**,** A31-A31.

VINCENT, M. A., BARRETT, E. J., LINDNER, J. R., CLARK, M. G. & RATTIGAN, S. 2003. Inhibiting NOS blocks microvascular recruitment and blunts muscle glucose uptake in response to insulin. *Am J Physiol Endocrinol Metab,* 285**,** E123-9.

VINCENT, M. A., CLERK, L. H., LINDNER, J. R., KLIBANOV, A. L., CLARK, M. G., RATTIGAN, S. & BARRETT, E. J. 2004. Microvascular recruitment is an early insulin effect that regulates skeletal muscle glucose uptake in vivo. *Diabetes,* 53**,** 1418-1423.

VINCENT, M. A., CLERK, L. H., LINDNER, J. R., PRICE, W. J., JAHN, L. A., LEONG-POI, H. & BARRETT, E. J. 2006. Mixed meal and light exercise each recruit muscle capillaries in healthy humans. *Am J Physiol Endocrinol Metab,* 290**,** E1191-7.

VIND, B. F., PEHMOLLER, C., TREEBAK, J. T., BIRK, J. B., HEY-MOGENSEN, M., BECK-NIELSEN, H., ZIERATH, J. R., WOJTASZEWSKI, J. F. & HOJLUND, K. 2011. Impaired insulin-induced site-specific phosphorylation of TBC1 domain family, member 4 (TBC1D4) in skeletal muscle of type 2 diabetes patients is restored by endurance exercise-training. *Diabetologia,* 54**,** 157-67.

WAGENMAKERS, A.J.M. 2005. Insulin resistance in the offspring of parents with type 2 diabetes. *PLoS Med,* 2, e289.

WAGENMAKERS, A. J., VAN RIEL, N. A., FRENNEAUX, M. P. & STEWART, P. M. 2006. Integration of the metabolic and cardiovascular effects of exercise. *Essays Biochem,* 42**,** 193-210.

WANG, W., HANSEN, P. A., MARSHALL, B. A., HOLLOSZY, J. O. & MUECKLER, M. 1996. Insulin unmasks a COOH-terminal Glut4 epitope and increases glucose transport across T-tubules in skeletal muscle. *J Cell Biol,* 135**,** 415-30.

WASSERMAN, D. H. 2009. Four grams of glucose. *Am J Physiol Endocrinol Metab,* 296**,** E11-21.

WASSERMAN, D. H. & AYALA, J. E. 2005. Interaction of physiological mechanisms in control of muscle glucose uptake. *Clin Exp Pharmacol Physiol,* 32**,** 319-23.

WATSON, R. T., KANZAKI, M. & PESSIN, J. E. 2004. Regulated membrane trafficking of the insulin-responsive glucose transporter 4 in adipocytes. *Endocr Rev,* 25**,** 177-204.

WEBER, T., ZEMELMAN, B. V., MCNEW, J. A., WESTERMANN, B., GMACHL, M., PARLATI, F., SOLLNER, T. H. & ROTHMAN, J. E. 1998. SNAREpins: minimal machinery for membrane fusion. *Cell,* 92**,** 759-72.

WEI, Y., CHEN, K., WHALEY-CONNELL, A. T., STUMP, C. S., IBDAH, J. A. & SOWERS, J. R. 2008. Skeletal muscle insulin resistance: role of inflammatory cytokines and reactive oxygen species. *Am J Physiol Regul Integr Comp Physiol,* 294**,** R673-80.

WHEATLEY, C. M., RATTIGAN, S., RICHARDS, S. M., BARRETT, E. J. & CLARK, M. G. 2004. Skeletal muscle contraction stimulates capillary recruitment and glucose uptake in insulin-resistant obese Zucker rats. *Am J Physiol Endocrinol Metab,* 287**,** E804-9.

WILSON, O. J., SHAW, C. S., SHERLOCK, M., STEWART, P. M. & WAGENMAKERS, A. J. 2012. Immunofluorescent visualisation of focal adhesion kinase in human skeletal muscle and its associated microvasculature. *Histochem Cell Biol,* 138**,** 617-26.

WOJTASZEWSKI, J. F., HANSEN, B. F., GADE, KIENS, B., MARKUNS, J. F., GOODYEAR, L. J. & RICHTER, E. A. 2000. Insulin signaling and insulin sensitivity after exercise in human skeletal muscle. *Diabetes,* 49**,** 325-31.

WOJTASZEWSKI, J. F., HANSEN, B. F., KIENS, B. & RICHTER, E. A. 1997. Insulin signaling in human skeletal muscle: time course and effect of exercise. *Diabetes,* 46**,** 1775-81.

WOJTASZEWSKI, J. F., HIGAKI, Y., HIRSHMAN, M. F., MICHAEL, M. D., DUFRESNE, S. D., KAHN, C. R. & GOODYEAR, L. J. 1999. Exercise modulates postreceptor insulin signaling and glucose transport in muscle-specific insulin receptor knockout mice. *J Clin Invest,* 104**,** 1257-64.

WOJTASZEWSKI, J. F. & RICHTER, E. A. 2006. Effects of acute exercise and training on insulin action and sensitivity: focus on molecular mechanisms in muscle. *Essays Biochem,* 42**,** 31-46.

WORLD HEALTH ORGANISATION. 2009. Global Health Risks: Mortality and Burden of Disease Attributable to Selected Major Risks. Geneva, Switzerland.

WRIGHT, D. C., GEIGER, P. C., HOLLOSZY, J. O. & HAN, D. H. 2005. Contraction- and hypoxia-stimulated glucose transport is mediated by a Ca2+-dependent mechanism in slow-twitch rat soleus muscle. *Am J Physiol Endocrinol Metab,* 288**,** E1062-6.

WRIGHT, D. C., HUCKER, K. A., HOLLOSZY, J. O. & HAN, D. H. 2004. Ca2+ and AMPK both mediate stimulation of glucose transport by muscle contractions. *Diabetes,* 53**,** 330-5.

YANG, C., MORA, S., RYDER, J. W., COKER, K. J., HANSEN, P., ALLEN, L. A. & PESSIN, J. E. 2001. VAMP3 null mice display normal constitutive, insulin- and exercise-regulated vesicle trafficking. *Mol Cell Biol,* 21**,** 1573-80.

YOSHIZAKI, T., IMAMURA, T., BABENDURE, J. L., LU, J. C., SONODA, N. & OLEFSKY, J. M. 2007. Myosin 5a is an insulin-stimulated Akt2 (protein kinase Bbeta) substrate modulating GLUT4 vesicle translocation. *Mol Cell Biol,* 27**,** 5172-83.

YOUN, J. H., GULVE, E. A. & HOLLOSZY, J. O. 1991. Calcium stimulates glucose transport in skeletal muscle by a pathway independent of contraction. *Am J Physiol,* 260**,** C555-61.

ZERIAL, M. & MCBRIDE, H. 2001. Rab proteins as membrane organizers. *Nat Rev Mol Cell Biol,* 2**,** 107-17.

ZHANG, L., VINCENT, M. A., RICHARDS, S. M., CLERK, L. H., RATTIGAN, S., CLARK, M. G. & BARRETT, E. J. 2004. Insulin sensitivity of muscle capillary recruitment in vivo. *Diabetes,* 53**,** 447-53.

ZHOU, W., LI, H., GU, Y., YU, L., HAN, J., XU, W., JIAN, W., TIAN, J., ZHOU, W., ZHANG, D., LIU, Y., YANG, J., LI, J., LI, G. & LUO, M. 2006. The ROC analysis for different time points during oral glucose tolerance test. *Diabetes Res Clin Pract,* 72**,** 88-92.

ZIERATH, J. R., HE, L., GUMA, A., ODEGOARD WAHLSTROM, E., KLIP, A. & WALLBERG-HENRIKSSON, H. 1996. Insulin action on glucose transport and plasma membrane GLUT4 content in skeletal muscle from patients with NIDDM. *Diabetologia,* 39**,** 1180-9.

ZISMAN, A., PERONI, O. D., ABEL, E. D., MICHAEL, M. D., MAUVAIS-JARVIS, F., LOWELL, B. B., WOJTASZEWSKI, J. F., HIRSHMAN, M. F., VIRKAMAKI, A., GOODYEAR, L. J., KAHN, C. R. & KAHN, B. B. 2000. Targeted disruption of the glucose transporter 4 selectively in muscle causes insulin resistance and glucose intolerance. *Nat Med,* 6**,** 924-8.

CHAPTER 2

GENERAL METHODS

2.1. Ethical approval

Ethical approval for all the studies included in this thesis was granted by NHS Research Ethics Committees in the Birmingham and West Midlands region or the Ethics Committee of the Capital Region of Denmark. Written informed consent was obtained from all participants, prior to their commencement of a study. All animal studies were conducted according to the UK Animal (Scientific Procedures) Act 1984.

2.2. Human skeletal muscle biopsy collection

Human skeletal muscle samples (~100 mg wet weight) for studies described in chapters 3, 4 and 6 were obtained under local anaesthesia (1 % lidocaine) from the *vastus lateralis* muscle using the Bergström percutaneous needle biopsy technique with suction (Bergstrom, 1975). Small incisions (~1 cm) were made in the skin and fascia over the *vastus lateralis* muscle, through which the biopsy needle was inserted. Samples were blotted to remove excess blood and any visible collagen or fat was discarded. For immunofluorescence microscopy analysis part of the sample was embedded in Tissue Tek OCT (Sakura, 4583) compound and immediately frozen in liquid nitrogen-cooled isopentane (Sigma Aldrich, 270342). The sample was then transferred to an aluminium cryotube (Caltag Medsystems, PA6003) for storage at $^{-}80\ ^{o}C$. The remaining sample was snap frozen in liquid nitrogen to be used for Western blot analysis where relevant.

2.3. Rat skeletal muscle collection

Immediately after completion of the experimental protocol (described fully in chapter 5) animals were sacrificed by anaesthetic overdose, via intraperitoneal administration of Inactin, followed by cervical dislocation. The *tibialis anterior* muscle was dissected free and any

visible non-muscle tissue or tendon was removed and discarded. The muscle was embedded to enable transverse sectioning of the tissue in Tissue Tek OCT (Sakura, 4583) compound and immediately frozen in liquid nitrogen-cooled isopentane (Sigma Aldrich, 270342). The sample was then stored at $^{-}80\ ^{o}C$ until use.

2.4. Sample homogenisation for Western blotting

Snap-frozen muscle samples of 20-50 mg, were homogenised in liquid nitrogen using a pestle and mortar. Radio-Immunoprecipitation Assay (RIPA) buffer (20 mM Tris-HCl (pH 7.5), 150 mM NaCl, 1 mM Na_2EDTA, 1 mM EGTA, 1% NP-40, 1% sodium deoxycholate, 2.5 mM sodium pyrophosphate, 1 mM β-glycerophosphate, 1 mM Na_3VO_4, 1 µg/ml leupeptin, Cell Signalling) with a protease inhibitor cocktail (Roche, 11836153001) was added to the muscle sample and the homogenate was left on ice for 10 min before being vortexed and again left on ice for 3 hr on a shaker. Further homogenisation was achieved using a polytron (Digital ULTRA-TURRAX, IKA). Finally samples were centrifuged for 20 min at 10 000 g at 4 ^{o}C (accuSpin^{TM} MicroR centrifuge, Fisher Scientific) and the resulting supernatant was aliquoted. A bicinchoninic acid (BCA) assay was run on the homogenate samples to determine the protein concentration, so concentration could be normalised to 2 µg/µl for all samples (BCA kit, Thermo Scientific, 23227). To achieve this 100 µl Laemmli buffer (0.004 % bromophenol blue, 400 mM DTT, 20 % glycerol, 4 % SDS, 0.125 M Tris, Sigma Aldrich) and an appropriate volume of RIPA buffer was added to the sample. Samples were not boiled prior to immunoblotting due to the tendency of hydrophobic membrane proteins to aggregate at high temperatures (Lee et al., 2005).

2.5. VO_{2max} determination

All participants recruited for the studies in chapters 3 and 4 performed an incremental exercise test to exhaustion on an electronically braked cycle ergometer (Lode BV, Groningen, The Netherlands) to determine their maximal aerobic capacity (VO_{2max}) using an on-line gas collection system (Oxycon Pro, Jaeger, Germany). The test began with cycling at a workload of 95 W with subsequent increases of 35 W every 3 min. The test was terminated when the participant's cadence dropped below 50 rpm. The VO_{2max} was recorded as the highest value reached within the final 30 s of the test. The data from the VO_{2max} test were also used to estimate the workload that corresponded to 65% VO_{2max}.

2.6. Venous blood sampling and plasma glucose and insulin analysis

Venous blood samples were collected from a cannula inserted into a forearm vein into ethylenediaminetetraacetic acid (EDTA)-containing tubes (BD vacutainer, USA). Samples were kept on ice before centrifuging for 15 min at 3500 rpm at 4^{o}C. Plasma was aliquoted and stored at -80^{o}C. Plasma glucose was analysed in duplicate in all samples spectrophotometrically using an ILab 600 analyser and the glucose oxidase kit (Instrumentation Laboratory Ltd, UK). Plasma insulin was analysed in duplicate in all samples using commercially available insulin ELISA kits (Invitrogen, UK).

2.7. Matsuda index calculation

Insulin sensitivity during OGTT in chapters 3, 4 and 6 was calculated using the Matsuda index, which was originally proposed by Matsuda and DeFronzo (1999), and has been shown to correlate highly with the gold standard assessment of insulin sensitivity using the

hyperinsulinaemic-euglycaemic clamp (Matsuda and DeFronzo, 1999). The Matsuda index was calculated as follows:

$$Matsuda\ ISI = \frac{10000}{\sqrt{(FPGxFPI)(MPGxMPI)}},$$

where FPG is fasting plasma glucose, FPI is fasting plasma insulin, MPG is mean plasma glucose during OGTT and MPI is mean plasma insulin during OGTT.

2.8. GLUT4 immunofluorescence microscopy method development

2.8.1. Sample preparation

Cryosections (5 µm) were cut using a Bright 5040 (Bright Instrument Company limited, Huntingdon, England) microtome within a Bright cryostat with temperature maintained at -25^{o}C. Sections were cut onto uncoated glass microscope slides (VWR international) and were either stained within 30 min or stored at -20 ^{o}C for staining on a subsequent occasion. Following storage slides were left at room temperature for 30 min prior to staining.

2.8.2. GLUT4 immunofluorescence staining protocol.

The GLUT4 staining protocol was optimised by checking different fixatives, antibody dilutions and incubation times to produce the optimal images. The fully optimised protocol is outlined below. Pre-cut cryosections on slides were fixed for 5 min in solution of 75 % acetone and 25 % ethanol. Following this sections were washed 3 times for 5 min in phosphate buffered saline (PBS, 1x, 137 mM sodium chloride, 3 mM potassium chloride, 8 mM sodium phosphate dibasic, 3 mM potassium phosphate monobasic, all Sigma Aldrich). For anti-GLUT4 staining sections were incubated in 1:200 anti-GLUT4 polyclonal antibody (abcam, UK, ab654) diluted in PBS with 5 % normal goat serum (NGS, Invitrogen) for 2 h at room temperature. Following primary antibody incubation, sections were again washed 3

times for 5 min in PBS. Sections were then incubated in a 1:200 dilution of appropriately targeted secondary antibodies diluted in PBS for 30 min at room temperature. GLUT4 antibody was targeted with goat anti-rabbit IgG 488 (Invitrogen, UK). Following secondary antibody incubation, sections were washed 3 times for 5 min in PBS and glass coverslips were mounted with 20 µl mowiol mounting medium (6 g glycerol (Sigma Aldrich, G5150), 2.4 g mowiol 4-88 (Fluka, 81381) and 0.026 g 1,4-diazobicyclo-[2,2,2]-octane (DABCO) (Fluka, 33490) dissolved in 18 ml 0.2M Tris-buffer (pH 8.5) (Sigma Aldrich, T5030)) to protect the sample and preserve the fluorescence signal. Slides were left to dry overnight before immunofluorescence visualisation.

GLUT4 staining has been combined with a number of different markers. The plasma membrane (PM) was stained with a monoclonal antibody against the protein dystrophin (1:400, Sigma Aldrich, UK, D8168) and T-tubule membranes were stained with a monoclonal antibody against dihydropyridine receptor (DHPR; 1:25, Abcam, UK, ab2864). Type I and type IIa muscle fibres were identified using monoclonal antibodies against myosin heavy chain type I (MHCI, 1:100, A4.840) and myosin heavy chain type IIa (MHCIIa. 1:100, N2.261), respectively (both DSHB, USA, developed by Dr Blau). The appropriately targeted secondary antibodies are as follows; dystrophin was targeted with goat anti-mouse (GAM) IgG_{2b} 594 (Invitrogen, UK) or GAM IgG_{2b} 633 (Invitrogen, UK), DHPR with GAM IgG_{2a} 594 (Invitrogen, UK), MHCI with GAM IgM 594 (Invitrogen, UK) or GAM IgM 488 (Invitrogen, UK) and MHCIIa with GAM $IgG_1$594. 4,6-Diamidino-2-phenylindole dihydrochloride (DAPI, Sigma Aldrich, UK) was used to identify cell nuclei and was applied with secondary antibody at a 1:500 dilution. Further details of these staining combinations will be provided in the individual chapters.

SNAP23 was stained in human muscle sections using an anti-SNAP23 polyclonal antibody (1:50, Synaptic Systems, Germany, 111 202) in combination with dytrophin. However due to limitations of antibody species GLUT4 and SNAP23 staining were not combined. These limitations will be further discussed in section 2.10 of this chapter.

2.8.3. Antibody validation.

The performance of accurate immunofluorescence microscopy requires a primary antibody which specifically targets only the desired protein of interest. There are a number of methods used to determine the specificity of an antibody (as described in (Saper, 2009, Saper, 2005, Burry, 2011)), but as there are inherent advantages and disadvantages of each method, in this thesis a number of methods were combined to provide convincing evidence of antibody specificity.

Western blotting was performed to confirm the antibody selected a single protein at the expected molecular weight. Protein extract (60 µg) was loaded onto a 7.5 % resolving gel (Biorad, UK) with 5 µl molecular weight markers (Biorad, UK) and run for 1 h at 40 mA in 1x Tris/Glycine/SDS buffer (Biorad, UK). Proteins were transferred to a PVDF membrane (Biorad, UK) for 2 h at 350mA in 1x Tris/Glycine buffer (Biorad, UK) with 20 % methanol. The membrane was blocked for 1 h in 5 % non-fat dry milk (Cell Signalling, USA) made up in tris-buffered saline (50mM Tris-HCl (Sigma Aldrich, UK), 150 mM NaCl (Sigma Aldrich, UK) with 0.05 % tween 20 (Sigma Aldrich, UK)) (TBST) and then incubated overnight at 4^{o}C in 1:2000 dilution of GLUT4 primary antibody (ab654, Abcam, UK) in 5 % milk. Membrane was subsequently washed 3 times for 10 min in TBST and blocked again for 1 h in 5 % milk prior to incubation in 1:2000 dilution of goat-anti rabbit IgG HRP conjugated secondary antibody (Cell Signalling, USA) in 5 % milk for 1 h. Membrane was then washed

twice in TBST and once in TBS without tween. Membrane was incubated in ECL substrate (GE Healthcare, UK) for 5 min prior to exposure to film (GE Healthcare, UK) and development of film. To confirm GLUT4 antibody specificity and selectivity in an immunofluoresence application experiments were carried out onsite at AstraZeneca in an L6 cell line overexpressing GLUT4 with a myc protein tag (GLUT4-myc) and non-transfected L6 cells. L6-GLUT4myc cells were purchased by AstraZeneca from Dr. Amira Klip and Dr. Philip Bilan (Department of Biochemistry, University of Toronto) and have been described previously (Kanai et al., 1993, Wang et al., 1998). GLUT4-myc and non-transfected cells (20,000 per well) were differentiated to myotubes and were fixed in 4 % formaldehyde for 5 min on ice and then kept for 20 min at room temperature. Cells were washed twice in PBS and 100 µl 0.1M glycine was added to quench the formaldehyde reaction. Cells were permeabilised in 100 µl 0.1 % triton X-100 in PBS for 5 min at room temperature and then washed once in PBS. Cells were blocked for 1 h at room temperature in 3 % BSA in PBS and then incubated in 25 µl 1:50 GLUT4 antibody in 3 % BSA with 1:50 mouse anti-myc (Sigma Aldrich, UK) for 1 h at room temperature. Some cells did not have GLUT4 primary antibody applied as a negative control to confirm secondary antibody specificity. Cells were then washed once in PBS and secondary antibodies were applied for 40 min at room temperature in 3 % BSA with a 1:500 Hoechst 33342 (Invitrogen, UK) counterstain for cell nuclei. Goat anti-rabbit IgG 594 (1:500) was used to detect GLUT4 primary antibody and 1:500 goat anti-mouse IgG 488 was used to detect myc primary antibody. Cells were then washed three times in PBS and left in PBS for viewing. Viewing was completed using ImageXpress with a 10x objective and contrast was adjusted consistently across all images. To confirm specificity of the GLUT4 antibody for the immunogen peptide the antibody was incubated with saturating concentrations (5 times higher than the antibody concentration) of the GLUT4 immunogen

peptide composed of the C terminal 15 amino acids of rat GLUT4 (Abcam, UK, ab115831) for 24 h at 4^{o}C, prior to application onto human skeletal muscle sections in place of primary antibody. All other stages of the staining protocol remained identical and the competition staining was completed alongside a positive control with primary antibody and a negative control in which primary antibody was omitted completely.

The specificity of the antibodies targeting MHCI and MHCII to identify muscle fibre type (Webster et al., 1988, Shepherd et al., 2013), dystrophin to mark the PM (Nguyen et al., 1990, Sedgwick et al., 1991, Koenig et al., 1988) and DHPR to identify the T-tubule membranes (Wilson et al., 2012) have all been confirmed in earlier studies.

2.8.4. Antibody controls

For each tissue, species and staining protocol certain controls were carried out. To confirm there was no tissue autofluorescence or non-specific secondary antibody binding PBS containing 5 % NGS was applied to the tissue in place of primary antibody. When visualised, an image free of positive staining confirmed there was no tissue autofluorescence or non-specific secondary antibody binding.

To ensure secondary antibodies did not cross react with the incorrect primary antibody, controls were performed in which only one primary antibody was applied to the tissue section with all secondary antibodies. Correct staining was confirmed with images in which signal was only observed from the secondary antibody targeted to the primary antibody applied to the tissue section.

To ensure each fluorophore only emitted signal that was detected in a single channel, controls were carried out in which only one target was stained. Images were captured in all channels to confirm signal was only detected in the channel specific to the target stained. It was important

to confirm there was no bleedthrough into other channels as this would have affected the images analysis.

2.8.5. Microscopy

Images were captured using a widefield or confocal fluorescence microscope. In widefield fluorescence microscopy fluorophores are illuminated through the entire depth of the muscle section not just in the plane of focus, which can result in images appearing blurry and out of focus (Smith, 2008). In contrast a confocal microscope only collects light from a single focus plane. In focus light is allowed through the confocal microscope pinhole aperture and reaches the detector, whereas out-of-focus light does not (Smith, 2008). Furthermore the lasers used for excitation in a confocal microscope lead to intense excitation of the fluorophores (Smith, 2008). Taken together these features allow generation of higher resolution images with less out-of focus light. Confocal microscopy was therefore used for colocalisation analysis, to reduce false colocalisation that would be caused by out-of-focus light with widefield microscopy. All staining was carried out in triplicate on separate slides, and subsequent image capture and analysis was completed on all three slides.

Widefield immunofluorescence images were visualised using a Nikon E600 microscope and captured with a SPOT RT KE colour three shot CCD camera (Diagnostic Instruments Inc., MI, USA). A 170 W Xenon light source was used for illumination. The Alexa Fluor 594 and 488 fluorophores were visualised using Texas red (540-580 nm) and FITC (465-495 nm) excitation filters, respectively, while the DAPI UV (340-380 nm) excitation filter was used to visualise cell nuclei stained with DAPI. Filters were changed using a semi-automated filterwheel (10B 10 Position Filterwheel, Sutter, USA). All widefield images were obtained using a 40x objective (0.75 NA).

In order to obtain higher resolution images suitable for colocalisation analysis, an inverted confocal microscope (Leica DMIRE2, Leica Microsystems) with a 63x oil immersion objective (1.4 NA) was used. AlexaFluor 488 fluorophores were excited with a 488 nm line of the argon laser and 498-571 nm emission. Alexa Fluor 594 fluorophores were excited with the 594 nm line of the helium-neon laser and 601-713 nm emission. Alexa Fluor 633 fluorophores were excited with the 633 nm line of the helium-neon laser and 639-734 nm emission.

2.8.6. Immunofluorescence image analysis

Images were processed and analysed using Image-Pro Plus 5.1 software (Media Cybernetics, MD, USA). The colocalisation of GLUT4 and dystrophin used to estimate PM GLUT4 was measured using the Pearson's correlation coefficient which was calculated by the ImagePro Plus 5.1 colocalisation tool. Prior to colocalisation all images underwent an ImagePro Plus 5.1 no neighbour deconvolution algorithm as a filter. Pearson's correlation coefficient has been routinely used to measure colocalisation of two proteins in immunofluorescence images (Dunn et al., 2011, Bolte and Cordelieres, 2006, Landmann and Marbet, 2004, Sedarat et al., 2004, Lachmanovich et al., 2003). All image processing and analysis was kept consistent between images across each analysis method.

2.9. Results of GLUT4 immunofluorescence method development

2.9.1. GLUT4 antibody validation

The online UniProt database Basic Local Alignment Search Tool (BLAST; http://www.uniprot.org) indicated that the immunogen sequence corresponding to the C terminal 15 amino acid sequence of rat GLUT4 was not present in any protein other than GLUT4 in human skeletal muscle. Therefore an antibody raised against this immunogen

sequence should only detect GLUT4 in human skeletal muscle sections. To confirm this experimentally Western blotting (Fig. 2.1A) was applied to human skeletal muscle and the GLUT4 antibody detected a single band at the expected molecular weight (approximately 45 kDa). In L6 cells overexpressing GLUT4 with a myc tag (GLUT4-myc), antibody staining against myc demonstrated extensive colocalisation with the staining generated by the GLUT4 antibody (Fig. 2.1B). Furthermore in non-transfected L6 cells, which exhibit very low expression of GLUT4, no positive GLUT4 staining was observed. The residual myc signal is attributable to endogenous myc in L6 cells (Denis et al., 1987). Incubation of the primary antibody with the immunogen peptide prior to application to the muscle section abolishes antibody staining, leaving only background fluorescence and confirming specificity of the antibody for the immunogen sequence (Fig. 2.1C, right panel). Omission of the GLUT4 primary antibody results in no staining, confirming secondary antibody specificity and absence of tissue autofluorescence (Fig. 2.1C, middle panel). Taken together these data validate the use of this GLUT4 primary antibody (abcam, ab654) in skeletal muscle.

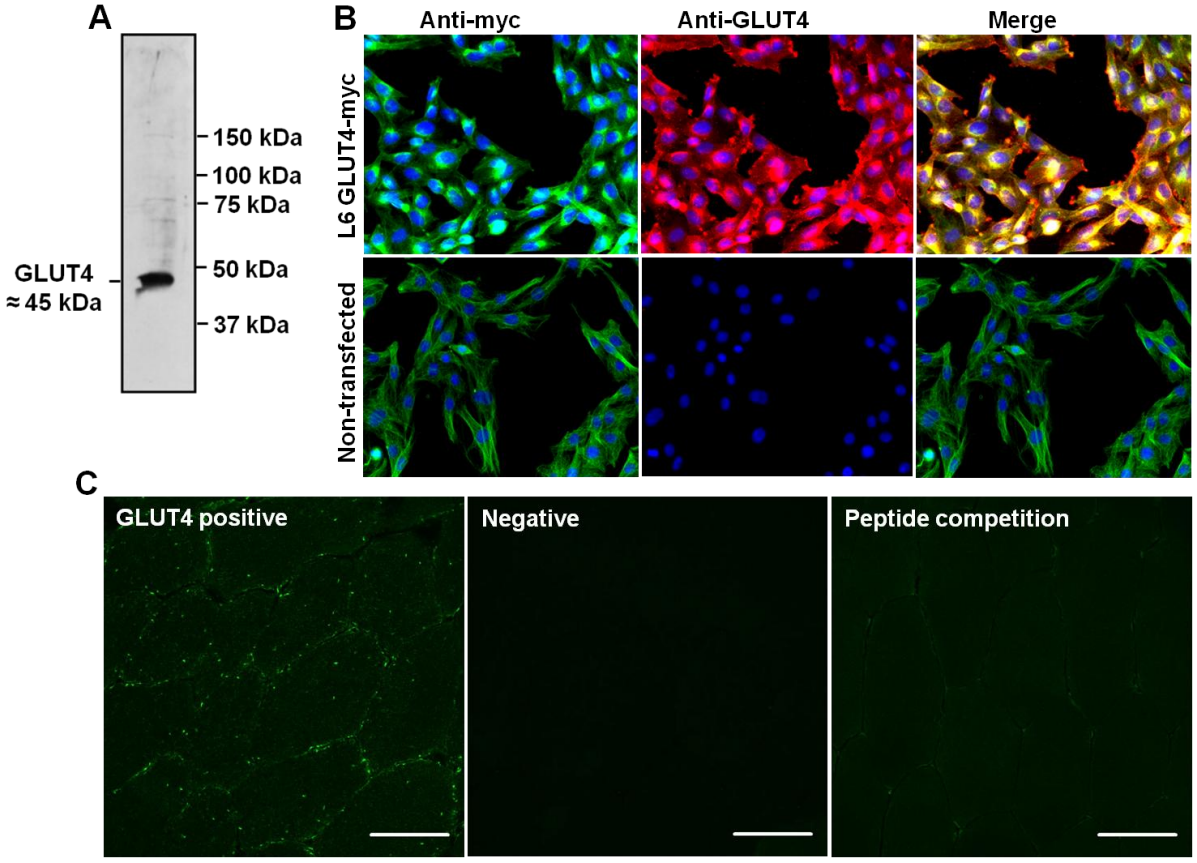

Fig. 2.1. *Validation of GLUT4 antibody. A) Human skeletal muscle Western blot. B) GLUT4-myc transfected L6 cells (and non-transfected L6 cells) stained with GLUT4 antibody (red) and myc antibody (green). Myc staining is apparent in non-transfected L6 cells because they express endogenous myc (Denis et al., 1987). C) Positive control GLUT4 antibody staining for comparison to primary antibody omission negative and peptide competition staining. Scale bars 50 µm.*

2.9.2. Basal GLUT4 localisation in human skeletal muscle

GLUT4 staining in human skeletal muscle appears as large clusters of staining with smaller spots dispersed throughout the cell interior as can be seen in Fig.2. 2. GLUT4 clusters are also observed close to or incorporated in the PM as indicated by the distinct colocalisation of GLUT4 with the PM marker dystrophin (Fig. 2.2). Another clear feature of human skeletal

muscle GLUT4 localisation is a perinuclear distribution, which is shown in Fig. 2.3 where GLUT4 staining surrounds the DAPI stain for cell nuclei. Importantly, the localisation of GLUT4 in human skeletal muscle revealed in this thesis is very similar to the results of published fluorescence microscopy studies in rodent skeletal muscle in which large and small clusters of GLUT4 staining were observed predominantly at the fibre periphery and at a high density in perinuclear regions (Ploug et al., 1998, Lauritzen et al., 2006). As well as staining in PM regions, Fig. 2.4 shows that GLUT4 is also localised at the T-tubule membranes in human skeletal muscle in the basal state. In longitudinally oriented muscle fibre sections staining for DHPR, a receptor found in high concentrations in the T-tubule membranes and therefore used as a marker for the T-tubule membranes, generates a striated pattern in which the striations run perpendicular to the long axis of the fibre (Fig. 2.4, middle panel). GLUT4 staining demonstrates the same striation pattern (Fig. 2.4, left panel), which correspond to the DHPR striations when the two stains are overlaid (Fig. 2.4, right panel). In Fig. 2.5 no difference in GLUT4 signal intensity is apparent between the type I fibres, which positively stain for MHCI, and the type II fibres.

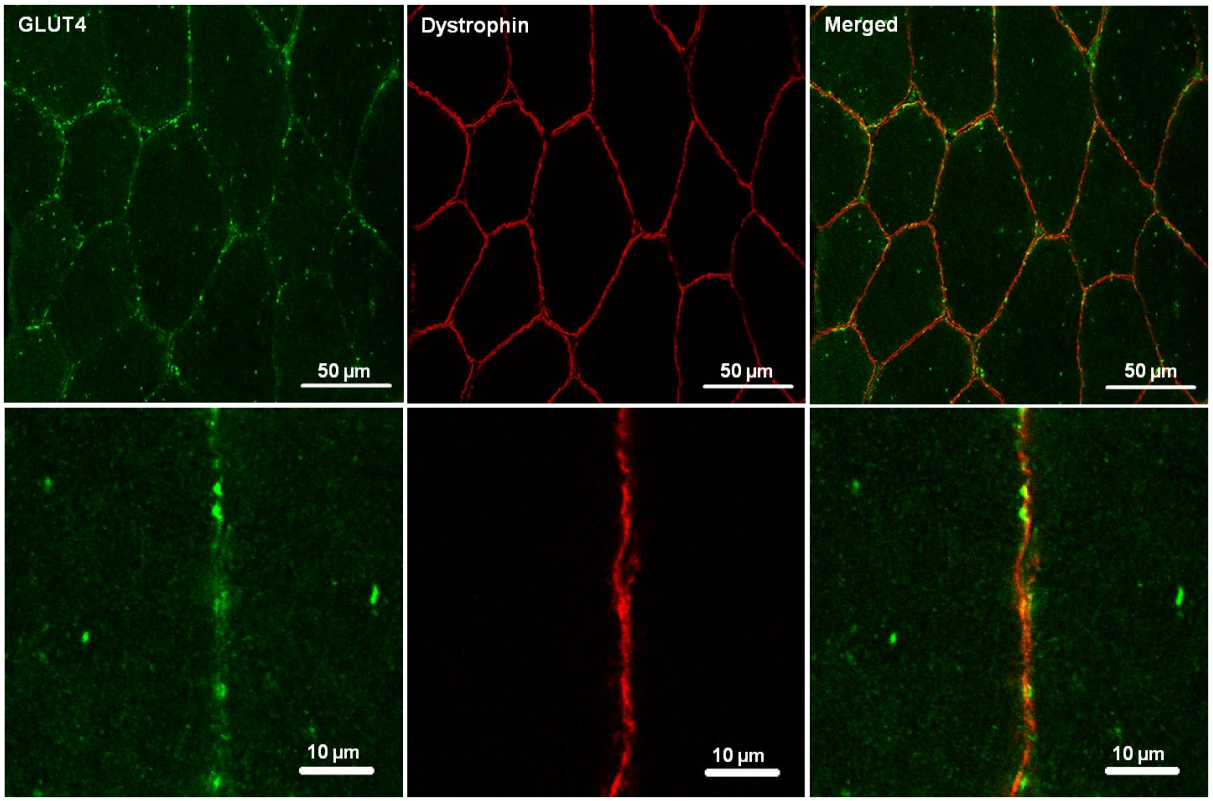

Fig. 2.2. *Representative confocal immunofluorescence microscopy images of GLUT4 (green) in human skeletal muscle stained in combination with dystrophin (red) to mark the PM.*

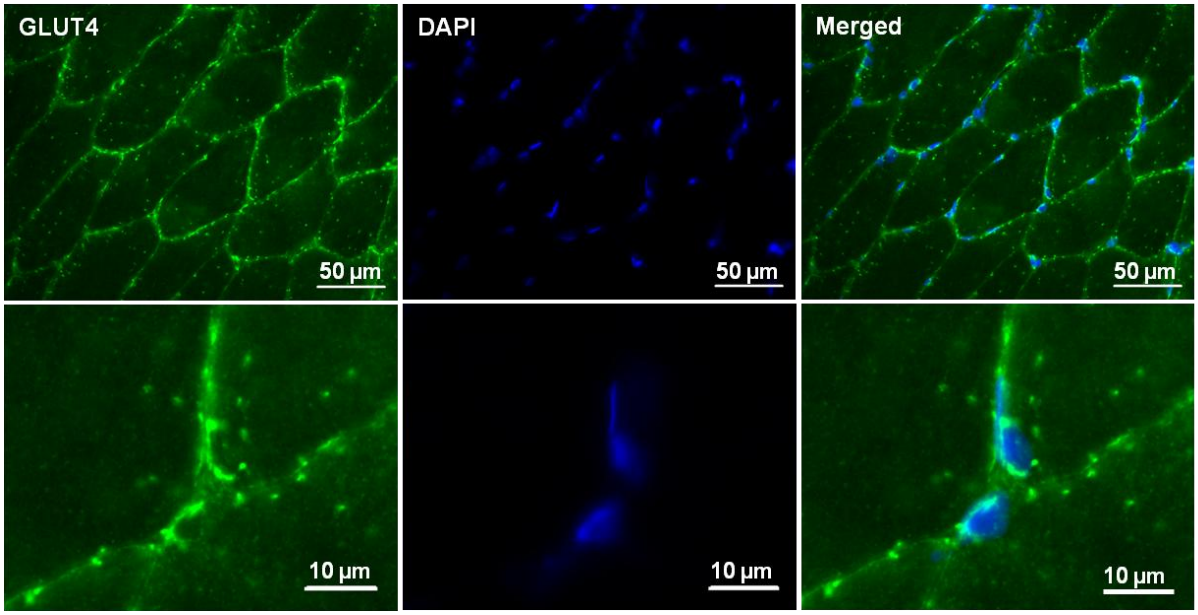

Fig. 2.3. *Representative widefield immunofluorescence microscopy images of GLUT4 (green) in human skeletal muscle stained in combination with DAPI (blue) to mark the cell nuclei.*

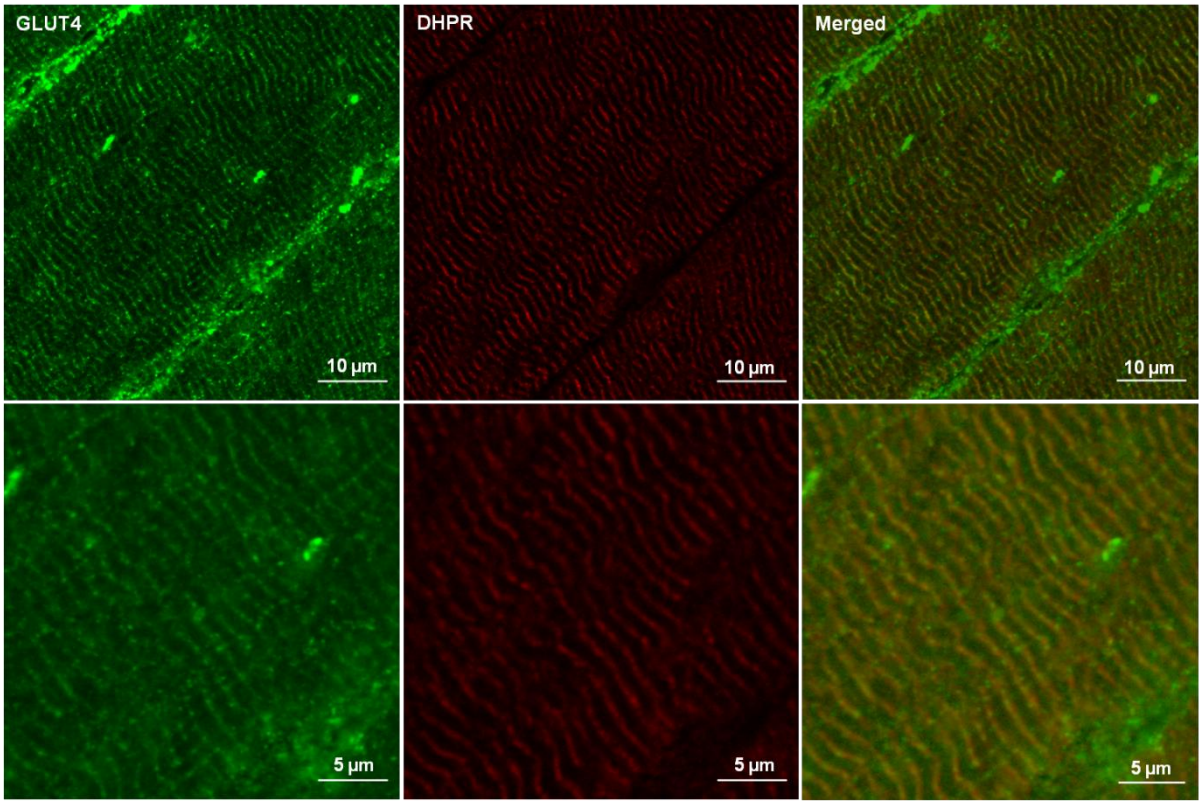

Fig. 2.4. *Representative confocal immunofluorescence microscopy images of GLUT4 (green) in human skeletal muscle stained in combination with DHPR (red) to mark the T-tubule membranes.*

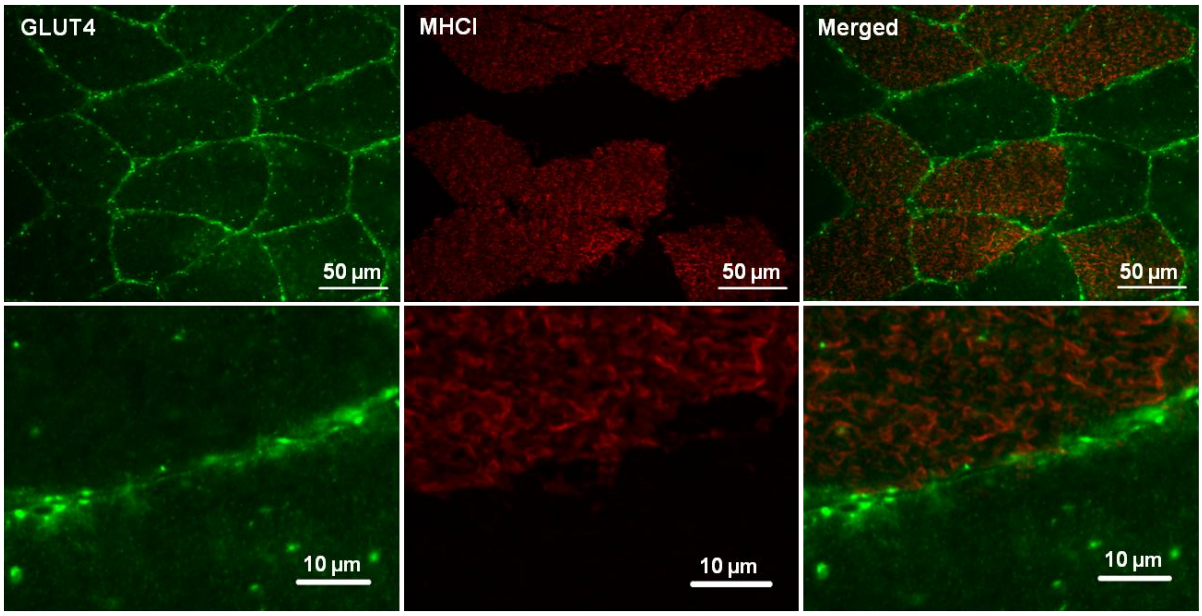

Fig. 2.5. *Representative widefield immunofluorescence microscopy images of GLUT4 (green) in human skeletal muscle stained in combination with MHCI (red) to mark the type I muscle fibres.*

2.9.3. Coefficient of variation of the Pearson's correlation coefficient to measure GLUT4 and dystrophin colocalisation

The Pearson's correlation coefficient to measure GLUT4 in PM regions has been used in all chapters of this thesis. During the development of this method staining was carried out on five serial sections of the same muscle piece each on a separate slide in order to determine the coefficient of variation of the analysis method. As with the full analysis carried out in each study of this thesis, five GLUT4 and dystrophin images were captured per section. The mean Pearson's correlation coefficient for each section is displayed in Fig. 2.6. The coefficient of variation across the five sections is 1 %.

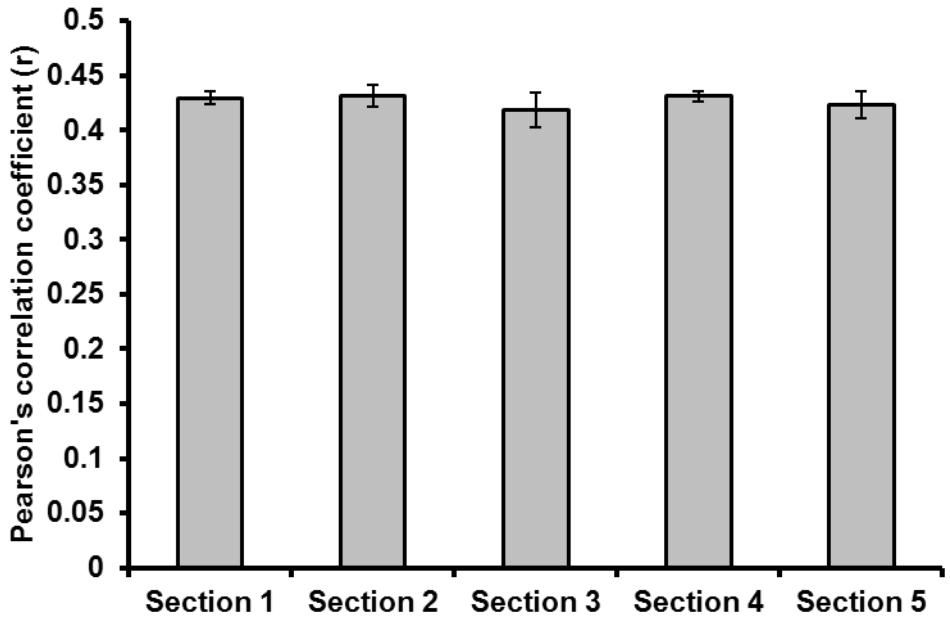

Fig. 2.6. *Pearson's correlation coefficient measuring GLUT4 and dystrophin colocalisation in five serial sections. Coefficient of variation between sections is 1 %. Mean ± SEM. N = 5.*

2.10. Attempts made to co-stain GLUT4 and SNAP23

Combined staining of GLUT4 and SNAP23 at the PM would enable assessment of whether regions of GLUT4 and SNAP23 staining overlap at the PM. If this were confirmed to be the case it would support the idea that GSV fusion with the PM occurs at specific PM domains (Chamberlain and Gould, 2002). Furthermore combination of GLUT4 and SNAP23 staining would allow further investigation of the SNARE highjacking hypothesis (Sollner, 2007) by determining whether increased lipid content reduces the colocalisation of GLUT4 and SNAP23 in the insulin stimulated state in T2D compared to insulin sensitive individuals. Therefore during these PhD studies attempts were made to co-stain GLUT4 and SNAP23.

2.10.1. Problem of species cross-reactivity

The GLUT4 and SNAP23 antibodies that have been fully validated, either as part of this thesis or in the thesis of Dr. Juliette Clark (Clark, 2012), are both the same isotype and were raised in the same species; rabbit IgG. Therefore the primary antibodies could not be targeted with secondary antibodies specific to each primary antibody (depicted in Fig. 2.7A). Alternative approaches were attempted and will be outlined in the sections below. A fundamental difference is that each target was stained sequentially. In brief, following fixation GLUT4 primary antibody and after subsequent washing a secondary detection system against the GLUT4 primary antibody were applied to the skeletal muscle section, followed by further washing and application of SNAP23 antibody, washing and application of a secondary detection system against the SNAP23 primary antibody. Finally sections were again washed and mounted. The potential pitfalls are; avoiding SNAP23 primary antibody binding to any available sites in the GLUT4 secondary detection system and avoiding the SNAP23 secondary detection system binding to any available sites on the GLUT4 primary antibody.

2.10.2. Fluorophore conjugated Fab fragment (Fig.2.7B)

Secondary antibodies have more than one binding site available for binding to a primary antibody. Therefore once the GLUT4 secondary antibody has bound to the GLUT4 primary antibody binding sites would still be available when the SNAP23 primary antibody was subsequently applied. A fab fragment only has one binding site available for primary antibody binding and, therefore, use of appropriate fab fragments could prevent binding of SNAP23 primary antibody to the GLUT4 secondary detection system. Furthermore, an excess of Fab fragments can be used to saturate all GLUT4 primary antibody binding sites.

Despite a number of different attempts using different fab fragment dilutions and with a fixation step after GLUT4 staining, Fig. 2.8E demonstrates that the fab fragment did not block

all GLUT4 primary antibody binding sites and the attempt to block binding between the SNAP23 secondary antibody and the GLUT4 primary antibody therefore was not successful.

2.10.3. Biotin-labelled primary antibody (Fig.2.7C)

In order to avoid the above pitfall an alternative SNAP23 secondary detection system was investigated. GLUT4 was labelled the same as above but a biotin-labelled SNAP23 primary antibody would be used to allow detection of SNAP23 with AlexaFluor 488 conjugated streptavidin, which has a high affinity for biotin. The same SNAP23 antibody was provided by Synaptic Systems with a biotin label (111-203BT), however staining with this antibody (Fig. 2.9B) differed to staining with the original antibody (Fig. 2.9A). Furthermore a control in which only streptavidin was applied to the muscle sections showed streptavidin binds to endogenous biotin in skeletal muscle (Fig. 2.9C). Therefore use of biotin-labelled SNAP23 antibody was also not an option.

2.10.4. GLUT4 and SNAP23 co-staining conclusions

As explained above, the attempts to co-stain GLUT4 and SNAP23 were not successful. Further options would be to use alternative antibodies raised in a different species. However time was not available to fully validate new antibodies. Therefore for this thesis where SNAP23 staining was required, it was completed on different sections to GLUT4 staining. This, however, prevented us from generating evidence that GLUT4 docking and fusion preferentially occurred in SNAP23 rich lipid rafts as previously observed in adipose tissue cells (Chamberlain and Gould, 2002).

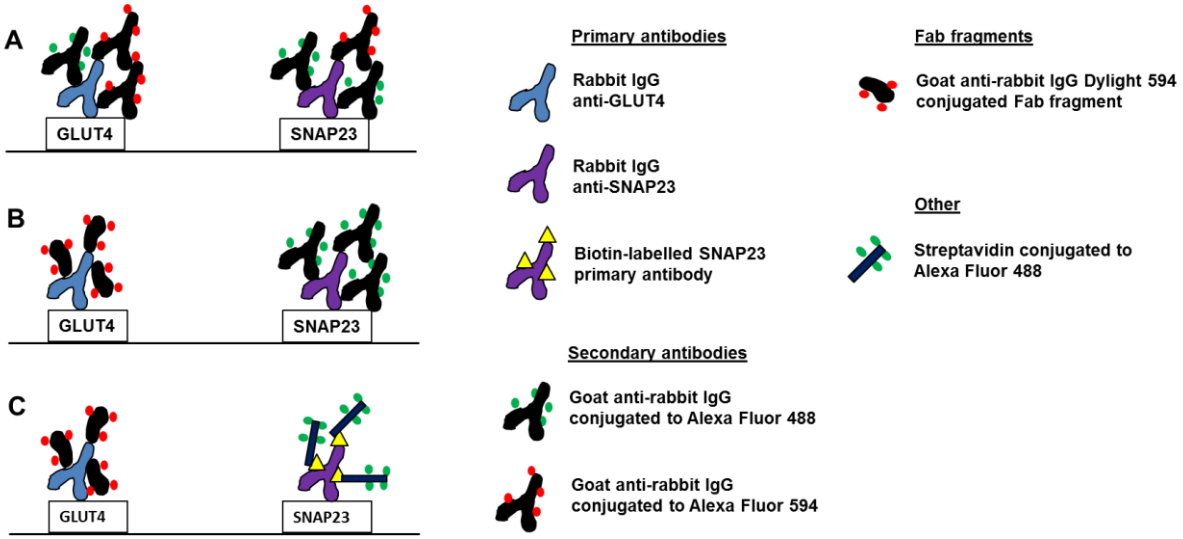

Fig. 2.7. M*ethodological problems and attempted solutions associated with GLUT4 and SNAP23 primary antibodies of the same species. A) Cross reactivity of goat-anti rabbit secondary antibodies against GLUT4 and SNAP23 secondary antibodies. B) Use of a goat anti-rabbit fab fragment to saturate all GLUT4 primary antibody and fab fragment binding sites prior to incubation with SNAP23 primary and then secondary antibody. C) Biotin-labelled SNAP23 primary antibody targeted with AlexaFluor 488 conjugated streptavidin.*

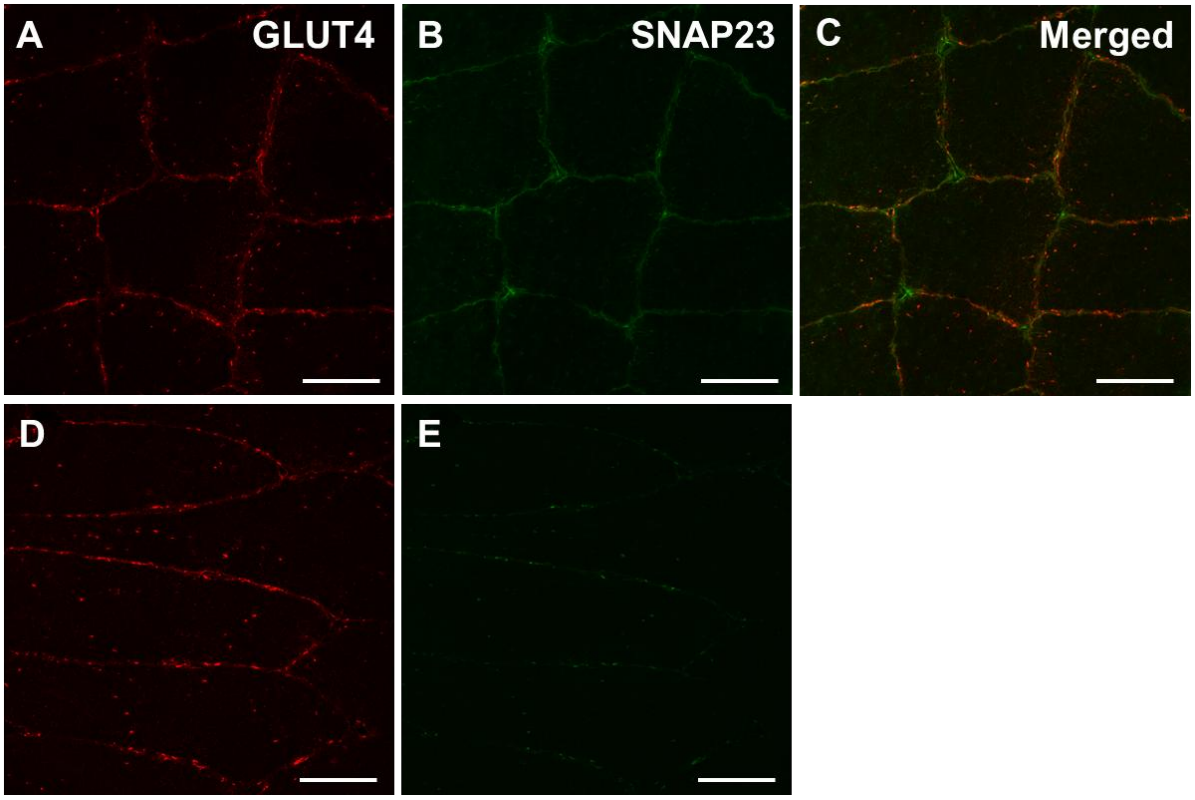

Fig. 2.8. *Confocal immunofluorescence microscopy images demonstrating attempts made to eliminate secondary antibody cross reactivity by targeting rabbit anti-GLUT4 primary antibody with goat anti-rabbit Dylight 594 fluorophore conjugated Fab fragment. A and D) GLUT4 staining with rabbit anti-GLUT4 primary antibody and goat anti-rabbit Dylight 594 fluorophore conjugated Fab fragment. B) Subsequent staining of SNAP23 with rabbit anti-SNAP23 primary antibody and AlexaFluor 488 conjugated goat anti-rabbit secondary antibody. C) Merged image of GLUT4 (red) and SNAP23 (green) staining. E) Omission of SNAP23 primary antibody with application of AlexaFluor 488 conjugated goat anti-rabbit secondary antibody shows binding of this secondary antibody to the GLUT4 primary antibody. Scale bars 50 µm.*

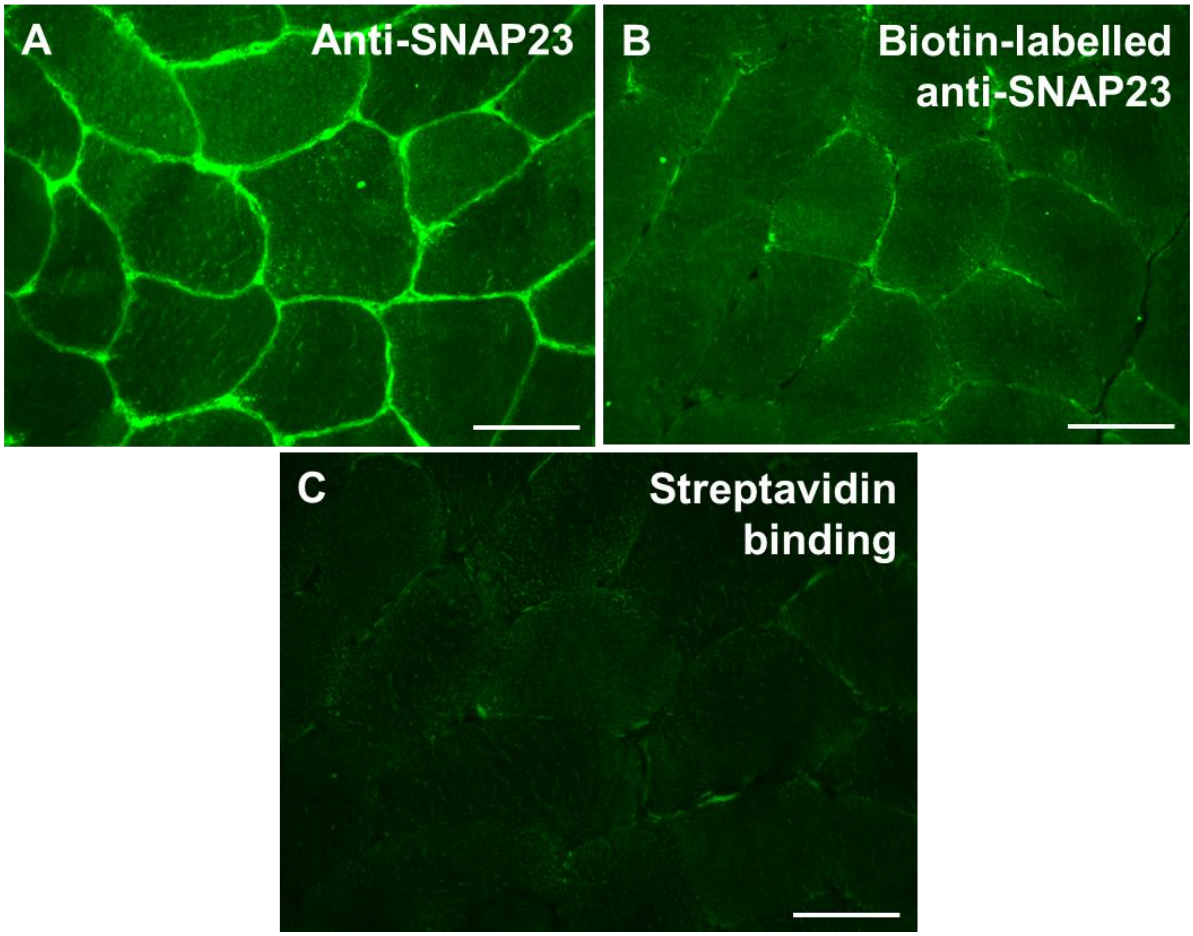

Fig. 2.9. *Widefield immunofluorescence microscopy images captured at the same settings demonstrating testing of biotin-labelled rabbit SNAP23 primary antibody. A) Rabbit anti-SNAP23 primary antibody targeted with AlexaFluor 488 conjugated goat anti-rabbit secondary antibody. B) Biotin-labelled rabbit anti-SNAP23 primary antibody targeted with AlexaFluor 488 conjugated streptavidin. C) Omission of biotin-labelled rabbit anti-SNAP23 primary antibody, therefore demonstrating direct binding of AlexaFluor 488 conjugated streptavidin to skeletal muscle section. Scale bars 50 µm.*

2.11. Attempts to quantify GLUT4 in the T-tubule membranes

The T-tubule membrane system comprises invaginations of the muscle PM which extend deep into the muscle fibre and is well characterised as a site of insulin- and contraction-mediated GLUT4 translocation in rodent muscle (Ploug et al., 1998, Lauritzen et al., 2006, Lauritzen et al., 2010). Therefore attempts were made to quantify GLUT4 in the T-tubule membranes with the aim to assess whether GLUT4 translocation to the T-tubule membranes of human skeletal muscle occurred following feeding and exercise. The first method considered was to create a mask from DHPR staining in longitudinally-oriented muscle fibres and to subsequently measure GLUT4 fluorescence intensity within this mask (Fig. 2.10A-D). The second method considered was to measure GLUT4 fluorescence intensity along a line drawn perpendicular to the GLUT4 striations in a longitudinally oriented muscle fibre (Fig. 2.10E-F) and to take the mean of the intensity peaks. Unfortunately, due to the nature of cryosections cutting through a single plane of muscle which was unlikely to correspond to the plane of an individual muscle fibre, the T-tubule membrane system network comes in and out of focus along the length of the fibre therefore making it difficult to achieve a repeatable and objective measure of GLUT4 in the T-tubule membrane using either of the above methods. Images of DHPR in three different Z positions in Fig. 2.11 demonstrate that the T-tubule membranes (DHPR stained regions) come in and out of focus even in different planes of an image stack. As discussed again in chapter 7, a potential solution may be to use these quantitation suggestions in single muscle fibres where the fibre can be visualised in one plane rather than cut through as in a cryosection. However unfortunately time constraints prevented development of the technique for this thesis, so only GLUT4 translocation to the PM has been assessed in a quantitative manner.

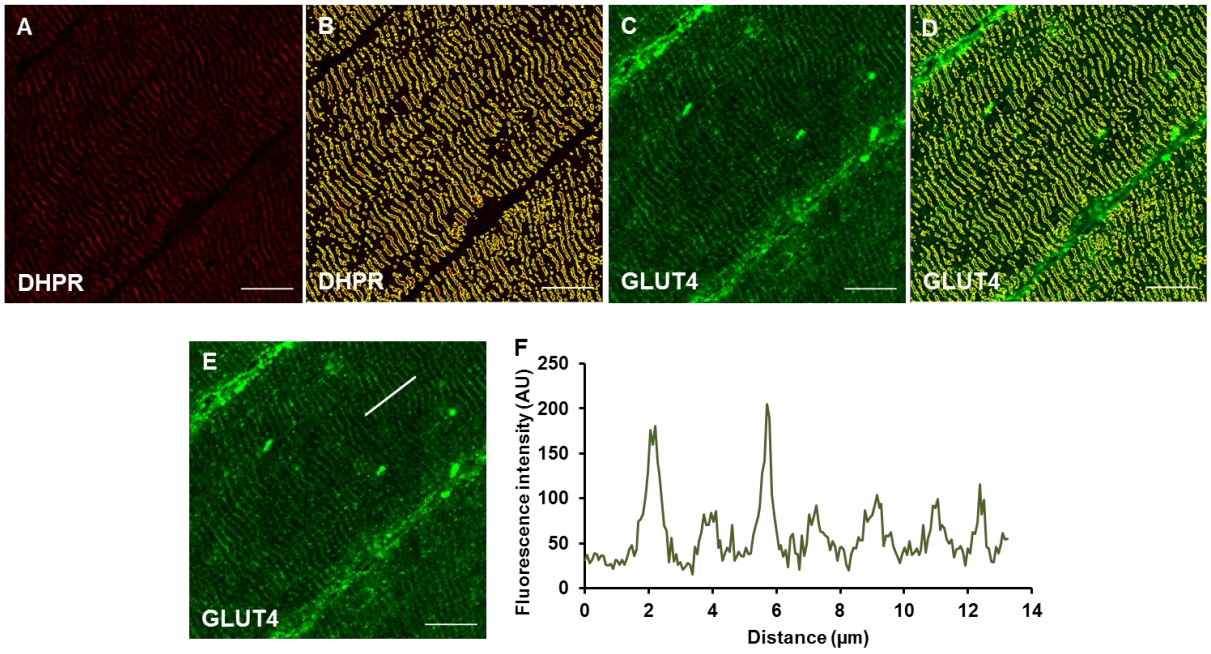

Fig. 2.10. *Quantitation methods attempted for GLUT4 in the T-tubule membranes. A-D GLUT4 fluorescence intensity within DHPR mask. E-F GLUT4 intensity along line running perpendicular to striations. Scale bars 10 µm.*

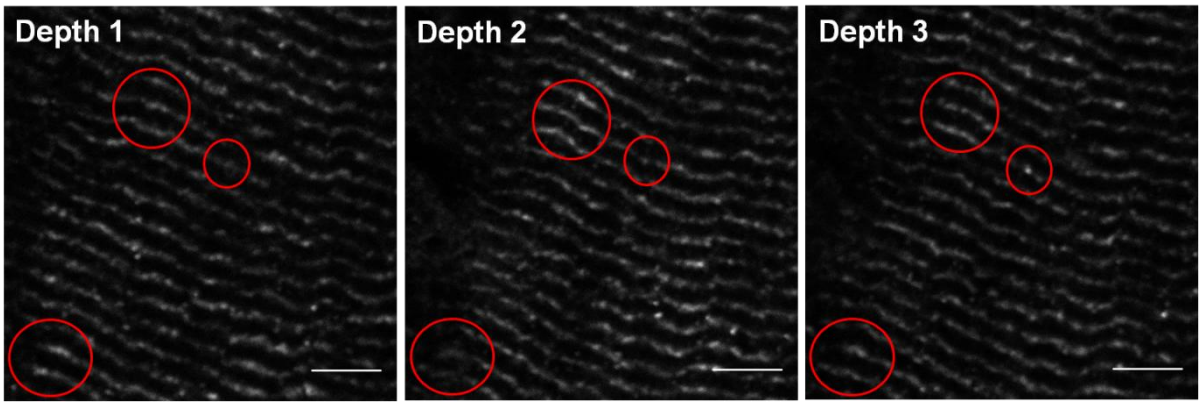

Fig. 2.11. *Confocal immunofluorescence images of DHPR staining at three different Z positions in image stack. Scale bars 5 µm.*

2.12. Acknowledgements

Dr Samantha Peel at AstraZeneca very kindly assisted with the GLUT4 antibody validation in GLUT4-myc and non-transfected L6 cells.

2.13. References

BERGSTROM, J. 1975. Percutaneous needle biopsy of skeletal muscle in physiological and clinical research. *Scand J Clin Lab Invest,* 35**,** 609-16.

BOLTE, S. & CORDELIERES, F. P. 2006. A guided tour into subcellular colocalization analysis in light microscopy. *J Microsc,* 224**,** 213-32.

BURRY, R. W. 2011. Controls for immunocytochemistry: an update. *J Histochem Cytochem,* 59**,** 6-12.

CHAMBERLAIN, L. H. & GOULD, G. W. 2002. The vesicle- and target-SNARE proteins that mediate Glut4 vesicle fusion are localized in detergent-insoluble lipid rafts present on distinct intracellular membranes. *J Biol Chem,* 277**,** 49750-4.

CLARK, J. A. 2012. *Subcellular distribution of lipid metabolising enzymes in human skeletal muscle.* University of Birmingham.

DENIS, N., BLANC, S., LEIBOVITCH, M. P., NICOLAIEW, N., DAUTRY, F., RAYMONDJEAN, M., KRUH, J. & KITZIS, A. 1987. c-myc oncogene expression inhibits the initiation of myogenic differentiation. *Exp Cell Res,* 172**,** 212-7.

DUNN, K. W., KAMOCKA, M. M. & MCDONALD, J. H. 2011. A practical guide to evaluating colocalization in biological microscopy. *Am J Physiol Cell Physiol,* 300**,** C723-42.

KANAI, F., NISHIOKA, Y., HAYASHI, H., KAMOHARA, S., TODAKA, M. & EBINA, Y. 1993. Direct demonstration of insulin-induced GLUT4 translocation to the surface of intact cells by insertion of a *c-myc* epitope into an exofacial GLUT4 domain. *J Biol Chem, 268, 14523-14526.*

KOENIG, M., MONACO, A. P. & KUNKEL, L. M. 1988. The complete sequence of dystrophin predicts a rod-shaped cytoskeletal protein. *Cell,* 53**,** 219-28.

LACHMANOVICH, E., SHVARTSMAN, D. E., MALKA, Y., BOTVIN, C., HENIS, Y. I. & WEISS, A. M. 2003. Co-localization analysis of complex formation among membrane proteins by computerized fluorescence microscopy: application to immunofluorescence co-patching studies. *J Microsc,* 212**,** 122-31.

LANDMANN, L. & MARBET, P. 2004. Colocalization analysis yields superior results after image restoration. *Microsc Res Tech,* 64**,** 103-12.

LAURITZEN, H. P., GALBO, H., TOYODA, T. & GOODYEAR, L. J. 2010. Kinetics of contraction-induced GLUT4 translocation in skeletal muscle fibers from living mice. *Diabetes,* 59**,** 2134-44.

LAURITZEN, H. P., PLOUG, T., PRATS, C., TAVARE, J. M. & GALBO, H. 2006. Imaging of insulin signaling in skeletal muscle of living mice shows major role of T-tubules. *Diabetes,* 55**,** 1300-6.

LEE, Y.N., CHEN, L.K., MA, H.C., YANG, H.H., LI, H.P. & LO, S.Y. 2005. Thermal aggregation of SARS-CoV memebrane protein. *J Virol Methods,* 129, 152-161.

MATSUDA, M. & DEFRONZO, R. A. 1999. Insulin sensitivity indices obtained from oral glucose tolerance testing: comparison with the euglycemic insulin clamp. *Diabetes Care,* 22**,** 1462-70.

NGUYEN, T. M., ELLIS, J. M., GINJAAR, I. B., VAN PAASSEN, M. M., VAN OMMEN, G. J., MOORMAN, A. F., CARTWRIGHT, A. J. & MORRIS, G. E. 1990. Monoclonal antibody evidence for structural similarities between the central rod regions of actinin and dystrophin. *FEBS Lett,* 272**,** 109-12.

PLOUG, T., VAN DEURS, B., AI, H., CUSHMAN, S. W. & RALSTON, E. 1998. Analysis of GLUT4 distribution in whole skeletal muscle fibers: identification of distinct storage compartments that are recruited by insulin and muscle contractions. *J Cell Biol,* 142**,** 1429-46.

SAPER, C. B. 2005. An open letter to our readers on the use of antibodies. *J Comp Neurol,* 493**,** 477-8.

SAPER, C. B. 2009. A guide to the perplexed on the specificity of antibodies. *J Histochem Cytochem,* 57**,** 1-5.

SEDARAT, F., LIN, E., MOORE, E. D. & TIBBITS, G. F. 2004. Deconvolution of confocal images of dihydropyridine and ryanodine receptors in developing cardiomyocytes. *J Appl Physiol,* 97**,** 1098-103.

SEDGWICK, S. G., NGUYEN, T. M., ELLIS, J. M., CROWNE, H. & MORRIS, G. E. 1991. Rapid mapping by transposon mutagenesis of epitopes on the muscular dystrophy protein, dystrophin. *Nucleic Acids Res,* 19**,** 5889-94.

SHEPHERD, S. O., COCKS, M., TIPTON, K. D., RANASINGHE, A. M., BARKER, T. A., BURNISTON, J. G., WAGENMAKERS, A. J. & SHAW, C. S. 2013. Sprint interval and traditional endurance training increase net intramuscular triglyceride breakdown and expression of perilipin 2 and 5. *J Physiol,* 591**,** 657-75.

SMITH, C. L. 2008. Basic confocal microscopy. *Curr Protoc Mol Biol,* Chapter 14**,** Unit 14 11.

SOLLNER, T. H. 2007. Lipid droplets highjack SNAREs. *Nat Cell Biol,* 9**,** 1219-20.

WANG, Q., KHAYAT, Z., KISHI, K., EBINA, Y. & KLIP, A. 1998. GLUT4 translocation by insulin in intact muscle cells: detection by a fast and quantitative assay. *FEBS lett,* 427, 193-197.

WEBSTER, C., SILBERSTEIN, L., HAYS, A. P. & BLAU, H. M. 1988. Fast muscle fibers are preferentially affected in Duchenne muscular dystrophy. *Cell,* 52**,** 503-13.

WILSON, O. J., SHAW, C. S., SHERLOCK, M., STEWART, P. M. & WAGENMAKERS, A. J. 2012. Immunofluorescent visualisation of focal adhesion kinase in human skeletal muscle and its associated microvasculature. *Histochem Cell Biol,* 138**,** 617-26.

CHAPTER 3

IMMUNOFLUORESCENCE VISUALISATION OF SUBCELLULAR GLUT4 DISTRIBUTION AND CONTENT IN HUMAN SKELETAL MUSCLE: EFFECTS OF ENDURANCE TRAINING AND SPRINT INTERVAL TRAINING

H. Bradley[1], C.S. Shaw[1,2], S.O. Shepherd[1,3], M. Cocks[1,3], and A.J.M. Wagenmakers[1,3]

[1]School of Sport and Exercise Sciences, University of Birmingham, UK

[2]Institute of Sport, Exercise and Active Living (ISEAL), Victoria University, Australia

[3]Research Institute for Sport and Exercise Sciences, Liverpool John Moores University, UK

3.1. Abstract

Increases in insulin-mediated glucose uptake following both endurance training (ET) and sprint interval training (SIT) have in part been attributed to concomitant increases in glucose transporter 4 (GLUT4) protein content in skeletal muscle. This study applied immunofluorescence methods developed in chapter 2 to investigate changes in GLUT4 content and subcellular localisation in human skeletal muscle in response to ET and SIT in order to further understand the mechanisms underpinning training-induced increases in insulin-mediated glucose uptake. Percutaneous muscle biopsy samples were taken from the *vastus lateralis* of 16 sedentary males in the rested overnight fasted state before and after 6 weeks of either ET or SIT. Large and smaller GLUT4-containing structures were located predominantly at the fibre periphery with a less dense punctate distribution in the rest of the muscle fibre. Total GLUT4 fluorescence intensity increased in type I and type II fibres following both ET and SIT. Number and staining area per fibre of intracellular clusters of GLUT4 staining increased both in type I and type II fibres. Large clusters (> 1 μm) increased predominantly in number, while the smaller clusters (< 1 μm) increased in size. There was no statistically significant increase in colocalisation of GLUT4 with the PM marker dystrophin. In conclusion, the immunofluorescence method developed in chapter 2 has been applied to human skeletal muscle to visualise GLUT4 distribution and content following ET and SIT. The increase in GLUT4 content observed following ET and SIT appears to be due primarily to an increase in the number of large intracellular GLUT4 storage clusters and the size of small GLUT4 storage clusters therefore increasing the GLUT4 available for translocation and likely contributing to the improvements in glucose homeostasis observed after both training modes.

3.2. Introduction

Skeletal muscle is the primary site of insulin-mediated glucose uptake (Katz et al., 1983, Wasserman et al., 2011) and is therefore important in determining whole body glucose disposal rates. Glucose transporter 4 (GLUT4) is the major facilitative glucose transporter isoform expressed in human skeletal muscle (Mueckler, 1994). Previous research in rat muscle has shown that GLUT4 is located in intracellular storage clusters which are predominantly located at the fibre periphery but also in deeper regions (Ploug et al., 1998). Following insulin stimulation GLUT4 storage vesicles (GSVs) dissociate from the larger intracellular storage clusters and translocate to fuse with both the plasma membrane (PM) and T-tubule membranes. This is assumed to lead to increases in PM GLUT4 content which enables increased glucose uptake into the muscle cell (Ploug et al., 1998, Lizunov et al., 2012, Bell et al., 1993, Lauritzen et al., 2008, Lauritzen et al., 2006).

Experimental increases in total muscle GLUT4 content are known to increase insulin stimulated glucose uptake rate, as demonstrated in animal models overexpressing GLUT4 in skeletal muscle (Ren et al., 1995, Leturque et al., 1996, Hansen et al., 1995). Similarly, in humans improvements in glucose homeostasis and increases in insulin sensitivity (measured during a hyperinsulinemic-euglycaemic clamp and/or an oral glucose tolerance test), that are seen following endurance exercise training (ET) and various forms of high intensity interval training (HIT), occur in parallel with robust increases in total skeletal muscle GLUT4 protein content (Hughes et al., 1993, Dela et al., 1996, Cox et al., 1999, Babraj et al., 2009, Richards et al., 2010, Houmard et al., 1991, Phillips et al., 1996, Daugaard et al., 2000, Burgomaster et al., 2007, Hood et al., 2011, Little et al., 2010). Increases in insulin-stimulated leg glucose uptake that occur in humans after training (Dela et al., 1996, Frosig et al., 2007, Dela et al., 1995, Dela et al., 1992) are driven by multiple mechanisms (Wasserman et al., 2011). The

main candidate mechanisms are training induced increases in: 1) insulin sensitivity leading to more GLUT4 translocation for the same insulin stimulus; 2) total number of GLUT4 molecules able to translocate to the PM (Hughes et al., 1993, Dela et al., 1996, Cox et al., 1999, Houmard et al., 1991, Phillips et al., 1996, Daugaard et al., 2000, Burgomaster et al., 2007); 3) mitochondrial oxidative capacity leading to steeper glucose gradients between capillary blood and the muscle cytosol (Hood et al., 2011, Little et al., 2010); and 4) capillary density leading to increased insulin induced microvascular dilation and a larger surface area available for the transendothelial transport of both insulin and glucose (Barrett et al., 2009, Barrett et al., 2011).

Studies in adipocytes have revealed that GLUT4 is stored in 50 – 70 nm insulin responsive vesicles termed GLUT4 storage vesicles (GSVs) and endosomal membranes estimated to be approximately 150 – 200 nm (Bogan, 2012, Bogan and Kandror, 2010, Larance et al., 2008, Stockli et al., 2011). GSVs in adipose tissue cells are formed by insulin stimulated budding of endosomal and trans-Golgi network (TGN) membranes (Bogan, 2012, Bogan and Kandror, 2010, Larance et al., 2008) followed by GSV translocation, docking and fusion with the PM to allow increased glucose uptake (Foley et al., 2011). Studies combining confocal immunofluorescence microscopy techniques with immunogold labelling electron microscopy (EM) applied to whole single fibres of rat soleus muscle have also demonstrated the presence of GLUT4 in TGN, endosomal membranes and GSVs (Lizunov et al., 2012, Lauritzen et al., 2008, Ploug et al., 1998, Rodnick et al., 1992). Immunofluorescence images have defined TGN GLUT4 stores as > 1 μm in size (Lauritzen et al., 2008), while based on EM images endosomal membrane stores appear to be smaller than TGN stores (Ploug et al., 1998) but larger than GSVs which have been reported as 40 nm (Lizunov et al., 2012). In muscle, GLUT4 stores are predominantly located at the fibre periphery in the basal state, with some

areas of intense intracellular staining. Large and smaller clusters of GLUT4 staining have been observed with a particularly high density in the perinuclear region. Staining in the PM region was present in the basal state, but was not continuous (Ploug et al., 1998, Lauritzen et al., 2006).

Other observations made in rodent muscle are that the large GLUT4 clusters did not translocate with insulin stimulation, rather they remained stationary and were locally depleted (Lauritzen et al., 2008). Similarly TGN stores of GLUT4 have been shown to reduce in size while endosomal stores and GSVs reduced in number following insulin stimulation (Ploug et al., 1998). Furthermore, total internal reflection fluorescence (TIRF) microscopy studies using a fluorescently labelled form of GLUT4 have shown that following insulin stimulation of isolated mouse muscle more than 80 % of insulin-stimulated fusion events emanated from stationary vesicles that had been pre-tethered at the PM or T-tubule membranes prior to stimulation, with only 10 % of all GLUT4 structures shown to be mobile (Lizunov et al., 2012). Taken together these data suggest that GLUT4 movement following stimulation is minimal and, therefore, implying basal state GLUT4 localisation close to the PM could impart a benefit for insulin action on glucose uptake. Brozinick *et al.* (1993) used membrane isolation and Western blotting methods to show increases in GLUT4 in the PM fraction of obese Zucker rat skeletal muscle following training (Brozinick et al., 1993). This led to the suggestion that GLUT4 localisation in regions close to the PM, as well as GLUT4 content, is important in the training-mediated increase in insulin stimulated glucose uptake (Ivy, 2004).

Two recent publications from our laboratory have shown that ET and sprint interval training (SIT, an extreme form of HIT involving 4-6 repeated 30 sec Wingate sprints) lead to similar magnitude increases in whole body insulin sensitivity, skeletal muscle mitochondrial content and skeletal muscle microvascular density and eNOS content (Shepherd et al., 2013, Cocks et

al., 2013). These observations support contributions of mechanism 1, 3 and 4 (introduced above) to the improved glucose homeostasis that is seen after training. In the current study we aimed to measure GLUT4 total protein content and subcellular distribution in muscle samples taken previously (studies published by Shepherd *et al.* (2013) and Cocks *et al.* (2013)) using the confocal immunofluorescence microscopy method developed in chapter 2 of this thesis to further investigate the contribution of GLUT4 total protein content (mechanism 2) to the improvements in glucose homeostasis after training. The immunofluorescence microscopy method was used to confirm the increase in total GLUT4 protein content observed previously in the literature and to further investigate whether any changes in GLUT4 subcellular distribution occur that may improve glucose homeostasis following training. In particular the immunofluorescence microscopy method was used to assess whether there are increases in colocalisation of GLUT4 and the PM marker dystrophin in the basal state or increases in the amount of the large and smaller intracellular GLUT4 clusters that would increase the amount of GLUT4 available for translocation and therefore improve glucose homeostasis following training.

3.3. Methods

Ethics, recruitment and informed consent. Sixteen sedentary, but otherwise healthy men (mean ± SEM, age 21 ± 1 y, BMI 23.7 ± 0.8 $kg.m^{-2}$, $VO_{2\ max}$ 41.8 ± 2.2 $mL.min^{-1}.kg^{-1}$) all gave written informed consent before being randomly divided into two age-, BMI- and VO_{2max}-matched groups to complete 6 weeks of either ET or SIT. Ethical approval was granted for the study by the Black Country Research Ethics Committee and all procedures conformed to the Helsinki declaration.

Training and testing. All procedures for pre- and post-training experiments and training interventions have been previously reported (Cocks et al., 2012, Shepherd et al., 2012). Briefly, all participants underwent a fasting muscle biopsy and a 2 h oral glucose tolerance test prior to and following 6 weeks of training. All post-training experiments were performed at least 48 h following the last training bout. On a separate day, participants performed an incremental exercise test to exhaustion on an electronically braked cycle ergometer to determine their VO_{2max} as an indicator of fitness and to set the exercise intensity during training sessions. ET consisted of 5 sessions per week of cycling on an electronically braked cycle ergometer at 65 % of $VO_{2\ max}$, with session duration increasing from 40 min to 60 min over the 6 week training period. SIT subjects completed 3 sessions per week each consisting of 4-6 Wingate tests (increasing over the 6 week training period). Each Wingate required a 30 s 'all out' sprint against a resistance of 0.075 kg/kg body mass followed by 4.5 min low intensity cycling on an electronically braked cycle ergometer.

Sample collection, preparation and storage. Full details of skeletal muscle biopsy and blood sample collection, processing and storage are provided in chapter 2. Skeletal muscle biopsy samples were processed for immunofluorescence staining and Western blotting; both are described in chapter 2.

Immunofluorescence staining protocol. The GLUT4 immunofluorescence staining protocol is described in full in chapter 2. In brief, muscle sections were fixed for 5 min in 75 % acetone 25 % ethanol and subsequently washed 3 times for 5 min in PBS. GLUT4 antibody (Abcam, UK) was applied to the sections at a dilution of 1:200 in 5 % normal goat serum (NGS, Invitrogen, UK) for 2 h at room temperature. GLUT4 primary antibody was combined with dystrophin (1:400, Sigma Aldrich, UK) and myosin heavy chain (MHCI; 1:100, developed by

Dr. Blau, DSHB, USA) antibodies. Following primary antibody incubation sections were washed 3 times for 5 min in PBS. Secondary antibodies were applied to sections for 30 min at room temperature at a dilution of 1:200 in PBS. GLUT4 antibody was targeted with goat anti-rabbit IgG 488 (Invitrogen, UK), dystrophin with goat anti-mouse IgG_{2b} 633 (Invitrogen, UK) and MHCI with goat anti-mouse IgM 594 (Invitrogen, UK). After secondary antibody incubation sections were washed 3 times for 5 min in PBS and coverslips were mounted with 20 µl mowiol.

Image capture. Confocal image capture was completed using an inverted confocal microscope (Leica DMIRE2, Leica Microsystems) with a 63x oil immersion objective (1.4 NA). AlexaFluor 488 fluorophores were excited with a 488 nm line of the argon laser and 498-571 nm emission. Alexa Fluor 594 fluorophores were excited with the 594 nm line of the helium-neon laser and 601-713 nm emission. Alexa Fluor 633 fluorophores were excited with the 633 nm line of the helium-neon laser and 639-734 nm emission.

Image quantitation. For each subject, 3 slide replicates, each with a pre-training and a post-training section, were stained, imaged and quantified. At least 5 type I fibre images and 5 type II fibre images were captured per section, therefore for each subject at least 30 images (15 type I fibres and 15 type II fibres) were analysed for both pre and post training. All image processing and quantitation was carried out in ImagePro Plus 5.1 and was kept consistent between images. GLUT4 fluorescence intensity was quantified by measuring the signal intensity within the intracellular regions of a mask created by the dystrophin stain in a fibre type specific manner as determined from the MHCI stain. No image processing was carried out prior to intensity analysis. Intracellular spot number and staining area per fibre was quantified by setting uniform threshold intensity and size values to identify spots within

intracellular regions of the dystrophin mask in a fibre type specific manner. In rodent muscle large GLUT4 stores which were stationary were greater than 1 µm in size. The small, mobile stores in rodent muscle were reported as < 1 µm in size (Lauritzen et al., 2008). Large and small spots in this paper were determined by limiting the threshold size values, whereby spots > 1 µm in diameter were classed as large spots and spots < 1 µm in diameter were classified as small spots. The mean size of spots was calculated by dividing the total area of spot staining by the number of spots per fibre. An ImagePro Plus no neighbour deconvolution algorithm and a HiGauss filter were applied to GLUT4 images prior to spot detection. Colocalisation in GLUT4 and dystrophin image pairs, to estimate GLUT4 PM content, was determined using the colocalisation tool in ImagePro Plus 5.1, to calculate the Pearson's correlation coefficient. Prior to colocalisation all images underwent an ImagePro Plus 5.1 no neighbour deconvolution algorithm as a filter.

Western blotting for GLUT4 content. Equal total protein quantities (60 µg) of all ET and SIT samples were separated by electrophoresis on 12 % polyacrylamide gels in 1x Tris/Glycine/SDS buffer (National Diagnostics, USA) for 20 min at 80 V and 2 hr at 120 V. Proteins were then transferred to nitrocellulose membrane using Invitrogen iblot apparatus (Invitrogen, UK) and Invitrogen iblot gel transfer stacks (Invitrogen, UK). Following transfer membranes were washed briefly in phosphate buffered saline (PBS, tablets, Merck Millipore, Germany) with 0.1 % tween-20 (Sigma Aldrich, UK) and bands were visualised with Ponceau S to confirm successful transfer. Ponceau S staining was removed with 3 washes for 2 min in PBST. Membranes were blocked for 1 h in 5 % milk (dried skimmed milk, Marvel) and incubated overnight at 4^{o}C on a shaker in 1: 2000 GLUT4 primary antibody in 5 % milk. Following incubation membranes were washed 4 times for 15 min in PBST and incubated in 1:15000 goat anti-rabbit IgG HRP secondary antibody (DAKO, Denmark) in 5 % milk at

room temperature for 1 h. Membranes were again washed 4 times for 15 min in PBST and were incubated for 5 min in ECL substrate (GE Healthcare, UK)) prior to exposure of membrane to film (Kodak, UK). Film was developed using a Xograph Imaging Systems Compact X4. To carry out protein loading control, membrane was washed 4 times for 15 min in PBST and incubated for 1 h in 1:2000 GAPDH (Cell Signalling, USA) antibody in 5 % milk. Following washing, membranes were incubated in 1:15000 goat anti-rabbit IgG HRP secondary antibody in 5 % milk for 1 h and after incubation were washed for the final time. Membranes were incubated in ECL for 5 min, exposed to film and developed as before. Imaging of blots was performed using a BIORAD GS-800 calibrated densitometer with QuantityOne 4.5.1 software (BIORAD) and band quantitation, normalised to a pooled standard and GAPDH, was carried out using ImagePro Plus 5.1.

Statistical analyses. Statistical analysis was carried out using PASW Statistics 18.0. Age-, BMI- and VO_{2max}-matched groups were confirmed using independent t-tests. Training effects were investigated using a repeated measures ANOVA with training and exercise mode as within and between group factors and post hoc Bonferroni pairwise comparisons. Graphical data show mean ± SEM.

3.4. Results

Participant characteristics. Participant characteristics are displayed in table 3.1. Participants were insulin sensitive before the start of training. The full description of training adaptations including insulin sensitivity improvements has been previously reported (Cocks et al., 2012, Shepherd et al., 2012) with the same insulin sensitivity data as displayed in this chapter. Insulin sensitivity, measured using the Matsuda insulin sensitivity index (Matsuda-ISI), and VO_{2max} improved following 6 weeks of both ET and SIT (see table 3.1).

Table 3.1 *Participant characteristics before and after training*

	ET		SIT	
	N = 8		N = 8	
	Pre	Post	Pre	Post
Age (y)	21 ± 1	-	22 ± 1	-
Height (m)	1.77 ± 0.03	1.77 ± 0.03	1.74 ± 0.02	1.74 ± 0.02
Body mass (kg)	70.8 ± 4.4	70.8 ± 4.5	75.1 ± 3.0	75.2 ± 3.1
BMI ($kg.m^{-2}$)	22.6 ± 1.2	22.6 ± 1.2	24.8 ± 0.8	24.8 ± 0.9
VO_{2max} ($mL.min^{-1}.kg^{-1}$)	41.7 ± 4.1	48.2 ± 5.0*	41.9 ± 1.8	45.1 ± 2.3*
W_{max} (W)	218.5 ± 11.2	253.8 ± 16.0*	221.1 ± 11.4	241.5 ± 14.3*
Fasting plasma glucose ($mmol.L^{-1}$)	5.6 ± 0.4	4.8 ± 0.6	4.9 ± 0.2	5.1 ± 0.2
2 hr OGTT plasma glucose ($mmol.L^{-1}$)	7.0 ± 0.6	6.1 ± 0.3	6.3 ± 0.5	5.6 ± 0.4
Fasting plasma insulin ($\mu IU.ml^{-1}$)	12.3 ± 3.0	13.2 ± 3.2	13.1 ± 2.1	7.2 ± 0.5
HOMA-IR	3.1 ± 0.7	2.7 ± 0.6	2.9 ± 0.5	1.6 ± 0.1
Matsuda-ISI	3.7 ± 0.5	4.7 ± 0.7*	3.9 ± 0.3	5.8 ± 0.4*

*Data displayed are mean ± SEM. Statistical significance was determined using a repeated measures ANOVA with post hoc Bonferroni analysis, pre- to post- training * P < 0.001.*

Immunofluorescence visualisation of baseline GLUT4 localisation in human skeletal muscle. GLUT4 staining in human skeletal muscle appears as large clusters of staining (> 1 µm) with smaller spots dispersed throughout the cell interior as can be seen in Fig. 3.1. GLUT4 clusters are also observed close to or incorporated in the PM (Fig. 3.1).

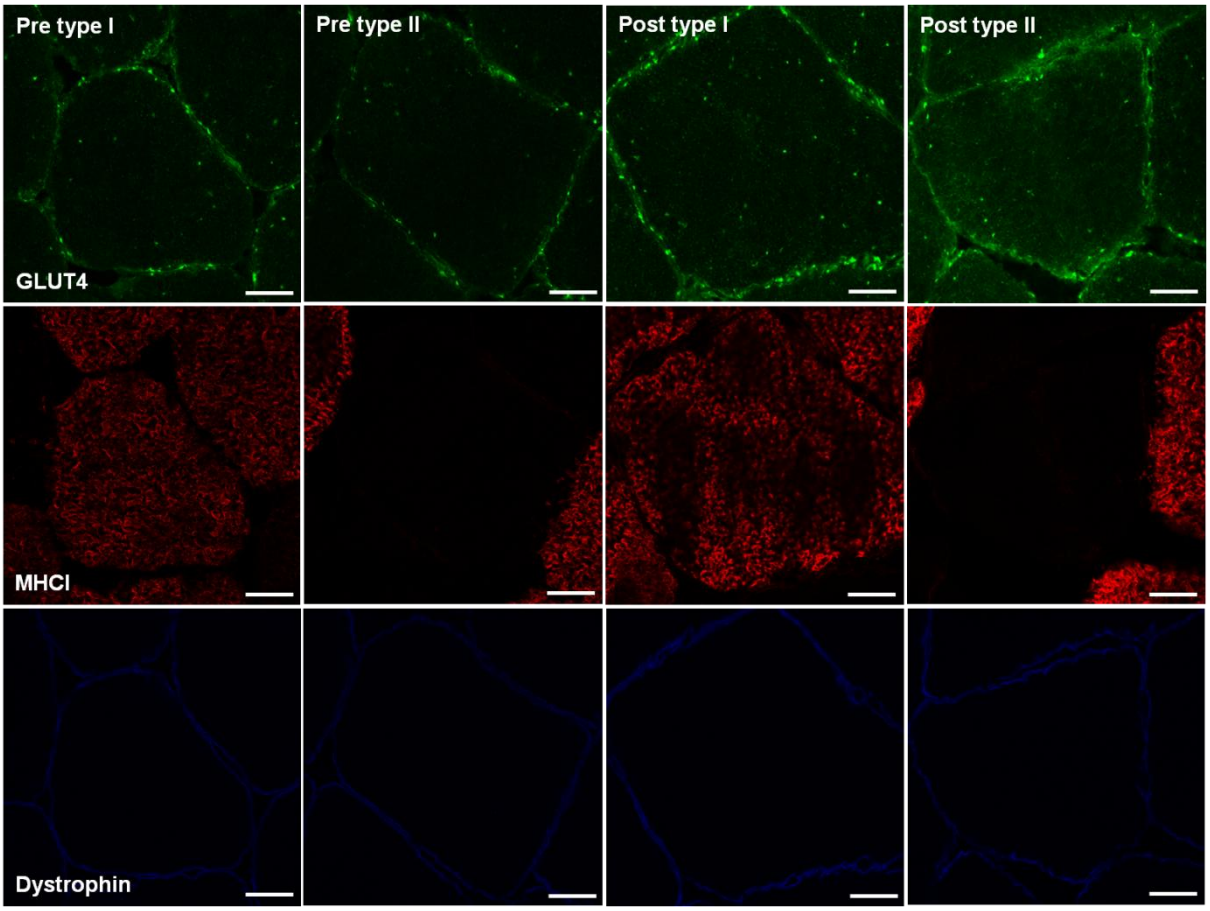

Fig. 3.1. *Representative confocal immunofluorescence images of type I and type II human skeletal muscle fibres in the basal state before and after ET. The images obtained after SIT look very similar and therefore are not shown. GLUT4 immunofluorescence staining is in green, staining for MHC1 to mark type I fibres is in red and staining for dystrophin to mark the PM is in blue. Scale bars 20 µm.*

Immunofluorescence visualisation of GLUT4 content and localisation following exercise training. Representative confocal immunofluorescence images in Fig. 3.1 show increased GLUT4 staining in both type I and type II muscle fibres following 6 weeks of training. GLUT4 fluorescence intensity increased with training (P = 0.018) with no significant difference between the magnitude of increase observed with each training type or between

type I and type II fibres (Fig. 3.2). In type I fibres GLUT4 fluorescence intensity increased by 15 ± 6 % following ET and 14 ± 5 % following SIT. In type II fibres GLUT4 fluorescence intensity increased by 16 ± 6 % following ET and 16 ± 5 % following SIT. These increases were confirmed using Western blotting which detected a 30 ± 12 % increase in GLUT4 content following ET and a 45 ± 27 % increase following SIT (Fig. 3.3) (training effect, P = 0.05).

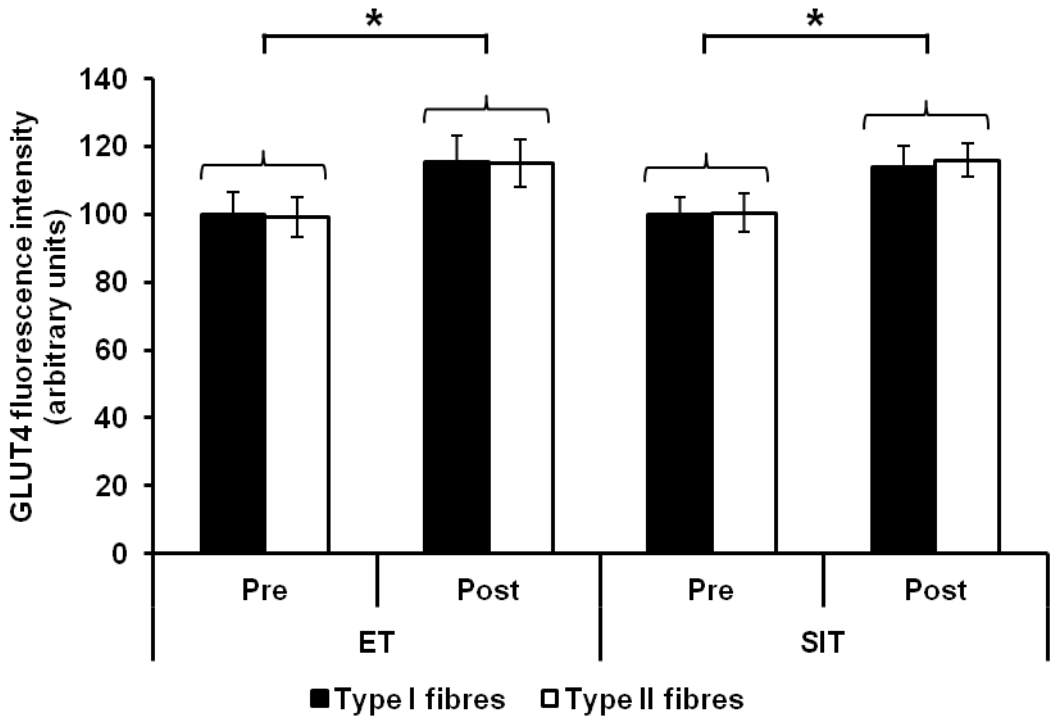

Fig. 3.2. *Total GLUT4 fluorescence intensity of type I and type II muscle fibres in the basal state before and after ET or SIT. Graph shows mean ± SEM relative to type I fibres pre training (n=8 per group). Repeated measures ANOVA training effect P = 0.018, training type P = 0.982, fibre type P = 0.878. * P < 0.05.*

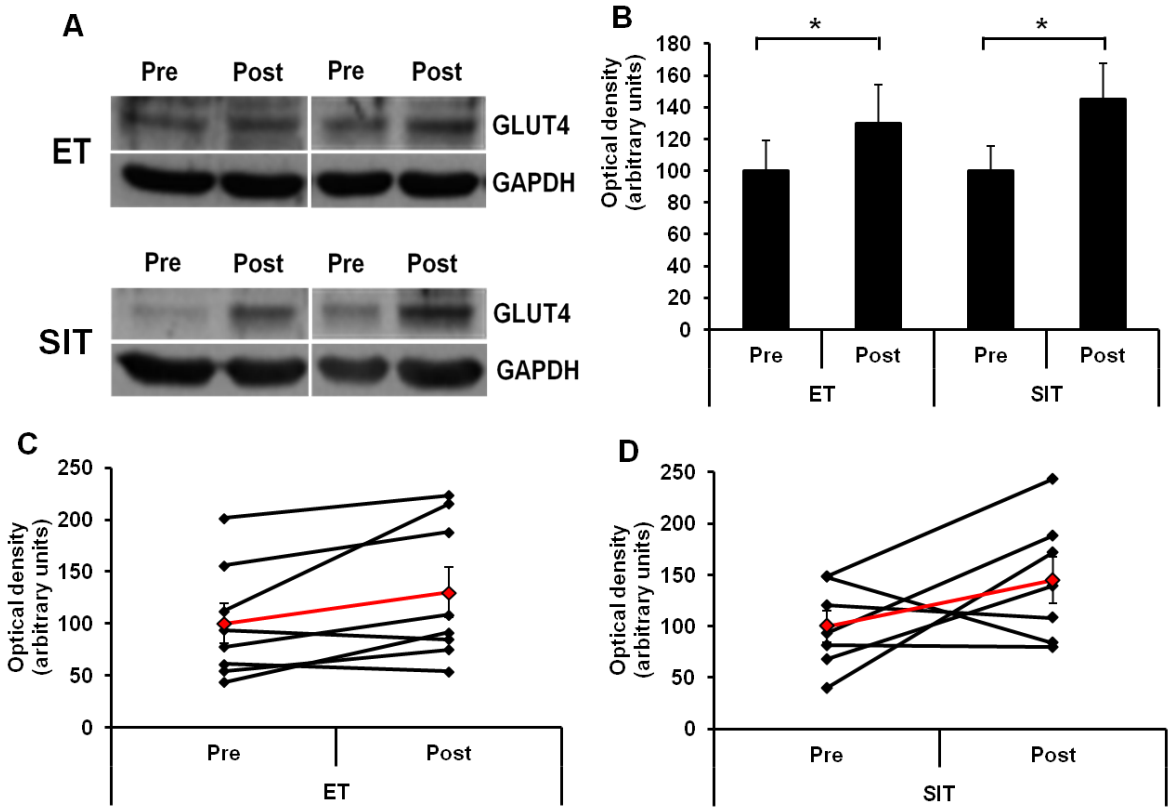

Fig. 3.3. *Representative Western blots of two ET and two SIT subjects showing skeletal muscle GLUT4 content before and after ET or SIT (A). B) GLUT4 content normalised to GAPDH and internal standard. Graph shows mean ± SEM relative to pre training (n=8 per group). Repeated measures ANOVA training effect P = 0.05, training type P = 0.626, interaction P = 0.43. * P < 0.05. C) and D) Individual responses in GLUT4 skeletal muscle content normalised to GAPDH and internal standard after ET and SIT, respectively.*

Training-induced increases in intracellular GLUT4 stores. GLUT4 immunofluorescence staining generates large bright clusters of GLUT4 staining as well as smaller stores which are dispersed throughout the cell interior (Fig. 3.1) and appear as a diffuse background stain in lower magnification images. Total (large plus small) intracellular spot number increased (*P* = 0.03) following ET (25 ± 9 % in type I fibres and 26 ± 13 % in type II fibres) and SIT (36 ±

16 % in type I fibres and 48 ± 16 % in type II fibres). As a result of the increase in number of spots, total intracellular GLUT4 spot area per fibre increased (P = 0.025) following ET (70 ± 30 % in type I fibres and 61 ± 26 % in type II fibres) and SIT (82 ± 34 % in type I fibres and 100 ± 33 % in type II fibres). Furthermore these intracellular spots can be quantified in subcategories of large and smaller spots by setting threshold limits on the spot sizes detected (> 1 µm diameter or < 1 µm diameter, as in Lauritzen *et al.* (2008)) (Lauritzen et al., 2008). Large intracellular spot number increased (P = 0.002) following ET (24 ± 15 % in type I fibres and 32 ± 6 % in type II fibres) and SIT (46 ± 12 % in type I fibres and 46 ± 13 % in type II fibres) (Fig. 3.4A). The total area covered by large intracellular spots per fibre also increased (P = 0.001) following ET (44 ± 15 % in type I fibres and 40 ± 8 % in type II fibres) and SIT (76 ± 18 % in type I fibres and 72 ± 19 % in type II fibres) (Fig. 3.4B). Mean individual large spot size in each fibre type increased (P = 0.011) following ET (10 ± 3 % in type I fibres and 4 ± 5 % in type II fibres) and SIT (21 ± 88 % in type I fibres and 17 ± 6 % in type II fibres) (Fig. 3.6A). There was no change in the number of small intracellular spots following ET or SIT (Fig. 3.5A). However the total area covered by small intracellular spots per fibre increased (P = 0.009) following ET (19 ± 7 % in type I fibres and 17 ± 9 % in type II fibres) and SIT (38 ± 12 % in type I fibres and 39 ± 12 % in type II fibres) (Fig. 3.5B), suggesting increased individual small spot size. Indeed, mean individual size of small spots increased (P = 0.028) following ET (17 ± 8 % in type I fibres and 18 ± 8 % in type II fibres) and SIT (36 ± 11 % in type I fibres and 31 ± 11 % in type II fibres) (Fig.3.6B). The response to training of large and small GLUT4 spot number, area and size was the same for ET and SIT and the same in type I and type II fibres.

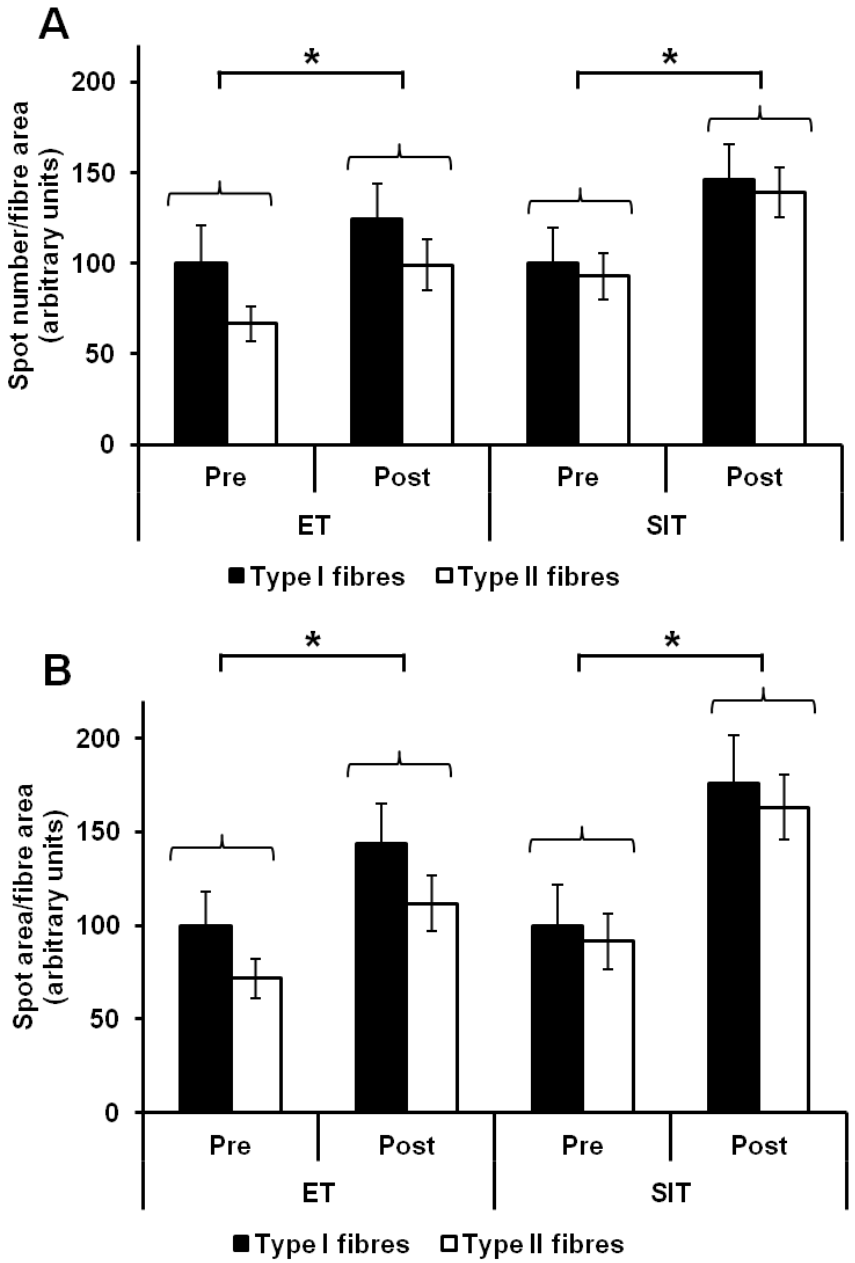

Fig. 3.4. *Quantitation of large spots of GLUT4 staining in type I and type II fibres in the basal state before and after ET or SIT. A) Number of large clusters per fibre area. Repeated measures ANOVA training effect P = 0.002, training type P = 0.35, fibre type 0.054. B) Area of large clusters per fibre area. Repeated measures ANOVA training effect P = 0.001, training type 0.241, fibre type 0.084. * P < 0.01. Graphs show mean ± SEM relative to pre training in type I fibres (n=8 per group).*

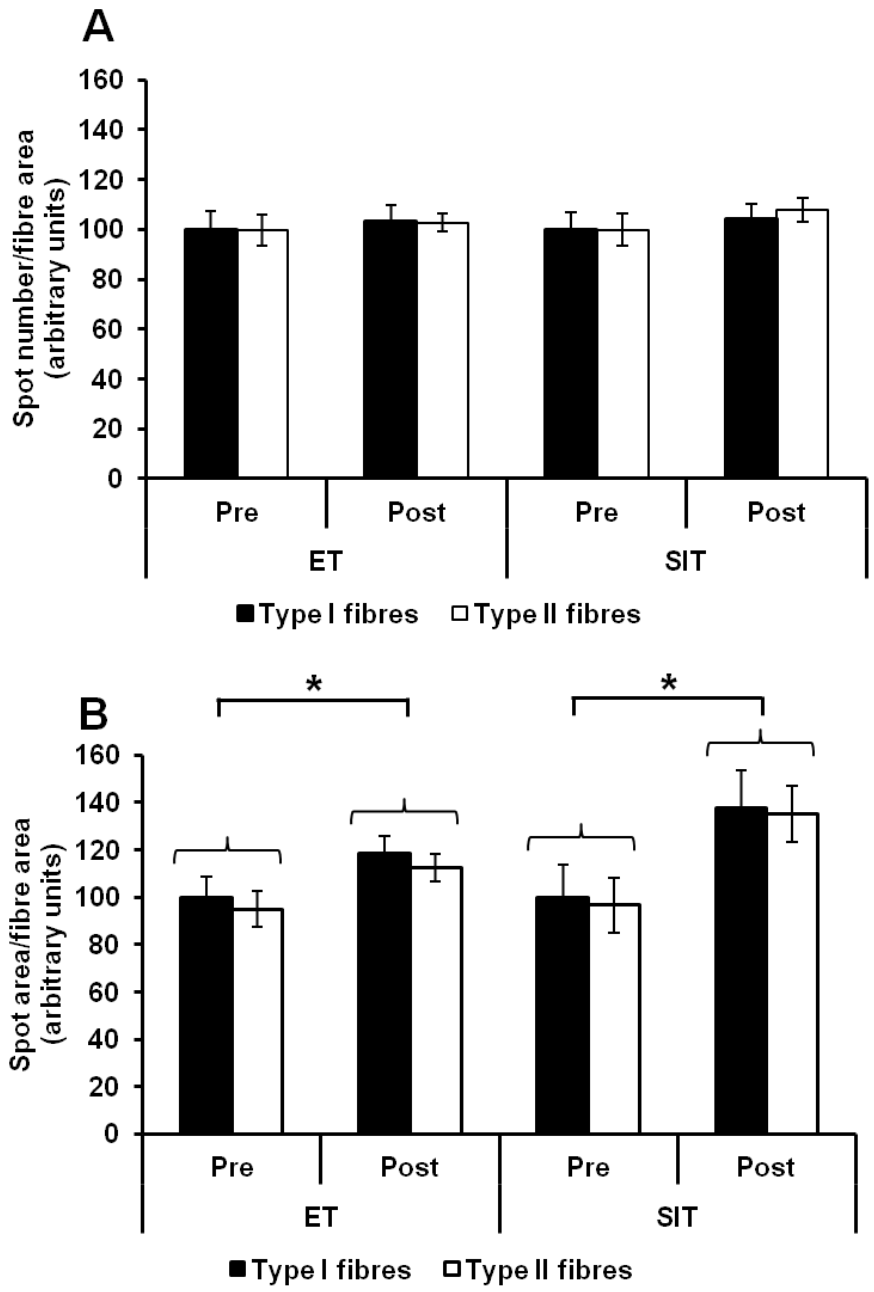

Fig. 3.5. *Quantitation of smaller spots of GLUT4 staining in type I and type II fibres in the basal state before and after ET or SIT. A) Number of spots per fibre area. Repeated measures ANOVA training P = 0.230, training type P = 0.858, fibre type P = 0.834. B) Area of spots per fibre area. Repeated measures ANOVA training effect P = 0.009, training type P = 0.438, fibre type P = 0.283. Graphs show mean ± SEM relative to pre training in type I fibres (n=8 per group). * P < 0.01.*

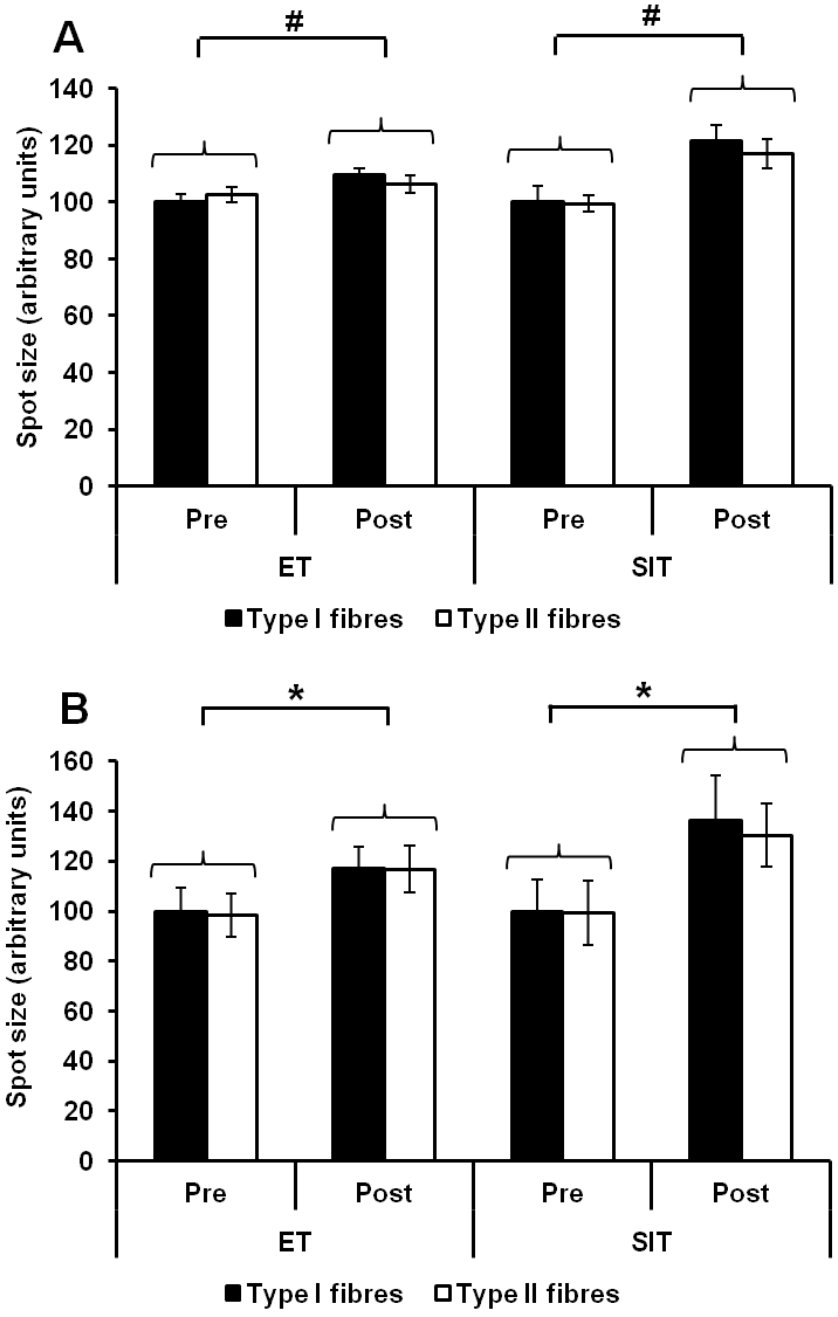

Fig. 3.6. *Quantitation of size of large (A) and smaller (B) spots of GLUT4 staining in type I and type II fibres in the basal state before and after ET or SIT. Large spots repeated measures ANOVA training effect P = 0.011, training type 0.245, fibre type 0.587. # P < 0.05. Small spots repeated measures ANOVA training P = 0.002, training type P = 0.053, fibre type P = 0.082. Graphs show mean ± SEM (n=7). * P < 0.01.Graphs show mean ± SEM relative to pre training in type I fibres (n=8).*

Quantitation of baseline PM GLUT4 content. Colocalisation of GLUT4 with the PM marker dystrophin can be quantified using the Pearson's correlation coefficient. This has been used as an estimate of baseline GLUT4 PM content. There was no significant change in baseline GLUT4 PM content following training (P = 0.075); before ET r = 0.33 ± 0.01 while after ET r = 0.38 ± 0.00, in comparison to before SIT r = 0.33 ± 0.02, while after SIT r = 0.33 ± 0.01 (repeated measures ANOVA training P = 0.075, training type P = 0.106, interaction P = 0.07).

3.5. Discussion

This study has demonstrated the immunofluorescence method developed in chapter 2 of this thesis is able to detect the well-established increase in total muscle GLUT4 protein content that occurs following training. Furthermore use of the immunofluorescence method has extended current knowledge by demonstrating the increase in total GLUT4 protein content is primarily due to an increase in number and area of intracellular clusters of GLUT4 staining, in particular large GLUT4 clusters increased in number while small clusters increased in size. No evidence was found to support the presence of increased GLUT4 content of the PM in the basal state.

Total GLUT4 protein content following ET and SIT. Six weeks of SIT and ET in the present study induced similar increases in the total protein content of GLUT4 in comparison to previous studies (Burgomaster et al., 2007, Little et al., 2010). The application of the immunofluorescence microscopy method in the current study also confirms the increase in GLUT4 protein expression and extends these findings by demonstrating that both modes of exercise increase GLUT4 expression in both type I and type II fibres. No fibre type differences in GLUT4 content were detected pre-training or following ET and SIT and

GLUT4 content increased in type I and type II fibres to the same extent following both ET and SIT. There is disparity in the current literature with some studies reporting higher GLUT4 content in type I fibres (Daugaard et al., 2000, Houmard et al., 1991, Houmard et al., 1993, Gaster et al., 2000), some finding no relationship between GLUT4 content and fibre type (Hardin et al., 1995, Andersen et al., 1993, Hughes et al., 1993) and one other observing higher GLUT4 content in type II fibres (Borghouts et al., 2000). In support of the current data Shepherd *et al.* (2013) showed increases in mitochondrial content in type I and type II fibres following both ET and SIT (Shepherd et al., 2013). Taken together these data suggest that PGC1α-regulated training adaptations (Ojuka et al., 2012), such as increases in GLUT4 and mitochondrial content (Shepherd et al., 2013), occur in response to both types of training in both type I and type II fibres. In summary, regardless of the discrepancy in the literature surrounding fibre-type specific increases, it is clear that both ET and SIT induce increases in total muscle GLUT4 protein content which can be assessed using the immunofluorescence microscopy method developed in chapter 2 of this thesis and likely contributes to training-induced increases in insulin mediated leg glucose uptake (Dela et al., 1996, Frosig et al., 2007, Dela et al., 1995, Dela et al., 1992).

GLUT4 storage structures in human skeletal muscle and their response to training. This study extends current knowledge on the training-induced increase in GLUT4 protein content in human skeletal muscle by demonstrating that the increase is primarily due to an increase in number and area of intracellular clusters of GLUT4 staining. Large clusters (> 1 µm diameter) increased predominantly in number, while the smaller clusters (< 1 µm diameter) increased in size, with no increases in number. The large GLUT4 stores visualised here in human skeletal muscle are likely to be TGN-associated stores, as large stores (> 1 µm) have been identified as such in rodent skeletal muscle (Rodnick et al., 1992, Ploug et al., 1998). Studies in

adipocytes report endosomal stores as approximately 150 - 200 nm and GSVs as 50 - 80 nm (Bogan, 2012, Bogan and Kandror, 2010, Larance et al., 2008, Stockli et al., 2011), while based on EM images endosomes appear to be in a similar range in rodent skeletal muscle (Ploug et al., 1998) and GSVs have been reported as 40 nm (Lizunov et al., 2012). Therefore due to the resolution of confocal miscroscopy (~ 200 nm) the small stores detected here in human skeletal muscle could be endosomal membrane stores or GSVs, either individually or in clusters of smaller vesicles (Stockli et al., 2011). It may confer an insulin-sensitivity advantage to have more TGN GLUT4 storage, as shown in this study, following training as this would increase the capacity for GSV budding at the TGN upon insulin stimulation (Bogan, 2012, Bogan and Kandror, 2010, Larance et al., 2008). The size of small GLUT4 stores also increases. If the small stores visualised here in human skeletal muscle are endosomal this will increase the capacity for GSV biogenesis at endosomal membranes (Bogan, 2012, Bogan and Kandror, 2010, Larance et al., 2008). If the small stores are visible clusters of GSVs, this will increase the capacity for GLUT4 docking and fusion at the PM (Foley et al., 2011). Co-staining with TGN, endosomal and GSV markers such as TGN38, transferrin receptor (TfR) and vesicle-associated membrane protein (VAMP) 2, respectively, will be required to generate harder evidence on the identity of the GLUT4 storage compartments observed here in human skeletal muscle. In summary, assuming that the increase in number of large and area of small intracellular GLUT4 storage also increases GLUT4 available for translocation, this will augment the capacity to increase GLUT4 at the surface membranes in response to insulin, thereby increasing the total capacity for glucose uptake and contributing to the well described improvements in glucose homeostasis with both ET and SIT (Hughes et al., 1993, Dela et al., 1996, Cox et al., 1999, Babraj et al., 2009,

Richards et al., 2010, Houmard et al., 1991, Phillips et al., 1996, Daugaard et al., 2000, Burgomaster et al., 2007, Hood et al., 2011, Little et al., 2010).

Peripheral GLUT4 localisation. In this study there was substantial colocalisation of GLUT4 with the PM marker dystrophin, indicating GLUT4 localisation close to the PM in the basal unstimulated state. However, due to the limits of confocal fluorescence microscopy, it is not possible to differentiate between cytosolic GLUT4 that is immediately adjacent to the PM or in vesicles pre-tethered at the PM (see next paragraph) and GLUT4 that is fully incorporated into the PM (Marette et al., 1992). Authoritative reviews on adipose cells conclude that GLUT4 is excluded from the PM in the basal state (Bogan, 2012, Bogan and Kandror, 2010, Larance et al., 2008, Stockli et al., 2011, Foley et al., 2011). Furthermore EM studies in rodent skeletal muscle report very little GLUT4 in the PM in the basal state (Ploug et al., 1998, Rodnick et al., 1992). The observed heterogeneous pattern of colocalisation of GLUT4 and dystrophin in the basal state is in line with data in rodent skeletal muscle showing that large clusters remain stationary at sarcolemmal regions following insulin stimulation (Lauritzen et al., 2008). Lauritzen *et al.* (2008) suggested that these stationary vesicles release small GLUT4 vesicles (probably GSVs) which then translocate to and fuse with the PM (Lauritzen et al., 2008). Furthermore, recently Lizunov *et al.* (2012) using TIRF microscopy in live mouse muscle fibres generated evidence that there are stationary vesicles which are pre-tethered at the PM and that 80 % of the total number of GLUT4-PM fusion events actually emanated from these pre-tethered vesicles (Lizunov et al., 2012). Considering the stationary nature of the majority of GLUT4 stores (Lauritzen et al., 2008, Lizunov et al., 2012), it may confer an insulin-sensitivity advantage to have more of these stores in close proximity to the PM following training. In the current study GLUT4 colocalisation with the PM marker dystrophin in the basal state did not change following training suggesting that

training does not increase the amount of GLUT4 located close to the PM. However future work should investigate this further and specifically assess the number and area of GLUT4 stores in close proximity to the PM in human skeletal muscle both before and after training to determine whether training increases the number and area of stores located close to the PM in particular.

Conclusions. This study has employed the immunofluorescence method developed in chapter 2 to visualise the subcellular distribution and content of GLUT4 following ET and SIT. The results show that comparable increases in total skeletal muscle GLUT4 content occur following the two training modes primarily through increases in the number of large GLUT4 clusters (> 1 µm; including TGN stores) and increases in size of the smaller GLUT4 clusters (< 1 µm; including endosomal membranes and clusters of GSVs). There were no differences between increases seen in type I and type II fibres, and there was no significant increase in the degree of colocalistion of GLUT4 with the PM marker dystrophin in the basal state following the two training modes. The increases in whole body insulin sensitivity observed following the two training modes (Table 3.1) and the training induced increases in insulin-stimulated leg glucose uptake in humans observed previously (Dela et al., 1996, Frosig et al., 2007, Dela et al., 1995, Dela et al., 1992) are therefore likely to be in part driven by increases in the number and size of intracellular GLUT4 storage compartments that are assumed to be the main sources for the biogenesis of GSVs and GLUT4 available for translocation.

3.6. Acknowledgements

The antibody against myosin (human slow twitch fibres, A4.840) used in the study was developed by Dr. Blau, and obtained from the Developmental Studies Hybridoma Bank

developed under the auspices of the NICHD and maintained by the University of Iowa, Department of Biological Sciences, Iowa City, IA 52242. Valued assistance in Western blotting was also provided by Dr Craig Doig, School of Clinical and Experimental Medicine, University of Birmingham.

3.7. References

ANDERSEN, P. H., LUND, S., SCHMITZ, O., JUNKER, S., KAHN, B. B. & PEDERSEN, O. 1993. Increased insulin-stimulated glucose uptake in athletes: the importance of GLUT4 mRNA, GLUT4 protein and fibre type composition of skeletal muscle. *Acta Physiol Scand,* 149**,** 393-404.

BABRAJ, J. A., VOLLAARD, N. B., KEAST, C., GUPPY, F. M., COTTRELL, G. & TIMMONS, J. A. 2009. Extremely short duration high intensity interval training substantially improves insulin action in young healthy males. *BMC Endocr Disord,* 9**,** 3.

BARRETT, E. J., EGGLESTON, E. M., INYARD, A. C., WANG, H., LI, G., CHAI, W. & LIU, Z. 2009. The vascular actions of insulin control its delivery to muscle and regulate the rate-limiting step in skeletal muscle insulin action. *Diabetologia,* 52**,** 752-64.

BARRETT, E. J., WANG, H., UPCHURCH, C. T. & LIU, Z. 2011. Insulin regulates its own delivery to skeletal muscle by feed-forward actions on the vasculature. *Am J Physiol Endocrinol Metab,* 301**,** E252-63.

BELL, G. I., BURANT, C. F., TAKEDA, J. & GOULD, G. W. 1993. Structure and function of mammalian facilitative sugar transporters. *J Biol Chem,* 268**,** 19161-4.

BOGAN, J. S. 2012. Regulation of glucose transporter translocation in health and diabetes. *Annu Rev Biochem,* 81**,** 507-32.

BOGAN, J. S. & KANDROR, K. V. 2010. Biogenesis and regulation of insulin-responsive vesicles containing GLUT4. *Curr Opin Cell Biol,* 22**,** 506-12.

BORGHOUTS, L. B., SCHAART, G., HESSELINK, M. K. & KEIZER, H. A. 2000. GLUT-4 expression is not consistently higher in type-1 than in type-2 fibres of rat and human vastus lateralis muscles; an immunohistochemical study. *Pflugers Arch,* 441**,** 351-8.

BROZINICK, J. T., JR., ETGEN, G. J., JR., YASPELKIS, B. B., 3RD, KANG, H. Y. & IVY, J. L. 1993. Effects of exercise training on muscle GLUT-4 protein content and translocation in obese Zucker rats. *Am J Physiol,* 265**,** E419-27.

BURGOMASTER, K. A., CERMAK, N. M., PHILLIPS, S. M., BENTON, C. R., BONEN, A. & GIBALA, M. J. 2007. Divergent response of metabolite transport proteins in human skeletal muscle after sprint interval training and detraining. *Am J Physiol Regul Integr Comp Physiol,* 292**,** R1970-6.

COCKS, M., SHAW, C. S., SHEPHERD, S. O., FISHER, J. P., RANASINGHE, A. M., BARKER, T. A., TIPTON, K. D. & WAGENMAKERS, A. J. 2013. Sprint interval and endurance training are equally effective in increasing muscle microvascular density and eNOS content in sedentary males. *J Physiol,* 591**,** 641-56.

COX, J. H., CORTRIGHT, R. N., DOHM, G. L. & HOUMARD, J. A. 1999. Effect of aging on response to exercise training in humans: skeletal muscle GLUT-4 and insulin sensitivity. *J Appl Physiol,* 86**,** 2019-25.

DAUGAARD, J. R., NIELSEN, J. N., KRISTIANSEN, S., ANDERSEN, J. L., HARGREAVES, M. & RICHTER, E. A. 2000. Fiber type-specific expression of GLUT4 in human skeletal muscle: influence of exercise training. *Diabetes,* 49**,** 1092-5.

DELA, F., LARSEN, J. J., MIKINES, K. J., PLOUG, T., PETERSEN, L. N. & GALBO, H. 1995. Insulin-stimulated muscle glucose clearance in patients with NIDDM. Effects of one-legged physical training. *Diabetes,* 44**,** 1010-20.

DELA, F., MIKINES, K. J., LARSEN, J. J. & GALBO, H. 1996. Training-induced enhancement of insulin action in human skeletal muscle: the influence of aging. *J Gerontol A Biol Sci Med Sci,* 51**,** B247-52.

DELA, F., MIKINES, K. J., VON LINSTOW, M., SECHER, N. H. & GALBO, H. 1992. Effect of training on insulin-mediated glucose uptake in human muscle. *Am J Physiol,* 263**,** E1134-43.

FOLEY, K., BOGUSLAVSKY, S. & KLIP, A. 2011. Endocytosis, recycling, and regulated exocytosis of glucose transporter 4. *Biochemistry,* 50**,** 3048-61.

FROSIG, C., ROSE, A. J., TREEBAK, J. T., KIENS, B., RICHTER, E. A. & WOJTASZEWSKI, J. F. 2007. Effects of endurance exercise training on insulin signaling in human skeletal muscle: interactions at the level of phosphatidylinositol 3-kinase, Akt, and AS160. *Diabetes,* 56**,** 2093-102.

GASTER, M., POULSEN, P., HANDBERG, A., SCHRODER, H. D. & BECK-NIELSEN, H. 2000. Direct evidence of fiber type-dependent GLUT-4 expression in human skeletal muscle. *Am J Physiol Endocrinol Metab,* 278**,** E910-6.

HANSEN, P. A., GULVE, E. A., MARSHALL, B. A., GAO, J., PESSIN, J. E., HOLLOSZY, J. O. & MUECKLER, M. 1995. Skeletal muscle glucose transport and metabolism are enhanced in transgenic mice overexpressing the Glut4 glucose transporter. *J Biol Chem,* 270**,** 1679-84.

HARDIN, D. S., AZZARELLI, B., EDWARDS, J., WIGGLESWORTH, J., MAIANU, L., BRECHTEL, G., JOHNSON, A., BARON, A. & GARVEY, W. T. 1995. Mechanisms of enhanced insulin sensitivity in endurance-trained athletes: effects on blood flow and differential expression of GLUT 4 in skeletal muscles. *J Clin Endocrinol Metab,* 80**,** 2437-46.

HOOD, M. S., LITTLE, J. P., TARNOPOLSKY, M. A., MYSLIK, F. & GIBALA, M. J. 2011. Low-volume interval training improves muscle oxidative capacity in sedentary adults. *Med Sci Sports Exerc,* 43**,** 1849-56.

HOUMARD, J. A., EGAN, P. C., NEUFER, P. D., FRIEDMAN, J. E., WHEELER, W. S., ISRAEL, R. G. & DOHM, G. L. 1991. Elevated skeletal muscle glucose transporter levels in exercise-trained middle-aged men. *Am J Physiol,* 261**,** E437-43.

HOUMARD, J. A., HORTOBAGYI, T., NEUFER, P. D., JOHNS, R. A., FRASER, D. D., ISRAEL, R. G. & DOHM, G. L. 1993. Training cessation does not alter GLUT-4 protein levels in human skeletal muscle. *J Appl Physiol,* 74**,** 776-81.

HUGHES, V. A., FIATARONE, M. A., FIELDING, R. A., KAHN, B. B., FERRARA, C. M., SHEPHERD, P., FISHER, E. C., WOLFE, R. R., ELAHI, D. & EVANS, W. J. 1993. Exercise increases muscle GLUT-4 levels and insulin action in subjects with impaired glucose tolerance. *Am J Physiol,* 264**,** E855-62.

IVY, J. L. 2004. Muscle insulin resistance amended with exercise training: role of GLUT4 expression. *Med Sci Sports Exerc,* 36**,** 1207-11.

KATZ, L. D., GLICKMAN, M. G., RAPOPORT, S., FERRANNINI, E. & DEFRONZO, R. A. 1983. Splanchnic and peripheral disposal of oral glucose in man. *Diabetes,* 32**,** 675-9.

LARANCE, M., RAMM, G. & JAMES, D. E. 2008. The GLUT4 code. *Mol Endocrinol,* 22**,** 226-33.

LAURITZEN, H. P., GALBO, H., BRANDAUER, J., GOODYEAR, L. J. & PLOUG, T. 2008. Large GLUT4 vesicles are stationary while locally and reversibly depleted during transient insulin stimulation of skeletal muscle of living mice: imaging analysis of GLUT4-enhanced green fluorescent protein vesicle dynamics. *Diabetes,* 57**,** 315-24.

LAURITZEN, H. P., PLOUG, T., PRATS, C., TAVARE, J. M. & GALBO, H. 2006. Imaging of insulin signaling in skeletal muscle of living mice shows major role of T-tubules. *Diabetes,* 55**,** 1300-6.

LETURQUE, A., LOIZEAU, M., VAULONT, S., SALMINEN, M. & GIRARD, J. 1996. Improvement of insulin action in diabetic transgenic mice selectively overexpressing GLUT4 in skeletal muscle. *Diabetes,* 45**,** 23-7.

LITTLE, J. P., SAFDAR, A., WILKIN, G. P., TARNOPOLSKY, M. A. & GIBALA, M. J. 2010. A practical model of low-volume high-intensity interval training induces mitochondrial biogenesis in human skeletal muscle: potential mechanisms. *J Physiol,* 588**,** 1011-22.

LIZUNOV, V. A., STENKULA, K. G., LISINSKI, I., GAVRILOVA, O., YVER, D. R., CHADT, A., AL-HASANI, H., ZIMMERBERG, J. & CUSHMAN, S. W. 2012. Insulin stimulates fusion, but not tethering, of GLUT4 vesicles in skeletal muscle of HA-GLUT4-GFP transgenic mice. *Am J Physiol Endocrinol Metab,* 302**,** E950-60.

MARETTE, A., RICHARDSON, J. M., RAMLAL, T., BALON, T. W., VRANIC, M., PESSIN, J. E. & KLIP, A. 1992. Abundance, localization, and insulin-induced translocation of glucose transporters in red and white muscle. *Am J Physiol,* 263**,** C443-52.

MUECKLER, M. 1994. Facilitative glucose transporters. *Eur J Biochem,* 219**,** 713-25.

OJUKA, E. O., GOYARAM, V. & SMITH, J. A. 2012. The role of CaMKII in regulating GLUT4 expression in skeletal muscle. *Am J Physiol Endocrinol Metab,* 303**,** E322-31.

PHILLIPS, S. M., HAN, X. X., GREEN, H. J. & BONEN, A. 1996. Increments in skeletal muscle GLUT-1 and GLUT-4 after endurance training in humans. *Am J Physiol,* 270**,** E456-62.

PLOUG, T., VAN DEURS, B., AI, H., CUSHMAN, S. W. & RALSTON, E. 1998. Analysis of GLUT4 distribution in whole skeletal muscle fibers: identification of distinct storage compartments that are recruited by insulin and muscle contractions. *J Cell Biol,* 142**,** 1429-46.

REN, J. M., MARSHALL, B. A., MUECKLER, M. M., MCCALEB, M., AMATRUDA, J. M. & SHULMAN, G. I. 1995. Overexpression of Glut4 protein in muscle increases basal and insulin-stimulated whole body glucose disposal in conscious mice. *J Clin Invest,* 95**,** 429-32.

RICHARDS, J. C., JOHNSON, T. K., KUZMA, J. N., LONAC, M. C., SCHWEDER, M. M., VOYLES, W. F. & BELL, C. 2010. Short-term sprint interval training increases insulin sensitivity in healthy adults but does not affect the thermogenic response to beta-adrenergic stimulation. *J Physiol,* 588**,** 2961-72.

RODNICK, K. J., SLOT, J. W., STUDELSKA, D. R., HANPETER, D. E., ROBINSON, L. J., GEUZE, H. J. & JAMES, D. E. 1992. Immunocytochemical and biochemical studies of GLUT4 in rat skeletal muscle. *J Biol Chem,* 267**,** 6278-85.

SHEPHERD, S. O., COCKS, M., TIPTON, K. D., RANASINGHE, A. M., BARKER, T. A., BURNISTON, J. G., WAGENMAKERS, A. J. & SHAW, C. S. 2013. Sprint interval and traditional endurance training increase net intramuscular triglyceride breakdown and expression of perilipin 2 and 5. *J Physiol,* 591**,** 657-75.

STOCKLI, J., FAZAKERLEY, D. J. & JAMES, D. E. 2011. GLUT4 exocytosis. *J Cell Sci,* 124**,** 4147-59.

WASSERMAN, D. H., KANG, L., AYALA, J. E., FUEGER, P. T. & LEE-YOUNG, R. S. 2011. The physiological regulation of glucose flux into muscle in vivo. *J Exp Biol,* 214**,** 254-62.

CHAPTER 4

VISUALISATION AND QUANTITATION OF GLUT4 TRANSLOCATION IN HUMAN SKELETAL MUSCLE FOLLOWING GLUCOSE INGESTION AND EXERCISE

H. Bradley[1], C.S. Shaw[1,2], O.J. Wilson[1], A. M. Turner[3,4], G.A. Wallis[1] and A.J.M. Wagenmakers[1,5]

[1]School of Sport and Exercise Sciences, University of Birmingham, UK

[2]Current address: Institute of Sport, Exercise and Active Living (ISEAL), Victoria University, Australia

[3]School of Clinical and Experimental Medicine, University of Birmingham, UK

[4]Heart of England NHS Foundation Trust, Bordesley Green East

[5]Current address: Research Institute for Sport and Exercise Sciences, Liverpool John Moores University, UK

4.1. Abstract

Insulin- and contraction-stimulated increases in glucose uptake into skeletal muscle occur at least in part as a result of the translocation of glucose transporter 4 (GLUT4) storage vesicles (GSVs) to and subsequent fusion of the GSVs with the plasma membrane (PM). This study aimed to use the immunofluorescence microscopy method developed in chapter 2 of this thesis to visualise and quantify increases in colocalisation of GLUT4 with the PM in response to glucose feeding, exercise and a combination of glucose feeding and exercise. Percutaneous muscle biopsy samples were taken from ten insulin sensitive males (age 21 ± 1 yrs, BMI 23.1 ± 0.4 $kg.m^{-2}$, VO_{2max} 52.5 ± 2.4 $ml.min^{-1}.kg^{-1}$) in the basal state and 90 min following ingestion of 75 g glucose, immediately following 30 min cycling exercise (65 % VO_{2max}) and 90 min following glucose feeding with 30 min exercise completed between 60 – 90 min. Subsequently muscle biopsy samples were taken from a second cohort of ten insulin sensitive males (25 ± 2 y, BMI 22.6 ± 0.5 $kg.m^{-2}$, VO_{2max} 50.7 ± 2.2 $ml.min^{-1}.kg^{-1}$) in the basal state and 30 min and 60 min following glucose feeding. Colocalisation of GLUT4 with the PM marker dystrophin was measured with the Pearson's correlation coefficient. Thirty minutes of cycling exercise resulted in a continuous GLUT4 signal at the PM and increased GLUT4 and dystrophin colocalisation (baseline $r = 0.47 \pm 0.01$; post exercise $r = 0.58 \pm 0.02$; $P < 0.001$). GLUT4 and dystrophin colocalisation increased 30 min after glucose ingestion (baseline $r = 0.42 \pm 0.02$; 30 min $r = 0.46 \pm 0.02$; $P < 0.05$) but not at 60 min (baseline $r = 0.42 \pm 0.02$; 60 min $r = 0.44 \pm 0.02$) or at 90 min (baseline $r = 0.47 \pm 0.01$; 90 min $r = 0.46 \pm 0.01$). Glucose ingestion 60 min prior to cycling exercise had no further effect on post-exercise GLUT4 and dystrophin colocalisation (baseline $r = 0.47 \pm 0.01$; post glucose ingestion and exercise $r = 0.57 \pm 0.02$; $P < 0.001$). This study has successfully used the immunofluorescence microscopy method developed in chapter 2 to quantify increases in GLUT4 and dystrophin

colocalisation as evidence of net GLUT4 translocation to the PM in response to glucose ingestion and exercise. Furthermore, this study demonstrates that the increase in GLUT4 and dystrophin colocalisation in response to glucose ingestion is transient, occurring only at 30 min following glucose ingestion, and appeared smaller than seen immediately following 30 min endurance exercise.

4.2. Introduction

Insulin and contraction are potent physiological stimulators of glucose uptake into skeletal muscle. Skeletal muscle is the primary site of postprandial glucose uptake (Katz et al., 1983, Ferrannini et al., 1985, Wasserman et al., 2011) and plasma glucose contributes significantly to ATP production in the working skeletal muscle during endurance exercise (Katz et al., 1991, Kjaer et al., 1991, van Loon et al., 2001). Glucose is taken up into the muscle cell via facilitated transport through glucose transporter proteins in the plasma membrane (PM) and T-tubule membranes (Bell et al., 1993). Glucose transporter 4 (GLUT4) translocates to the muscle cell PM in response to insulin and contraction and is the major glucose transporter isoform expressed in skeletal muscle (Mueckler, 1994, Gaster et al., 2000). Global or muscle-specific GLUT4 knockout in mice resulted in reduced basal muscle glucose uptake and reduced insulin and contraction stimulated muscle glucose uptake in vitro, demonstrating the vital role of GLUT4 in glucose uptake into muscle cells (Ryder et al., 1999a, Ryder et al., 1999b, Zisman et al., 2000).

Leg glucose uptake increased 3-fold during the 4 h period following glucose feeding (Katz et al., 1983), approximately 5-fold during a hyperinsulinaemic-euglycaemic clamp (DeFronzo et al., 1985) and approximately 15-fold during cycling exercise at 50-60% $VO_{2\ max}$ (Katz et al., 1986, Martin et al., 1995). Previous studies aiming to investigate GLUT4 translocation to the

muscle cell PM in humans in response to increases in plasma insulin concentrations or cycling exercise have used density gradient centrifugation methods with the aim to isolate pure PM fractions of *vastus lateralis* muscle biopsies and measure their GLUT4 content with Western blots. In insulin sensitive individuals, these studies have demonstrated increases in GLUT4 PM content of *vastus lateralis* of 27% 1 h following ingestion of 75 g of glucose (Goodyear et al., 1996) and of 60%, 30 - 40 min after the start of a hyperinsulinaemic-euglycaemic clamp (Guma et al., 1995). Furthermore, cycling exercise at 60 - 70% VO_{2max} for 45 - 60 min resulted in 70% increases in GLUT4 content in the *vastus lateralis* PM fraction (Kennedy et al., 1999). Kristiansen *et al.* (1997) prepared PM giant vesicles from *vastus lateralis* muscle biopsies obtained from healthy men at rest and during cycling exercise at 75% VO_{2max} and observed increases in GLUT4 content of 38% and 93% after 5 min and 40 min of exercise, respectively (Kristiansen et al., 1997). Subcellular membrane fractionation studies suggested that the effects of insulin and cycling exercise on GLUT4 translocation are additive in human *vastus lateralis* (Thorell et al., 1999).

A series of detailed immunofluorescence and electron microscopy studies in rat and mouse skeletal muscle suggest that GLUT4 is present predominantly at the fibre periphery and in perinuclear regions in the basal state and appears as large and small GLUT4 storage clusters which are likely pretethered at the PM and T tubule membranes (Ploug et al., 1998, Lauritzen et al., 2006, Lauritzen et al., 2008, Lizunov et al., 2012). GLUT4 storage depots have been characterised as the membranes of the trans-Golgi network (TGN), endosomal membranes and GLUT4 storage vesicles (GSVs) (Rodnick et al., 1992, Ploug et al., 1998, Lizunov et al., 2012). Furthermore studies in transgenic mouse muscle fibres using labelling of exofacially tagged GLUT4 demonstrate GLUT4 fusion with the PM in the basal state; with one study describing a small amount of exofacially-tagged GLUT4 labelling in the basal state (Lizunov

et al., 2012) and another reporting a more substantial amount with externalised *myc* labelling under basal conditions approximately 50 % of that after insulin stimulation (Schertzer et al., 2009). A representation of the spatial distribution of intracellular GLUT4 stores is presented in Fig. 1.1 in chapter 1 of this thesis.

Insulin injection and electrical muscle stimulation led to a redistribution of GLUT4 from intracellular clusters to the PM and T-tubule membranes in immunofluorescence microscopy studies in rodent muscle (Ploug et al., 1998) and in *in vivo* studies of rodent muscle transiently transfected with GFP-tagged GLUT4 (Lauritzen et al., 2006, Lauritzen et al., 2010). Immuno-gold particle electron microscopy studies have demonstrated that the effects of insulin and contraction on GLUT4 redistribution to the PM and T-tubule membranes are additive in rat skeletal muscle with 14-fold increases in immunogold particle density in the PM, in comparison to 7-fold and 9-fold increases following insulin and exercise alone, respectively (Ploug et al., 1998).

Once GSVs have translocated to and tethered at the PM, docking and fusion of GSVs with the PM is a critical step to permit glucose uptake via GLUT4. This process requires soluble *N*-ethylmaleimide-sensitive factor attachment protein receptors (SNARES). Cognate vesicle (v)- and target (t)-SNARES must form a SNARE complex to bring the vesicle and target membranes into close proximity for fusion to occur (Chen and Scheller, 2001). GSVs have been shown to contain the v-SNARE VAMP2, which interacts with the t-SNARES syntaxin 4 and SNAP23 at the PM (Bryant et al., 2002). This interaction has been shown to be vital for insulin-stimulated GLUT4 translocation (Kawanishi et al., 2000) and is likely to be the same for contraction stimulated GLUT4 translocation as VAMP2 has been shown to translocate to cell surface membranes, where the t-SNARES are already located, in response to contraction

(Rose et al., 2009). There is however also evidence that VAMP3 may be the v-SNARE responsible for contraction stimulated GLUT4 translocation (Schwenk et al., 2010).

In chapter 2 of this thesis a confocal immunofluorescence microscopy method for assessment of GLUT4 localisation in cross-sections and longitudinal sections of human skeletal muscle was developed to avoid the methodological flaws inherent in existing techniques (as described in chapter 1). The overarching aim of the current study was to visualise and characterise the translocation of GLUT4 in human skeletal muscle in response to physiological stimuli known to elevate rates of muscle glucose uptake using this newly developed technique. We specifically investigated changes in the colocalisation of GLUT4 with the PM marker dystrophin 30, 60 and 90 min following oral glucose ingestion to elevate insulin to physiological levels, in response to 30 min cycling exercise at 65% VO_{2max} and following a combination of glucose ingestion and exercise. It was hypothesized that GLUT4 and dystrophin colocalisation will increase in response to both glucose ingestion and exercise, and that the effects of these interventions will be additive.

4.3. Methods

The data presented in this chapter were obtained from two separate participant cohorts and sets of experiments, which will be termed experiment 1 and experiment 2.

*Ethics, recruitment and informed consent***.** Ethical approval was granted by Birmingham East, North and Solihull and West Midlands Black Country NHS Research Ethics Committees, for experiment 1 and experiment 2, respectively. Ten healthy, lean, recreationally active men were recruited for each experiment (experiment 1 age 21 ± 1 y, BMI 23.1 ± 0.4 $kg.m^{-2}$, VO_{2max} 52.5 ± 2.4 $ml.min^{-1}.kg^{-1}$, experiment 2 age 25 ± 2 y, BMI 22.6 ± 0.5 $kg.m^{-2}$, VO_{2max}

50.7 ± 2.2 $ml.min^{-1}.kg^{-1}$) and written informed consent was obtained prior to their participation in the study.

Study protocol. All participants performed an incremental exercise test to exhaustion on an electronically braked cycle ergometer (Lode BV, Groningen, The Netherlands) to determine their maximal aerobic capacity (VO_{2max}) using an on-line respiratory gas collection system (Oxycon Pro, Jaeger, Germany). Workload began at 95 W and increased by 35 W every 3 min until volitional fatigue.

Experiment 1. Following the incremental exercise test, there were three subsequent visits, which took place in a randomised order at least 1 week apart. Participants were asked to refrain from strenuous physical activity for 48 hr prior to each visit. For all visits participants arrived at the laboratory at 7 am following an overnight fast. A blood sample was drawn from a forearm vein and a percutaneous needle biopsy sample (Bergstrom, 1975) was taken from the *m. vastus lateralis* under local anaesthesia (1 % lidocaine). To investigate insulin-stimulated GLUT4 translocation, 75 g glucose was ingested as a 25 % solution and a second needle biopsy was taken 90 min after glucose ingestion. Blood samples were drawn 30, 60, 75, 90 and 120 min after glucose ingestion. To investigate contraction-stimulated GLUT4 translocation participants completed 30 min cycling exercise on an electronically braked cycle ergometer at a workload equivalent to 65 % VO_{2max} and a second needle biopsy was taken immediately upon completion of exercise. Blood samples were taken after 15 and 30 min of exercise. To investigate whether glucose ingestion and exercise exert additive effects on GLUT4 translocation 75 g glucose was ingested as a 25 % solution and between 60 and 90 min after glucose ingestion subjects completed 30 min of cycling exercise. A second needle biopsy was taken immediately at cessation of exercise. Blood samples were drawn 30, 60, 75

and 90 min after glucose ingestion, the final two samples being taken during exercise. The protocol is displayed in figure 4.1.

Experiment 2. Following the incremental exercise test there was one subsequent visit. Participants were asked to refrain from strenuous physical activity for 48 hr prior to the visit and arrived at the laboratory at 7 am following an overnight fast. A percutaneous needle biopsy sample was taken from the *m. vastus lateralis* under local anaesthesia (1 % lidocaine) and a blood sample was drawn from a forearm vein. Participants then ingested 75 g glucose as a 25 % solution and subsequent needle biopsy samples were taken from the *m. vastus lateralis* 30 min and 60 min after glucose ingestion. Blood samples were drawn 30, 60, 90 and 120 min after glucose ingestion. The protocol is displayed in Fig. 4.1.

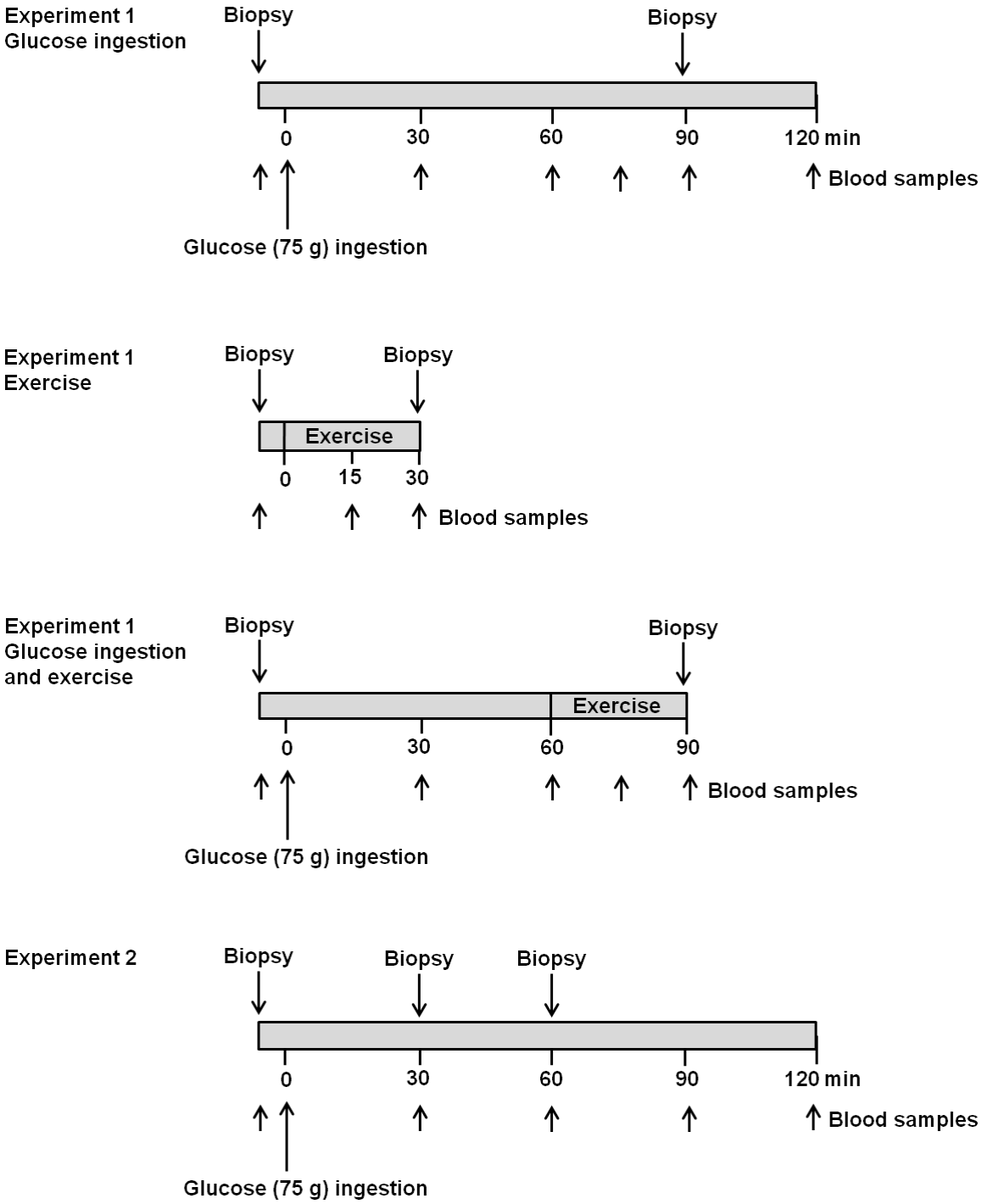

Fig. 4.1. *Glucose ingestion and exercise participant testing protocol for experiment 1 and experiment 2.*

Sample collection and storage. Full details of sample processing and storage are outlined in chapter 2.

Plasma glucose and insulin analysis. Full details of plasma glucose and insulin analysis is provided in chapter 2.

Immunofluorescence staining and microscopy. Frozen muscle biopsy samples were cryosectioned (Bright Instrument Company Limited, Huntingdon, England) to a thickness of 5 µm onto uncoated glass microscope slides (VWR international, USA). For each participant in experiment 1, three slides were processed for GLUT4 and dystrophin and three slides for SNAP23 and dystrophin and on each slide was a section for all six samples. For experiment 2, three slides were processed for GLUT4 and dystrophin with a section for all three samples on each slide. Slides were either stained within 30 min of sectioning or stored at -20^{o}C. Following storage slides were left at room temperature for 30 min prior to staining. The GLUT4 staining protocol is described in full in chapter 2. SNAP23 immunofluorescence staining followed the same protocol with SNAP23 primary antibody (Synaptic Systems, Germany) applied at a 1 in 50 dilution and the secondary antibody (AlexaFluor 488-conjugated goat anti-rabbit IgG secondary antibody, Invitrogen, UK) applied at a 1 in 200 dilution. Slides were left to dry overnight before confocal immunofluorescence visualisation. Confocal image capture was as described in chapter 2 using an inverted confocal microscope (Leica DMIRE2, Leica Microsystems) with a 63x oil immersion objective (1.4 NA).

Immunofluorescence image analysis. Images were processed and analysed using Image-Pro Plus 5.1 software (Media Cybernetics, MD, USA). All image processing and analysis was kept consistent between images within each experiment. An average of 51 ± 2 muscle fibres

were analysed for each participant. See chapter 2 for a full description of the image processing and analysis, however in brief, the Pearson's correlation coefficient between two images was calculated using the colocalisation tool in Image-Pro Plus 5.1 to measure colocalisation of GLUT4 and dystrophin or SNAP23 and dystrophin. Pearson's correlation coefficient has been routinely used to measure colocalisation of two proteins in immunofluorescence images (Lachmanovich et al., 2003, Landmann and Marbet, 2004, Sedarat et al., 2004, Bolte and Cordelieres, 2006, Dunn et al., 2011).

Statistical analysis. Plasma glucose and insulin data were analysed for statistical significance using a repeated measures ANOVA separately for each experiment with post hoc Bonferroni pairwise comparisons to locate the significant differences. Pearson's correlation coefficient data from immunofluorescence images for experiment 1 were analysed for statistical significance using paired t tests for each trial. For experiment 2 a repeated measures ANOVA was used to compare Pearson's correlation coefficient at baseline and 30 min and 60 min after glucose ingestion, with post hoc Bonferroni pairwise comparisons used to locate the significant differences. The subject characteristics of the two groups were compared using independent T tests. Data are displayed as mean ± SEM. Significance was set at $P < 0.05$.

4.4. Results

Subject characteristics. Subject characteristics are shown in table 4.1. Ten healthy, lean, recreationally active men were recruited separately for experiments 1 and 2. All subjects were insulin sensitive, according to classification of fasting plasma glucose of less than 5.6 mM and 2 h OGTT plasma glucose of less than 7.8 mM (Genuth et al., 2003). All subjects were in the normal BMI classification range of 18.5 – 25 $kg.m^{-2}$. There were no significant differences

in VO_{2max}, BMI, fasting plasma glucose, fasting plasma insulin or ISI-Matsuda between the cohorts for experiments 1 and 2.

Table 4.1 Participant characteristics

	Experiment 1	Experiment 2
	N = 10	N = 10
Age (y)	21 ± 1	25 ± 2
Height (m)	1.81 ± 0.02	1.83 ± 0.01
Body mass (kg)	75.9 ± 2.4	75.3 ± 2.0
BMI ($kg.m^{-2}$)	23.1 ± 0.4	22.6 ± 0.5
$VO_{2\,max}$ ($ml.min^{-1}.kg^{-1}$)	52.5 ± 2.4	50.7 ± 2.2
W_{max} (W)	278 ± 15	285 ± 13
Fasting plasma glucose ($mmol.l^{-1}$)	5.3 ± 0.1	5.1 ± 0.2
2 hr OGTT plasma glucose ($mmol.l^{-1}$)	5.0 ± 0.3	5.4 ± 0.4
Fasting plasma insulin ($\mu IU.ml^{-1}$)	14.3 ± 1.4	12.7 ± 1.7
2 hr OGTT plasma insulin ($\mu IU.ml^{-1}$)	31.4 ± 4.2	41.4 ± 7.3#
ISI-Matsuda	3.1 ± 0.3	4.4 ± 0.6

Significant difference to fasting insulin concentration, $P < 0.05$, repeated measures ANOVA.

Experiment 1 plasma glucose and insulin concentrations. Fig. 4.2 displays the mean glucose and insulin concentrations during the three trials for experiment 1. In the glucose ingestion only trial plasma glucose peaked at 30 min increasing significantly above baseline (baseline

5.3 ± 0.1 mM, 30 min 9.5 ± 0.5 mM, $P < 0.001$), then remained above baseline until 75 min (6.9 ± 0.2 mM, $P < 0.001$) and returned to baseline by 90 min (6.1 ± 0.3 mM, $P > 0.05$). Plasma insulin peaked at 30 min increasing significantly above baseline (baseline 14.3 ± 1.4 $\mu IU.mL^{-1}$, 30 min 97.6 ± 13.1 $\mu IU.mL^{-1}$, $P < 0.001$), then remained above baseline until 90 min (50.1 ± 6.2 $\mu IU.mL^{-1}$, $P < 0.01$) and returned to baseline by 120 min (31.4 ± 4.2 $\mu IU.mL^{-1}$, $P > 0.05$). In the glucose ingestion and exercise trial plasma glucose peaked at 30 min increasing significantly above baseline (baseline 5.3 ± 0.1 mM, 30 min 9.1 ± 0.4 mM, $P < 0.01$) and returned to baseline by 60 min (7.0 ± 0.4 mM, $P > 0.05$). After 75 min plasma glucose dropped below baseline (3.8 ± 0.3 mM, $P < 0.01$) and remained below baseline at 90 min (4.4 ± 0.2 mM, $P < 0.01$). Plasma insulin peaked at 30 min increasing significantly above baseline (baseline 15.7 ± 1.3 $\mu IU.mL^{-1}$, 30 min 90.8 ± 7.2 $\mu IU.mL^{-1}$, $P < 0.001$), then remained above baseline until 60 min (67.7 ± 6.4 $\mu IU.mL^{-1}$, $P < 0.01$) and returned to baseline by 75 min (23.1 ± 3.6 $\mu IU.mL^{-1}$, $P > 0.05$). Both plasma glucose and insulin remained constant throughout the 30 min exercise bout alone.

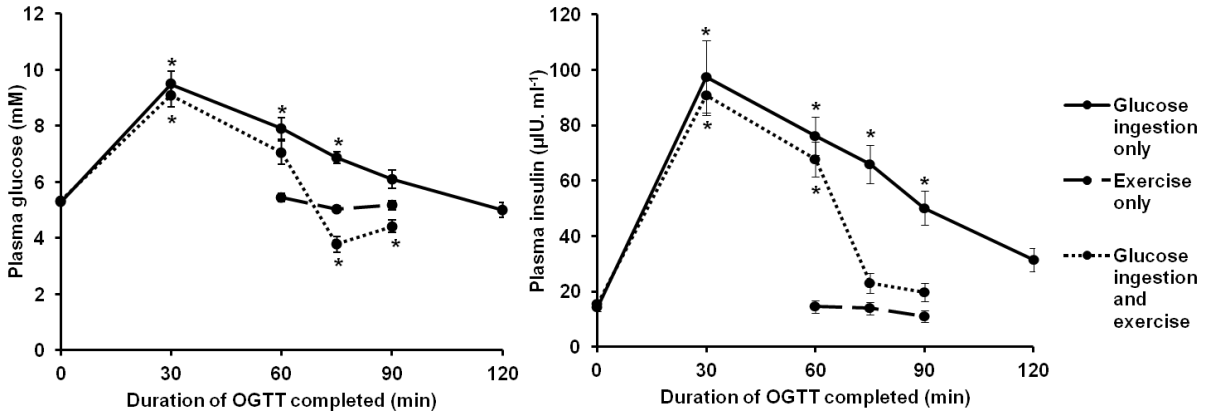

Fig. 4.2. *Plasma glucose and insulin during OGTT, exercise and combination of glucose ingestion and exercise for experiment 1. Data presented are mean ± SEM. N = 10. Repeated measures ANOVA for OGTT and glucose ingestion and exercise glucose P < 0.001, insulin P < 0.001, post hoc Bonferroni pairwise comparisons * P < 0.01 compared to baseline.*

Basal state GLUT4 localisation. Consistent with previous studies (Ploug et al., 1998, Lauritzen et al., 2006, Lauritzen et al., 2008) and as shown in chapter 2 of this thesis GLUT4 immunofluorescence staining (Fig. 4.3A and 4.3B) is observed in large clusters, as well as smaller punctate structures which at a lower magnification appear as a diffuse background stain. The large clusters appear at the fibre periphery as well as intracellular regions. Immunofluorescence staining of the protein dystrophin (Fig. 4.3C) was used to mark the PM. Fig. 4.3D shows the colocalisation of GLUT4 and dystrophin. Perinuclear GLUT4 distribution is also observed when stained in combination with 4,6'-diamidino-2-phenylindole (DAPI) (see Fig. 2.3 in chapter 2 for combined GLUT4 and DAPI staining, and Fig. 4.3B and 4.3D of this chapter indicate perinuclear GLUT4 localisation).

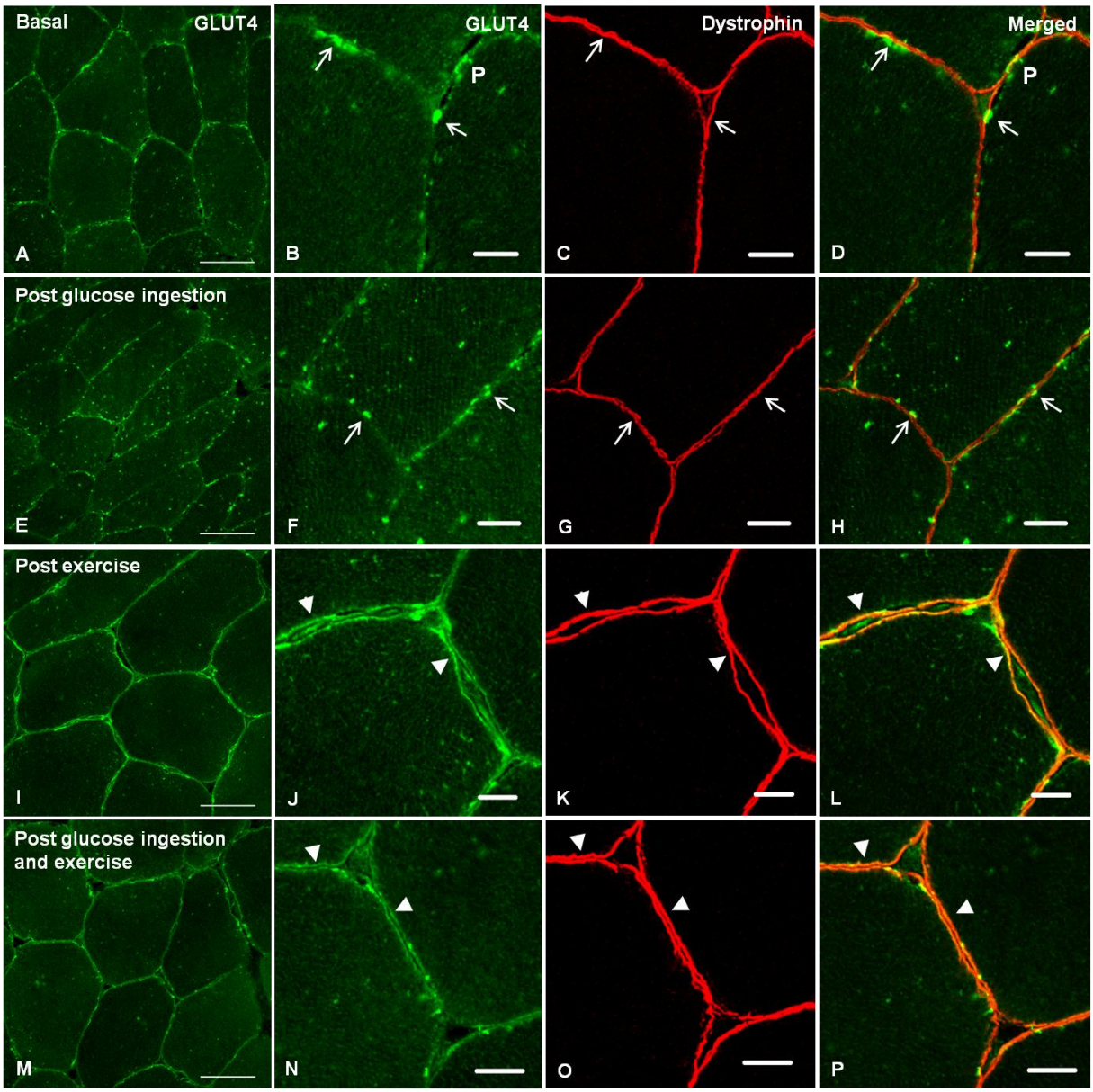

Fig. 4.3. *Representative confocal GLUT4 immunofluorescence of human skeletal muscle fibres in the basal state (A-D), 90 min post glucose ingestion (E-H), post exercise (I-L) and post glucose ingestion and exercise combined (M-P) from experiment 1. Images A, E, I and M show GLUT4 localisation in green (scale bars 50 µm). Images B, F, J and N show more detailed images of GLUT4 in PM regions, GLUT4 shown in green (scale bars 10 µm). Images C, G, K and O show the PM marker dystrophin in red (scale bars 10 µm). Merged images in D, H, L and P demonstrate colocalisation of GLUT4 with the PM marker dystrophin (scale*

bars 10 µm). Open arrows indicate clusters of GLUT4 at the PM, while filled arrow heads indicate GLUT4 redistributed to a continuous PM signal. P indicates perinuclear GLUT4 localisation.

GLUT4 localisation 90 min after glucose ingestion and after 30 min exercise (experiment 1). Ninety minutes after glucose ingestion there was no apparent change in GLUT4 localisation (Fig.4.3E and 4.3F) with GLUT4 distributed in clusters at the PM and in intracellular regions. In line with the visual observations, Pearson's correlation coefficient was unchanged following 90 min glucose ingestion (pre $r = 0.47 \pm 0.01$, post $r = 0.46 \pm 0.01$, $P > 0.05$, Fig 4.4A), indicating no change in GLUT4 PM association (Fig. 4.3H). In contrast, immediately following 30 min of cycling exercise at 65 % of VO_{2max}, GLUT4 staining redistributed around the PM (Fig. 4.3I and 4.3J). GLUT4 exhibited a continuous PM signal that demonstrated a clear increase in colocalisation between GLUT4 and dystrophin staining (Fig. 4.3L). Pearson's correlation coefficient increased significantly from $r = 0.47 \pm 0.01$ before exercise to $r = 0.58 \pm 0.02$ after exercise ($P < 0.001$, Fig. 4.4B), indicating an increase in GLUT4 and dystrophin colocalisation and GLUT4 PM association. When glucose ingestion and exercise were combined, GLUT4 redistributed to a continuous PM signal (Fig. 4.3M and 4.3N) and increases in GLUT4 and dystrophin colocalisation (Fig. 4.3P) occurred. Similarly, following glucose ingestion and exercise Pearson's correlation coefficient increased significantly from $r = 0.47 \pm 0.01$ at baseline to $r = 0.57 \pm 0.02$ after feeding and exercise ($P < 0.001$, Fig.4.4C), however this increase was similar to the response to exercise alone.

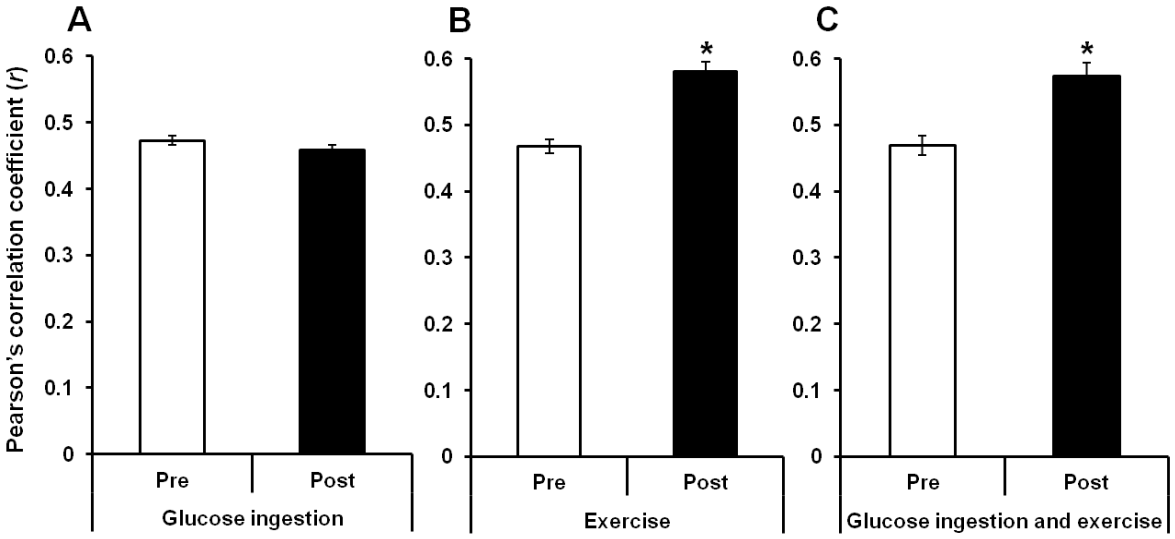

Fig. 4.4. *Colocalisation of GLUT4 with PM marker dystrophin, measured using Pearson's correlation coefficient, from experiment 1. A) Pre and post glucose ingestion, B) pre and post exercise and C) pre and post glucose ingestion and exercise combined. Mean ± SEM, n = 10, *P < 0.001, paired t test.*

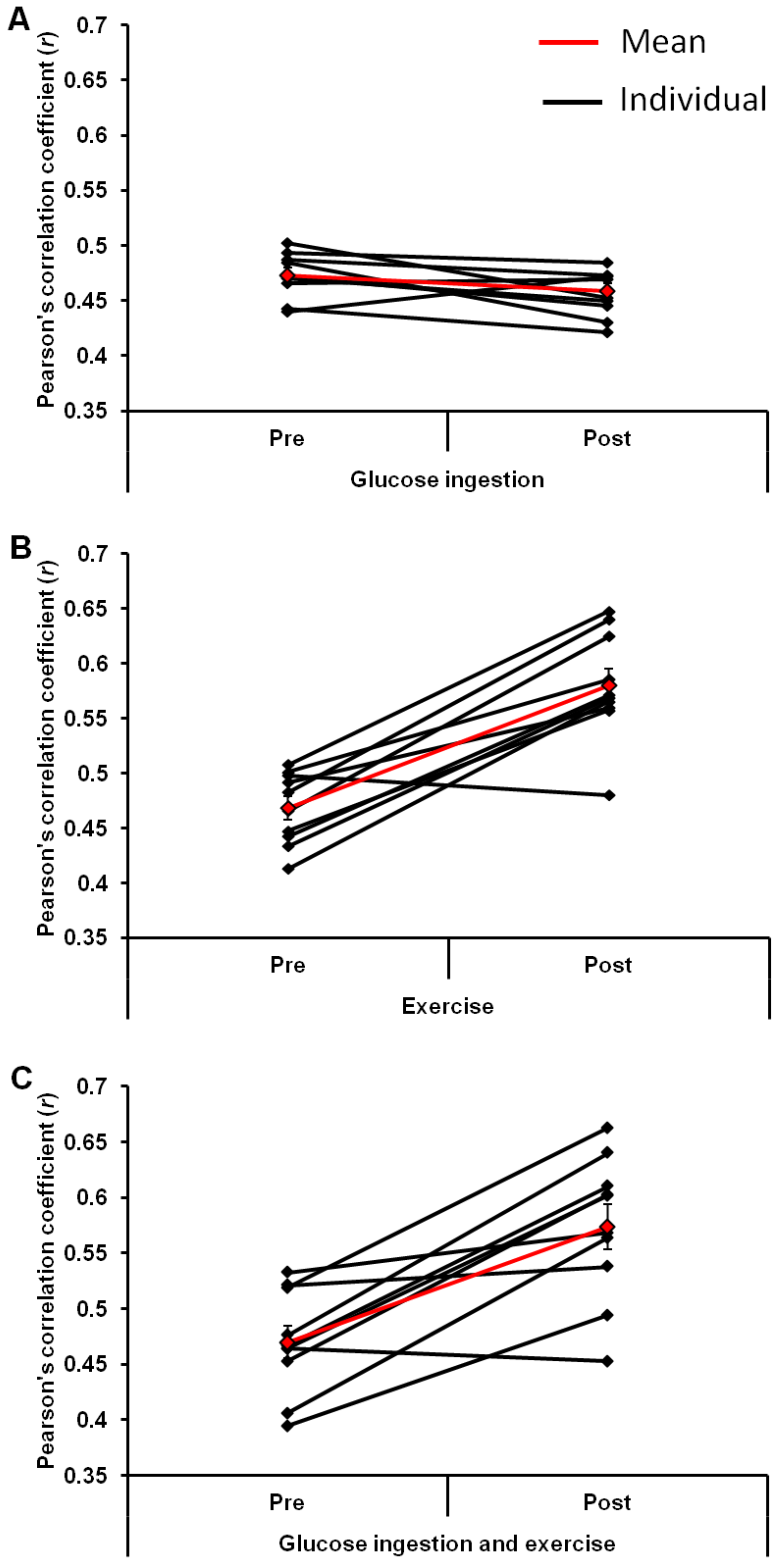

Fig. 4.5. *Colocalisation of GLUT4 with PM marker dystrophin, measured using Pearson's correlation coefficient, from individual participants in experiment 1. A) Pre and post glucose*

ingestion, B) pre and post exercise and C) pre and post glucose ingestion and exercise combined.

SNAP23 localisation 90 min after glucose ingestion and after 30 min exercise (experiment 1). Immunofluorescence staining of SNAP23 displays a strong PM signal which is confirmed by SNAP23 and dystrophin colocalisation (Fig. 4.6D, 4.5H, 4.5L and 4.5P). Pearson's correlation coefficient measuring SNAP23 and dystrophin colocalisation did not change following glucose ingestion (pre $r = 0.42 \pm 0.01$, post $r = 0.42 \pm 0.02$, Fig. 4.7A), exercise (pre $r = 0.47 \pm 0.01$, post $r = 0.46 \pm 0.02$, Fig. 4.7B) or a combination of glucose ingestion and exercise (pre $r = 0.41 \pm 0.03$, post $r = 0.41 \pm 0.04$, Fig. 4.7C), indicating there are no changes in SNAP23 PM content following glucose ingestion or exercise.

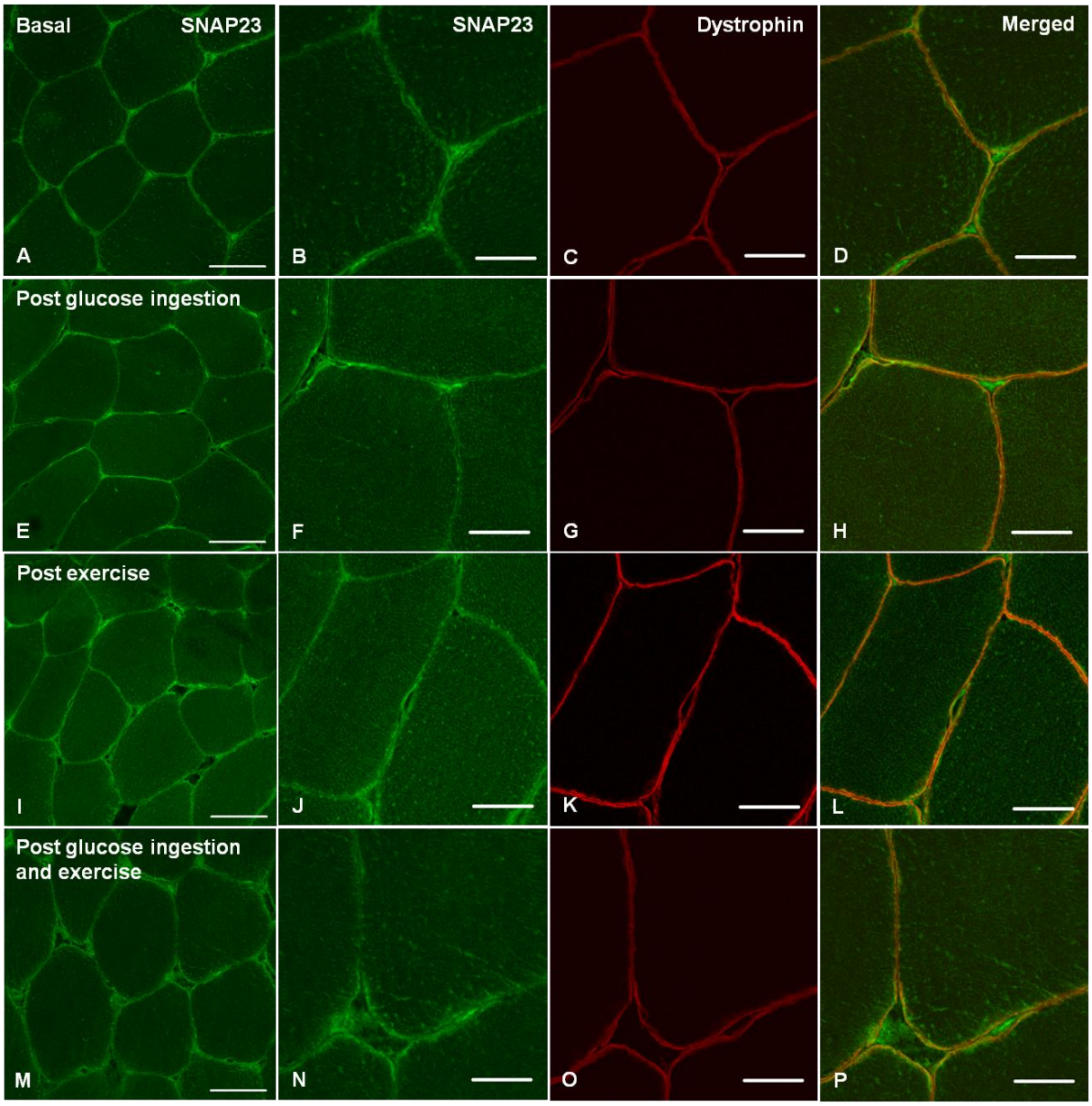

Fig. 4.6. *Representative confocal SNAP23 immunofluorescence images of human skeletal muscle fibres in the basal state (A-D), post glucose ingestion (E-H), post exercise (I-L) and post glucose ingestion and exercise combined (M-P) from experiment 1. Images A, E, I and M show SNAP23 localisation in green (scale bars 50 µm). Images B, F, J and N show more detailed images of SNAP23 in PM regions, SNAP23 shown in green (scale bars 10 µm). Images C, G, K and O show the PM marker dystrophin in red (scale bars 10 µm). Merged*

images in D, H, L and P demonstrate colocalisation of SNAP23 with the PM marker dystrophin (scale bars 10 µm).

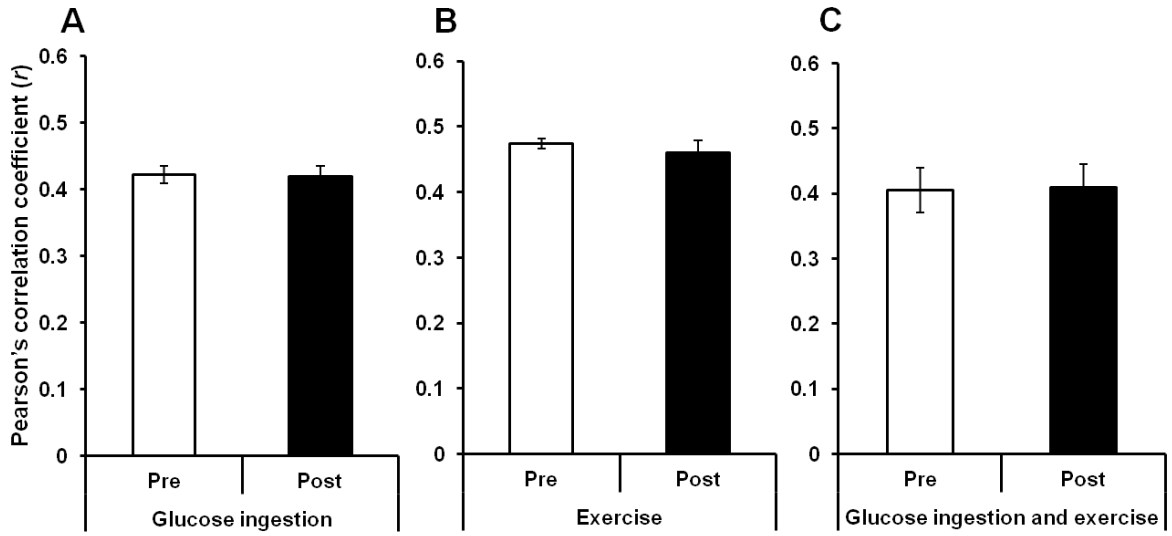

Fig. 4.7. *Colocalisation of SNAP23 with the PM marker dystrophin, measured using Pearson's correlation coefficient, from experiment 1. A) Pre and post glucose ingestion, B) pre and post exercise and C) pre and post glucose ingestion and exercise combined. Mean ± SEM, N = 10.*

Experiment 2 plasma glucose and insulin concentrations. To further investigate the time course of GLUT4 translocation in response to glucose ingestion, GLUT4 and dystrophin colocalisation was investigated in *vastus lateralis* samples taken in the basal state and 30 min and 60 min after glucose ingestion. Fig. 4.8 displays plasma glucose and insulin concentrations during OGTT in experiment 2. Plasma glucose increased above baseline at 30 min (baseline 5.1 ± 0.2 mM, 30 min 8.1 ± 0.6 mM, $P < 0.05$) and returned to baseline by 60 min (6.5 ± 0.5 mM, $P > 0.05$). Plasma insulin peaked at 30 min increasing above baseline

(baseline 12.7 ± 1.7 µIU.mL^{-1}, 30 min 61.3 ± 7.2 µIU.mL^{-1}, $P < 0.001$) and remained increased above baseline at 120 min (41.4 ± 7.3 µIU.mL^{-1}, $P < 0.05$).

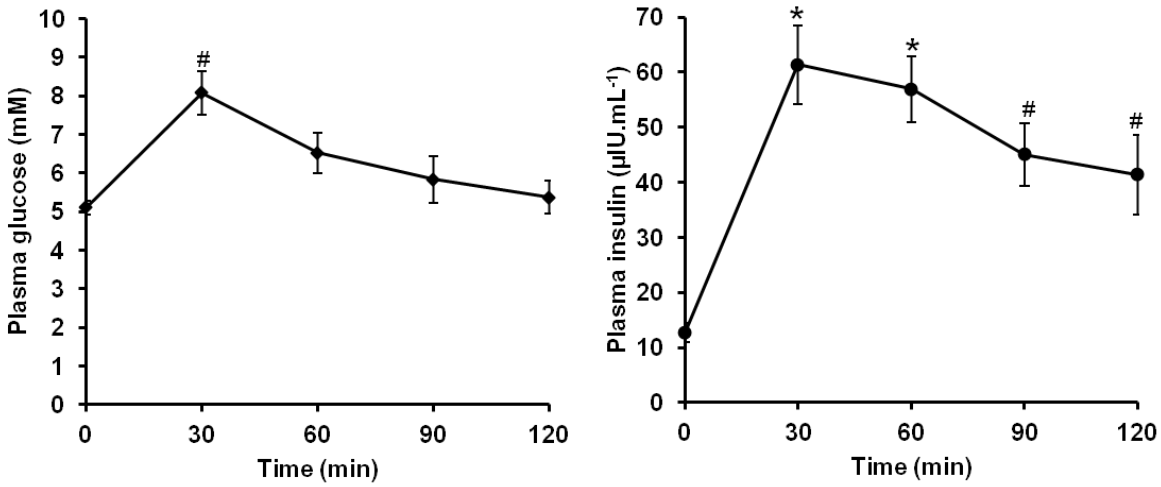

Fig. 4.8. *Plasma glucose and insulin during OGTT for experiment 2. Data presented are mean ± SEM. N = 10. Repeated measures ANOVA glucose P < 0.001, insulin P < 0.001, post hoc Bonferroni pairwise comparisons * P < 0.01, # P < 0.05 compared to baseline.*

GLUT4 localisation 30 min and 60 min after glucose ingestion (experiment 2). Thirty minutes after glucose ingestion, GLUT4 clusters localised to the PM remained clearly visible with the additional appearance of moderate continuous staining along the PM (Fig. 4.9E-H). Pearson's correlation coefficient values to measure GLUT4 and dystrophin colocalisation increased significantly from baseline at 30 min post-glucose ingestion. GLUT4 and dystrophin colocalisation returned to baseline 60 min after glucose ingestion (pre $r = 0.42 \pm 0.02$, 30 min $r = 0.46 \pm 0.02$, 60 min $r = 0.44 \pm 0.02$, repeated measures ANOVA $P = 0.008$, Fig. 4.10).

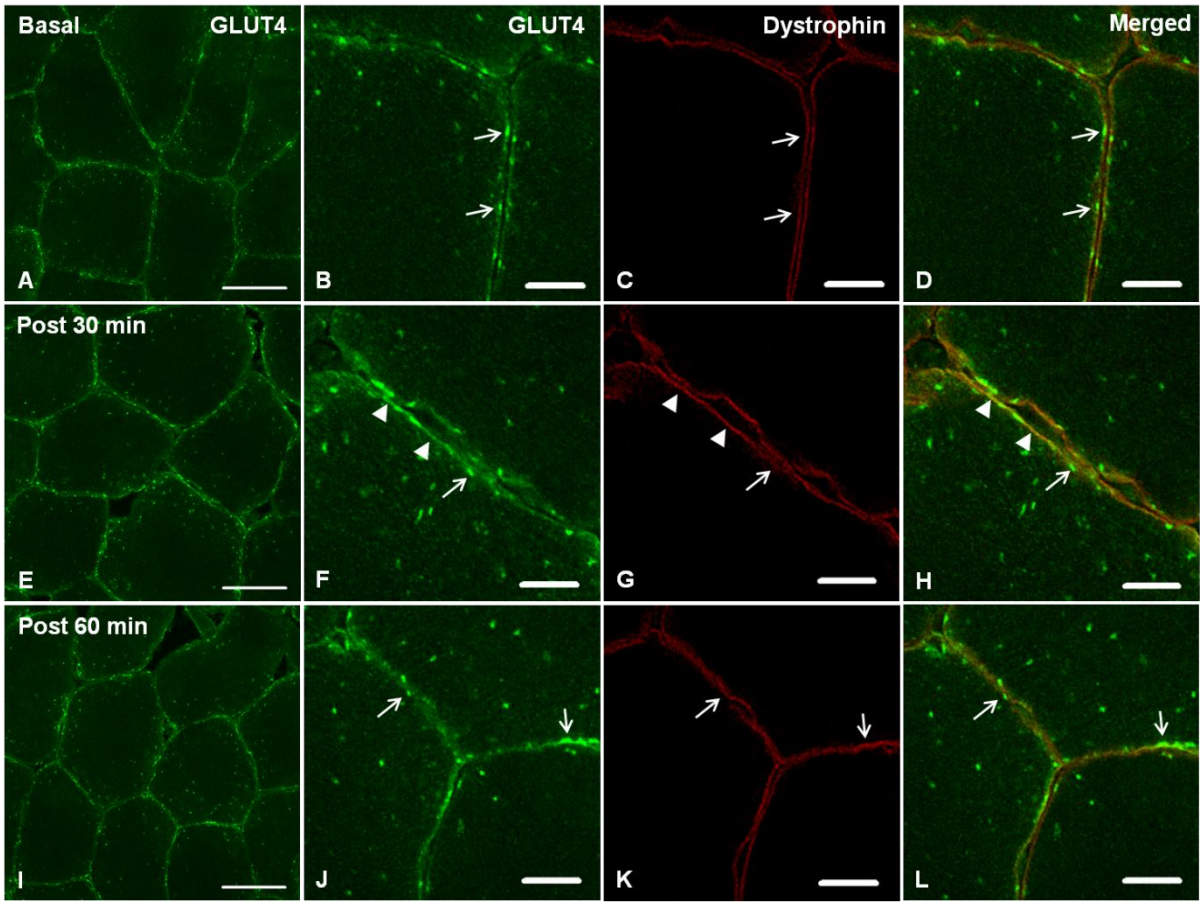

Fig. 4.9. *Representative confocal immunofluorescence images of GLUT4 immunofluorescence in human skeletal muscle fibres in the basal state (A,B), 30 min post glucose ingestion (E,F) and 60 min post glucose ingestion (I,J) from experiment 2. Images A, E and I show GLUT4 localisation in green (scale bars 50 µm). Images B, F and J show more detailed images of GLUT4 in PM regions (scale bars 10 µm). Images C,G and K show the PM marker dystrophin in red (scale bars 10 µm). Merged images in D, H amd L demonstrate colocalisation of GLUT4 with the PM marker dystrophin (scale bars 10 µm). Open arrows indicate clusters of GLUT4 at the PM, while filled arrow heads indicate moderate continuous GLUT4 signal at the PM..*

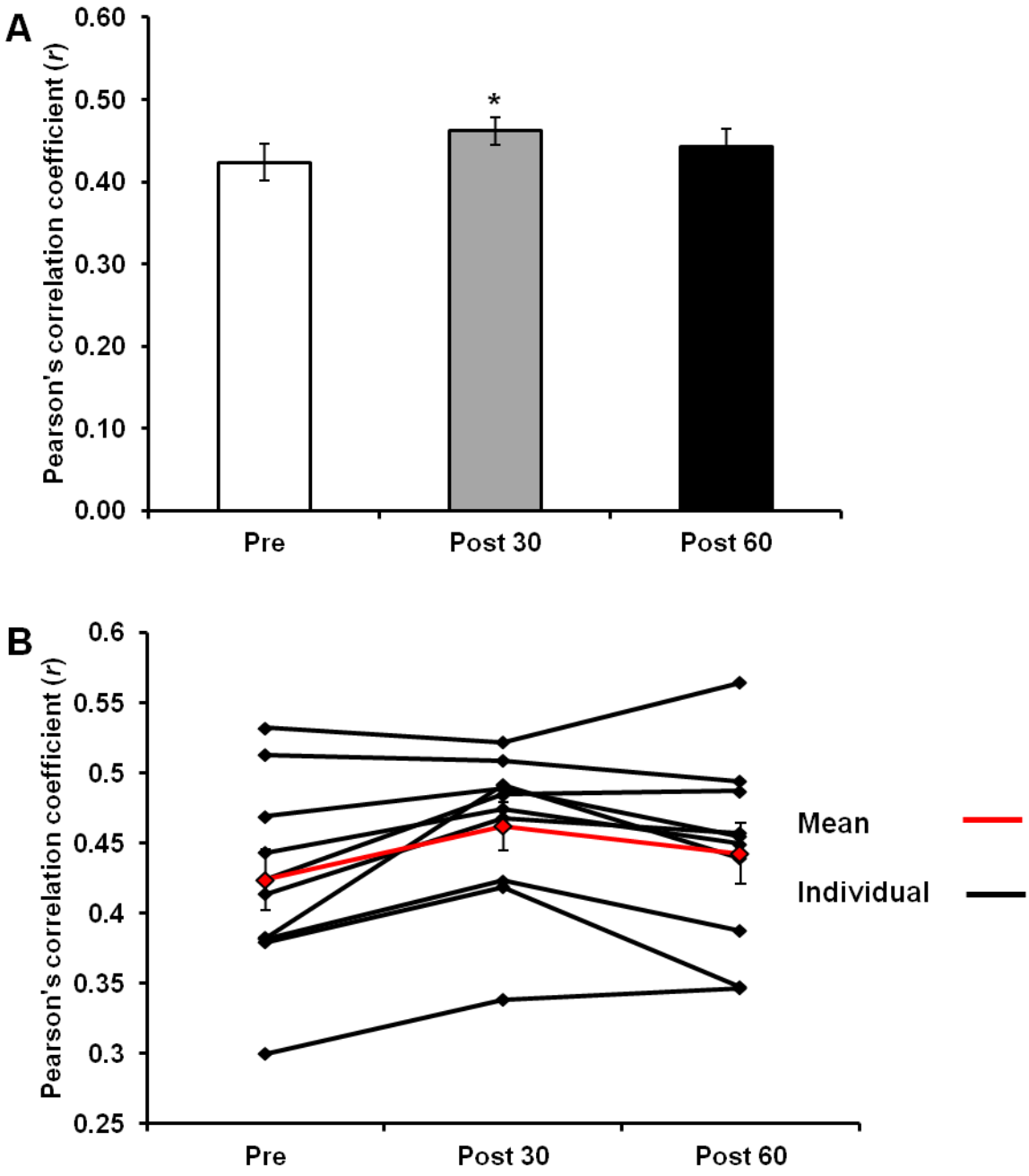

Fig. 4.10. *Colocalisation of GLUT4 with the PM marker dystrophin, measured using Pearson's correlation coefficient, in the basal state and 30 min and 60 min following glucose ingestion from experiment 2. A) Data presented are mean ± SEM, N = 10. Repeated measures ANOVA P = 0.008, * post hoc Bonferroni pairwise comparisons P < 0.05 compared to baseline. B) Individual participant responses.*

4.5. Discussion

Immunofluorescence visualisation of GLUT4 translocation following glucose ingestion and exercise. In the current study, the immunofluorescence microscopy method developed in chapter 2 of this thesis has been used successfully to detect GLUT4 translocation to the PM in human skeletal muscle 30 min following glucose ingestion, after 30 min of cycling exercise at 65% VO_{2max} and following a combination of glucose feeding and exercise.

Cycling exercise at 60-70% VO_{2max} has been shown to increase PM GLUT4 by 71 % in human *vastus lateralis* muscle using cellular subfractionation methods (Kennedy et al., 1999). In addition, just 5 min of electrical stimulation of rodent muscle induces a significant increase in GLUT4 PM content measured using fluorescence microscopy (Ploug et al., 1998, Lauritzen et al., 2010). In line with these previous observations, the immunofluorescence images presented in this study show marked redistribution of GLUT4 around PM regions in response to exercise. This can be observed by the clear appearance of a continuous GLUT4 signal along the cell border, which colocalised with the PM marker dystrophin following exercise (Fig 4.3). Furthermore, these observations are confirmed by the significant increase in GLUT4 and dystrophin colocalisation post-exercise.

Furthermore, in the current study, the appearance of moderate continuous GLUT4 staining at the cell border was observed in skeletal muscle 30 min following glucose ingestion (Fig. 4.9) and was also confirmed by a significant increase in GLUT4 and dystrophin colocalisation. This finding was expected given that skeletal muscle accounts for the majority of insulin-mediated glucose disposal (Katz et al., 1983, Ferrannini et al., 1985) and GLUT4 is the main insulin responsive GLUT isoform in skeletal muscle (Mueckler, 1994). These findings are in line with previous observations of increased GLUT4 content of isoloated PM fractions in

human *vastus lateralis* muscle 30-40 min following a hyperinsulinaemic-euglycaemic clamp (Guma et al., 1995) and the rapid translocation of GLUT4 into the PM region in rodent muscle following insulin injection (Lauritzen et al., 2006). However, we did not observe a significant increase above baseline in GLUT4 and dystrophin colocalisation either at 60 or 90 min following glucose ingestion, contrary to the original hypothesis. This finding is in contrast to previous studies using subcellular fractionation techniques, which reported a 27 % increase in GLUT4 in the PM 60 min after ingestion of an OGTT load (Goodyear et al., 1996) and is somewhat surprising given previous observations that rates of glucose disposal (Ferrannini et al., 1985, Breen et al., 2011) and leg glucose uptake (Katz et al., 1983) are still elevated 90 min following glucose ingestion.

Glucose ingestion 60 min prior to cycling exercise had no further effect on post-exercise GLUT4 and dystrophin colocalisation, therefore no additive effect on GLUT4 translocation was observed of combined glucose feeding and exercise. However while the muscle biopsy was sampled immediately after 30 min cycling exercise, this was 90 min after glucose ingestion; the time point at which no insulin-mediated GLUT4 translocation was detected.

Interestingly and perhaps of relevance, the GLUT4 translocation measured in the current study following glucose ingestion appears to mirror the peak concentration of plasma insulin, which peaked 30 min following glucose ingestion. The results from this study suggest that physiological GLUT4 translocation to the PM in response to glucose ingestion is transient. Furthermore the GLUT4 translocation response following glucose ingestion appears to be modest in comparison to that following exercise. This suggestion will be discussed further in a subsequent paragraph.

Importance of peripheral GLUT4 localisation. In previous rat and mouse studies skeletal muscle GLUT4 was located predominantly at the fibre periphery in both the basal and stimulated states (Ploug et al., 1998, Lauritzen et al., 2006, Lizunov et al., 2012). The images presented in this study confirm that this also is the case in human skeletal muscle as GLUT4 and dystrophin colocalisation was present in both the basal and stimulated states. Two previous studies using different transgenic mouse models with specific GLUT4 exofacial labelling techniques have visualised the incorporation of GLUT4 in the PM and both detected GLUT4 in the PM in the basal state (Schertzer et al., 2009, Lizunov et al., 2012). One study described a small amount of exofacially-tagged GLUT4 labelling in the basal state (Lizunov et al., 2012) and the other reported a more substantial amount with externalised *myc* labelling under basal conditions approximately 50 % of that after insulin stimulation (Schertzer et al., 2009). This suggests there is GLUT4 incorporation into the PM even in the basal state, which is in agreement with data indicating a role for GLUT4 in basal glucose uptake (Hansen et al., 1995).

TIRF microscopy studies in skeletal muscle have shown that eighty percent of insulin-mediated GSV fusion events emanated from vesicles that were within 100 nm of the PM and pre-tethered at the PM prior to insulin stimulation (Lizunov et al., 2012). Therefore the limit of resolution of confocal microscopy (~ 200 nm) dictates that it is not possible to distinguish between a vesicle that is fused at the PM, pre-tethered at the PM or simply in close proximity to the PM (Schertzer et al., 2009). Therefore, it should be noted that the transition from tethered to fused GLUT4 may not have been detected in the current study. This potentially limits the sensitivity of measuring increases in GLUT4 and dystrophin colocalisation using this method.

Comments on the magnitude of glucose ingestion- and exercise-mediated increases in GLUT4 and dystrophin colocalisation. In adipocytes a mode of GLUT4 exocytosis has been proposed to occur whereby in the basal state GLUT4 is retained in clusters in PM regions, while insulin stimulation increased the prevalence of these clusters but also elicited dispersal of GLUT4 molecules into the PM (Stenkula et al., 2010). The observations presented here in human skeletal muscle have similarities to this data. Clusters of GLUT4 are clearly observed in PM regions in the basal state (Fig. 4.3 and Fig. 4.9). However, following exercise, the clusters of GLUT4 staining are absent and GLUT4 staining is instead continuous along the PM, indicative of GLUT4 dispersal in the PM. On the other hand, following glucose ingestion, GLUT4 clusters localised to the PM remain clearly visible despite the appearance of moderate continuous staining along the PM at 30 min following glucose ingestion. This suggests that the magnitude of GLUT4 redistribution around the PM in human skeletal muscle is greater following exercise at 65% VO_{2max} than 30 min following glucose ingestion. Supporting this suggestion is a significant difference between the magnitude of increase in Pearson's correlation coefficient following 30 min exercise at 65% VO_{2max} and 30 min following glucose ingestion (mean increase following exercise $r = 0.11 \pm 0.02$, mean increase following glucose ingestion $r = 0.04 \pm 0.01$, independent samples t test $P < 0.01$). Furthermore the suggestion that GLUT4 redistribution around the PM is greater following exercise compared to glucose ingestion is consistent with previous studies in which leg glucose uptake increased 3-fold during the 4 h period following glucose feeding (Katz et al., 1983) and approximately 15-fold during cycling exercise at 50-60% $VO_{2\,max}$ (Katz et al., 1986, Martin et al., 1995).

SNAP23 localisation following glucose feeding and exercise. SNAP23 is a t-SNARE, which, in combination with another t-SNARE syntaxin 4 and the v-SNARE VAMP2, is required for insulin mediated GLUT4 fusion at the PM (Kawanishi et al., 2000, Chen and Scheller, 2001).

The SNAREs required for contraction-mediated GLUT4 fusion at the PM are yet to be fully characterised, but are likely to be the same as insulin-mediated GLUT4 translocation as VAMP2 has been shown to translocate to cell surface membranes, where the t-SNARES are already located, in response to contraction (Rose et al., 2009). In the present study, GLUT4 redistribution in response to exercise occurred without any changes in basal state SNAP23 localisation. This is consistent with SNAP23 being a t-SNARE, therefore constitutively present at the PM (Bryant et al., 2002). The images presented here, in particular highlighted in Fig. 4.11, suggest SNAP23 and post-exercise GLUT4 staining of the PM are heterogeneous. Chamberlain and Gould (2002) observed that the majority of SNAP23 was present in PM lipid rafts in 3T3-L1 adipocytes (Chamberlain and Gould, 2002). Future studies should therefore explore whether this also is the case in human skeletal muscle, implying that the lipid rafts would be the sections of the PM where preferential docking and fusion of GLUT4 occurs.

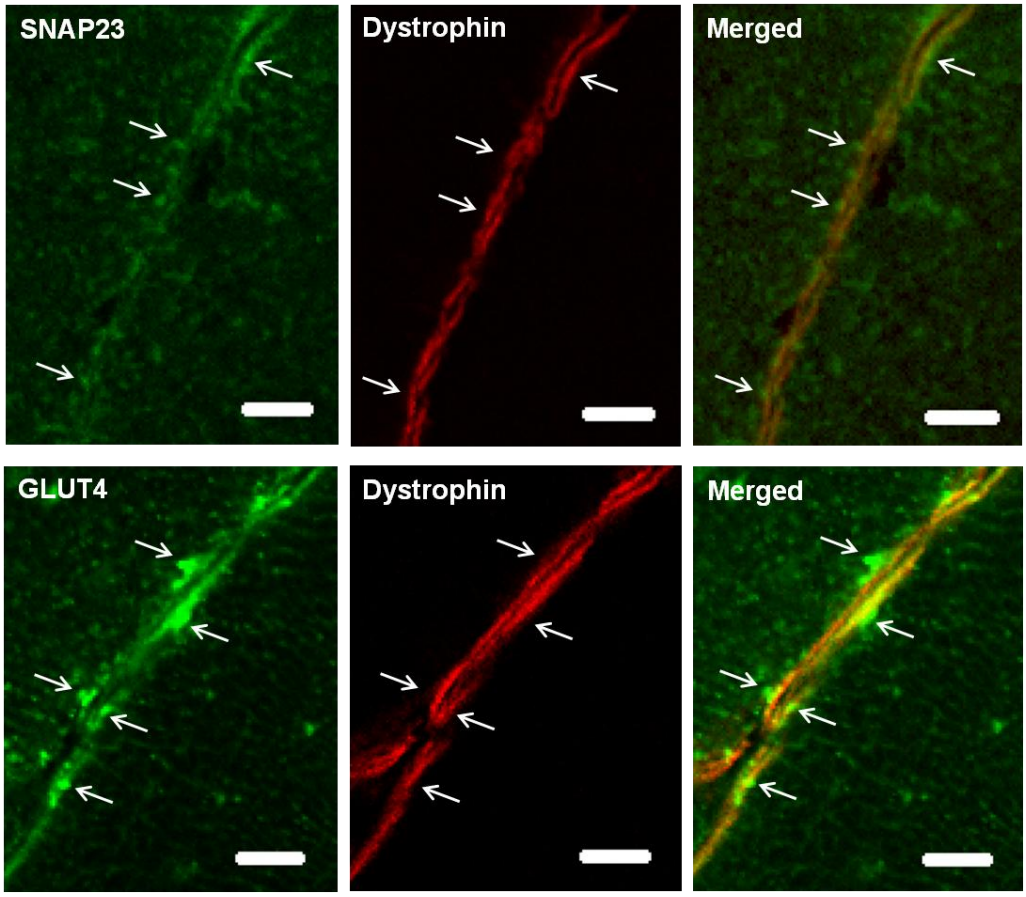

Fig. 4.11. *Post exercise SNAP23 and GLUT4 staining in combination with the PM marker dystrophin highlighting inhomogeneity in SNAP23 and GLUT4 staining at the PM. Arrows indicate regions of greater SNAP23 and GLUT4 staining at the PM. Scale bars 5 µm.*

Other factors contributing to insulin- and contraction-mediated increases in glucose uptake. The magnitude of increase in PM GLUT4 association following glucose feeding and exercise in this study and GLUT4 in PM subfractions in others (Goodyear et al., 1996, Kennedy et al., 1999) does not seem to account for the large increases in glucose uptake observed in the 4 h period following glucose feeding (3-fold) (Katz et al., 1983), during hyperinsulinaemic-euglycaemic clamp (5-fold) (DeFronzo et al., 1985) and during exercise at 50-60% $VO_{2\ max}$ (15-fold) (Katz et al., 1986, Martin et al., 1995). Therefore it appears that mechanisms other

than GLUT4 translocation to the PM contribute to the large increases in glucose uptake following either stimulus. In Chapter 2 of this thesis we observed that GLUT4 staining was present in the T-tubule membranes of human skeletal muscle in the basal state as there was substantial colocalisation of GLUT4 and dihydropyridine receptor (DHPR) staining. However, colocalisation of GLUT4 with DPHR was not quantified in the current chapter, due to the methodological difficulties as explained in chapter 2 leading to large variability in the data. It, nevertheless, cannot be excluded that translocation to T-tubule membranes was more prominent at the sampled time-points than to the PM.

Other mechanisms that may contribute to the increases in glucose uptake following glucose ingestion and during endurance exercise are increases in GLUT4 intrinsic activity (Furtado et al., 2002, Michelle Furtado et al., 2003), increases in hexokinase (HKII) activity and glycogen synthesis resulting in increased glucose phosphorylation and a steeper glucose concentration gradient between the interstitium and muscle cell interior (Wasserman et al., 2011) and increases in skeletal muscle microvascular recruitment, leading to increases in capillary permeability surface area product (Steinberg et al., 1994, Gudbjornsdottir et al., 2003, Vincent et al., 2006) and therefore increases in transendothelial transport rates of insulin and glucose.

Future investigation of a potential additive effect of glucose ingestion and exercise on GLUT4 translocation. In order to investigate whether the effects of exercise and glucose ingestion on GLUT4 translocation are additive the following study design was chosen; ingestion of 75 g of glucose was followed after 1 h with 30 min of exercise. The rationale behind this design was that increases in leg glucose uptake were maintained 90 min after glucose ingestion (Katz et al., 1983). Therefore a biopsy, and measurement of GLUT4 colocalisation with dystrophin, 90 min after glucose ingestion should be a time-point at which GLUT4 translocation was maximal and that the 30 min of exercise could lead to an additional increase in GLUT4

translocation. However, significant increases in GLUT4 and dystrophin colocalisation were only observed 30 min after oral glucose ingestion. Therefore, in hindsight, a better study design to investigate whether glucose ingestion and exercise exert additive effects on GLUT4 translocation, would be to start the exercise immediately after glucose ingestion with the biopsy therefore taken 30 min after both glucose ingestion and the start of exercise. The data in Fig. 4.2 and 4.8 show that 30 min after glucose ingestion the mean plasma insulin concentration was higher than the very low plasma insulin concentration seen when exercise was performed 60-90 min after glucose ingestion. This higher plasma insulin concentration 30 min after glucose ingestion could better allow investigation of additive effects of glucose ingestion and exercise using the alternative study design proposed above.

Another possible design would have been to start with 30 min of exercise, and follow this immediately with glucose ingestion and take biopsies 30, 60 and 90 min after glucose ingestion. It is difficult to suggest what the outcome would be as there are a number of variables. Firstly, it is unknown how long the contraction-induced increase in GLUT4 and dystrophin colocalisation is maintained. Data obtained in rodents suggest that exercise-mediated increases in skeletal muscle GLUT4 PM content are reduced by 20% 30 min after the termination of exercise and return to baseline by 2 h (Ivy and Kuo, 1998). Secondly, if the exercise bout occurs before glucose ingestion, post-exercise improvements in glucose tolerance may affect GLUT4 translocation rather than an assessment of whether the individual glucose ingestion and exercise responses are additive. However it is not known whether the 30 min of prior exercise leads to sufficient glycogen depletion to increase the rate of insulin-stimulated glycogen resynthesis (Wojtaszewski et al., 2000) and contribute to potential post-exercise increases in insulin-mediated GLUT4 translocation. In summary, reversing the order

of glucose ingestion and exercise would be complicated by many unanswered questions that need further research to comprehend.

Conclusions. This study has successfully used the immunofluorescence technique developed in chapter 2 of this thesis to demonstrate increases in GLUT4 and dystrophin colocalisation 30 min following glucose ingestion and immediately after 30 min exercise performed at 65% $VO_{2\ max}$; indicative of GLUT4 translocation to the PM stimulated by insulin and contraction, respectively. GLUT4 translocation following glucose ingestion was transient and did not mirror the prolonged elevated rates of glucose disposal previously observed following oral glucose ingestion. This methodology raises the possibility to further explore the mechanisms regulating glucose uptake in response to insulin and contraction in human skeletal muscle, the mechanisms underlying the development of insulin resistance in obesity and ageing and the beneficial effects of lifestyle changes and pharmaceutical interventions.

4.6. References

BELL, G. I., BURANT, C. F., TAKEDA, J. & GOULD, G. W. 1993. Structure and function of mammalian facilitative sugar transporters. *J Biol Chem,* 268**,** 19161-4.

BOLTE, S. & CORDELIERES, F. P. 2006. A guided tour into subcellular colocalization analysis in light microscopy. *J Microsc,* 224**,** 213-32.

BREEN, L., PHILP, A., SHAW, C. S., JEUKENDRUP, A. E., BAAR, K. & TIPTON, K. D. 2011. Beneficial effects of resistance exercise on glycemic control are not further improved by protein ingestion. *PLoS One,* 6**,** e20613.

BRYANT, N. J., GOVERS, R. & JAMES, D. E. 2002. Regulated transport of the glucose transporter GLUT4. *Nat Rev Mol Cell Biol,* 3**,** 267-77.

CHAMBERLAIN, L. H. & GOULD, G. W. 2002. The vesicle- and target-SNARE proteins that mediate Glut4 vesicle fusion are localized in detergent-insoluble lipid rafts present on distinct intracellular membranes. *J Biol Chem,* 277**,** 49750-4.

CHEN, Y. A. & SCHELLER, R. H. 2001. SNARE-mediated membrane fusion. *Nat Rev Mol Cell Biol,* 2**,** 98-106.

DEFRONZO, R. A., GUNNARSSON, R., BJORKMAN, O., OLSSON, M. & WAHREN, J. 1985. Effects of insulin on peripheral and splanchnic glucose metabolism in noninsulin-dependent (type II) diabetes mellitus. *J Clin Invest,* 76**,** 149-55.

DUNN, K. W., KAMOCKA, M. M. & MCDONALD, J. H. 2011. A practical guide to evaluating colocalization in biological microscopy. *Am J Physiol Cell Physiol,* 300**,** C723-42.

FERRANNINI, E., BJORKMAN, O., REICHARD, G. A., JR., PILO, A., OLSSON, M., WAHREN, J. & DEFRONZO, R. A. 1985. The disposal of an oral glucose load in healthy subjects. A quantitative study. *Diabetes,* 34**,** 580-8.

FURTADO, L. M., SOMWAR, R., SWEENEY, G., NIU, W. & KLIP, A. 2002. Activation of the glucose transporter GLUT4 by insulin. *Biochem Cell Biol,* 80**,** 569-78.

GASTER, M., HANDBERG, A., BECK-NIELSEN, H. & SCHRODER, H. D. 2000. Glucose transporter expression in human skeletal muscle fibers. *Am J Physiol Endocrinol Metab,* 279**,** E529-38.

GENUTH, S., ALBERTI, K. G., BENNETT, P., BUSE, J., DEFRONZO, R., KAHN, R., KITZMILLER, J., KNOWLER, W. C., LEBOVITZ, H., LERNMARK, A., NATHAN, D., PALMER, J., RIZZA, R., SAUDEK, C., SHAW, J., STEFFES, M., STERN, M., TUOMILEHTO, J., ZIMMET, P., EXPERT COMMITTEE ON THE, D. & CLASSIFICATION OF DIABETES, M. 2003. Follow-up report on the diagnosis of diabetes mellitus. *Diabetes Care,* 26**,** 3160-7.

GOODYEAR, L. J., HIRSHMAN, M. F., NAPOLI, R., CALLES, J., MARKUNS, J. F., LJUNGQVIST, O. & HORTON, E. S. 1996. Glucose ingestion causes GLUT4 translocation in human skeletal muscle. *Diabetes,* 45**,** 1051-6.

GUDBJORNSDOTTIR, S., SJOSTRAND, M., STRINDBERG, L., WAHREN, J. & LONNROTH, P. 2003. Direct measurements of the permeability surface area for insulin and glucose in human skeletal muscle. *J Clin Endocrinol Metab,* 88**,** 4559-64.

GUMA, A., ZIERATH, J. R., WALLBERG-HENRIKSSON, H. & KLIP, A. 1995. Insulin induces translocation of GLUT-4 glucose transporters in human skeletal muscle. *Am J Physiol,* 268**,** E613-22.

HANSEN, P. A., GULVE, E. A., MARSHALL, B. A., GAO, J., PESSIN, J. E., HOLLOSZY, J. O. & MUECKLER, M. 1995. Skeletal muscle glucose transport and metabolism are enhanced in transgenic mice overexpressing the Glut4 glucose transporter. *J Biol Chem,* 270**,** 1679-84.

IVY, J.L. & KUO, C.H. 1998. Regulation of GLUT4 protein and glycogen synthase during muscle glycogen synthesis after exercise. *Acta Physiol Scand,* 162, 295-304.

KATZ, A., BROBERG, S., SAHLIN, K. & WAHREN, J. 1986. Leg glucose uptake during maximal dynamic exercise in humans. *Am J Physiol,* 251**,** E65-70.

KATZ, A., SAHLIN, K. & BROBERG, S. 1991. Regulation of glucose utilization in human skeletal muscle during moderate dynamic exercise. *Am J Physiol,* 260**,** E411-5.

KATZ, L. D., GLICKMAN, M. G., RAPOPORT, S., FERRANNINI, E. & DEFRONZO, R. A. 1983. Splanchnic and peripheral disposal of oral glucose in man. *Diabetes,* 32**,** 675-9.

KAWANISHI, M., TAMORI, Y., OKAZAWA, H., ARAKI, S., SHINODA, H. & KASUGA, M. 2000. Role of SNAP23 in insulin-induced translocation of GLUT4 in 3T3-L1 adipocytes. Mediation of complex formation between syntaxin4 and VAMP2. *J Biol Chem,* 275**,** 8240-7.

KENNEDY, J. W., HIRSHMAN, M. F., GERVINO, E. V., OCEL, J. V., FORSE, R. A., HOENIG, S. J., ARONSON, D., GOODYEAR, L. J. & HORTON, E. S. 1999. Acute exercise induces GLUT4 translocation in skeletal muscle of normal human subjects and subjects with type 2 diabetes. *Diabetes,* 48**,** 1192-7.

KJAER, M., KIENS, B., HARGREAVES, M. & RICHTER, E. A. 1991. Influence of active muscle mass on glucose homeostasis during exercise in humans. *J Appl Physiol,* 71**,** 552-7.

KRISTIANSEN, S., HARGREAVES, M. & RICHTER, E. A. 1997. Progressive increase in glucose transport and GLUT-4 in human sarcolemmal vesicles during moderate exercise. *Am J Physiol,* 272**,** E385-9.

LACHMANOVICH, E., SHVARTSMAN, D. E., MALKA, Y., BOTVIN, C., HENIS, Y. I. & WEISS, A. M. 2003. Co-localization analysis of complex formation among membrane proteins by computerized fluorescence microscopy: application to immunofluorescence co-patching studies. *J Microsc,* 212**,** 122-31.

LANDMANN, L. & MARBET, P. 2004. Colocalization analysis yields superior results after image restoration. *Microsc Res Tech,* 64**,** 103-12.

LAURITZEN, H. P., GALBO, H., BRANDAUER, J., GOODYEAR, L. J. & PLOUG, T. 2008. Large GLUT4 vesicles are stationary while locally and reversibly depleted during transient insulin stimulation of skeletal muscle of living mice: imaging analysis of GLUT4-enhanced green fluorescent protein vesicle dynamics. *Diabetes,* 57**,** 315-24.

LAURITZEN, H. P., GALBO, H., TOYODA, T. & GOODYEAR, L. J. 2010. Kinetics of contraction-induced GLUT4 translocation in skeletal muscle fibers from living mice. *Diabetes,* 59**,** 2134-44.

LAURITZEN, H. P., PLOUG, T., PRATS, C., TAVARE, J. M. & GALBO, H. 2006. Imaging of insulin signaling in skeletal muscle of living mice shows major role of T-tubules. *Diabetes,* 55**,** 1300-6.

LIZUNOV, V. A., STENKULA, K. G., LISINSKI, I., GAVRILOVA, O., YVER, D. R., CHADT, A., AL-HASANI, H., ZIMMERBERG, J. & CUSHMAN, S. W. 2012. Insulin stimulates fusion, but not tethering, of GLUT4 vesicles in skeletal muscle of HA-GLUT4-GFP transgenic mice. *Am J Physiol Endocrinol Metab,* 302**,** E950-60.

MARTIN, I. K., KATZ, A. & WAHREN, J. 1995. Splanchnic and muscle metabolism during exercise in NIDDM patients. *Am J Physiol,* 269**,** E583-90.

MICHELLE FURTADO, L., POON, V. & KLIP, A. 2003. GLUT4 activation: thoughts on possible mechanisms. *Acta Physiol Scand,* 178**,** 287-96.

MUECKLER, M. 1994. Facilitative glucose transporters. *Eur J Biochem,* 219**,** 713-25.

PLOUG, T., VAN DEURS, B., AI, H., CUSHMAN, S. W. & RALSTON, E. 1998. Analysis of GLUT4 distribution in whole skeletal muscle fibers: identification of distinct storage compartments that are recruited by insulin and muscle contractions. *J Cell Biol,* 142**,** 1429-46.

RODNICK, K. J., SLOT, J. W., STUDELSKA, D. R., HANPETER, D. E., ROBINSON, L. J., GEUZE, H. J. & JAMES, D. E. 1992. Immunocytochemical and biochemical studies of GLUT4 in rat skeletal muscle. *J Biol Chem,* 267**,** 6278-85.

ROSE, A. J., JEPPESEN, J., KIENS, B. & RICHTER, E. A. 2009. Effects of contraction on localization of GLUT4 and v-SNARE isoforms in rat skeletal muscle. *Am J Physiol Regul Integr Comp Physiol,* 297**,** R1228-37.

RYDER, J. W., KAWANO, Y., CHIBALIN, A. V., RINCON, J., TSAO, T. S., STENBIT, A. E., COMBATSIARIS, T., YANG, J., HOLMAN, G. D., CHARRON, M. J. & ZIERATH, J. R. 1999a. In vitro analysis of the glucose-transport system in GLUT4-null skeletal muscle. *Biochem J,* 342 (Pt 2)**,** 321-8.

RYDER, J. W., KAWANO, Y., GALUSKA, D., FAHLMAN, R., WALLBERG-HENRIKSSON, H., CHARRON, M. J. & ZIERATH, J. R. 1999b. Postexercise glucose uptake and glycogen synthesis in skeletal muscle from GLUT4-deficient mice. *FASEB J,* 13**,** 2246-56.

SCHERTZER, J. D., ANTONESCU, C. N., BILAN, P. J., JAIN, S., HUANG, X., LIU, Z., BONEN, A. & KLIP, A. 2009. A transgenic mouse model to study glucose transporter 4myc regulation in skeletal muscle. *Endocrinology,* 150**,** 1935-40.

SCHWENK, R. W., DIRKX, E., COUMANS, W. A., BONEN, A., KLIP, A., GLATZ, J. F. & LUIKEN, J. J. 2010. Requirement for distinct vesicle-associated membrane proteins in insulin- and AMP-activated protein kinase (AMPK)-induced translocation of GLUT4 and CD36 in cultured cardiomyocytes. *Diabetologia,* 53**,** 2209-19.

SEDARAT, F., LIN, E., MOORE, E. D. & TIBBITS, G. F. 2004. Deconvolution of confocal images of dihydropyridine and ryanodine receptors in developing cardiomyocytes. *J Appl Physiol,* 97**,** 1098-103.

STEINBERG, H. O., BRECHTEL, G., JOHNSON, A., FINEBERG, N. & BARON, A. D. 1994. Insulin-mediated skeletal muscle vasodilation is nitric oxide dependent. A novel action of insulin to increase nitric oxide release. *J Clin Invest,* 94**,** 1172-9.

STENKULA, K. G., LIZUNOV, V. A., CUSHMAN, S. W. & ZIMMERBERG, J. 2010. Insulin controls the spatial distribution of GLUT4 on the cell surface through regulation of its postfusion dispersal. *Cell Metab,* 12**,** 250-9.

THORELL, A., HIRSHMAN, M. F., NYGREN, J., JORFELDT, L., WOJTASZEWSKI, J. F., DUFRESNE, S. D., HORTON, E. S., LJUNGQVIST, O. & GOODYEAR, L. J. 1999. Exercise and insulin cause GLUT-4 translocation in human skeletal muscle. *Am J Physiol,* 277**,** E733-41.

VAN LOON, L. J., GREENHAFF, P. L., CONSTANTIN-TEODOSIU, D., SARIS, W. H. & WAGENMAKERS, A. J. 2001. The effects of increasing exercise intensity on muscle fuel utilisation in humans. *J Physiol,* 536**,** 295-304.

VINCENT, M. A., CLERK, L. H., LINDNER, J. R., PRICE, W. J., JAHN, L. A., LEONG-POI, H. & BARRETT, E. J. 2006. Mixed meal and light exercise each recruit muscle capillaries in healthy humans. *Am J Physiol Endocrinol Metab,* 290**,** E1191-7.

WASSERMAN, D. H., KANG, L., AYALA, J. E., FUEGER, P. T. & LEE-YOUNG, R. S. 2011. The physiological regulation of glucose flux into muscle in vivo. *J Exp Biol,* 214**,** 254-62.

WOJTASZEWSKI, J.F.P., HANSEN, B.F., GADE, J., KIENS, B., MARKUNS, J.F., GOODYEAR, L.J. & RICHTER, E.A. 2000. Insulin signalling and insulin sensitivity after exercise in human skeletal muscle. *Diabetes,* 49, 325-331.

ZISMAN, A., PERONI, O. D., ABEL, E. D., MICHAEL, M. D., MAUVAIS-JARVIS, F., LOWELL, B. B., WOJTASZEWSKI, J. F., HIRSHMAN, M. F., VIRKAMAKI, A., GOODYEAR, L. J., KAHN, C. R. & KAHN, B. B. 2000. Targeted disruption of the glucose transporter 4 selectively in muscle causes insulin resistance and glucose intolerance. *Nat Med,* 6**,** 924-8.

CHAPTER 5

AN 80 MINUTE HYPERINSULINAEMIC-ISOGLYCAEMIC CLAMP DOES NOT INCREASE GLUT4 AND DYSTROPHIN COLOCALISATION IN TIBIALIS ANTERIOR MUSCLE FIBRES OF LEAN AND OBESE ZUCKER RATS

H. Bradley[1], A. Stride[2], C.S. Shaw[1,3], F.R. Macdonald[4], J.M. Marshall[2], S.M. Poucher[4] and A.J.M. Wagenmakers[5]

[1] School of Sport and Exercise Sciences, University of Birmingham, UK

[2] School of Clinical and Experimental Medicine, University of Birmingham, UK

[3] Institute of Sport, Exercise and Active Living (ISEAL), Victoria University, Australia

[4] CVGI Discovery iMED, AstraZeneca Pharmaceuticals, Mereside, Alderley Park, UK

[5] Research Institute of Sport and Exercise Sciences, Liverpool John Moores University, UK

5.1. Abstract

The Obese Zucker rat (OZR) is a genetic model of the metabolic syndrome and previous research has shown that OZR in comparison to Lean Zucker rats (LZR) exhibit a marked reduction in insulin-mediated skeletal muscle glucose uptake during a hyperinsulinaemic-isoglycaemic clamp. The aim of this study was to use immunofluorescence microscopy to assess the translocation of GLUT4 to the plasma membrane (PM) in LZR and OZR in response to a hyperinsulinaemic-isoglycaemic clamp. Insulin was infused at 10 $mIU.min^{-1}.kg^{-1}$ and 20 $mIU.min^{-1}.kg^{-1}$ and glucose clamped at approximately 4 mM and 6mM in LZR and OZR, respectively. Seven rats in each group (LZR basal, LZR stimulated, OZR basal and OZR stimulated) were sacrificed either in the post-absorptive state or 80 min after the start of a hyperinsulinaemic-isoglycaemic clamp. Colocalisation of GLUT4 with the PM marker dystrophin in *tibialis anterior* (TA) muscle was measured using the Pearson's correlation coefficient. GLUT4 and dystrophin colocalisation was not different between LZR and OZR in the post-absorptive state (LZR basal $r = 0.40 \pm 0.02$, OZR basal $r = 0.38 \pm 0.02$) and did not increase in either LZR or OZR following the 80 min hyperinsulinaemic-isoglycaemic clamp (LZR stimulated $r = 0.38 \pm 0.02$, OZR stimulated $r = 0.38 \pm 0.03$). There were no differences in fibre type composition of the TA between LZR and OZR, with approximately 1 % type I fibres, 21 % type IIa fibres and 78 % type IIb fibres. Total intracellular GLUT4 fluorescence intensity was highest in type IIa fibres both in LZR and OZR with no difference between the groups. In conclusion, 80 min of insulin stimulation did not increase the colocalisation of GLUT4 with the PM marker dystrophin in the fast twitch TA muscle of LZR and OZR. This suggests that mechanisms other than GLUT4 translocation to the skeletal muscle PM in the TA muscle are responsible for the gradual increase in whole body glucose disposal rates during the 80 min hyperinsulinaemic-isoglycaemic clamps in both groups. Furthermore

impairments in GLUT4 translocation to the skeletal muscle PM in TA muscle do not seem to explain the insulin resistance in the OZR during the hyperinsulinaemic-isoglycaemic clamp.

5.2. Introduction

Skeletal muscle is the major site of insulin-mediated glucose disposal (Katz et al., 1983) and glucose transporter 4 (GLUT4) is the primary insulin responsive glucose transporter expressed in skeletal muscle (Mueckler, 1994). Chapters 1-4 of this thesis describe in detail the spatial distribution of the intracellular storage depots of GLUT4 and the increases that have been observed in GLUT4 content of the plasma membrane (PM) region in response to insulin stimulation in rodent and human skeletal muscle. In brief, immunofluorescence microscopy studies in rodent soleus, quadriceps and flexor digitorum brevis muscles have shown GLUT4 is present predominantly at the fibre periphery and in perinuclear regions and appears as large and small GLUT4 storage clusters which are likely pretethered at the PM and T-tubule membranes (Ploug et al., 1998, Lauritzen et al., 2006, Lizunov et al., 2012). Following insulin stimulation resulting from insulin injection into a tail vein, GLUT4 redistributed to the PM and T-tubule membranes whereby continuous staining of the PM and T-tubule membranes was observed (Ploug et al., 1998, Lauritzen et al., 2006). Maximal GLUT4 staining of the PM occurred 20 min after insulin stimulation (Lauritzen et al., 2006) and was maintained for 150 min (Lauritzen et al., 2008).

Obesity is associated with insulin resistance of the skeletal muscle. This is characterised by lower rates of insulin-stimulated glucose uptake from the blood into skeletal muscle, which results in hyperglycaemia (Krook et al., 2004). The obese Zucker rat (OZR) has a mutation in the leptin gene and is characterised by hyperphagia, hyperlipidaemia, hyperinsulinaemia, and insulin resistance (Oana et al., 2005, Mathe, 1995). Therefore the OZR is considered a good

model of the metabolic syndrome; a condition which results from accumulation of the pathologies listed above (Frisbee and Delp, 2006). A previous study has measured hind-limb (which primarily reflects skeletal muscle) glucose uptake at the end of a 2 h hyperinsulinaemic-isoglycaemic clamp in the lean Zucker rat (LZR) and OZR and observed a marked reduction in hind-limb glucose uptake in the OZR in comparison to the LZR (Wallis et al., 2002).

The reduction in insulin-stimulated glucose uptake in skeletal muscle of OZR in comparison to LZR has been suggested to be a consequence of reductions in protein content and activation of insulin signalling cascade proteins in all skeletal muscle fibre types (Ivy, 2004, Sherman et al., 1988). There were no differences in the total protein content of GLUT4 between OZR and LZR in red quadriceps or gastrocnemius muscle, though GLUT4 total protein content was lower in white quadriceps muscle in OZR compared to LZR (Banks et al., 1992, Friedman et al., 1990). To further explore the reduction in skeletal muscle glucose uptake in the OZR upon insulin stimulation, the GLUT4 content of the isolated PM fraction has been measured in LZR and OZR. King *et al.* (1992) observed a 40 % increase in GLUT4 content of the PM fractions of the *soleus* and *gastrocnemius* muscle 30 min following intraperitoneal insulin injection in LZR, but there was no significant increase in the OZR (King et al., 1992). In contrast, Galante *et al.* (1994) observed a 1.9-fold increase in GLUT4 content of the PM fraction of hind-limb muscles in both LZR and OZR 20 min following intraperitoneal insulin injection with no difference between groups (Galante et al., 1994). However in this study the insulin dose was increased in the OZR to achieve a decline in blood glucose comparable to that seen in the LZR, therefore implying more insulin was required in OZR compared to LZR to achieve the same increase in GLUT4 content of the PM fraction.

As the use of isolated PM fractions to measure PM GLUT4 content has been criticised due to potential contamination with intracellular membranes (Schertzer et al., 2009, Fazakerley et al., 2009), we here used the immunofluorescence microscopy method developed in chapter 2 of this thesis to investigate insulin-mediated GLUT4 translocation in LZR and OZR.

This study, therefore, aimed to visualise the localisation of GLUT4 in *tibialis anterior* (TA) muscle fibres of LZR and OZR in the post-absorptive state and at the end of an 80 min hyperinsulinaemic-isoglycaemic clamp. GLUT4 translocation to the PM was assessed using the Pearson's correlation coefficient to measure the colocalisation of GLUT4 and the PM marker dystrophin (as described in chapter 2 of this thesis). This was a collaborative study between the School of Sport and Exercise Sciences, the Medical School and AstraZeneca with multiple aims to investigate both the vascular and skeletal muscle responses to insulin stimulation. The hypotheses investigated in this chapter of the thesis were that: 1) the colocalisation of GLUT4 with dystrophin in TA muscle fibres will be increased at the end of the hyperinsulinaemic-isoglycaemic clamp in the LZR in comparison to the post-absorptive state; and 2) this increase will be absent or blunted in the OZR in comparison to the LZR.

5.3. Methods

Animals. All *in vivo* rat experiments were carried out at AstraZeneca in Alderley Park (Cheshire, UK). All procedures conformed to the Animal (Scientific Procedures) Act 1986 (UK). Lean (Fa/Fa or Fa/fa) and obese (fa/fa) male, 20 week old Zucker rats (Charles River Laboratories, France) were fed standard rat chow and water ad libitum and were housed on a 12 hr light-dark cycle .

Hyperinsulinaemic-isoglycaemic clamp protocol. LZR and OZR were randomly divided into two groups; either fasted or insulin stimulated (N = 7 per group). On the day prior to the experiment rats received a controlled portion of rat chow (16g obese, 10g lean) at 16:00 hours with the aim to provide sufficient food until midnight and obtain the post-absorptive state, rather than starved, for the clamp protocol. LZR and OZR in the insulin-stimulated group underwent a hyperinsulinaemic-isoglycaemic clamp as follows. Rats were anaesthetised at 9 am (160-190 $mg.kg^{-1}$ Inactin, intraperitoneal) and catheters were placed in the right jugular vein for insulin and glucose infusion and the left carotid artery for blood sampling. A 60 min recovery period was then allowed following surgical procedures and the hyperinsulinaemic-isoglycaemic clamp was subsequently initiated and terminated at 80 min. LZR received 10 $mIU.min^{-1}.kg^{-1}$ insulin, while OZR received 20 $mIU.min^{-1}.kg^{-1}$insulin. Different infusion rates were chosen to reflect the increases in plasma insulin normally seen in LZR and OZR. Similarly blood glucose concentration was maintained at 4 mM in the LZR and 6 mM in the OZR to reflect physiological conditions. Blood glucose concentrations were measured with an automated glucose analyser (AccuChek Aviva Glucose Meter, Roche Diagnostics GmbH, Mannheim, Germany) and appropriate adjustments in glucose infusion rates were made. Immediately following the clamp animals were sacrificed by intraperitoneal overdose of Inactin and cervical dislocation and the *TA* muscle was then immediately dissected free and embedded in Tissue Tek OCT (Sakura Finetek, The Netherlands) before freezing in liquid nitrogen-cooled isopentane (Sigma Aldrich, UK) for storage at -80^{o}C. LZR and OZR in the fasted state were sacrificed in the same way without any prior experimentation.

Glucose infusion rate (GIR, µmol.kg lean body $mass^{-1}.min^{-1}$) was calculated and was assumed to equal the rate of disappearance of glucose from the blood into skeletal muscle and other tissues. The assumption was made because blood glucose concentration was maintained at a

constant level. During the 60-80 min steady state period insulin sensitivity was calculated using GIR (µmol.kg lean body mass^{-1}.min^{-1}) divided by plasma insulin (pmol.L^{-1}) values at each time point (Muniyappa et al., 2008). Lean body mass was calculated from formulae developed in-house at AstraZeneca (Cardiovascular and Gastrointestinal Group, AstraZeneca, Alderley Park); LZR lbm (g) = 31 + (0.77 x body mass (g)), OZR lbm (g) = 59 + (0.5 x body mass (g)).

Immunofluorescence staining protocol. The GLUT4 immunofluorescence staining protocol is described in detail in chapter 2. All analysis was completed in triplicate. Seven sets of slides were prepared with each set comprising a LZR basal and insulin stimulated and OZR basal and insulin stimulated section on each slide. For analysis of GLUT4 and dystrophin colocalisation, dystrophin primary antibody was included in the primary antibody incubation step of the protocol described in chapter 2 at a 1:400 dilution (Sigma Aldrich, UK). For fibre type analysis, MHCI primary antibody at 1:100 dilution (developed by Dr. Blau, DSHB, USA) or MHCIIa primary antibody at 1:100 dilution if targeted with AlexaFluor488-conjugated secondary antibody or 1:200 dilution if targeted with AlexaFluor594-conjugated secondary antibody (developed by Dr. Blau, N2.261, DSHB, University of Iowa) were added to the primary antibody incubation. Dystrophin was targeted with AlexaFluor594-conjugated goat anti-mouse IgG_{2b} (Invitrogen, UK), MHCI with either AlexaFluor488- or AlexaFluor594-conjugated goat anti-mouse IgM (Invitrogen, UK) and MHCIIa with AlexaFluor488- or AlexaFluor594-conjugated goat anti-mouse IgG_1 (Invitrogen, UK). For staining of the muscle fibre border during fibre type analysis, sections were incubated in AlexaFluor350-conjugated wheat germ agglutinin (WGA, Invitrogen, WGA) after secondary antibody incubation for 15 min at a 1:50 dilution in PBS and finally were washed for 2 min in PBS and subsequently mounted. Negative control staining was also completed. GLUT4

primary antibody was omitted from the fibre type staining to confirm MHCIIa signal did not bleed through into the channel in which GLUT4 was imaged. In separate staining MHCIIa antibody was also omitted from GLUT4 staining to confirm that some fibres retain stronger fluorescence intensity even when MHCIIa antibody is absent. These images are shown in Fig. 5.1. and confirmed that MHCIIa signal did not bleed through into the channel in which GLUT4 was imaged, therefore showing that GLUT4 quantitation is unaffected by MHCIIa co-staining.

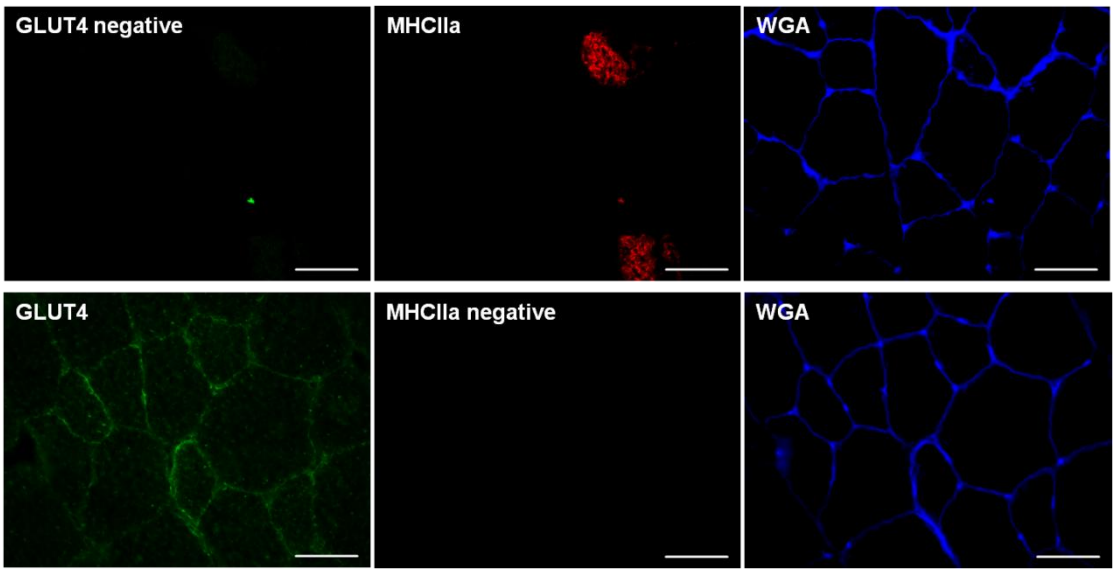

Fig. 5.1. *Representative widefield immunofluorescence microscopy images of negative control staining for fibre type analysis of rat TA muscle. In the top row of images GLUT4 primary antibody was omitted. In the bottom row of images MHCIIa antibody was omitted. GLUT4 was stained in green, MHCIIa in red and WGA was used to mark cell borders in blue. These images demonstrate that GLUT4 quantitation is unaffected by MHC co-staining. Scale bars = 50 µm.*

Immunofluorescence image capture, processing and analysis. Further details of image capture, processing and analysis are provided in chapter 2. GLUT4 and dystrophin images for colocalisation analysis were captured using an inverted confocal microscope (Leica DMIRE2, Leica Microsystems) with a 63x oil immersion objective (1.4 NA). For each animal 5 images were captured per muscle section, with sections analysed in triplicate for each condition. GLUT4 and dystrophin images for colocalisation analysis had a no neighbour deconvolution algorithm inbuilt into Image-Pro Plus 5.1 applied to them. The colocalisation tool in Image-Pro Plus 5.1 was then used to calculate the Pearson's correlation coefficient of each image pair. Images for fibre type composition analysis and fibre-type specific GLUT4 fluorescence intensity analysis were captured using a Nikon E600 microscope coupled to a SPOT RT KE colour three shot CCD camera (Diagnostic Instruments Inc., MI, USA). To ensure fibre type composition was consistent across all sections analysed images were captured of MHCI (594) for type I fibres, MHCIIa (488) for type IIa fibres and WGA (350) to mark the cell borders across a single section for each animal using a 20x objective (0.4 NA). Unstained fibres were considered type IIb. The number of type I, type IIa and type IIb muscle fibres in each image were counted and the sum for each section calculated. The mean number of fibres counted per section was as follows; total fibres 488 ± 58, type I fibres 5 ± 1, type IIa fibres 121 ± 23 and type IIb fibres 362 ± 38. The percentage composition of type I, type IIa and type IIb fibres of each section was then calculated. For analysis of fibre type specific GLUT4 fluorescence intensity serial sections were imaged from 7 lean basal and 7 obese basal animals. On one section images were captured of MHCI (594), MHCIIa (488) and WGA (350) using the 20x objective, then corresponding fibres were found on the serial section stained for GLUT4 (488), MHCIIa (594) and WGA (350) and images were captured using both the 20x and 40x (0.75 NA) objectives. Analysis of GLUT4 fluorescence intensity was completed using the

GLUT4 images captured with the 40x objective in 250 ± 37 fibres (type I; 4 ± 2, type IIa; 51 ± 16, type IIb; 195 ± 26) per lean animal section and 278 ± 46 fibres (type I; 2 ± 1 , type IIa 66 ± 20, type IIb 210 ± 36) per obese animal section. No processing was carried out on the GLUT4 images. The appropriate WGA image was used to create an outline of fibres; firstly a flatten background filter was applied and fibres were identified using consistent intensity and size thresholds. The WGA fibre outline was applied to the raw GLUT4 image to measure GLUT4 fluorescence intensity in a fibre type specific manner, with fibre type determined using the 20x serial sections stained for MHCI and MHCIIa.

Statistical analysis. All statistical analysis was performed using SPSS version 19 (Chicago, IL). Significant differences in animal characteristics between LZR and OZR were detected using independent T tests. Statistical analysis of Pearson's correlation coefficient data to measure GLUT4 translocation was completed using a repeated measures ANOVA with obesity and stimulation state as independent factors. Equivalent fibre type compositions of sections across the groups were confirmed using a repeated measures ANOVA with group and fibre type as independent factors. Significant main effects were investigated using Bonferroni pair-wise comparisons within the significant factor. Differences in GLUT4 fluorescence intensity between LZR and OZR and between fibre types were analysed using a repeated measures ANOVA with obesity and fibre type as independent factors. Where significant main effects were detected Least Significant Difference (LSD) pair-wise comparisons were performed within the significant factor. GLUT4 fluorescence intensity data of one animal was more than 2 standard deviations away from the mean and were therefore excluded as an outlier. Significance was set at $P \leq 0.05$. Data is presented as mean ± SEM.

5.4. Results

Animal characteristics. Seven rats were studied in each group (LZR and OZR) both in the fasted state and at the end of an 80 min hyperinsulinaemic-isoglycaemic clamp (insulin-stimulated). Characteristics of LZR and OZR are shown in Table 5.1. Body mass (LZR 300 ± 7 g, OZR 422 ± 21 g, $P = 0.001$) and basal blood glucose (LZR 4.1 ± 0.1 mM, OZR 6.1 ± 0.3 mM, $P = 0.001$) were significantly higher in the OZR, while insulin sensitivity in the final 20 min of the clamp was significantly higher in the LZR (LZR 0.048 ± 0.004 µmol.kg $lbm^{-1}.min^{-1}/pmol.L^{-1}$, OZR 0.009 ± 0.002 µmol.kg $lbm^{-1}.min^{-1}/pmol.L^{-1}$, $P < 0.001$).

Table 5.1 Animal characteristics

	LZR	OZR
	N = 7	N = 7
Body mass (g)	300 ± 7	422 ± 21 *
Basal blood glucose (mM)	4.1 ± 0.1	6.1 ± 0.3 *
Insulin sensitivity at 60-80 min steady state (µmol.kg lean body $mass^{-1}.min^{-1}/pmol.L^{-1}$)	0.048 ± 0.004	0.009 ± 0.002 *

Data shown are mean ± SEM for animals that underwent a hyperinsulinaemic-isoglycaemic clamp. Independent samples T test * $P < 0.01$.

Blood glucose, plasma insulin and glucose infusion rate (GIR). Blood glucose concentration was clamped at the blood glucose concentration in the post-absorptive state; approximately 4 mM in the LZR and 6 mM in the OZR (Fig 5.2). Plasma insulin concentration data (Fig. 5.3) were obtained at three time-points (basal, 40 min, 80 min). Plasma insulin concentration was significantly higher in OZR compared to LZR at all time points ($P < 0.05$) and plasma insulin concentration was significantly increased above basal levels in both LZR and OZR ($P < 0.05$). GIR during the hyperinsulinaemic-isoglycaemic clamp is shown in Fig. 5.4. There was

no significant difference between the mean GIR for LZR and OZR during the steady state 60-80 min time period (LZR 15.3 ± 0.6 µmol.kg lbm^{-1}.min^{-1}, OZR 13.1 ± 1.6 µmol.kg lbm^{-1}.min^{-1}, P = 0.257).

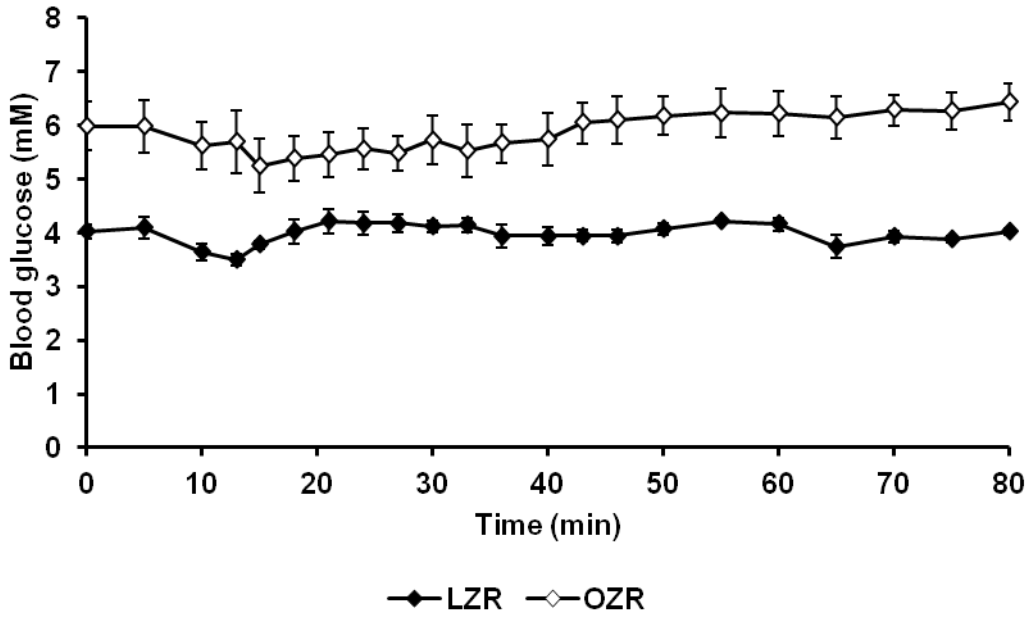

Fig. 5.2. *Blood glucose concentration during 80 min hyperinsulinaemic-isoglycaemic clamp in LZR (filled diamonds) and OZR (open diamonds). Graph shows mean ± SEM. This data has been obtained from the thesis of Ann Stride (University of Birmingham, 2012, Fig. 4.5).*

A

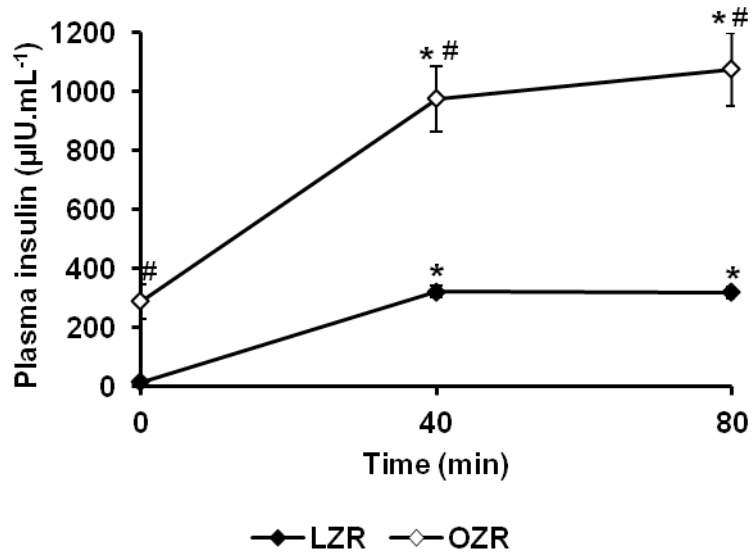

B

	Plasma insulin (µlU.mL^{-1})		
	Basal	40 min	80 min
LZR	15.4 ± 1.7	321.5 ± 19.2	321.1 ± 19.2
OZR	288.1 ± 58.8	974.8 ± 111.5	1075.9 ± 122.3

Fig. 5.3. *Plasma insulin concentration during 80 min hyperinsulinaemic-isoglycaemic clamp in LZR (filled diamonds) and OZR (open diamonds) (A). Plasma insulin values (mean ± SEM) are also provided in Table in B to improve clarity of graph axis in A. Insulin infusion was at 10 mU.min^{-1}.kg^{-1} in LZR and 20 mU.min^{-1}.kg^{-1} in OZR. * P < 0.05 compared to basal. $^{\#}$ P < 0.05 OZR compared to LZR. Graph shows mean ± SEM. This data has been obtained from the thesis of Ann Stride (University of Birmingham, 2012, Fig. 4.8).*

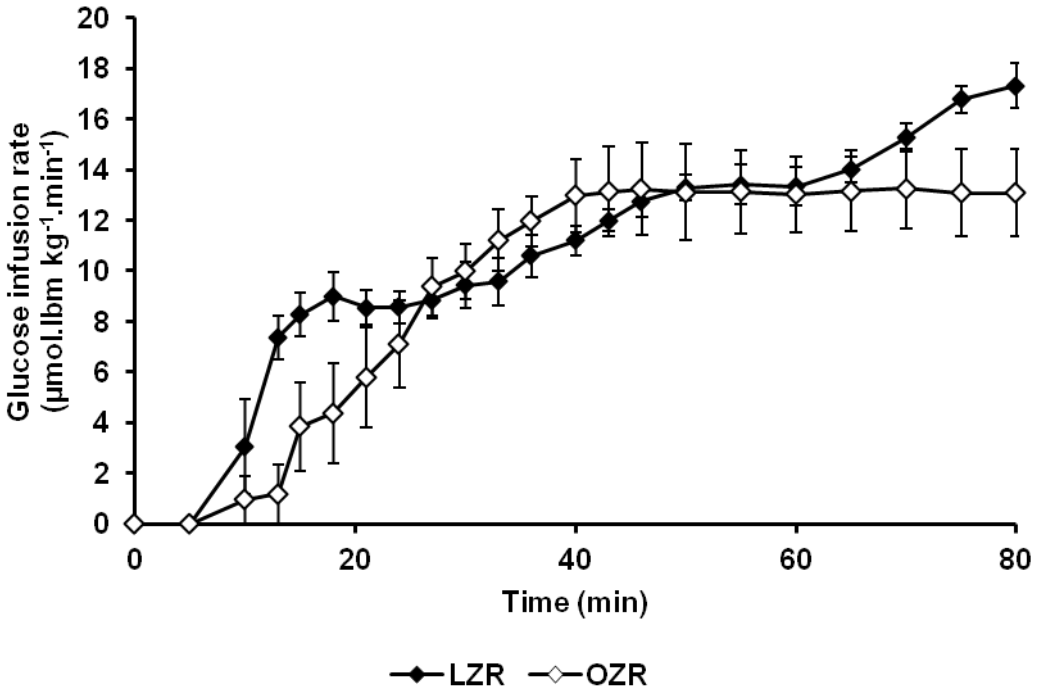

Fig. 5.4. *Glucose infusion rate during 80 min hyperinsulinaemic-isoglycaemic clamp in LZR (filled diamonds) and OZR (open diamonds). Insulin infusion is at 10 mU.min^{-1}.kg^{-1} in LZR and 20 mU.min^{-1}.kg^{-1} in OZR. Graph shows mean ± SEM. This data has been obtained from the thesis of Ann Stride (University of Birmingham, 2012, Fig. 4.6).*

GLUT4 localisation in TA muscle from LZR and OZR. Intracellular GLUT4 staining of LZR and OZR TA muscle fibres appears as large and small clusters, the latter of which appear as a diffuse background stain under lower magnification (Fig. 5.5). Strong staining is present at the fibre periphery in both the basal and insulin stimulated rats. A striking feature of the images is brighter staining in some fibres compared to others.

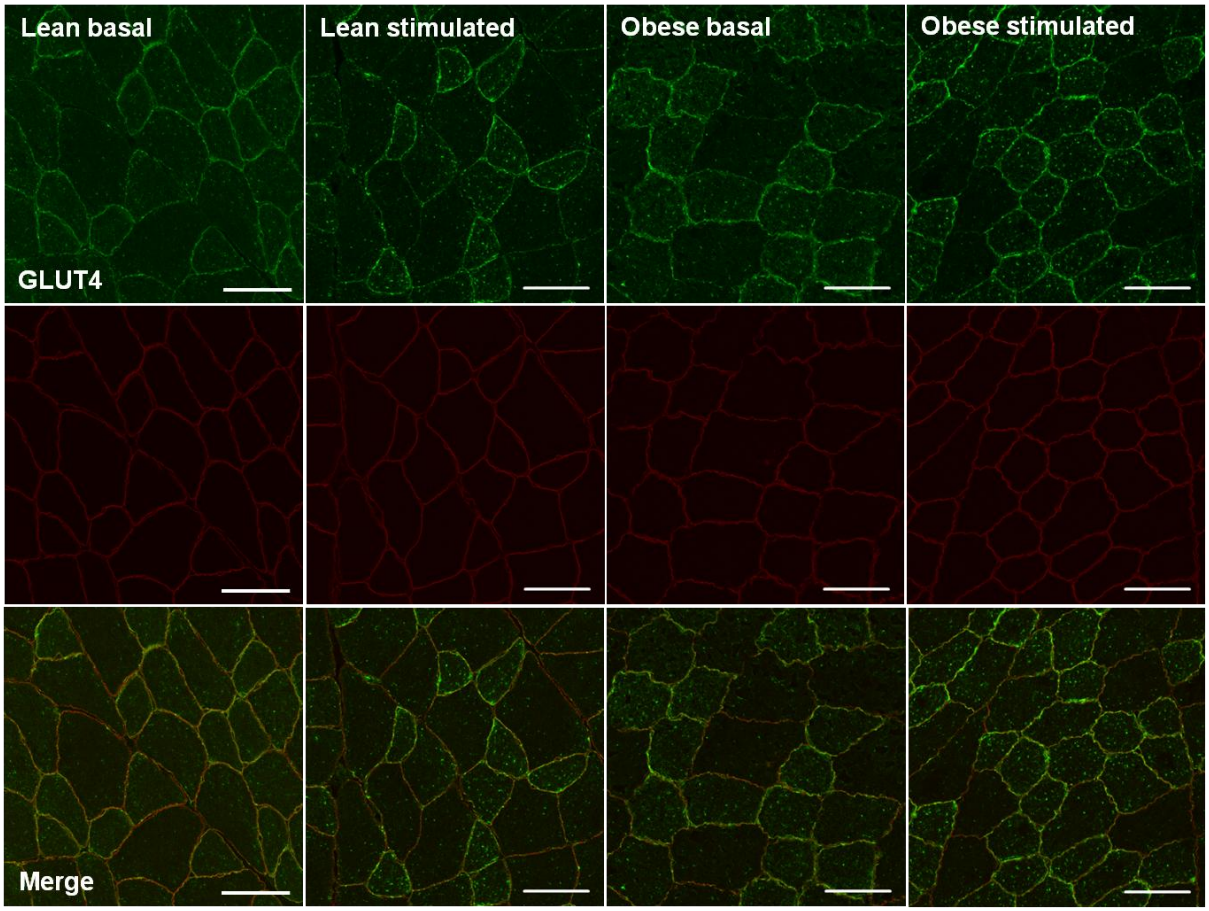

Fig. 5.5. *Representative confocal immunofluorescence microscopy images of GLUT4 (green) and dystrophin (red), a PM marker, in TA muscle from LZR and OZR sampled in the basal state and at the end of an 80 min hyperinsulinaemic-isoglycaemic clamp. Scale bars 50 µm.*

GLUT4 and dystrophin colocalisation. Fig. 5.5. shows immunofluorescence images of GLUT4 in green and dystrophin in red stained in TA muscle of LZR and OZR sampled in the basal state and at the end of an 80 min hyperinsulinaemic-isoglycaemic clamp. Merged images display colocalisation of GLUT4 and dystrophin. There was no difference in Pearson's correlation coefficient, therefore no difference in GLUT4 and dystrophin colocalisation, between the TA of LZR and OZR in the fasted state (LZR r = 0.40 ± 0.02, OZR r = 0.38 ± 0.02) (Fig. 5.6). Furthermore there was no increase in Pearson's correlation

coefficient following insulin stimulation in either LZR or OZR, indicating there was no increase in GLUT4 and dystrophin colocalisation (LZR post r = 0.38 ± 0.02, OZR post r = 0.38 ± 0.03) (Fig. 5.6).

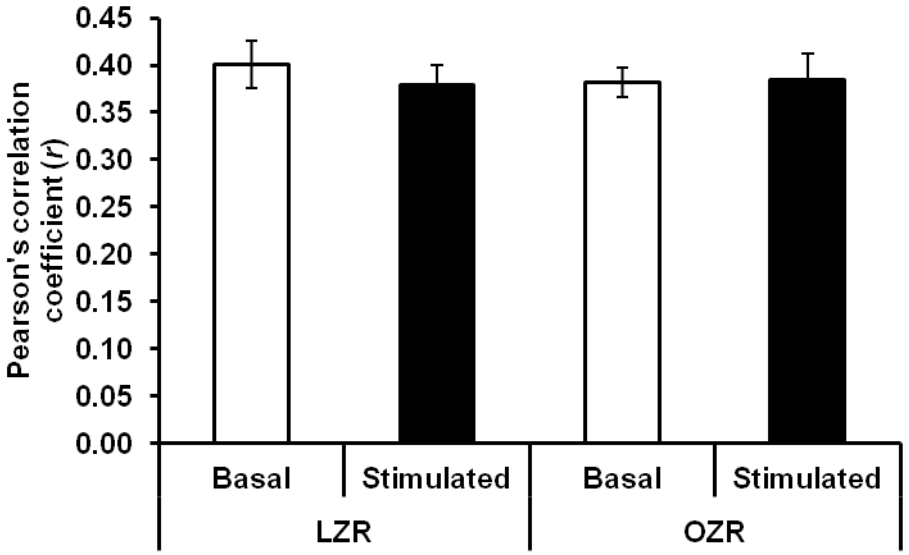

Fig. 5.6. *Pearson's correlation coefficient values representing GLUT4 and dystrophin colocalisation in TA muscle of LZR and OZR sampled in the basal state and following an 80 min hyperinsulinaemic-isoglycaemic clamp. Graph shows mean ± SEM. Repeated measures ANOVA group effect P = 0.763, stimulation effect P = 0.732, interaction effect P = 0.539.*

Fibre type composition of TA sections. Staining of MHCI for type I fibres, MHCIIa for type IIa fibres and WGA to mark the cell borders (Fig. 5.7) across a single section for each animal confirmed that there were no significant differences in the percentage composition of type I, type IIa and type IIb fibres between the four groups of animals (repeated measures ANOVA group effect, P = 0.315). For all four groups of animals type I fibres composed approximately

1 % of the total fibres, type IIa approximately 21 % and type IIb approximately 78 % (Fig. 5.8).

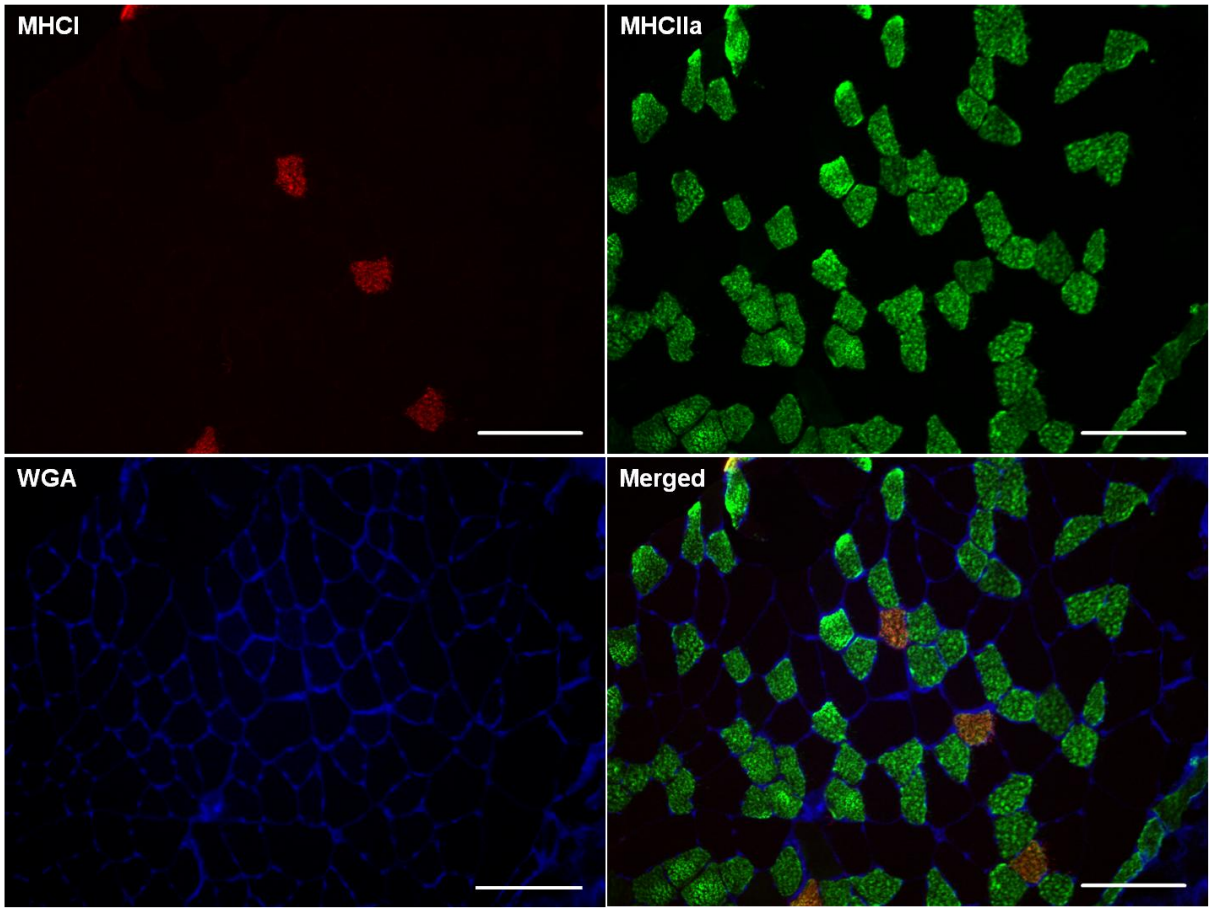

Fig. 5.7. *Representative widefield immunofluorescence images showing fibre type composition of TA muscle of LZR. Type I muscle fibres are stained in red for MHCI, type II muscle fibres are stained in green for MHCIIa, while WGA, shown in blue, marks the cell borders. Scale bars 100 µm.*

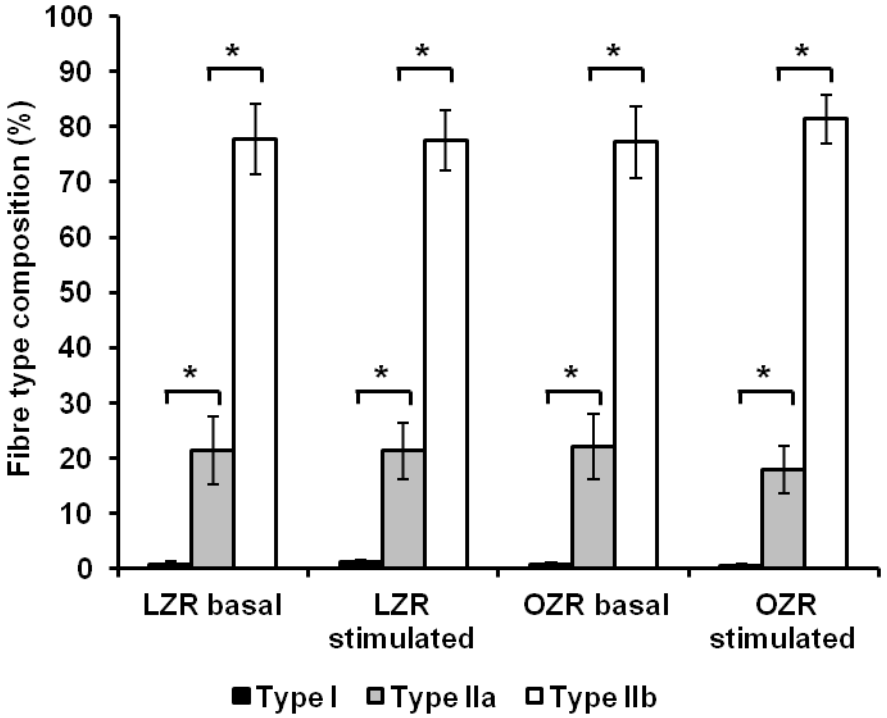

Fig. 5.8. *Fibre type composition of TA muscle sections analysed for GLUT4 and dystrophin colocalisation from LZR and OZR sampled in the basal state and following an 80 min hyperinsulinaemic-isoglycaemic clamp. Graph shows mean ± SEM. Repeated measures ANOVA fibre type effect P < 0.001, group effect P = 0.315, interaction effect P = 0.996.* Post hoc Bonferroni pairwise comparisons * P < 0.001.

Fibre type specific GLUT4 expression. To investigate GLUT4 content in different fibre types, total intracellular GLUT4 fluorescence intensity was analysed in a fibre type specific manner in TA muscle of LZR and OZR in the basal state. Total GLUT4 fluorescence intensity was measured within each fibre with the border delineated using the WGA stain (Fig. 5.9). Total intracellular GLUT4 fluorescence intensity was highest in type IIa fibres (LZR 20 ± 3, OZR 23 ± 1), intermediate in type I fibres (LZR 17 ± 1, OZR 20 ± 1) and lowest in type IIb fibres (LZR 14 ± 1, OZR 17 ± 1) (Fig. 5.10). The difference in total GLUT4 content between fibre

type was significant (P = 0.013) with no difference in total GLUT4 content between lean and obese Zucker rats (P = 0.668).

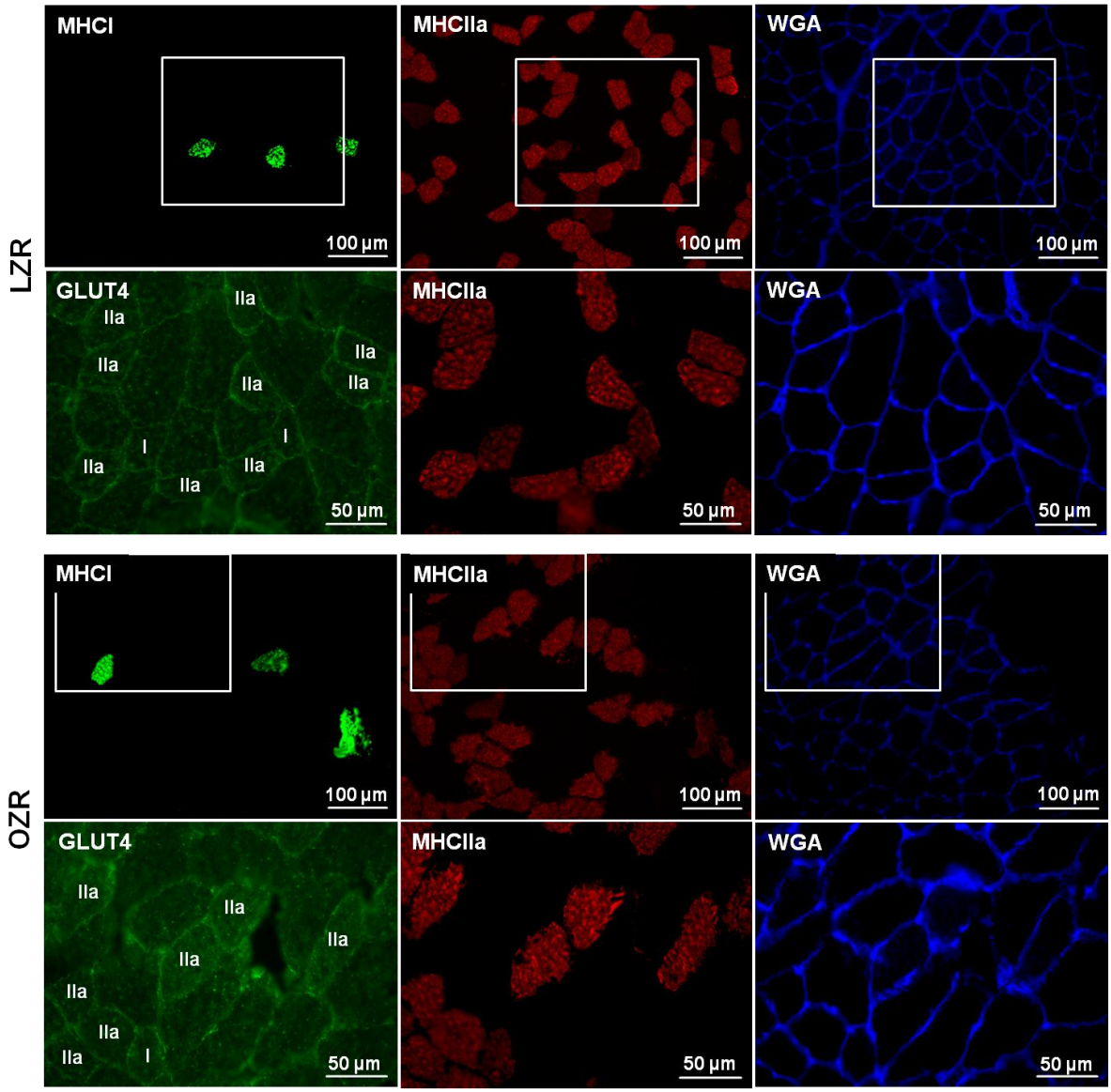

Fig. 5.9. *Representative widefield immunofluorescence microscopy images demonstrating analysis of GLUT4 fluorescence intensity in a fibre type specific manner in TA muscle of LZR and OZR in the basal state. Serial sections were stained for either MHCI in green, MHCIIa in red and WGA in blue or GLUT4 in green, MHCIIa in red and WGA in blue. Lower magnification images taken with 20x objective (100 µm scale bars) show section stained for fibre type, while higher magnification images taken with 40x objective (50 µm scale bar) show equivalent fibres in section stained for GLUT4 from which fluorescence intensity quantitation was carried out using WGA stain to mark cell borders.*

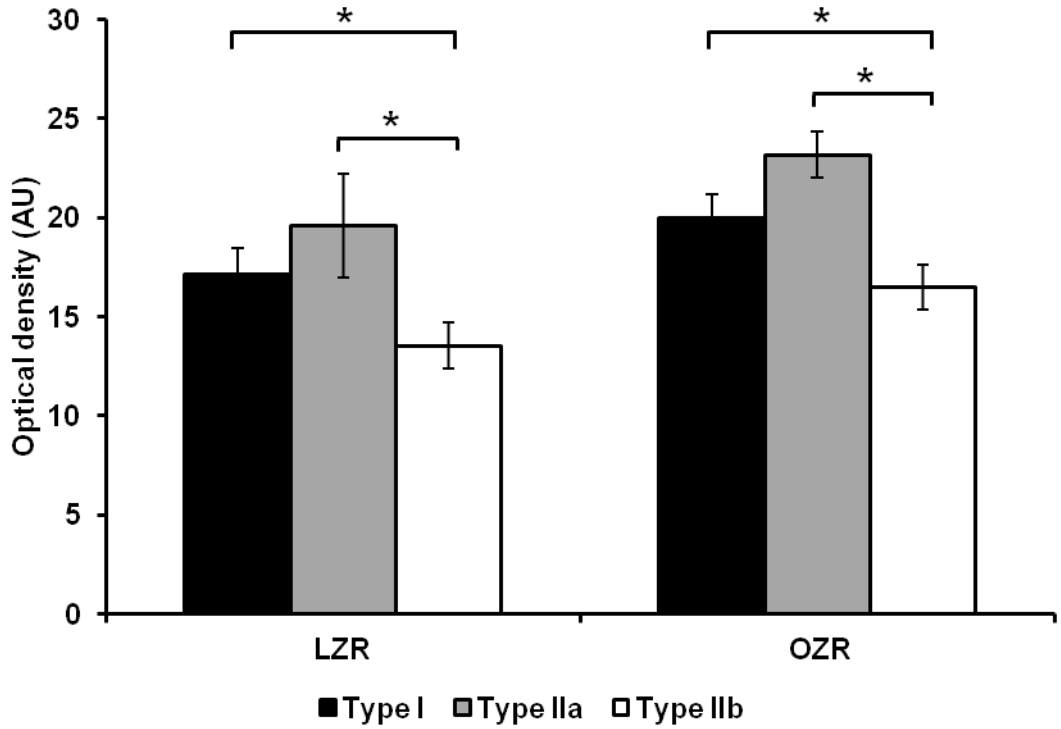

Fig. 5.10. *GLUT4 fluorescence intensity in type I, type IIa and type IIb fibres of the TA in LZR and OZR in the basal state. Graph shows mean ± SEM. Repeated measures ANOVA fibre type effect P = 0.013, group effect P = 0.668, interaction effect P = 0.423.* Least Significant Difference (LSD) pair-wise comparisons were performed to investigate the effect of fibre type, * $P < 0.05$.

5.5. Discussion

The immunofluorescence techniques developed and tested in human skeletal muscle in chapter 2-4 of this thesis have been used in this study to investigate the colocalisation of GLUT4 with the PM marker dystrophin in the fast twitch TA muscle fibres of LZR and OZR in the basal state and at the end of an 80 min hyperinsulinaemic-isoglycaemic clamp. In contrast to the a priori hypothesis and despite substantially elevated rates of whole body glucose disposal during the clamp there was no increase in colocalisation of GLUT4 with the

PM marker dystrophin 80 min after the onset of a hyperinsulinaemic-isoglycaemic clamp in TA muscle fibres of the LZR. Furthermore, there were no differences in GLUT4 and dystrophin colocalisation in TA muscle fibres between LZR and OZR either in the fasted state or at the end of the hyperinsulinaemic-isoglycaemic clamp.

Glucose infusion rate (GIR) and insulin sensitivity. GIR during the clamp was recorded for LZR and OZR and the data is presented in Fig. 5.4. There was no significant difference in mean GIR between LZR and OZR during the 60-80 min steady state time period. Also, area under the GIR curve over the 80 min clamp period was not different between LZR and OZR (LZR 837 ± 45 µmol.lbm kg^{-1}, OZR 752 ± 91 µmol.lbm kg^{-1}, P = 0.458). It is important to note that similar increases in GIR were obtained by using different insulin infusion rates in the 2 groups (10 $mIU.min^{-1}.kg^{-1}$ for LZR and 20 $mIU.min^{-1}.kg^{-1}$ for OZR). The difference in infusion rate was chosen to achieve the same proportional increases in plasma insulin levels in a range that is normally seen in the LZR and OZR. Also for this reason blood glucose concentration was maintained at 4 mM in the LZR and at 6 mM in the OZR. This implies that the same GIR was achieved in the LZR and OZR with markedly higher blood glucose and insulin concentrations at the end of the hyperinsulinaemic-isoglycaemic clamp in OZR which explains why the insulin sensitivity over the 60-80 min time period was approximately 5-fold higher in the LZR compared to the OZR (LZR 0.048 ± 0.004 $\mu mol.kg^{-1}.min^{-1}/pmol.L^{-1}$, OZR 0.009 ± 0.002 $\mu mol.kg^{-1}.min^{-}1/pmol.L^{-1}$).

GLUT4 translocation in LZR. The observation that GLUT4 and dystrophin colocalisation in TA muscle fibres did not change at the end of 80 min hyperinsulinaemic-isoglycaemic clamp in LZR was in contrast to the a priori hypothesis. The expectation was that in the LZR GLUT4 translocation would remain high for at least the 80 min of the hyperinsulinaemic-isoglycaemic clamp and this expectation was based on the following previously published

observations. Previous work has shown that insulin stimulation via intraperitoneal injection (King et al., 1992, Galante et al., 1994) increases GLUT4 content of skeletal muscle isolated PM fractions between 1.5- and 1.9-fold above basal levels in LZR 20-30 min after insulin injection. However as indicated in the introduction the measurement of the GLUT4 content in isolated PM fractions has been criticised. Lauritzen *et al.* (2006) used immunofluorescence microscopy to visualise *in vivo* GLUT4-GFP and observed that GLUT4 accumulated close to the mouse muscle fibre border 10 min after injection of insulin into a tail vein and suggested that this reflected GLUT4 translocation without investigating colocalisation with a PM marker (Lauritzen et al., 2006). Maximum values were reached after 20 min (Lauritzen et al., 2006) and the accumulation of GLUT4 clusters in the PM region remained elevated for 150 min (Lauritzen et al., 2008). It should, however, be noted that the amount of insulin injected was very high in the latter study and that the plasma insulin concentrations reached were equally high. Peak plasma insulin concentrations in LZR during hyperinsulinaemic-isoglycaemic clamp in the current study (presented in the PhD thesis of Ann Stride, University of Birmingham, 2012 and in Fig. 5.3 of this chapter) were approximately 320 $\mu IU.mL^{-1}$, in comparison to 200 000 $\mu IU.mL^{-1}$ in the study by Lauritzen *et al.* (Lauritzen et al., 2008).

Wallis *et al.* (2002) have previously measured hind-limb (which primarily reflects skeletal muscle) glucose uptake at the end of a 2 h hyperinsulinaemic-isoglycaemic clamp using a high infusion rate of insulin (20 $mIU.min^{-1}.kg^{-1}$) in LZR and OZR. This led to a 3-fold higher increase in whole body GIR in the LZR than the OZR. Furthermore the increase in hind-limb glucose uptake rate in the LZR was 5-fold greater than the fasted state, while this increase in the OZR was only 30% greater than in the fasted state (Wallis et al., 2002). On the basis of these findings it comes as a surprise that increases in colocalisation of GLUT4 and dystrophin

in skeletal muscle were not observed at the end of the 80 min hyperinsulinaemic-isoglycaemic clamp in the LZR in the current study.

A possible explanation is that GLUT4 translocation occurred at an earlier time point than 80 min after the start of the hyperinsulinaemic-isoglycaemic clamp in LZR. Chapter 4 of this thesis showed modest but significant increases in GLUT4 and dystrophin colocalisation in human skeletal muscle at 30 min after oral glucose ingestion and not after 60 and 90 min in response to physiological rises in plasma insulin. Therefore, it is possible that GLUT4 translocation is an early and transient event in LZR, which had returned to basal levels at 80 min. Unfortunately, due to the study design (collaborative study with AstraZeneca and the Medical School, UoB) it was not possible to collect muscle samples from earlier time points in the current study.

In addition it must be noted that the current study examined GLUT4 translocation in TA muscle, which is a fast twitch muscle composed primarily of type IIb fibres (Fig. 5.8). Therefore it remains possible that in soleus or quadriceps muscle with a much higher proportion of oxidative muscle fibres (Sherman et al., 1988) GLUT4 translocation may have been detected at the end of the 80 min hyperinsulinaemic-isoglycaemic clamp, therefore accounting for the increased hindlimb glucose uptake observed previously (Wallis et al., 2002). TA was the only muscle available for use in the current study due to damage incurred in other muscles during the freezing process.

GLUT4 translocation in OZR. Hind-limb glucose uptake has been shown to increase 5-fold in LZR during a 2 h hyperinsulinaemic-isoglycaemic clamp, while in contrast increases in hind-limb glucose uptake in OZR were only 30% ($P < 0.05$ in comparison to LZR) (Wallis et al., 2002). On the basis of these glucose uptake rates the a priori hypothesis was that the GLUT4

translocation to the PM TA muscle fibres in the OZR would be blunted. Our data are in line with the a priori hypothesis as no increase was seen in the colocalisation of GLUT4 with dystrophin at the end of an 80 min hyperinsulinaemic-isoglycaemic clamp in OZR. Previous studies measuring the GLUT4 content of isolated PM fractions also have come to the conclusion that no increase in GLUT4 content was seen following intraperitoneal insulin injections in OZR (King et al., 1992). Furthermore, the colocalisation of GLUT4 with dystrophin in the fasted state in the current study was the same for LZR and OZR. This is consistent with previous studies that have shown equivalent fasted state GLUT4 content of PM fractions isolated from skeletal muscles of LZR and OZR (King et al., 1992, Etgen et al., 1996).

Other factors apart from PM GLUT4, which may influence insulin-mediated increases in glucose disposal in LZR and OZR at end of 80 min hyperinsulinaemic-isoglycaemic clamp. Glucose disposal in LZR and OZR was elevated throughout the 80 min clamp as shown in the glucose infusion rate graph in Fig. 5.4. Wallis *et al.* (2002) observed 5-fold increases in insulin-mediated hind-limb glucose uptake during 2 h hyperinsulinaemic-isoglycaemic clamp in LZR (Wallis et al., 2002), therefore suggesting that insulin-mediated increases in glucose disposal in LZR in the current study likely reflect skeletal muscle glucose uptake. This leads to the conclusion that other mechanisms apart from GLUT4 translocation to the PM in TA muscle fibres are responsible for insulin-mediated increases in skeletal muscle glucose uptake in LZR. Insulin-mediated terminal arteriole vasodilation allows recruitment of previously underperfused skeletal muscle capillaries. This will increase insulin and glucose delivery to the skeletal muscle (Clark, 2008). Insulin-mediated skeletal muscle microvascular vasodilation begins 5-10 min into a hyperinsulinaemic-euglycaemic clamp in rats and is maintained for 120 min (Steinberg et al., 1994, Vincent and Barrett, 2002, Vincent et al.,

2004). Furthermore Gudbjornsdottir *et al.* (2003) have provided evidence that increases in capillary permeability surface area (PSA) product resulting from microvascular recruitment contribute to the increases in glucose uptake that occur 90-120 min after the start of an OGTT or a hyperinsulinaemic-euglycaemic clamp with physiological insulin levels (Gudbjornsdottir et al., 2003). Other mechanisms receiving attention that could explain increases in glucose uptake at later time points without increased GLUT4 at the PM is the intrinsic activation of GLUT4 already present in the PM (Furtado et al., 2002) and increased hexokinase (HKII) activity and glycogen synthesis, therefore leading to increased glucose phosphorylation and a steeper glucose concentration gradient between the muscle interstitium and fibre interior (Wasserman et al., 2011).

Although glucose disposal in OZR was elevated throughout the 80 min clamp in the current study (Fig. 5.2), Wallis *et al.* (2002) observed that insulin-mediated increases in hind-limb glucose uptake during 2 h hyperinsulinaemic-isoglycaemic clamp were negligible in OZR (Wallis et al., 2002), therefore suggesting that the majority of glucose disposal in OZR in the current study occurred into tissues other than skeletal muscle. GLUT4 and dystrophin colocalisation was not different between LZR and OZR after an 80 min hyperinsulinaemic-isoglycaemic clamp. Therefore the current study suggests the reduction in skeletal muscle glucose uptake observed by Wallis *et al.* (2002) was due to mechanisms that did not involve impairments in GLUT4 translocation to the PM in TA muscle fibres. Impaired insulin-mediated increases in skeletal muscle microvascular volume which occur early in a hyperinsulinaemic-euglycaemic clamp in LZR is a likely candidate mechanism for the reduced skeletal muscle glucose uptake observed in OZR (Steinberg et al., 1994, Rattigan et al., 2013). In support capillary PSA available for insulin and glucose delivery is reduced in OZR due to reductions in insulin-mediated recruitment of the microvasculature (Wallis et al.,

2002) and capillary rarefaction (Frisbee, 2003). Considering that capillary PSA has a major impact on glucose uptake 90-120 min into an OGTT or hyperinsulinaemic-euglycaemic clamp with physiological insulin levels (Gudbjornsdottir et al., 2003), the reduced capillary PSA in the OZR may be a major determinant in the reduced skeletal muscle glucose uptake observed previously in OZR (Wallis et al., 2002).

Intracellular GLUT4 localisation and total GLUT4 protein content. GLUT4 immunofluorescence staining of TA muscle sections from LZR and OZR generated a staining pattern featuring large bright intracellular clusters of GLUT4 staining and smaller clusters of GLUT4 which contribute to a diffuse background stain. Clusters of staining appear predominantly at the muscle fibre periphery but also in deeper regions (Fig. 5.5). These images are consistent with previous immunofluorescence data in rodent muscle (Ploug et al., 1998, Lauritzen et al., 2006, Lauritzen et al., 2008), as well as the images shown in chapter 2 of this thesis in the development of GLUT4 immunofluorescence staining in human skeletal muscle.

Strikingly, the staining in some fibres of LZR and OZR TA muscle is more intense than others (Fig. 5.5). This was confirmed to be due to differences in GLUT4 content of type I, type IIa and type IIb muscle fibres (Fig. 5.9 and Fig. 5.10). Type I and IIa muscle fibres had the highest GLUT4 content with lower GLUT4 content in type IIb muscle fibres. Similar GLUT4 expression patterns have been reported previously in rat muscle with higher GLUT4 content in oxidative fibres (Marette et al., 1992, Daugaard and Richter, 2001, Henriksen et al., 1990). There were no differences in total GLUT4 content of the different fibre types between LZR and OZR (Fig. 5.9) which is in line with previous studies in the Zucker rat (Banks et al., 1992, Friedman et al., 1990) and studies comparing insulin sensitive and insulin resistant human skeletal muscle (Handberg et al., 1990, Pedersen et al., 1990). Therefore, these

findings confirm that impairments in insulin-mediated glucose uptake in the muscle of the OZR are not due to a reduction in total GLUT4 protein content.

There are differing fibre type compositions along the proximal-distal length of the TA muscle (Wang and Kernell, 2000). While it is unknown from which region of the TA muscle sections were taken in this study, the fibre type compositions were consistent with sectioning from the more distal TA region (Wang and Kernell, 2000). In addition, as it was confirmed in the current study there were no differences in fibre type composition between the sections analysed for GLUT4 and dytrophin colocalisation, differences in fibre type composition could not have affected the results.

Conclusions. In conclusion using immunofluorescence microscopy techniques which were developed in chapter 2 of this thesis, this study has shown a higher GLUT4 protein content in type I and type IIa fibres of LZR and OZR TA muscle compared to type IIb fibres, with no differences in GLUT4 protein content between fibre types in LZR and OZR. Furthermore there were no differences in GLUT4 and dystrophin colocalisation between LZR and OZR in the basal state in TA muscle fibres. There was no increase in GLUT4 and dystrophin colocalisation in OZR at the end of an 80 min hyperinsulinaemic-isoglycaemic clamp which was in line with the a priori hypothesis. However in contrast to the a priori hypothesis GLUT4 and dystrophin colocalisation also did not increase at the end of an 80 min hyperinsulinaemic-isoglycaemic clamp in LZR. The absence of an increase in colocalisation of GLUT4 and dystrophin in LZR at the end of an 80 min hyperinsulinaemic-isoglycaemic clamp is in line with the observation of chapter 4 of this thesis that GLUT4 and dystrophin colocalisation is transiently increased 30 min after glucose feeding and returned to baseline by 60 min therefore suggesting that GLUT4 translocation may also be transient in TA muscle fibres of LZR and OZR despite sustained insulin stimulation. In addition the data presented in the

current study suggest differences in insulin sensitivity between LZR and OZR in the final 20 min of an 80 min hyperinsulinaemic-isoglycaemic clamp are not due to differences in skeletal muscle GLUT4 translocation in fast twitch TA muscle fibres.

5.6. Acknowledgements

The antibodies against myosin heavy chain type I (A4.840) and myosin heavy chain type IIa (N2.261) used in the study were developed by Dr. Blau, and obtained from the Developmental Studies Hybridoma Bank (DSHB) developed under the auspices of the NICHD and maintained by the University of Iowa, Department of Biological Sciences, Iowa City, IA 52242.

5.7. References

BANKS, E. A., BROZINICK, J. T., JR., YASPELKIS, B. B., 3RD, KANG, H. Y. & IVY, J. L. 1992. Muscle glucose transport, GLUT-4 content, and degree of exercise training in obese Zucker rats. *Am J Physiol,* 263**,** E1010-5.

CLARK, M. G. 2008. Impaired microvascular perfusion: a consequence of vascular dysfunction and a potential cause of insulin resistance in muscle. *Am J Physiol Endocrinol Metab,* 295**,** E732-50.

DAUGAARD, J. R. & RICHTER, E. A. 2001. Relationship between muscle fibre composition, glucose transporter protein 4 and exercise training: possible consequences in non-insulin-dependent diabetes mellitus. *Acta Physiol Scand,* 171**,** 267-76.

ETGEN, G. J., JR., WILSON, C. M., JENSEN, J., CUSHMAN, S. W. & IVY, J. L. 1996. Glucose transport and cell surface GLUT-4 protein in skeletal muscle of the obese Zucker rat. *Am J Physiol,* 271**,** E294-301.

FAZAKERLEY, D. J., LAWRENCE, S. P., LIZUNOV, V. A., CUSHMAN, S. W. & HOLMAN, G. D. 2009. A common trafficking route for GLUT4 in cardiomyocytes in response to insulin, contraction and energy-status signalling. *J Cell Sci,* 122**,** 727-34.

FRIEDMAN, J. E., SHERMAN, W. M., REED, M. J., ELTON, C. W. & DOHM, G. L. 1990. Exercise training increases glucose transporter protein GLUT-4 in skeletal muscle of obese Zucker (fa/fa) rats. *FEBS Lett,* 268**,** 13-6.

FRISBEE, J. C. 2003. Remodeling of the skeletal muscle microcirculation increases resistance to perfusion in obese Zucker rats. *Am J Physiol Heart Circ Physiol,* 285**,** H104-11.

FRISBEE, J. C. & DELP, M. D. 2006. Vascular function in the metabolic syndrome and the effects on skeletal muscle perfusion: lessons from the obese Zucker rat. *Essays Biochem,* 42**,** 145-61.

FURTADO, L. M., SOMWAR, R., SWEENEY, G., NIU, W. & KLIP, A. 2002. Activation of the glucose transporter GLUT4 by insulin. *Biochem Cell Biol,* 80**,** 569-78.

GALANTE, P., MAERKER, E., SCHOLZ, R., RETT, K., HERBERG, L., MOSTHAF, L. & HARING, H. U. 1994. Insulin-induced translocation of GLUT 4 in skeletal muscle of insulin-resistant Zucker rats. *Diabetologia,* 37**,** 3-9.

GUDBJORNSDOTTIR, S., SJOSTRAND, M., STRINDBERG, L., WAHREN, J. & LONNROTH, P. 2003. Direct measurements of the permeability surface area for insulin and glucose in human skeletal muscle. *J Clin Endocrinol Metab,* 88**,** 4559-64.

HANDBERG, A., VAAG, A., DAMSBO, P., BECK-NIELSEN, H. & VINTEN, J. 1990. Expression of insulin regulatable glucose transporters in skeletal muscle from type 2 (non-insulin-dependent) diabetic patients. *Diabetologia,* 33**,** 625-7.

HENRIKSEN, E. J., BOUREY, R. E., RODNICK, K. J., KORANYI, L., PERMUTT, M. A. & HOLLOSZY, J. O. 1990. Glucose transporter protein content and glucose transport capacity in rat skeletal muscles. *Am J Physiol,* 259**,** E593-8.

IVY, J. L. 2004. Muscle insulin resistance amended with exercise training: role of GLUT4 expression. *Med Sci Sports Exerc,* 36**,** 1207-11.

KATZ, L. D., GLICKMAN, M. G., RAPOPORT, S., FERRANNINI, E. & DEFRONZO, R. A. 1983. Splanchnic and peripheral disposal of oral glucose in man. *Diabetes,* 32**,** 675-9.

KING, P. A., HORTON, E. D., HIRSHMAN, M. F. & HORTON, E. S. 1992. Insulin resistance in obese Zucker rat (fa/fa) skeletal muscle is associated with a failure of glucose transporter translocation. *J Clin Invest,* 90**,** 1568-75.

KROOK, A., WALLBERG-HENRIKSSON, H. & ZIERATH, J. R. 2004. Sending the signal: molecular mechanisms regulating glucose uptake. *Med Sci Sports Exerc,* 36**,** 1212-7.

LAURITZEN, H. P., GALBO, H., BRANDAUER, J., GOODYEAR, L. J. & PLOUG, T. 2008. Large GLUT4 vesicles are stationary while locally and reversibly depleted during transient insulin stimulation of skeletal muscle of living mice: imaging analysis

of GLUT4-enhanced green fluorescent protein vesicle dynamics. *Diabetes,* 57**,** 315-24.

LAURITZEN, H. P., PLOUG, T., PRATS, C., TAVARE, J. M. & GALBO, H. 2006. Imaging of insulin signaling in skeletal muscle of living mice shows major role of T-tubules. *Diabetes,* 55**,** 1300-6.

LIZUNOV, V. A., STENKULA, K. G., LISINSKI, I., GAVRILOVA, O., YVER, D. R., CHADT, A., AL-HASANI, H., ZIMMERBERG, J. & CUSHMAN, S. W. 2012. Insulin stimulates fusion, but not tethering, of GLUT4 vesicles in skeletal muscle of HA-GLUT4-GFP transgenic mice. *Am J Physiol Endocrinol Metab,* 302**,** E950-60.

MARETTE, A., RICHARDSON, J. M., RAMLAL, T., BALON, T. W., VRANIC, M., PESSIN, J. E. & KLIP, A. 1992. Abundance, localization, and insulin-induced translocation of glucose transporters in red and white muscle. *Am J Physiol,* 263**,** C443-52.

MATHE, D. 1995. Dyslipidemia and diabetes: animal models. *Diabete Metab,* 21**,** 106-11.

MUECKLER, M. 1994. Facilitative glucose transporters. *Eur J Biochem,* 219**,** 713-25.

MUNIYAPPA, R., LEE, S., CHEN, H. & QUON, M. J. 2008. Current approaches for assessing insulin sensitivity and resistance in vivo: advantages, limitations, and appropriate usage. *Am J Physiol Endocrinol Metab,* 294**,** E15-26.

OANA, F., TAKEDA, H., HAYAKAWA, K., MATSUZAWA, A., AKAHANE, S., ISAJI, M. & AKAHANE, M. 2005. Physiological difference between obese (fa/fa) Zucker rats and lean Zucker rats concerning adiponectin. *Metabolism,* 54**,** 995-1001.

PEDERSEN, O., BAK, J. F., ANDERSEN, P. H., LUND, S., MOLLER, D. E., FLIER, J. S. & KAHN, B. B. 1990. Evidence against altered expression of GLUT1 or GLUT4 in skeletal muscle of patients with obesity or NIDDM. *Diabetes,* 39**,** 865-70.

PLOUG, T., VAN DEURS, B., AI, H., CUSHMAN, S. W. & RALSTON, E. 1998. Analysis of GLUT4 distribution in whole skeletal muscle fibers: identification of distinct storage compartments that are recruited by insulin and muscle contractions. *J Cell Biol,* 142**,** 1429-46.

RATTIGAN, S., RICHARDS, S. M. & KESKE, M. A. 2013. Microvascular contributions to insulin resistance. *Diabetes,* 62**,** 343-5.

SCHERTZER, J. D., ANTONESCU, C. N., BILAN, P. J., JAIN, S., HUANG, X., LIU, Z., BONEN, A. & KLIP, A. 2009. A transgenic mouse model to study glucose transporter 4myc regulation in skeletal muscle. *Endocrinology,* 150**,** 1935-40.

SHERMAN, W. M., KATZ, A. L., CUTLER, C. L., WITHERS, R. T. & IVY, J. L. 1988. Glucose transport: locus of muscle insulin resistance in obese Zucker rats. *Am J Physiol,* 255**,** E374-82.

STEINBERG, H. O., BRECHTEL, G., JOHNSON, A., FINEBERG, N. & BARON, A. D. 1994. Insulin-mediated skeletal muscle vasodilation is nitric oxide dependent. A novel action of insulin to increase nitric oxide release. *J Clin Invest,* 94**,** 1172-9.

VINCENT, M. A. & BARRETT, E. J. 2002. Insulin-induced capillary recruitment precedes changes in skeletal muscle glucose uptake. *Diabetes,* 51**,** A31-A31.

VINCENT, M. A., CLERK, L. H., LINDNER, J. R., KLIBANOV, A. L., CLARK, M. G., RATTIGAN, S. & BARRETT, E. J. 2004. Microvascular recruitment is an early insulin effect that regulates skeletal muscle glucose uptake in vivo. *Diabetes,* 53**,** 1418-1423.

WALLIS, M. G., WHEATLEY, C. M., RATTIGAN, S., BARRETT, E. J., CLARK, A. D. & CLARK, M. G. 2002. Insulin-mediated hemodynamic changes are impaired in muscle of Zucker obese rats. *Diabetes,* 51**,** 3492-8.

WANG, L. C. & KERNELL, D. 2000. Proximo-distal organization and fibre type regionalization in rat hindlimb muscles. *J Muscle Res Cell Motil,* 21**,** 587-98.

WASSERMAN, D. H., KANG, L., AYALA, J. E., FUEGER, P. T. & LEE-YOUNG, R. S. 2011. The physiological regulation of glucose flux into muscle in vivo. *J Exp Biol,* 214**,** 254-62.

CHAPTER 6

PROLONGED HYPERGLYCAEMIA DOES NOT INCREASE COLOCALISATION OF GLUT4 WITH THE PLASMA MEMBRANE MARKER DYSTROPHIN IN THE SKELETAL MUSCLE OF MEN WITH NORMAL GLUCOSE TOLERANCE AND TYPE 2 DIABETES

H. Bradley[1], T.P.J. Solomon[2], C.S. Shaw[1,3] and A.J.M. Wagenmakers[1,4]

[1] School of Sport and Exercise Sciences, University of Birmingham, UK

[2] The Centre of Inflammation and Metabolism, Rigshospitalet, Denmark

[3] Institute of Sport, Exercise and Active Living (ISEAL), Victoria University, Australia

[4] Research Institute of Sport and Exercise Sciences, Liverpool John Moores University, UK

6.1. Abstract

Hyperglycaemia, a feature of type 2 Diabetes Mellitus, has been shown to reduce insulin-mediated glucose disposal in experiments performed in isolated rat muscles and cultured skeletal muscle cells. This occurred in combination with reductions in glucose transporter 4 (GLUT4) translocation to the plasma membrane (PM). The aim of this study was to investigate the hypothesis that 24 h of hyperglycaemia would lower insulin sensitivity and reduce colocalisation of GLUT4 with the PM marker dystrophin. Ten overweight normal glucose tolerant (NGT) volunteers underwent a hyperglycaemic clamp (5.4 mM above the overnight fasted state) and muscle biopsies were collected from the *vastus lateralis* muscle in the overnight fasted state and after 2 h and 24 h of hyperglycaemia. The same measurements were taken in 10 age and weight matched type 2 diabetes patients (T2D) in the overnight fasted state and after 2 h of a hyperglycaemic clamp (again 5.4 mM above the blood glucose concentration seen in these subjects in the overnight fasted state). Two and 24 hours of hyperglycaemia increased plasma insulin concentration (NGT overnight fasted 12.9 ± 1.9 $\mu IU.mL^{-1}$, 2 h 73.1 ± 16.2 $\mu IU.mL^{-1}$, 24 h 166.5 ± 30.3 $\mu IU.mL^{-1}$, $P < 0.001$; T2D overnight fasted 12.8 ± 1.4 $\mu IU.mL^{-1}$, 2 h 36.1 ± 8.9 $\mu IU.mL^{-1}$, $P < 0.05$) and elicited increased rates of whole body glucose disposal in NGT (overnight fasted 8.9 ± 0.6 $\mu mol.kg^{-1}.min^{-1}$, 2 h 36.0 ± 7.6 $\mu mol.kg^{-1}.min^{-1}$, 24 h 47.0 ± 3.6 $\mu mol.kg^{-1}.min^{-1}$, $P < 0.05$). In comparison, rates of whole body glucose disposal did not increase as a result of 2 h hyperglycaemia in T2D (overnight fasted 14.4 ± 2.1 $\mu mol.kg^{-1}.min^{-1}$, 2 h 15.3 ± 1.8 $\mu mol.kg^{-1}.min^{-1}$). Following 24 h of hyperglycaemia in NGT, insulin sensitivity was significantly reduced to levels observed after 2 h of hyperglycaemia in the T2D patients. Hyperglycaemia did not change colocalisation of GLUT4 with the PM marker dystrophin, expressed as the Pearson's correlation coefficient, in either group (NGT overnight fasted $r = 0.38 \pm 0.01$, 2 h $r = 0.37 \pm 0.01$, 24 h $r = 0.38 \pm 0.01$,

P = 0.525; T2D overnight fasted r = 0.39 ± 0.01, 2 h r = 0.38 ± 0.01, P = 0.160). Collectively these data suggest that the increased rate of whole body glucose disposal in NGT observed after 2 h and 24 h of hyperglycaemia is not the result of an increase in the PM GLUT4 content of skeletal muscle. Furthermore, the lack of increase in whole body glucose disposal in T2D and inhibition of insulin sensitivity observed in NGT after 24 h of hyperglycaemia are likely to involve other mechanisms than impairments in GLUT4 translocation to the PM.

6.2. Introduction

Skeletal muscle is the major site of insulin-mediated glucose uptake (Katz et al., 1983, Ferrannini et al., 1985). As reported in previous chapters glucose transporter 4 (GLUT4) is the best characterised glucose transporter isoform responsible for the transmembrane transport of glucose during insulin-mediated glucose uptake (Mueckler, 1994). A detailed description of GLUT4 localisation and redistribution in response to insulin is provided across chapters 1-4. In brief, immunofluorescence microscopy studies in rodent soleus, quadriceps and flexor digitorum brevis skeletal muscle have reported large and small intracellular GLUT4 storage clusters located predominantly at the fibre periphery, from which GLUT4 storage vesicles (GSVs) translocate following insulin stimulation and dock and fuse with the plasma membrane (PM) (Ploug et al., 1998, Lauritzen et al., 2006). Furthermore chapters 2-4 of this thesis have demonstrated the presence of large and small clusters of intracellular GLUT4 staining in human skeletal muscle and a significant increase in colocalisation of GLUT4 with the PM marker dystrophin in human skeletal muscle 30 min after the start of an oral glucose tolerance test.

Type 2 Diabetes Mellitus (T2D) is characterized by a failure to increase glucose uptake into peripheral tissues such as skeletal muscle in response to physiological increases in plasma

insulin concentration that results in chronic hyperglycaemia. Skeletal muscle is regarded to be the most significant site of insulin resistance with leg glucose uptake, presumably representative of skeletal muscle, being reduced by 45 % in patients with T2D compared to insulin sensitive controls (DeFronzo et al., 1985). Impairments in insulin-induced translocation of GLUT4 to the PM of skeletal muscle are assumed to make an important contribution to skeletal muscle and whole body insulin resistance. The underlying mechanisms have been described in chapter 1 of this thesis (Zierath et al., 1996).

Chronic hyperglycaemia plays a key role in the pathogenesis and complications of T2D in humans *in vivo* by impairing insulin secretion and exacerbating peripheral insulin resistance (Zierath et al., 2000). A number of studies, which are outlined below, have also explored the acute effect of hyperglycaemia on whole body glucose disposal and skeletal muscle and endothelial cell insulin sensitivity *in vivo* and *in vitro*. Two hour glucose infusion, with somatostatin to inhibit insulin release, raised plasma glucose concentration to approximately 26 mM and increased whole body glucose disposal in healthy insulin sensitive participants (Katz et al., 1991). In contrast perfusion of rat hindquarters with 5 – 25 mM glucose for 2 h has been shown to reduce insulin-mediated skeletal muscle glucose uptake (Hansen et al., 1992). Similarly 5 h of hyperglycaemia reduced insulin-stimulated glucose uptake in rat hindlimbs (Richter et al., 1988). Furthermore incubation of human myotubes in hyperglycaemic conditions (20 mM glucose) reduced insulin sensitivity and glucose uptake (Aas et al., 2011). Human satellite cells from the *vastus lateralis* differentiated in 20 mM glucose for 4-7 days exhibited reduced insulin-stimulated glucose uptake compared to cells incubated in 5 mM glucose with no differences in GLUT4 protein content or mRNA concentration (Aas et al., 2004, Green et al., 2012). Furthermore, exposure of bovine aortic endothelial cells to high glucose (25 mM) for 24 h impaired insulin-mediated activation of

eNOS and production of NO (Kim et al., 2005), potentially suggesting that 24 h of hyperglycaemia *in vivo* may impair insulin-mediated capillary recruitment and, therefore, reduce glucose uptake in skeletal muscle (Steinberg et al., 1994, Vincent et al., 2003). Finally, normalising plasma glucose concentrations through 3 week subcutaneous insulin infusion in T2D patients improved insulin sensitivity as measured using a hyperinsulinaemic-euglycaemic clamp (Garvey et al., 1985).

Intraperitoneal injection of Wistar rats with glucose (2 ml, 15 mM) and somatostatin, the latter to inhibit the endogenous insulin response, increased the GLUT4 content of isolated PM fractions 20 min after injection by 150 % suggesting that acute increases in glycaemia induce GLUT4 translocation to the PM (Galante et al., 1995). A 70 % increase in GLUT4 content of the PM fraction was also seen after a rat hind-limb perfusion with 25 mM glucose (Galante et al., 1995). To the author's knowledge no measurements have been made of GLUT4 content of the PM in response to acute hyperglycaemia in skeletal muscle obtained from normal glucose tolerant (NGT) and T2D human volunteers. Furthermore in the published experiments presented above GLUT4 content of the PM was measured by isolation of the PM fraction by centrifugation followed by a Western blot to measure GLUT content. This method has been criticised previously (Schertzer et al., 2009, Fazakerley et al., 2009) as isolated PM fractions can be contaminated in such studies with intracellular GLUT4-containing membranes and because this method does not discriminate between GLUT4 in the vicinity of the PM or fused with the PM.

This study, therefore aimed to investigate the effect of acute hyperglycaemia on whole body glucose disposal rates, insulin sensitivity and colocalisation of GLUT4 with the PM marker dystrophin in human skeletal muscle using the immunofluorescence microscopy method described in chapter 2 of this thesis. Measurements are made following 2 h hyperglycaemia in

individuals with NGT and in patients with T2D and following 24 h hyperglycaemia in the NGT group only. We investigate the hypotheses that whole body glucose disposal rates and the colocalisation of GLUT4 and dystrophin are higher in NGT compared to T2D following 2 h of hyperglycaemia. Secondly we hypothesise that insulin sensitivity and colocalisation of GLUT4 and dystrophin are reduced in response to 24 h hyperglycaemia in the NGT group due to hyperglycaemia-induced impairments in translocation of GLUT4.

6.3. Methods

Ethics and recruitment. All protocols in this study were approved by the Ethics Committee of the Capital Region of Denmark and conformed to the Declaration of Helsinki. Inclusion criteria were age 18 – 30 y, BMI 20 – 35 $kg.m^{-2}$, < 150 min exercise per week, free from cardiovascular, pulmonary, renal and hepatic disease and non-insulin treated. Ten gender-, age- and BMI-matched individuals with NGT and patients with T2D were recruited and gave written informed consent before participating. Type 2 diabetes was controlled with metformin (n = 7), sulfonylureas (n = 1), and liraglutide (n = 2). Drugs were withdrawn 7 days before testing. All participants completed preliminary testing consisting of an oral glucose tolerance test (OGTT) and VO_{2peak} determination. For the OGTT an overnight fasted baseline venous blood sample was collected prior to ingestion of 300 ml of a 25 % glucose solution. Subsequent blood samples were then collected 60 min and 120 min after glucose ingestion to analyse plasma glucose and insulin concentration and determine insulin sensitivity through calculation of the Matsuda index. VO_{2peak} was determined using a modified Bruce protocol on a treadmill. There was a 2% increase in incline every 2 min with subjects at a constant self-determined fast-paced walking speed. VO_2 and VCO_2 were measured on-line using a CPET

system (Cosmed; Rome, Italy). VO_{2peak} was taken as the mean of the 3-values of VO_2 measured around the maximum recorded VO_2 value.

Testing protocol. All NGT and T2D participants arrived at the laboratory after an overnight fast at 8 am (day 1) for experiment 1 of the testing procedures. All procedures were carried out at The Centre of Inflammation and Metabolism in Copenhagen and have been detailed in full previously (Solomon et al., 2012). The protocol is depicted in Fig. 6.1. An overnight fasted baseline muscle biopsy sample was taken from the *vastus lateralis* using the Bergström percutaneous needle biopsy technique (Bergstrom, 1975) and the sample was immediately processed as below. The following morning (day 2) one antecubital *iv* line was placed for glucose infusion and one dorsal hand *iv* line for blood sampling. Blood was arterialised by placing the sampling hand in a heated blanket (~60^{o}C) and an overnight fasted baseline sample was collected. At t = -2 h (~8 am) a primed (20 µmol.kg^{-1} multiplied by fasting glucose divided by 5 mM), continuous (0.2 µmol.kg^{-1}.min^{-1}) infusion of [6,6-$^{2}H_2$] glucose commenced. At t = 0 h a 2 h variable rate glucose infusion was initiated to elevate plasma glucose by 5.4 mM above basal (2 h hyperglycaemia). The infusion rate of [6,6-$^{2}H_2$] glucose was increased to 0.6 µmol.kg^{-1}.min^{-1}. Arterialised blood samples were taken every 5 min, glucose concentrations were measured (ABL 725; Radiometer, Copenhagen, Denmark), and the glucose infusion rate was adjusted as required to clamp glucose 5.4 mM above basal. At t = 2 h a second muscle biopsy was taken and processed as below. On a separate occasion, NGT participants also completed experiment 2. Participants arrived at the laboratory after an overnight fast (day 1); two iv lines were placed and a variable rate glucose infusion was initiated (at ~ 8 am) as in experiment 1 on this occasion to elevate plasma glucose 5.4 mM above basal for 24 h (24 h hyperglycaemia). The following day (day 2) a final muscle biopsy was taken 24 h after the commencement of hyperglycaemia and processed as below. After 22

h of hyperglycaemic clamp a primed, continuous (0.6 µmol.kg $^{-1}$.min^{-1}) infusion of [6,6-$^{2}H_2$] glucose was commenced for 2 h to measure whole body glucose disposal rate. Blood samples were collected into plain vacuettes for determination of plasma insulin concentration and sodium fluoride (NaF, Greiner Bio-One, Kremsmünster, Austria) vacuettes to determine plasma glucose tracer enrichment by GC-MS. Plasma was separated by centrifugation for 15 min at 2000 *g* at 4^{o}C and stored at -80^{o}C until analysis.

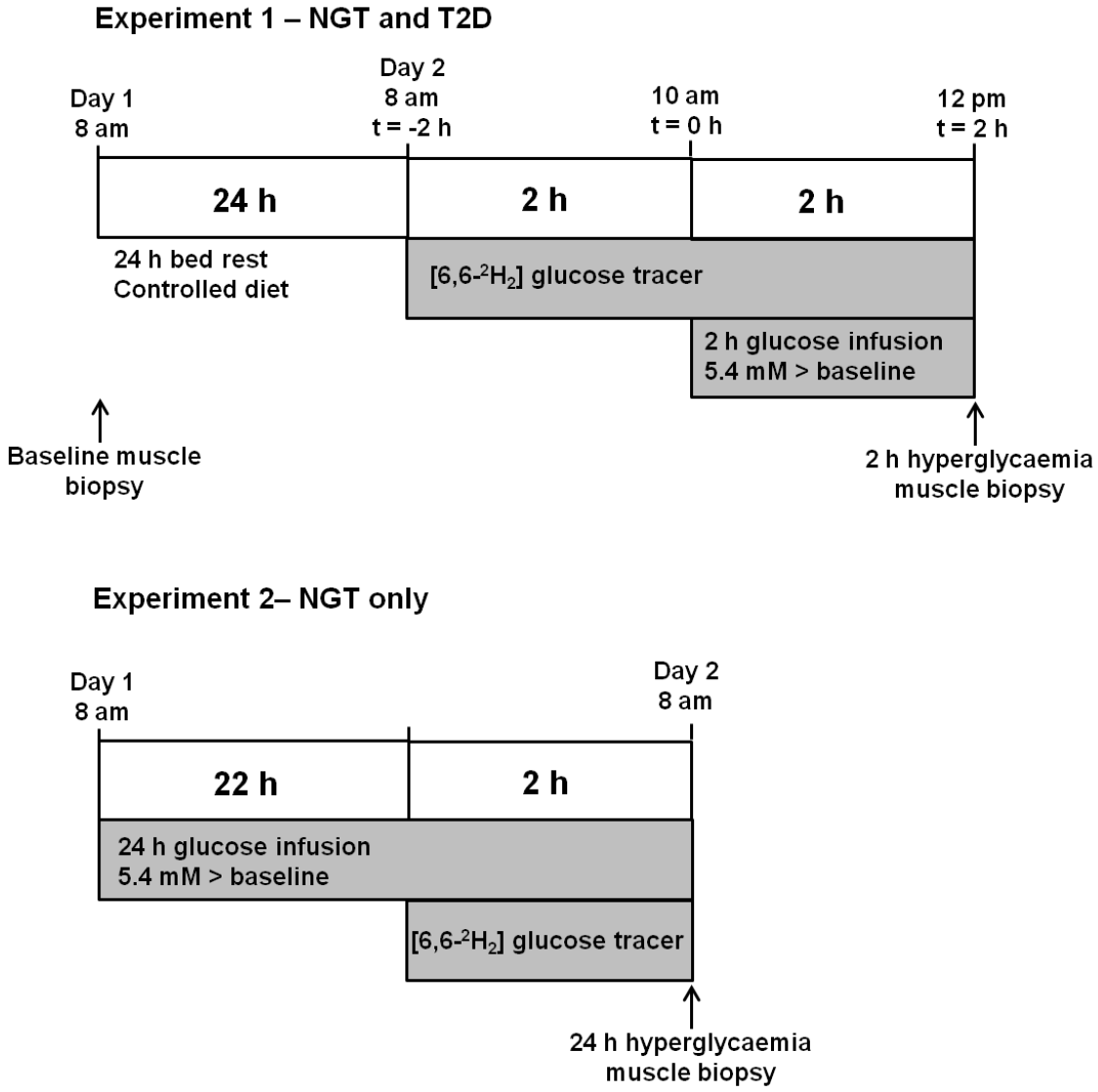

Fig. 6. 1. *Hyperglcyaemic glucose clamp participant testing protocol.*

Calculation of insulin sensitivity. A single pool model was used to calculate glucose flux rates (Steele, 1959). Glucose disposal rate was corrected for urinary glucose output. Glucose kinetics data have been published previously (Solomon et al., 2012) and are duplicated in the results section of this chapter (section 6.4) to enable interpretation of the GLUT4 and dystrophin colocalisation data.

To calculate whole-body insulin sensitivity, glucose disposal rate was divided by mean plasma insulin (Rd/[I]) during the final 30 min of the hyperglycaemic clamp. As subjects were clamped ~5.4 mM above basal glucose concentration each subject was clamped at a different absolute glucose concentration. In order to correct for this, insulin sensitivity was divided by mean plasma glucose during the final 30 min of the glucose-only stage of the clamp. Therefore insulin sensitivity was calculated as glucose disposal rate divided by plasma insulin multiplied by plasma glucose (Rd/[I][G]).

Muscle sample collection and processing. All post-sample collection processing and storage is described in detail in chapter 2.

Immunofluorescence staining protocol. NGT and T2D participants were pair matched and for each pair NGT cryosections for overnight fasted baseline (NGT baseline), 2 h hyperglyaemia (NGT 2 h) and 24 hr hyperglycaemia (NGT 24 h) and T2D cryosections for overnight fasted baseline (T2D baseline) and 2 h hyperglycaemia (T2D 2 h) were cut onto one slide. Slides were prepared and analysed in triplicate. Sections were either stained immediately or stored at -20^{o}C prior to use.

Full details of the GLUT4 and dystrophin immunofluorescence staining protocol are provided in chapter 2.

Image capture. Images were captured using an inverted confocal microscope (Leica DMIRE2, Leica Microsystems) with a 63x oil immersion objective (1.4 NA). AlexaFluor 488 fluorophores were excited with a 488 nm line of the argon laser and 498-571 nm emission. Alexa Fluor 594 fluorophores were excited with the 594 nm line of the helium-neon laser and 601-713 nm emission. For all subjects (N = 20) images were captured from 3 sections for each condition (NGT baseline, 2 h and 24 h hyperglycaemia and T2D overnight fasted baseline and 2 h hyperglycaemia), with 5 images captured per section. This equated to 179 ± 19, 154 ± 17, 145 ± 24, 161 ± 12 and 123 ± 16 fibres analysed for NGT pre, post 2 h, post 24 h, T2D pre and post 2 h, respectively.

Image quantitation. Full details of image analysis of GLUT4 and dystrophin colocalisation are presented in chapter 2. In brief, GLUT4 and dystrophin image pairs had a no neighbour deconvolution algorithm inbuilt into Image-Pro Plus 5.1 applied to them. The colocalisation tool in Image-Pro Plus 5.1 was then used to calculate the Pearson's correlation coefficient of each image pair. Analysis of GLUT4 fluorescence intensity within each muscle fibre was completed using the GLUT4 images with muscle fibres delineated based on the dystrophin image. No processing was carried out on the GLUT4 images. The appropriate dystrophin image was used to create an outline of fibres; firstly a flatten background filter was applied and fibres were identified using consistent intensity and size thresholds. The dystrophin fibre outline was applied to the GLUT4 images to measure GLUT4 fluorescence intensity within each fibre.

Statistics. All statistical testing was completed using SPSS statistics 19 (Chicago, IL). Age-, BMI- and VO_{2max}-matched NGT and T2D groups were confirmed using independent samples T tests. Statistical significance of insulin sensitivity data during hyperglycaemia was assessed using a repeated measures ANOVA with post hoc Bonferroni used to investigate significance

of pairwise comparisons. Plasma glucose and insulin, GLUT4 and dystrophin colocalisation and GLUT4 fluorescence intensity were assessed using a repeated measures ANOVA in NGT subjects, with post hoc Bonferroni analysis of significant main effects, and a paired T test in T2D subjects. Independent T tests were used to compare overnight fasted baseline NGT and T2D data and 2 h NGT and T2D data. Significance was set at $P < 0.05$. Data is displayed at mean ± SEM.

6.4. Results

Subject characteristics. Subject characteristics and OGTT-derived insulin sensitivity measures are shown in Table 6.1. Ten NGT and 10 T2D were matched according to gender (male:female, 8:2), age (NGT 56 ± 3 y, T2D 54 ± 2 y), BMI (NGT 31.3 ± 1.2 $kg.m^{-2}$, T2D 28.9 ± 1.0 $kg.m^{-2}$) and VO_{2peak} (NGT 32.1 ± 1.7 $mL.min^{-1}.kg^{-1}$, T2D 28.3 ± 1.2 $mL.min^{-1}.kg^{-1}$).

Table 6.1. *Participant characteristics*

	NGT	T2D
	N = 10	N = 10
Gender (M/F)	8/2	8/2
Age (y)	56 ± 3	54 ± 2
BMI ($kg.m^{-2}$)	31.3 ± 1.2	28.9 ± 1.0
VO_{2peak} ($mL.min^{-1}.kg^{-1}$)	32.1 ± 1.7	28.3 ± 1.2
Fasting plasma glucose (mM)	5.3 ± 0.2	9.1 ± 1.0*
2 hr OGTT plasma glucose (mM)	6.6 ± 0.3	16.5 ± 1.0*$^{\#}$
Fasting insulin ($\mu IU.ml^{-1}$)	12.9 ± 1.9	12.8 ± 1.4
HOMA-IR	3.7 ± 1.0	6.6 ± 0.6*
Matsuda ISI	5.7 ± 1.7	2.2 ± 0.2*

*Data shown is mean ± SEM. * T2D significantly different to NGT, independent samples T test, P < 0.05. #2 hr plasma glucose significantly different to baseline, paired samples T test, P < 0.01.*

Plasma glucose and insulin concentrations in the overnight fasted state and during hyperglycaemia. Plasma glucose and insulin at time of biopsy are shown in Fig. 6.2. In the overnight fasted state plasma glucose was 5.8 ± 0.2 mM in NGT and 10.0 ± 1.3 mM in T2D (P = 0.006). Plasma glucose was increased by approximately 5.4 mM following 2 h hyperglycaemia in both groups (NGT 10.8 ± 0.1 mM, T2D 15.3 ± 1.3 mM) and remained at this level following 24 h hyperglycaemia in NGT (11.3 ± 0.1 mM). There were no differences in plasma insulin concentrations between groups in the overnight fasted state (NGT 12.9 ± 1.9

μIU.mL^{-1}, T2D 12.8 ± 1.4 μIU.mL^{-1}, P = 0.997). In NGT plasma insulin was significantly increased above the overnight fasted baseline following 2 h (73.1 ± 16.2 μIU.mL^{-1}, *P* = 0.007) and 24 h hyperglycaemia (166.5 ± 30.3 μIU.mL^{-1}, *P* = 0.001). Plasma insulin increased significantly from 2 h to 24 h hyperglycaemia (*P* = 0.002). In T2D plasma insulin increased significantly above the overnight fasted baseline following 2 h hyperglycaemia (36.1 ± 8.9 μIU.mL^{-1}, *P* = 0.023).

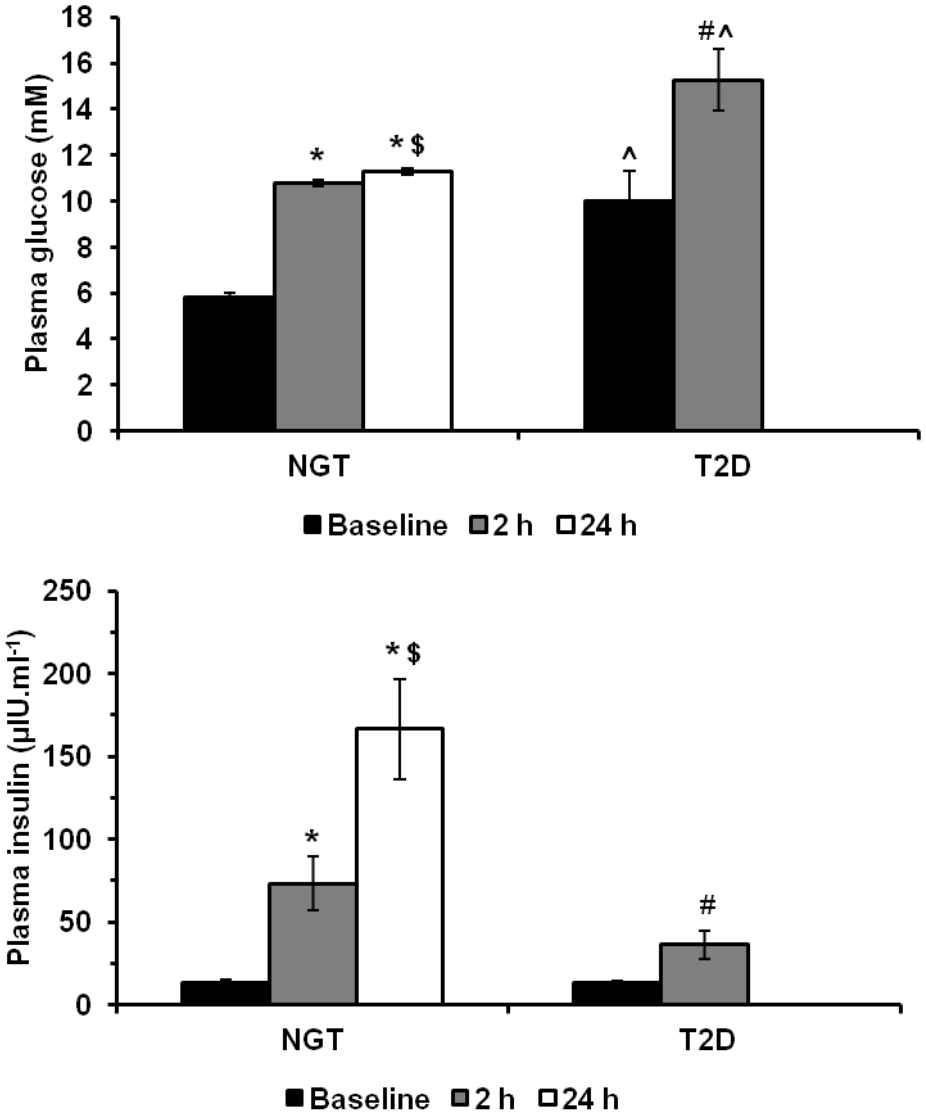

Fig. 6.2. *Plasma glucose and insulin concentrations in the overnight fasted state and during hyperglycaemia. Graphs shown mean ± SEM. NGT repeated measures ANOVA P < 0.001 for glucose and insulin, post hoc Bonferroni * significantly different to overnight fasted state P < 0.01, $ 2 h significantly different to 24 h P < 0.01. T2D paired T test, # significantly different to baseline P < 0.05. Independent samples T test to compare NGT and T2D plasma glucose and insulin at equivalent timepoints, ^ P < 0.01.*

Glucose disposal, endogenous glucose production and insulin sensitivity. Rates of glucose disposal (Rd) and endogenous glucose production (EGP) have been previously reported (Solomon et al., 2012) and are displayed in Fig. 6.3. Baseline Rd was higher in T2D than NGT. Rd during the final 30 min of 2 h and 24 h hyperglycaemic clamp was increased above baseline in NGT (NGT baseline 8.9 ± 0.6 μmol.kg^{-1}.min^{-1}, NGT 2 h 36.0 ± 7.6 μmol.kg^{-1}.min^{-1}, NGT 24 h 47.0 ± 3.6 μmol.kg^{-1}.min^{-1}, $P < 0.05$). In contrast, Rd during the final 30 min of 2 h hyperglycaemic clamp in T2D was not significantly elevated above baseline (T2D baseline 14.4 ± 2.1 μmol.kg^{-1}.min^{-1}, T2D 2 h 15.3 ± 1.8 μmol.kg^{-1}.min^{-1}). Rd during the final 30 min of hyperglycaemic clamp was significantly lower in T2D 2 h compared to both NGT 2 h and NGT 24 h ($P < 0.05$). EGP was higher in T2D compared to NGT at baseline (NGT 8.9 ± 0.6 μmol.kg^{-1}.min^{-1}, T2D 14.4 ± 2.1 μmol.kg^{-1}.min^{-1}, $P < 0.05$). EGP was suppressed in response to hyperglycaemia in both NGT and T2D, but remained higher in T2D (9.6 ± 1.6 μmol.kg^{-1}.min^{-}1) compared to NGT throughout (2.8 ± 1.3 μmol.kg^{-1}.min^{-1} and 1.1 ± 0.9 μmol.kg^{-1}.min^{-1} for 2 h and 24 h, respectively). When glucose disposal was corrected for plasma insulin concentration (Rd/[I]) there was no difference between NGT 2 h, 24 h or T2D 2 h during the final 30 min of hyperglycaemia (NGT 2 h 0.078 ± 0.015 μmol.kg^{-1}.min^{-1}.pmol^{-1}.L, NGT 24 h 0.057 ± 0.012 μmol.kg^{-1}.min^{-1}.pmol^{-1}.L, T2D 2h 0.069 ± 0.015 μmol.kg^{-1}.min^{-1}.pmol^{-1}.L, $P = 0.138$, Fig. 6.4A). Rd/[I][G], which is a measure of insulin sensitivity, was significantly lower during the final 30 min of the hyperglycaemic clamp in NGT 24 h and T2D 2 h compared to NGT 2 h (NGT 2 h 8.1 ± 1.4 x 10^{-3} μmol.kg^{-1}.min^{-1}.pmol^{-1}.L.mmol^{-1}.L, NGT 24 h 5.1 ± 1.1 x 10^{-3} μmol.kg^{-1}.min^{-1}.pmol^{-1}.L.mmol^{-1}.L, T2D 2 h 4.7 ± 0.7 x 10^{-3} μmol.kg^{-1}.min^{-1}.pmol^{-1}.L.mmol^{-1}.L, $P = 0.004$, Fig 6.4B). There was no difference between Rd/[I][G] in the final 30 min of hyperglycaemic clamp between NGT 24 h and T2D 2 h.

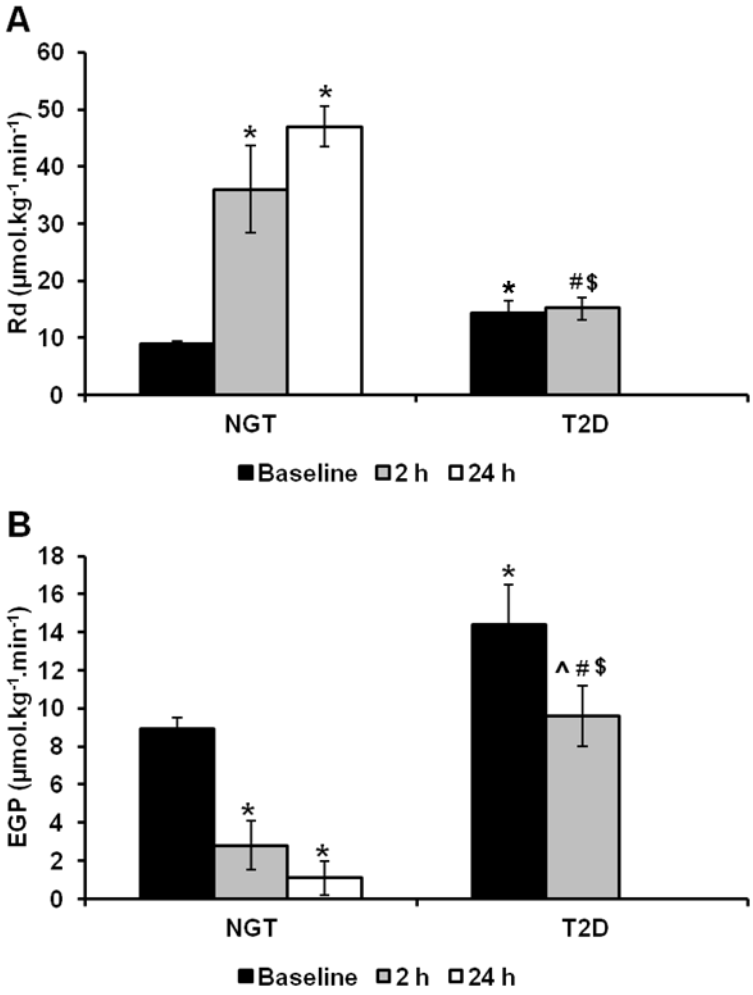

Fig. 6.3. *Mean glucose disposal rate (Rd, A) and mean endogenous glucose production (EGP, B) at baseline and during the final 30 min of 2 h and 24 h hyperglycaemic clamp. Graph shows mean ± SEM. * P < 0.05 compared to NGT baseline.* [#] *P < 0.05 compared to NGT 2 h.* [$] *P < 0.05 compared to NGT 24 h. ^ P < 0.05 compared to T2D baseline. Glucose kinetics data have been previously published (Solomon et al., 2012).*

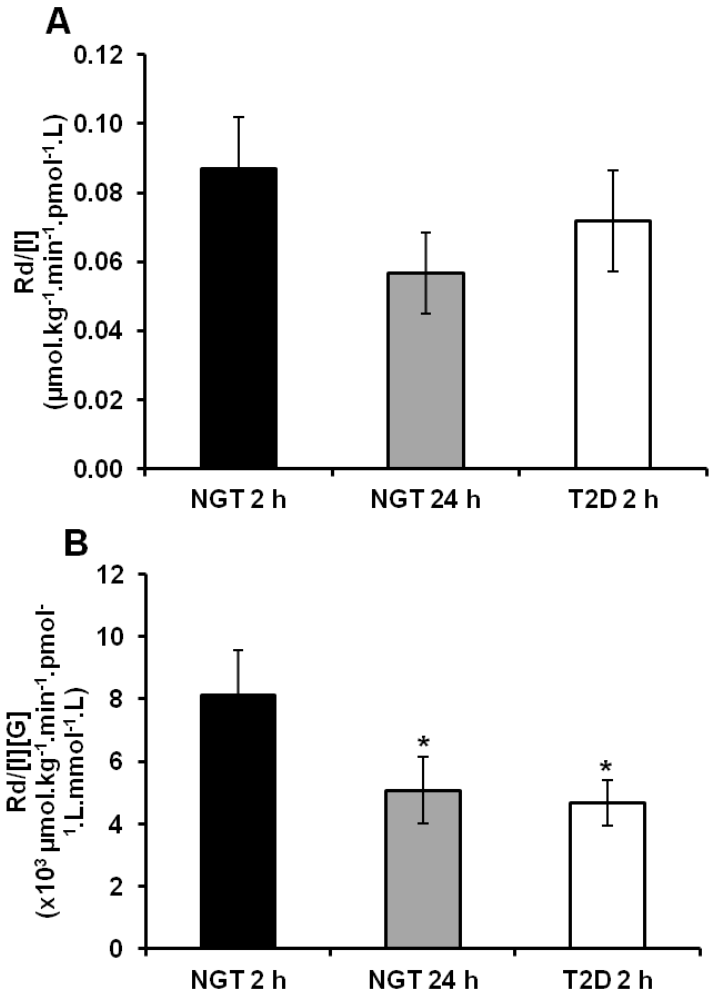

Fig. 6.4. *Mean glucose disposal corrected for plasma insulin concentration (A) and corrected for both plasma insulin and plasma glucose concentration (B) during final 30 min of 2 h and 24 h hyperglycaemic clamp. Insulin sensitivity is calculated from mean glucose disposal rate corrected for plasma glucose and insulin concentrations. Repeated measures ANOVA (A) P = 0.138 and (B) P = 0.004. Post hoc Bonferroni pairwise comparisons *significantly different to NGT 2hr P < 0.05, # significantly different to NGT 24 hr P < 0.001.*

GLUT4 and dystrophin colocalisation. The Pearson's correlation coefficient was used to measure the degree of colocalisation between GLUT4 and dystrophin immunofluorescence staining. GLUT4 and dystrophin images are shown in Fig. 6.5. The merged images display

the degree of colocalisation between GLUT4 and dystrophin. The Pearson's correlation coefficient data is shown in Fig. 6.6. There were no differences in Pearson's correlation coefficient between NGT and T2D in the overnight fasted state (NGT r = 0.38 ± 0.01, T2D r = 0.39 ± 0.01, P = 0.665). In NGT there was no difference in Pearson's correlation coefficient from the overnight fasted state following 2 h (r = 0.37 ± 0.01) and 24 h (r = 0.38± 0.01) of hyperglycaemia (P = 0.525). Similarly in T2D subjects there was no difference in Pearson's correlation coefficient between the overnight fasted state and following 2 h of hyperglycaemia (r = 0.38 ± 0.01, P = 0.160). Furthermore there were no differences in Pearson's correlation coefficient between NGT and T2D following 2 hr hyperglycaemia (P = 0.420). Therefore the degree of colocalisation between GLUT4 and dystrophin was similar in all conditions studied.

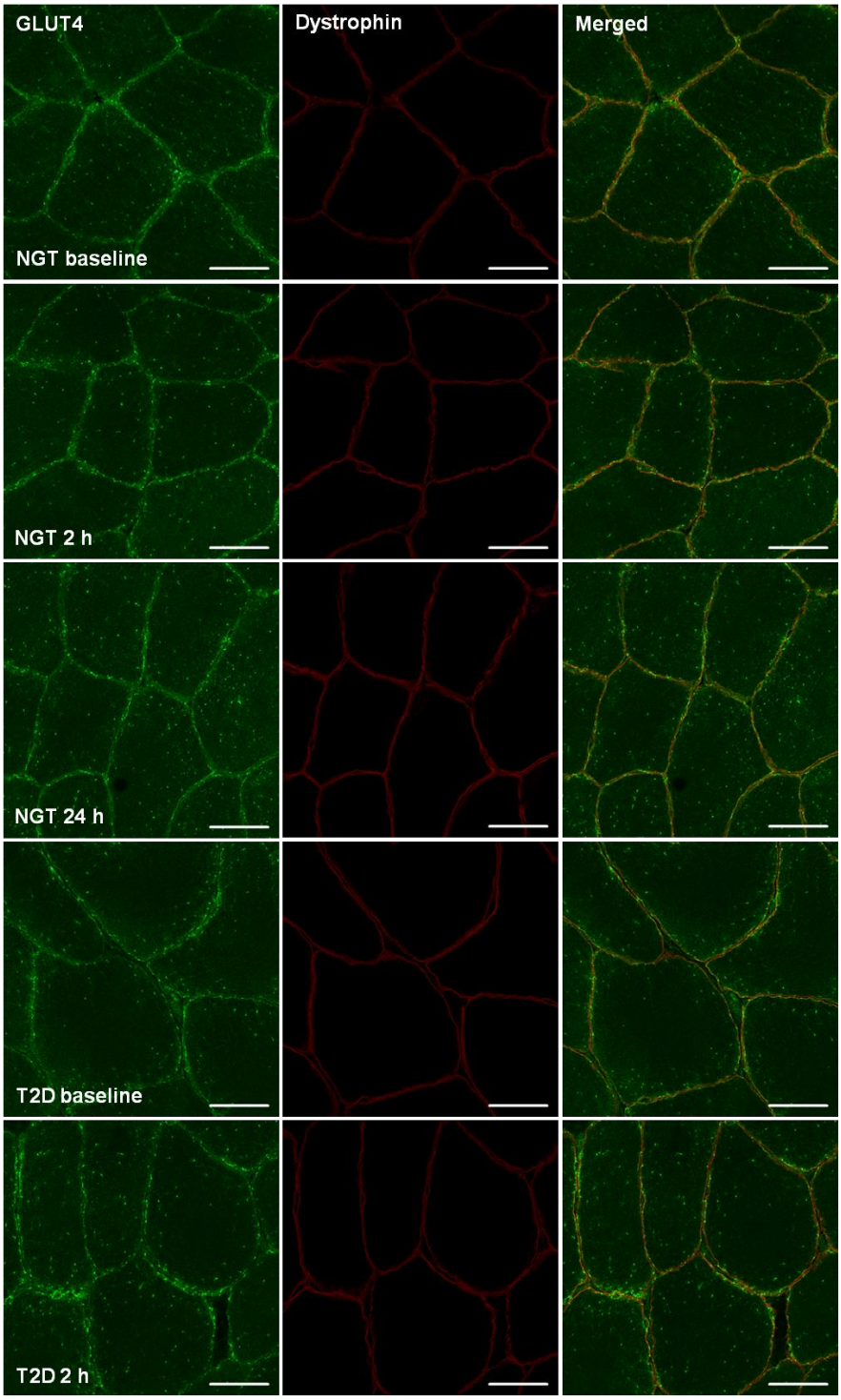

Fig. 6.5. *Representative confocal images of GLUT4 (green) and dystrophin (red) in skeletal muscle fibres of NGT and T2D participants in the overnight fasted state and following 2 h and 24 h (NGT only) hyperglyaemia. Merged images represent GLUT4 and dystrophin colocalisation. Scale bars 50 µm.*

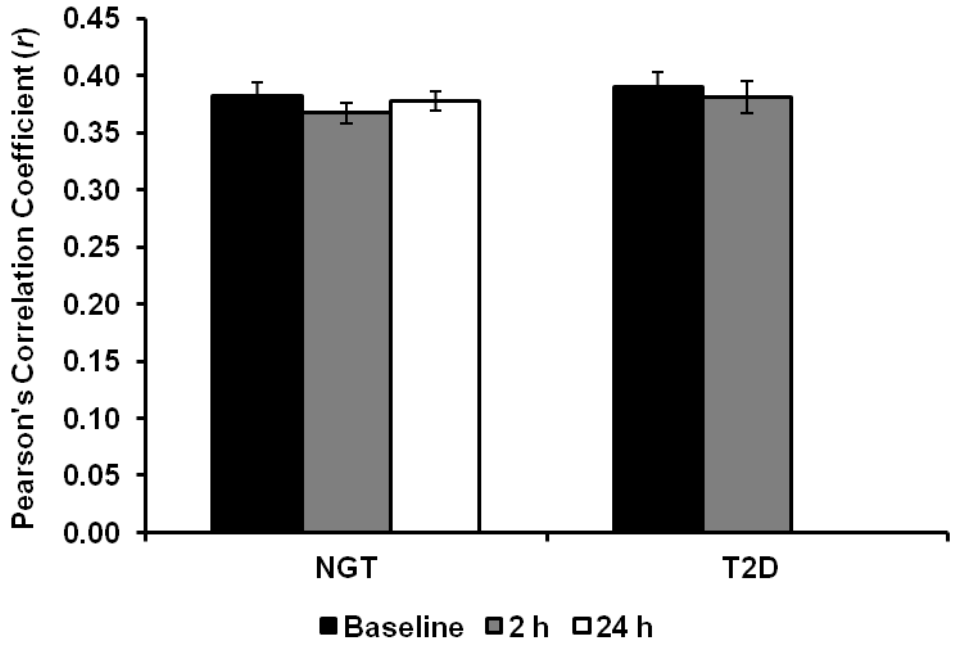

Fig. 6.6. *Pearson's correlation coefficient to measure colocalisation of GLUT4 and dystrophin in skeletal muscle fibres of NGT and T2D participants in the overnight fasted state and following 2 hr and 24 hr (NGT only) of hyperglyaemia. Graph shows mean ± SEM. NGT repeated measures ANOVA P = 0.525. T2D paired T test P = 0.160. Independent samples T test to compare NGT and T2D in the overnight fasted state P = 0.665. Independent samples T test to compare NGT and T2D 2 h P = 0.420.*

GLUT4 fluorescence intensity. The total GLUT4 protein content in the overnight fasted state and following 2 h and 24 h of hyperglycaemia was assessed by measuring the fluorescence intensity of the GLUT4 stain within the muscle fibres (mean of > 100 fibres in each condition). The data is shown in Fig. 6.7. There were no differences in GLUT4 fluorescence intensity, therefore no differences in total GLUT4 protein content, between NGT and T2D in the overnight fasted state or after any duration of hyperglycaemia.

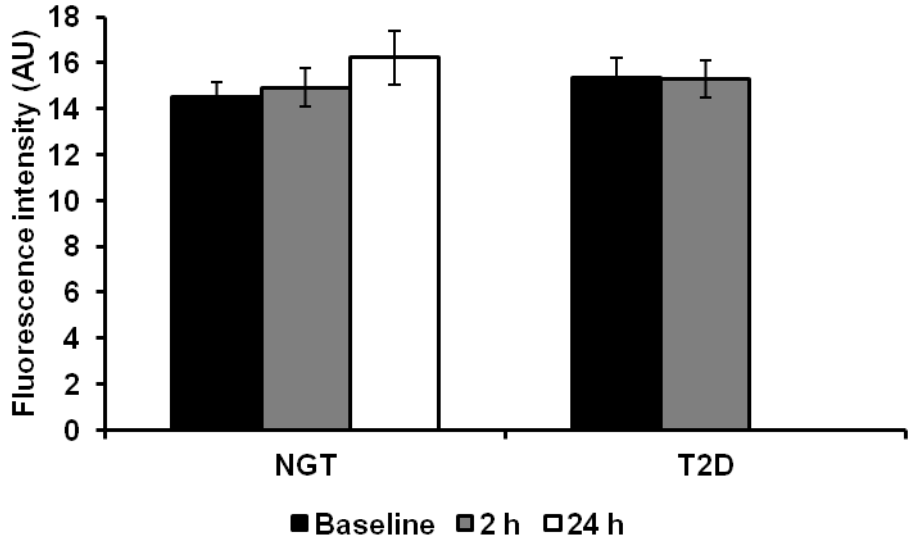

Fig. 6.7. *GLUT4 fluorescence intensity as a measure of total GLUT4 protein content in skeletal muscle fibres of NGT and T2D participants in the overnight fasted state and following 2 h and 24 h (NGT only) hyperglycaemia. Graph shows mean ± SEM. NGT repeated measures ANOVA P = 0.089. T2D paired T test P = 0.696. Independent samples T test to compare NGT and T2D in the overnight fasted state P = 0.460. Independent samples T test to compare NGT and T2D 2 h P = 0.760.*

6.5. Discussion

In the current study, 2 h of hyperglycaemia in both NGT and T2D was sufficient to raise plasma insulin concentrations above values seen in the overnight fasted state and was sufficient to increase rates of whole body glucose disposal above baseline in NGT. However, despite this increase in whole body glucose disposal following 2 h hyperglycaemia in NGT and in contrast to our initial hypothesis, there was no increase in the colocalisation of GLUT4 with the PM marker dystrophin. Furthermore, colocalisation of GLUT4 and dystrophin was the same in NGT and T2D following 2 h hyperglycaemia despite significantly higher whole body glucose disposal rates in NGT compared to T2D. These results indicate that GLUT4 PM

content was not responsible for the increased whole body glucose disposal rates that occurred following 2 h hyperglycaemia in NGT nor the lower glucose disposal rate observed in T2D. Following 24 h of hyperglycaemia in NGT, insulin sensitivity, measured as Rd/[I][G] (Rd corrected for prevailing insulin and glucose concentrations), was reduced to comparable levels as seen in T2D after 2 h of hyperglycaemia, however there were again no significant changes in GLUT4 and dystrophin colocalisation.

Glucose disposal rates. Baseline endogenous glucose production and glucose disposal rates were higher in T2D than NGT. This is in agreement with previous studies (DeFronzo et al., 1989) and is in line with the well described mass action effect on glucose transport, which is explained by the higher prevailing glucose concentrations in T2D (Yki-Jarvinen et al., 1987a, Yki-Jarvinen et al., 1987b). Glucose disposal rates increased significantly above baseline in the final 30 min of 2 h and 24 h hyperglycaemic clamp in NGT. In contrast glucose disposal rates were not increased above baseline in the final 30 min of hyperglycaemic clamp in T2D and furthermore were significantly lower in T2D compared to NGT in the final 30 min of 2 h hyperglycaemic clamp. This is likely due to a combination of lower insulin secretion rates resulting in lower plasma insulin concentrations and peripheral insulin resistance, which both characterise T2D. Interestingly, when corrected for plasma insulin concentrations there were no differences in glucose disposal between NGT and T2D. This can be explained by the ability of glucose to increase its own uptake (termed mass action effect of glucose) given the higher plasma glucose concentrations in T2D. This is in line with previous studies where glucose disposal is not different in T2D when measured using a hyperinsulinemic-isoglycemic clamp, where plasma glucose is clamped at fasting glucose concentration (Mandarino et al., 1990, Vaag et al., 1992). In the current study, impairments in insulin

sensitivity are observed in T2D when corrected for both prevailing plasma glucose and plasma insulin concentrations.

GLUT4 and dystrophin colocalisation after 2 h hyperglycaemia. Acute elevations in plasma glucose and insulin concentrations have been shown to independently induce GLUT4 translocation in skeletal muscle of Wistar rats using subcellular fractionation methods (Galante et al., 1995). It was therefore surprising that there was no increase in GLUT4 and dystrophin colocalisation following 2 h of hyperglycaemia in NGT in the study presented here, despite elevated plasma glucose and insulin concentrations and increased rates of whole body glucose disposal above baseline. A possible explanation for this unexpected finding is provided in chapter 4 of this thesis, in which we observed increases in GLUT4 and dystrophin colocalisation 30 min after the start of an OGTT, which returned to overnight fasted basal levels at 60 and 90 minutes post glucose ingestion. Therefore it is possible that GLUT4 translocation to the PM in the present study may have occurred at an earlier time point during the hyperglycaemic clamp.

Glucose disposal (Rd) was lower in the final 30 min of hyperglycaemia in T2D 2 h compared to NGT 2 h. However there were no differences in GLUT4 and dystrophin colocalisation between NGT 2h and T2D 2h, indicating that skeletal muscle PM GLUT4 content is not the primary determinant of the lower rates of glucose disposal in T2D.

GLUT4 and dystrophin colocalisation after 24 h hyperglycaemia in NGT. GLUT4 and dystrophin colocalisation was again unchanged following 24 h of hyperglycaemia despite the persistent and very large elevations in plasma insulin and the sustained high rates of glucose disposal. There was no difference in whole body glucose disposal in the final 30 min of 2 h and 24 h hyperglycaemia in NGT, though plasma insulin concentration was significantly

higher following 24 h hyperglycaemia compared to 2 h. Therefore, when correcting glucose disposal for plasma glucose and insulin concentrations, insulin sensitivity (Rd/[I][G]) in the final 30 min of 24 h hyperglycaemia in NGT was reduced to comparable levels to T2D following 2 h hyperglycaemia, indicating more insulin is required to achieve an equivalent glucose disposal response. However, as GLUT4 and dystrophin colocalisation is unchanged in NGT during elevated rates of glucose disposal, and is not different between NGT and T2D despite marked differences in glucose disposal rates, it appears unlikely to be the major determinant of elevated rates of glucose disposal or impaired insulin action following 24 h of hyperglycaemia.

Alternative mechanisms that may contribute to the increased rates of whole body glucose disposal following hyperglycaemia in NGT. As GLUT4 PM content does not change following hyperglycaemia in NGT there must be alternative mechanisms that contribute to the elevated rates of whole body glucose disposal.

As discussed above, during hyperglycaemia the mass action effect resulting from the steeper concentration gradient between arterial and intracellular glucose are highly likely to contribute to the high rates of glucose disposal in the present study (Yki-Jarvinen et al., 1987a). In support of this, whole body glucose disposal is almost doubled as a result of doubling the plasma glucose concentration without increases in plasma insulin concentrations (Yki-Jarvinen et al., 1987b). Therefore baseline glucose transporter PM content in peripheral tissues may be sufficient to drive the increased whole body glucose disposal during hyperglycaemia in NGT via the mass action effect.

GLUT4 localisation at the T-tubule membranes has not been analysed in the current study due to methodological difficulties in quantitation which are explained in chapter 2. However

chapter 2 of this thesis did demonstrate the presence of GLUT4 in the T tubule membranes of human skeletal muscle. Therefore, it is possible that increases in GLUT4 localisation may have been more prominent at the T-tubule membranes compared to the PM in the current study. This raises the possibility that GLUT4 in the T-tubule membranes may have contributed to skeletal muscle glucose uptake and the increased whole body glucose disposal observed during hyperglycaemia in NGT. However, further methodological advances are needed in order to examine this possibility in human muscle.

An additional alternative mechanism that is likely to make significant contributions to increased whole body glucose disposal rates and skeletal muscle glucose uptake in particular during 2 h hyperglycaemia in NGT is increased skeletal muscle microvascular recruitment induced by the elevated plasma insulin concentrations. An increase in the capillary permeability surface area product and glucose delivery to the muscle fibre is known to be a key determinant of skeletal muscle glucose uptake in response to insulin (Steinberg et al., 1994, Vincent et al., 2006, Gudbjornsdottir et al., 2003).

Although skeletal muscle is generally considered the quantitatively most important tissue for glucose disposal, even during hyperglycaemia (Baron et al., 1988), it is also important to consider that tissues other than skeletal muscle, namely liver and adipose tissue, may contribute significantly to whole body glucose disposal in conditions of hyperglycaemia. Muscle, adipose tissue and liver may all contribute to the high rates of whole body glucose disposal measured in the current study. For example, intravenous glucose infusion to induce hyperglycaemic-hyperinsulinaemia resulted in a doubling of splanchnic (primarily liver, gut and pancreas) glucose uptake in comparison to euglycaemic-hyperinsulinaemia (Ferrannini et al., 1980, DeFronzo et al., 1978). Furthermore in animal models exhibiting reduced capillary density through muscle specific vascular endothelial growth factor (VEGF) knockout, whole

body glucose disposal did not change in comparison to wild type animals, however more glucose was deposited as glycogen in the liver during hyperinsulinaemic-euglycaemic clamp suggesting increased liver glucose uptake (Bonner et al., 2013). Therefore in the current study in which hyperglycaemia (24 h in particular) may have impaired microvascular recruitment (see subsequent section, Kim et al., 2005), high whole body glucose disposal rates may have been maintained in part through increased splanchic glucose uptake. In addition during hyperinsulinaemic-euglycaemic clamp in obese rats adipose tissue glucose utilisation was increased compared to lean rats (Penicaud et al., 1987). Therefore it is possible that increased rates of whole body glucose disposal were achieved in part at least through increased glucose uptake into other tissues than skeletal muscle during hyperglycaemia in NGT.

Alternative mechanisms that may contribute to reduced rates of whole body glucose disposal in T2D. Obesity and T2D have been associated with reduced insulin-mediated NO production from vascular endothelial cells and reduced capillary density (Barrett et al., 2009, Barrett et al., 2011, Wagenmakers et al., 2006). The subsequent impairment in insulin-mediated skeletal muscle microvascular recruitment and lower glucose and insulin delivery to the muscle bed, has been shown to be reduced in obese compared to lean humans and has been suggested to significantly contribute to the development of skeletal muscle insulin resistance (Clerk et al., 2002, Clerk et al., 2006, Keske et al., 2009). Therefore, it is likely that reduced glucose delivery to the skeletal muscle contributes to the reduced skeletal muscle glucose uptake and therefore reduced whole body glucose disposal observed following 2 h hyperglycaemia in T2D compared to NGT.

Alternative mechanisms that may contribute to reduced insulin sensitivity in NGT following 24 h hyperglycaemia. In the current study high rates of whole body glucose disposal were maintained following 24 h hyperglycaemia in NGT, without changes in skeletal muscle PM

GLUT4 content. However insulin sensitivity (calculated by correcting glucose disposal for plasma glucose and insulin concentrations, (Rd/[I][G])) in the final 30 min of 24 h hyperglycaemia in NGT was reduced to comparable levels to T2D following 2 h hyperglycaemia. It has been shown previously that exposure of muscle cells to hyperglycaemic conditions in vitro induces defects in the insulin signalling pathway (Pillay et al., 1996). However, as there was no apparent change in GLUT4 localisation in the current study, it seems that mechanisms other than impaired GLUT4 translocation explain the reduction in insulin action following 24 h of hyperglycaemia in humans.

A previous study showed that bovine aortic endothelial cells exposed to high glucose (25 mM) for 24 h exhibit impaired insulin mediated activation of eNOS and production of NO (Kim et al., 2005). If such an effect were to occur in humans in vivo, then it would impair terminal arteriole dilation and microvascular recruitment in skeletal muscle and contribute to skeletal muscle insulin resistance (Kim et al., 2005, Steinberg et al., 1994, Vincent et al., 2003). Therefore it is possible that in the current study 24 h hyperglycaemia *in vivo* in humans may induce insulin resistance through impaired eNOS activation and microvascular recruitment and this is an important area for future investigation.

Conclusions. In conclusion, 2 h and 24 h of hyperglycaemia did not influence the colocalisation of GLUT4 with the PM marker dystrophin in NGT despite substantial elevations in plasma insulin concentrations and increased rates of whole body glucose disposal. According to this study, factors other than GLUT4 presence at the skeletal muscle PM, such as T-tubule membrane GLUT4 localisation, microvascular recruitment (Clark, 2008), glucose uptake into other tissues (Ferrannini et al., 1980, DeFronzo et al., 1978), and the glucose mass action effect (Yki-Jarvinen et al., 1987a) may be responsible for the elevation in whole body glucose disposal rate in the final 30 min of 2 h hyperglycaemia in

NGT compared to baseline. In addition, neither the lower whole body glucose disposal rate that occurred in the final 30 min of 2 h hyperglycaemia in T2D nor the insulin resistance that developed after 24 h of hyperglycaemia coincided with a decrease in GLUT4 and dystrophin colocalisation. Impairments in insulin-stimulated activation of microvascular eNOS and skeletal muscle capillary recruitment are potential alternative mechanism by which prolonged hyperglycaemia reduces insulin sensitivity.

6.6. References

AAS, V., HESSVIK, N. P., WETTERGREEN, M., HVAMMEN, A. W., HALLEN, S., THORESEN, G. H. & RUSTAN, A. C. 2011. Chronic hyperglycemia reduces substrate oxidation and impairs metabolic switching of human myotubes. *Biochim Biophys Acta,* 1812**,** 94-105.

AAS, V., KASE, E. T., SOLBERG, R., JENSEN, J. & RUSTAN, A. C. 2004. Chronic hyperglycaemia promotes lipogenesis and triacylglycerol accumulation in human skeletal muscle cells. *Diabetologia,* 47**,** 1452-61.

BARON, A. D., BRECHTEL, G., WALLACE, P. & EDELMAN, S. V. 1988. Rates and tissue sites of non-insulin- and insulin-mediated glucose uptake in humans. *Am J Physiol,* 255**,** E769-74.

BERGSTROM, J. 1975. Percutaneous needle biopsy of skeletal muscle in physiological and clinical research. *Scand J Clin Lab Invest,* 35**,** 609-16.

BONNER, J. S., LANTIER, L., HASENOUR, C. M., JAMES, F. D., BRACY, D. P. & WASSERMAN, D. H. 2013. Muscle-specific vascular endothelial growth factor deletion induces muscle capillary rarefaction creating muscle insulin resistance. *Diabetes,* 62**,** 572-80.

CLARK, M. G. 2008. Impaired microvascular perfusion: a consequence of vascular dysfunction and a potential cause of insulin resistance in muscle. *Am J Physiol Endocrinol Metab,* 295**,** E732-50.

CLERK, L. H., RATTIGAN, S. & CLARK, M. G. 2002. Lipid infusion impairs physiologic insulin-mediated capillary recruitment and muscle glucose uptake in vivo. *Diabetes,* 51**,** 1138-45.

CLERK, L. H., VINCENT, M. A., JAHN, L. A., LIU, Z., LINDNER, J. R. & BARRETT, E. J. 2006. Obesity blunts insulin-mediated microvascular recruitment in human forearm muscle. *Diabetes,* 55**,** 1436-42.

DEFRONZO, R. A., FERRANNINI, E., HENDLER, R., WAHREN, J. & FELIG, P. 1978. Influence of hyperinsulinemia, hyperglycemia, and the route of glucose administration on splanchnic glucose exchange. *Proc Natl Acad Sci U S A,* 75**,** 5173-7.

DEFRONZO, R. A., FERRANNINI, E. & SIMONSON, D. C. 1989. Fasting hyperglycemia in non-insulin-dependent diabetes mellitus: contributions of excessive hepatic glucose production and impaired tissue glucose uptake. *Metabolism,* 38**,** 387-95.

DEFRONZO, R. A., GUNNARSSON, R., BJORKMAN, O., OLSSON, M. & WAHREN, J. 1985. Effects of insulin on peripheral and splanchnic glucose metabolism in noninsulin-dependent (type II) diabetes mellitus. *J Clin Invest,* 76**,** 149-55.

FAZAKERLEY, D. J., LAWRENCE, S. P., LIZUNOV, V. A., CUSHMAN, S. W. & HOLMAN, G. D. 2009. A common trafficking route for GLUT4 in cardiomyocytes in response to insulin, contraction and energy-status signalling. *J Cell Sci,* 122**,** 727-34.

FERRANNINI, E., BJORKMAN, O., REICHARD, G. A., JR., PILO, A., OLSSON, M., WAHREN, J. & DEFRONZO, R. A. 1985. The disposal of an oral glucose load in healthy subjects. A quantitative study. *Diabetes,* 34**,** 580-8.

FERRANNINI, E., WAHREN, J., FELIG, P. & DEFRONZO, R. A. 1980. The role of fractional glucose extraction in the regulation of splanchnic glucose metabolism in normal and diabetic man. *Metabolism,* 29**,** 28-35.

GALANTE, P., MOSTHAF, L., KELLERER, M., BERTI, L., TIPPMER, S., BOSSENMAIER, B., FUJIWARA, T., OKUNO, A., HORIKOSHI, H. & HARING, H. U. 1995. Acute hyperglycemia provides an insulin-independent inducer for GLUT4 translocation in C2C12 myotubes and rat skeletal muscle. *Diabetes,* 44**,** 646-51.

GARVEY, W. T., OLEFSKY, J. M., GRIFFIN, J., HAMMAN, R. F. & KOLTERMAN, O. G. 1985. The effect of insulin treatment on insulin secretion and insulin action in type II diabetes mellitus. *Diabetes,* 34**,** 222-34.

GREEN, C. J., HENRIKSEN, T. I., PEDERSEN, B. K. & SOLOMON, T. P. 2012. Glucagon like peptide-1-induced glucose metabolism in differentiated human muscle satellite cells is attenuated by hyperglycemia. *PLoS One,* 7**,** e44284.

HANSEN, B. F., HANSEN, S. A., PLOUG, T., BAK, J. F. & RICHTER, E. A. 1992. Effects of glucose and insulin on development of impaired insulin action in muscle. *Am J Physiol,* 262**,** E440-6.

KATZ, A., RAZ, I., SPENCER, M. K., RISING, R. & MOTT, D. M. 1991. Hyperglycemia induces accumulation of glucose in human skeletal muscle. *Am J Physiol,* 260**,** R698-703.

KATZ, L. D., GLICKMAN, M. G., RAPOPORT, S., FERRANNINI, E. & DEFRONZO, R. A. 1983. Splanchnic and peripheral disposal of oral glucose in man. *Diabetes,* 32**,** 675-9.

KESKE, M. A., CLERK, L. H., PRICE, W. J., JAHN, L. A. & BARRETT, E. J. 2009. Obesity blunts microvascular recruitment in human forearm muscle after a mixed meal. *Diabetes Care,* 32**,** 1672-7.

KIM, F., TYSSELING, K. A., RICE, J., GALLIS, B., HAJI, L., GIACHELLI, C. M., RAINES, E. W., CORSON, M. A. & SCHWARTZ, M. W. 2005. Activation of IKKbeta by glucose is necessary and sufficient to impair insulin signaling and nitric oxide production in endothelial cells. *J Mol Cell Cardiol,* 39**,** 327-34.

LAURITZEN, H. P., PLOUG, T., PRATS, C., TAVARE, J. M. & GALBO, H. 2006. Imaging of insulin signaling in skeletal muscle of living mice shows major role of T-tubules. *Diabetes,* 55**,** 1300-6.

MANDARINO, L. J., CONSOLI, A., KELLEY, D. E., REILLY, J. J. & NURJHAN, N. 1990. Fasting hyperglycemia normalizes oxidative and nonoxidative pathways of insulin-stimulated glucose metabolism in noninsulin-dependent diabetes mellitus. *J Clin Endocrinol Metab,* 71**,** 1544-51.

MUECKLER, M. 1994. Facilitative glucose transporters. *Eur J Biochem,* 219**,** 713-25.

PENICAUD, L., FERRE, P., TERRETAZ, J., KINEBANYAN, M. F., LETURQUE, A., DORE, E., GIRARD, J., JEANRENAUD, B. & PICON, L. 1987. Development of obesity in Zucker rats. Early insulin resistance in muscles but normal sensitivity in white adipose tissue. *Diabetes,* 36**,** 626-31.

PILLAY, T. S., XIAO, S. & OLEFSKY, J. M. 1996. Glucose-induced phosphorylation of the insulin receptor. Functional effects and characterization of phosphorylation sites. *J Clin Invest,* 97**,** 613-20.

PLOUG, T., VAN DEURS, B., AI, H., CUSHMAN, S. W. & RALSTON, E. 1998. Analysis of GLUT4 distribution in whole skeletal muscle fibers: identification of distinct storage compartments that are recruited by insulin and muscle contractions. *J Cell Biol,* 142**,** 1429-46.

RICHTER, E. A., HANSEN, B. F. & HANSEN, S. A. 1988. Glucose-induced insulin resistance of skeletal-muscle glucose transport and uptake. *Biochem J,* 252**,** 733-7.

SCHERTZER, J. D., ANTONESCU, C. N., BILAN, P. J., JAIN, S., HUANG, X., LIU, Z., BONEN, A. & KLIP, A. 2009. A transgenic mouse model to study glucose transporter 4myc regulation in skeletal muscle. *Endocrinology,* 150**,** 1935-40.

SOLOMON, T. P., KNUDSEN, S. H., KARSTOFT, K., WINDING, K., HOLST, J. J. & PEDERSEN, B. K. 2012. Examining the Effects of Hyperglycemia on Pancreatic

Endocrine Function in Humans: Evidence for in Vivo Glucotoxicity. *J Clin Endocrinol Metab,* 97, 4682-91.

STEELE, R. 1959. Influences of glucose loading and of injected insulin on hepatic glucose output. *Ann N Y Acad Sci,* 82**,** 420-30.

STEINBERG, H. O., BRECHTEL, G., JOHNSON, A., FINEBERG, N. & BARON, A. D. 1994. Insulin-mediated skeletal muscle vasodilation is nitric oxide dependent. A novel action of insulin to increase nitric oxide release. *J Clin Invest,* 94**,** 1172-9.

VAAG, A., DAMSBO, P., HOTHER-NIELSEN, O. & BECK-NIELSEN, H. 1992. Hyperglycaemia compensates for the defects in insulin-mediated glucose metabolism and in the activation of glycogen synthase in the skeletal muscle of patients with type 2 (non-insulin-dependent) diabetes mellitus. *Diabetologia,* 35**,** 80-8.

VINCENT, M. A., BARRETT, E. J., LINDNER, J. R., CLARK, M. G. & RATTIGAN, S. 2003. Inhibiting NOS blocks microvascular recruitment and blunts muscle glucose uptake in response to insulin. *Am J Physiol Endocrinol Metab,* 285**,** E123-9.

YKI-JARVINEN, H., BOGARDUS, C. & HOWARD, B. V. 1987a. Hyperglycemia stimulates carbohydrate oxidation in humans. *Am J Physiol,* 253**,** E376-82.

YKI-JARVINEN, H., YOUNG, A. A., LAMKIN, C. & FOLEY, J. E. 1987b. Kinetics of glucose disposal in whole body and across the forearm in man. *J Clin Invest,* 79**,** 1713-9.

ZIERATH, J. R., HE, L., GUMA, A., ODEGOARD WAHLSTROM, E., KLIP, A. & WALLBERG-HENRIKSSON, H. 1996. Insulin action on glucose transport and plasma membrane GLUT4 content in skeletal muscle from patients with NIDDM. *Diabetologia,* 39**,** 1180-9.

ZIERATH, J. R., KROOK, A. & WALLBERG-HENRIKSSON, H. 2000. Insulin action and insulin resistance in human skeletal muscle. *Diabetologia,* 43**,** 821-35.

CHAPTER 7

GENERAL DISCUSSION

7.1. Introduction

Excess calorific intake and reduced levels of physical activity are contributing to the increasing prevalence of obesity and type 2 diabetes (T2D) worldwide. Overt T2D is preceded by insulin resistance; a phenomenon whereby peripheral tissues do not respond adequately to insulin resulting in hyperglycaemia and related complications. The mechanisms that contribute to increased postprandial glucose uptake in healthy individuals need to be further investigated in order to identify the main targets for interventions to combat the increasing prevalence of T2D. Skeletal muscle is both the primary site of postprandial glucose uptake in insulin sensitive individuals (Katz et al., 1983, Ferrannini et al., 1985) and a major site of insulin resistance in obesity and T2D (DeFronzo et al., 1985). GLUT4 is the major glucose transporter isoform expressed in skeletal muscle (Mueckler, 1994). As such GLUT4 has a significant role to play in the successful, or unsuccessful, maintenance of glucose homeostasis. In the published literature membrane fractionation methods have been used to isolate the plasma membrane (PM) fraction of human skeletal muscle and estimate its GLUT4 content. However these methods have been criticised as they have a number of methodological limitations. Firstly membrane fractionation requires very large muscle samples (~1g) which would be impractical to achieve using the Bergstrom percutaneous needle biopsy technique (Bergstrom, 1975). However of greater importance is the potential contamination of PM fractions with myofibrillar proteins and other GLUT4-containing membranes (Fazakerley et al., 2009b) and the inability to discriminate between GLUT4 just adjacent to the PM and GLUT4 fully incorporated into the PM and able to transport glucose (Schertzer et al., 2009). Both of these limitations may lead to overestimation of the GLUT4 content of the PM. Therefore an overarching aim of this thesis was to develop an immunofluorescence microscopy method suitable for measurement of both the subcellular

distribution of GLUT4 in storage vesicles of various sizes and the colocalisation of GLUT4 with the PM marker dystrophin in sections of human skeletal muscle (chapter 2). This method was then used in the subsequent chapters to compare the effect of 2 modes of exercise training (chapter 3), acute oral glucose ingestion, endurance exercise and the combination of the two (chapter 4), a hyperinsulinaemic-isoglycaemic clamp in lean and obese Zucker rats (chapter 5) and a hyperglycaemic clamp in human volunteers with normal glucose tolerance (NGT) and T2D (chapter 6) on size and distribution of the GLUT4 stores and colocalisation with the PM marker dystrophin.

7.2. Novel findings of this thesis and relevance to the existing literature

7.2.1. GLUT4 immunofluorescence microscopy method development

An immunofluorescence microscopy method has been developed using a fully validated GLUT4 antibody to visualise the subcellular distribution of GLUT4 in human and rat skeletal muscle (chapter 2). This method has shown that GLUT4 in human *vastus lateralis* muscle in the overnight fasted state is present in large clusters (> 1 µm diameter) and in smaller clusters (< 1µm diameter), which are both dispersed throughout the cell interior. GLUT4 clusters of both sizes are also observed close to or colocalising with the PM marker dystrophin, in particular in perinuclear regions. This subcellular distribution is very similar to the distribution seen previously in the published literature in rodent skeletal muscle using confocal fluorescence and transmission electron microscopy with the majority of GLUT4 localised to the fibre periphery and in large and small clusters (Ploug et al., 1998, Lauritzen et al., 2006). This similarity provides the first indication that the immunofluorescence microscopy method developed in this thesis is valid. A Pearson's correlation coefficient of approximately 0.4 in the overnight fasted state indicated that substantial GLUT4 and

dystrophin colocalisation was already present in the overnight fasted state. In support of this observation studies in transgenic mouse muscle fibres using labelling of exofacially tagged GLUT4 demonstrate GLUT4 fusion with the PM in the basal state; with one study describing a small amount of exofacially-tagged GLUT4 labelling in the basal state (Lizunov et al., 2012) and another reporting a more substantial amount with externalised *myc* labelling under basal conditions approximately 50 % of that after insulin stimulation (Schertzer et al., 2009). In addition the images in chapter 2 also show that GLUT4 colocalises with the T-tubule membrane marker DHPR in the overnight fasted state. These findings are in contrast to EM studies in rodent skeletal muscle using the immunogold labelling technique that report very little GLUT4 in the PM and T-tubule membranes in the basal state (Ploug et al., 1998, Rodnick et al., 1992). As explained, however, in chapter 1 there are some methodological issues with immunogold labelling of GLUT4 which may lead to an underestimation of the GLUT4 content of the PM in the basal state. The above immunofluorescence method was subsequently used to generate the novel results described in the following chapters of the thesis, which are summarised in the subsequent sections.

7.2.2. Training induced changes in subcellular GLUT4 distribution and GLUT4 content

In chapter 3 a comparison was made between the effect of 6 weeks sprint interval training (SIT, repeated Wingate sprints) and traditional endurance training (ET) on total GLUT4 protein content and subcellular distribution in human *vastus lateralis* muscle of previously sedentary young men. This immunofluorescence microscopy technique confirmed equivalent increases in total muscle GLUT4 content seen previously using Western blot analysis following ET and SIT (Burgomaster et al., 2007, Little et al., 2010) and furthermore showed that the increases in total GLUT4 protein content were primarily due to an increase in number and area of the intracellular GLUT4 staining clusters. Large clusters (> 1 μm diameter)

increased predominantly in number, while the smaller clusters (< 1 μm diameter) increased in size, with no increase in number. Assuming that the increases in the intracellular GLUT4 stores also increase the total amount of GLUT4 available for translocation, this may contribute to the improved glucose homeostasis that was seen both after ET and SIT interventions of 1 -12 weeks in duration (Hughes et al., 1993, Dela et al., 1996, Cox et al., 1999, Babraj et al., 2009, Richards et al., 2010, Phillips et al., 1996, Daugaard et al., 2000, Burgomaster et al., 2007, Hood et al., 2011, Little et al., 2010). The colocalisation of GLUT4 with the PM marker dystrophin in biopsies taken in the overnight fasted state did not change following training. However, a more detailed analysis of the GLUT4 stores in close proximity to the PM is required to further investigate the subcellular localisation of increases in GLUT4 content. This will be discussed in section 7.5 of this chapter. Previous literature suggested that the increase in GLUT4 following training occurs in insulin responsive stores in particular, therefore, increasing the GLUT4 available for GLUT4 translocation in response to a given insulin stimulus (Ivy, 2004).

7.2.3. Effect of acute exercise and oral glucose ingestion on GLUT4 localisation

In chapter 4 immunofluorescence visualisation of GLUT4 using the method developed in chapter 2 has clearly shown an increase in GLUT4 staining around the PM following 30 min of cycling exercise at 65 % of VO_{2max} in human skeletal muscle. GLUT4 exhibited a continuous PM signal following exercise and marked increases were seen in colocalisation of GLUT4 with dystrophin staining both visually and through quantitation using the Pearson's correlation coefficient. Therefore, these results suggest that this newly developed immunofluorescence colocalisation method can be used to show exercise-induced increases in GLUT4 translocation to the PM in human skeletal muscle. The data presented in this thesis is in line with immunofluorescence data in rodent skeletal muscle in which just 5 min of

electrical stimulation induced an ~50 % increase in GLUT4 PM content, which was maintained during 30 min electrical stimulation (Ploug et al., 1998, Lauritzen et al., 2010). In addition chapter 4 showed that the redistribution of GLUT4 in response to exercise occurred without any changes in the content and distribution of SNAP23 in the PM, suggesting that there is enough SNAP23 present in the overnight fasted state to allow increased docking and fusion of GLUT4 in the PM in response to exercise.

Colocalisation of GLUT4 with dystrophin has also been measured in chapter 4 to investigate the effect that an oral glucose tolerance test has on GLUT4 translocation in human skeletal muscle. Thirty minutes after glucose ingestion moderate continuous GLUT4 staining along the PM was observed with significant increases in Pearson's correlation coefficient, though distinct GLUT4 clusters remained clearly visible. In contrast, the moderate continuous stain was not seen after 60 min and 90 min. Collectively these data suggest that GLUT4 translocation to the PM in response to the physiological rises in plasma insulin following glucose feeding is transient. This observation is novel and is somewhat surprising given previous observations that rates of glucose disposal (Ferrannini et al., 1985, Breen et al., 2011) and leg glucose uptake (Katz et al., 1983) are still elevated 90 min following glucose ingestion. In addition while Lauritzen *et al.* (2006) observed accumulation of GLUT4-GFP at the mouse muscle fibre border 10 min after injection of insulin into a tail vein, with maximum values reached after 20 min (Lauritzen et al., 2006), the accumulation of GLUT clusters in the PM region remained elevated for 150 min (Lauritzen et al., 2008). It should, however, be noted that the amount of insulin injected was very high in this study and that the plasma insulin concentrations reached were equally high (approximately 200 000 $\mu IU.mL^{-1}$) (Lauritzen et al., 2008). For comparison, the hyperinsulinaemic-isoglycaemic clamp in

chapter 5 in the lean Zucker rats led to a mean plasma insulin concentration of ~ 320 μIU.mL^{-1}.

In addition the results of chapter 4 suggest that the magnitude of GLUT4 translocation in human skeletal muscle is greater following 30 min exercise at 65% VO_{2max} than 30 min following glucose ingestion. In adipocytes two modes of insulin-mediated GLUT4 exocytosis have been proposed to occur whereby 1) the prevalence of distinct GLUT4 clusters in PM regions already present in the basal state increases and 2) GLUT4 molecules disperse into the PM (Stenkula et al., 2010). The GLUT4 translocation data in human skeletal muscle presented in this thesis may be of relevance to the work of Stenkula *et al.* (2010). Following exercise, the clusters of GLUT4 staining are absent and GLUT4 staining is instead continuous along the PM, indicative of GLUT4 dispersal in the PM. On the other hand, following glucose ingestion, GLUT4 clusters localised to the PM remain clearly visible despite the appearance of moderate continuous staining along the PM at 30 min following glucose ingestion. These observations that exercise appears to induce greater GLUT4 dispersal through the PM in comparison to glucose ingestion, in combination with the differing magnitude of the increase in Pearson's correlation coefficient, led to the suggestion in chapter 4 that the magnitude of GLUT4 translocation in human skeletal muscle is greater following exercise at 65% VO_{2max} than 30 min following glucose ingestion. This is consistent with skeletal muscle glucose uptake data which showed 3-fold increases in leg glucose uptake in the 4 h period following glucose feeding (Katz et al., 1983) and 15-fold increases in leg glucose uptake during exercise at 50-60% VO_{2max} (Katz et al., 1986, Martin et al., 1995).

7.2.4. Effect of a hyperinsulinaemic-isoglycaemic clamp on GLUT4 localisation in Zucker rats

Eighty minutes after the start of a hyperinsulinaemic-isoglycaemic clamp in lean (LZR) and obese (OZR) Zucker rats, there was no increase in the colocalisation of GLUT4 with dystrophin in skeletal muscle fibres in comparison to the post-absorptive state despite substantially elevated rates of glucose disposal (chapter 5). A potential explanation for the lack of increase in GLUT4 and dystrophin colocalisation during the hyperinsulinaemic-isoglycaemic clamp is that the effect of the insulin stimulation, similar to the effect of the OGTT in chapter 4, is transient. Reinternalization of the fused GLUT4 molecules may then occur, in this case despite the continuously high insulin concentrations, with the insulin signal switched off at the later time points. This would imply that other mechanism take over at the later time points to explain the continuously high glucose disposal rates observed in this study and the continuously high muscle glucose uptake rates observed previously during a 2 h hyperinsulinaemic-isoglycaemic clamp in rats (Wallis et al., 2002). Unfortunately, as the study design was formulated based on the expectation that GLUT4 translocation would occur at 80 min muscle samples were not collected at earlier time points and, therefore, this explanation cannot be supported with hard evidence.

There were also no differences in GLUT4 and dystrophin colocalisation between LZR and OZR in the overnight fasted and the insulin-stimulated states, despite previous studies reporting significant reductions in skeletal muscle glucose uptake during a 2 h hyperinsulinaemic-isoglycaemic clamp in OZR compared to LZR (Wallis et al., 2002). This implied that there are other mechanisms than impaired GLUT4 translocation behind the skeletal muscle insulin resistance in the OZR.

7.2.5. Effect of a hyperglycaemic glucose clamp 5.4 mM above the overnight fasted level in human volunteers with NGT and T2D

A 2 h intravenous glucose infusion with the aim to create hyperglycaemic conditions, with the plasma glucose concentration elevated 5.4 mM above overnight fasted levels, was sufficient to raise plasma insulin concentrations markedly above baseline and elevate rates of whole body glucose disposal in NGT, therefore insulin sensitive, volunteers (chapter 6). However, the expected increase in colocalisation of GLUT4 with dystrophin following 2 h hyperglycaemia compared to the overnight fasted state did not occur. These data seem to suggest that after 2 h intravenous glucose infusion, GLUT4 PM content is not responsible for the elevated rates of whole body glucose disposal. It is possible that similar to the OGTT (chapter 4), intravenous glucose infusion also leads to transient increases in colocalisation between GLUT4 and dystrophin. These muscle samples were part of a research collaboration and no biopsy was taken at earlier timepoints to enable investigation of this possibility. There also were no increases compared to the overnight fasted state in the colocalisation of GLUT4 with dystrophin in the patients with T2D. Pearson's correlation coefficients in fact were the same for both groups both in the overnight fasted state and after 2 h of hyperglycaemia. This suggests that the insulin resistance of T2D does not lead to a reduction in the colocalisation of GLUT4 with the PM marker dystrophin either in the overnight fasted state or following 2 h intravenous glucose infusion. Following 24 h of hyperglycaemia in NGT, insulin sensitivity was reduced to values seen in T2D following 2 h hyperglycaemia, again with no changes in GLUT4 and dystrophin colocalisation. Similar to the observations made in chapter 5, the data resulting from intravenous glucose infusion suggests that changes in GLUT4 fusion with the skeletal muscle fibre PM are not responsible for decreases in whole body glucose disposal that occur in T2D individuals following 2 h hyperglycaemia compared to NGT and are also

not important in the development of insulin resistance following 24 h of hyperglycaemia in NGT.

7.3. Comments on methodology in relation to the published literature

The limitations of membrane fractionation methods in combination with Western blot analysis to investigate GLUT4 translocation in response to insulin and contraction are discussed in section 1.4.1 of the general introduction. These limitations provided the rationale for the development of a new method to investigate GLUT4 subcellular localisation and translocation to the PM in human skeletal muscle in this thesis. Confocal fluorescence microscopy studies published in the literature in rodent skeletal muscle and the data presented in chapter 4 of this thesis in human skeletal muscle have both shown insulin- and contraction-mediated translocation of GLUT4 to the PM (Lauritzen et al., 2008, Lauritzen et al., 2006, Lauritzen et al., 2010). The method presented in this thesis is superior to that in the confocal fluorescence microscopy studies (Lauritzen et al., 2006, Lauritzen et al., 2008, Lauritzen et al., 2010) in the sense that it utilises the PM marker dystrophin to identify the PM and quantifies GLUT4 and dystrophin colocalisation rather than quantifying GLUT4 intensity in a peripheral region of interest assumed to be the PM. One technique that can be utilised in rodent muscle but not human muscle *in vivo* due to technological limitations is exofacial tagging of GLUT4 with GFP, haemaglutinnin (HA) or myc protein tags. GLUT4-GFP fusion protein has enabled highly elegant analysis of the temporal response of GLUT4 translocation to insulin and contraction *in vivo* in mouse muscle (Lauritzen et al., 2006, Lauritzen et al., 2008, Lauritzen et al., 2010). HA and myc protein tags on the first extracellular loop of GLUT4, which becomes extracellular only when GLUT4 is inserted into the PM, has allowed confirmation of GLUT4 insertion into the PM in isolated muscle cells through detection of the externalised tag with an anti-myc (Schertzer et al., 2009) or anti-HA antibody (Fazakerley et

al., 2009a). However as specified neither method can be applied to human skeletal muscle *in vivo*.

While confocal microscopy achieves superior resolution in comparison to widefield microscopy, all light microscopy methods have a resolution limit of approximately 200 nm. The significance of this resolution limit to the data presented in this thesis and the previously published literature became apparent towards the end of the PhD studies comprising this thesis. TIRF microscopy studies in mouse skeletal muscle that endogenously expressed a HA-GLUT4-GFP protein, have shown that eighty percent of insulin-mediated GSV fusion events emanated from stationary vesicles that were within 100 nm of the PM and therefore likely pre-tethered at the PM prior to insulin stimulation (Lizunov et al., 2012). The small pool of mobile GSVs was not affected by insulin (Lizunov et al., 2012). This demonstrates the importance of pre-tethered GLUT4 localised within 100 nm of the PM (Lizunov et al., 2012).

Therefore given the resolution limit of light microscopy it is not possible to distinguish between a vesicle that is fused at the PM, pre-tethered at the PM or simply in close proximity to the PM (Schertzer et al., 2009, Lauritzen and Schertzer, 2010). Therefore, it should be noted that the transition from tethered to fused GLUT4 may not have been detected in the current study, which potentially limits the sensitivity of measuring increases in GLUT4 and dystrophin colocalisation using this method. However it is important to emphasise that this is a limitation observed with all standard confocal microscopy methods and similarly with measurement of GLUT4 content in isolated membrane fractions (Schertzer et al., 2009). The TIRF microscopy method also relies on expression of GLUT4 tagged with a fluorescent protein which means the method is not suitable for replication in human skeletal muscle *in vivo*. Despite the resolution limit of confocal microscopy, the immunofluorescence microscopy method developed in this thesis has been able to generate novel information

regarding GLUT4 localisation and GLUT4 translocation in human skeletal muscle. Therefore considering the limitations of subcellular fractionation methods and the inability to use TIRF methodology in human skeletal muscle *in vivo,* the immunofluorescence microscopy method developed in this thesis is the best method currently available to generate novel information on GLUT4 localisation in human skeletal muscle. The results obtained in this thesis have shown that this method can be used to measure fibre type specific GLUT4 content, changes in the number and size of GLUT4 clusters induced by training interventions, and changes in the colocalisation of GLUT4 with the PM marker dystrophin induced by moderate intensity exercise and ingestion of a 75 g bolus of glucose.

7.4. Mechanisms in addition to GLUT4 fusion with the skeletal muscle fibre PM that may contribute to increases in skeletal muscle glucose uptake

The modest transient increase in GLUT4 and dystrophin colocalisation seen after glucose ingestion in chapter 4 does not seem to account for the 3-fold increase in skeletal muscle glucose uptake observed in the 4 h period following glucose feeding (Katz et al., 1983). The increase in Pearson's correlation coefficient seen after 30 min of exercise also does not seem to explain the 15-fold increase in muscle glucose uptake that is seen during exercise at 50-60% VO_{2max} (Katz et al., 1986, Martin et al., 1995). In addition the absence of an increase in GLUT4 and dystrophin colocalisation 80 min into a hyperinsulinaemic-isoglycaemic clamp in LZR (chapter 5) does not explain the 5-fold increase in glucose infusion rate observed in chapter 5 or the 5-fold increase in hind-limb glucose uptake observed previously during a 2 h hyperinsulinaemic-isoglycaemic clamp in LZR (Wallis et al., 2002). This implies that in these conditions there must be additional parallel mechanisms or alternative mechanisms that lead to these marked increases in muscle glucose uptake.

In chapter 2 we observed colocalisation of GLUT4 with the dihydropyridine receptor (DHPR) which confirms GLUT4 is also present in the T-tubule membranes in human skeletal muscle similar to observations made before in rodent muscle. The T-tubule membrane system comprises invaginations of the muscle PM which extend deep into the muscle fibre and is well characterised as a site of insulin- and contraction-mediated GLUT4 translocation in rodent muscle (Ploug et al., 1998, Lauritzen et al., 2006, Lauritzen et al., 2010). The T-tubule membrane surface area has been suggested to be two- to three-fold larger than that of the PM (Lauritzen et al., 2006), with suggestions that it may even be nine times larger and may contribute as much as 94 % of the GLUT4-mediated glucose uptake in rodent skeletal muscle (Wang et al., 1996). Regretfully it was not possible to quantify GLUT4 translocation to the T-tubule membranes due to methodological difficulties that have been discussed in chapter 2. Suggestions that may help to improve the quantitation of GLUT4 translocation to the T-tubule membranes in human skeletal muscle in future studies are given in section 7.5 of this chapter. It, however, remains possible that at the time points sampled in this study, increases in GLUT4 localisation may have been much more prominent at the T-tubule membranes compared to the PM.

Insulin-mediated skeletal muscle microvascular vasodilation leading to increases in skeletal muscle capillary blood flow is a second mechanism that may lead to increases in the delivery of both glucose and insulin to the interstitial fluid that surrounds the muscle fibres and that, therefore, may increase skeletal muscle glucose uptake (Clark, 2008, Steinberg et al., 1994). Insulin-mediated skeletal muscle microvascular vasodilation begins 5-10 min into a hyperinsulinaemic-euglycaemic clamp in rats and precedes the activation of the insulin signalling cascade and increases in glucose uptake in skeletal muscle (Vincent and Barrett, 2002, Vincent et al., 2004). Of relevance to the later time points in particular, Gudbjornsdottir

et al. (2003) have shown that there are marked increases in the capillary permeability surface area (PSA) product which are proportional to the increase in glucose uptake that has been observed 90-120 min after the start of an OGTT and even larger increases in that period during a hyperinsulinaemic-euglycaemic clamp using physiological insulin levels (Gudbjornsdottir et al., 2003). In addition increases in total leg and muscle blood flow that are beginning to occur approximately 2 h after the start of a hyperglycaemic-euglycaemic clamp (Laakso et al., 1990, Utriainen et al., 1995, Yki-Jarvinen and Utriainen, 1998) may also contribute to the high glucose disposal rate observed at later time-points in chapters 5 (hyperinsulinaemic-isoglycaemic clamp in rats) and 6 (hyperglycaemic glucose clamp in individuals with NGT), conditions in which no increases in colocalisation of GLUT4 with dystrophin were observed.

A number of studies have provided evidence that an increase in GLUT4 intrinsic activity may occur after GLUT4 has translocated to and fused with the PM and this is a third mechanism that may thus contribute to the increase in glucose uptake under insulin-stimulated conditions (Michelle Furtado et al., 2003). Potential mechanisms proposed for the increase in GLUT4 intrinsic activity include phosphorylation and binding of enhancer or inhibitor proteins, the latter of which is suggested to change the activity of GLUT4 through changes in its 3D structure (Michelle Furtado et al., 2003).

The final step in glucose uptake into the skeletal muscle is the irreversible phosphorylation of glucose to glucose 6-phosphate by the enzyme hexokinase (HKII), thereby trapping the glucose molecule inside the muscle cell (Wasserman et al., 2011). A negative feedback mechanism also exists whereby glucose 6-phosphate inhibits HKII activity (Wasserman et al., 2011). Studies in transgenic mice that over-express HKII in skeletal muscle have shown increased muscle glucose uptake during hyperinsulinaemic-euglycaemic clamp in comparison

to wild type controls (Fueger et al., 2004). In addition transgenic mice in which HKII activity is impaired by approximately 50 % in heart, muscle and adipose tissue displayed reduced whole body insulin sensitivity assessed during a hyperinsulinaemic-euglycaemic clamp (Fueger et al., 2007). Mechanisms that lead to activation of HKII should, therefore, also be considered as a mechanism that may increase muscle glucose uptake, providing sufficient GLUT4 is available at the PM for glucose transport into the muscle cell (Wasserman et al., 2011). In addition downstream processes such as increased glycogen synthesis may have a role to play in increasing rates of muscle glucose uptake. For example, increased glycogen synthesis will reduce intracellular glucose 6-phosphate concentration thereby increasing HKII activity and increasing phosphorylation of glucose. This in turn would decrease the free glucose concentration in the muscle and increase the concentration gradient between arterial blood, the interstitium and the muscle fibres, thereby leading to increased rates of GLUT4-mediated glucose transport (Wasserman et al., 2011).

In summary while chapter 4 clearly shows GLUT4 translocation occurs in human skeletal muscle 30 min following glucose ingestion and following 30 min cycling exercise at 65 % VO_{2max}, there are additional mechanisms that may contribute to insulin- and contraction-mediated increases in skeletal muscle glucose uptake which may predominate when the colocalisation of GLUT4 and dystrophin returns to the overnight fasted baseline values (at 60 and 90 min into the OGTT) or does not increase above the overnight fasted baseline values (chapter 5 and 6). These mechanisms were beyond the scope of this thesis and, therefore, have not been investigated.

7.5. Suggestions for future research

7.5.1. Possibilities for improvement in the GLUT4 translocation assay in human skeletal muscle

As mentioned in the previous section a major aspect of the role that GLUT4 translocation may play in increases in skeletal muscle glucose uptake that could not be evaluated in the studies contributing to this thesis is the translocation of GLUT4 to and fusion with the T-tubule membranes. Methodological issues associated with the quantitation of T-tubule GLUT4 content (chapter 2) prevented its assessment in response to glucose ingestion, acute exercise, a hyperinsulinaemic-isoglycaemic clamp and a hyperglycaemic glucose clamp. The development of a method to quantify GLUT4 content in the T-tubule membranes remains an important target for future research. Immunofluorescence microscopy of single human muscle fibres might offer a solution as it allows elongation of the sarcomeres and, therefore, may allow clearer visualisation of GLUT4 in T-tubule membranes (Murphy et al., 2009). This muscle fibre preparation method should be combined with assessment of colocalisation of the GLUT4 stain with the T-tubule membrane marker DHPR and assessment of the intensity of the GLUT4 striations using line profiling techniques (Sylow et al., 2013).

Further information on GLUT4 localisation changes in response to exercise training, glucose and insulin administration and acute exercise could be gained through more detailed analysis of the large and small intracellular GLUT4 clusters. One option to contribute towards this would be to use specific markers to label GSVs, endosomes and TGN associated membranes, such as VAMP2 (Foley et al., 2011), tranferrin receptor (TfR) (Ploug et al., 1998) and TGN38 (Ploug et al., 1998), respectively. Assessment of colocalisation of GLUT4 with these markers using confocal immunofluorescence microscopy could generate further information on whether training increases GLUT4 content in a particular storage location and whether

glucose feeding and exercise recruit GLUT4 from a particular storage location in human skeletal muscle. Furthermore it could be helpful to measure the content of the GLUT4 clusters observed in this thesis in concentric layers extending into the fibre from the PM to determine 1) whether training induces greater increases in GLUT4 stores in layers closer to the PM and 2) whether insulin and contraction deplete GLUT4 to a greater extent from stores closer to the PM as observed in rodent muscle by (Lizunov et al., 2012). Such measurements would require additional software which is commercially available (MATLAB, v. 2012b, The MathWorks Inc., Natick, MA, 2012).

The above methods to further investigate the identity of GLUT4 storage clusters in human skeletal muscle could all be carried out using standard confocal immunofluorescence microscopy methods; albeit with the consideration of the 200 nm resolution limit of light microscopy methods. However to fully confirm GLUT4 and the TGN, endosomal or GSV markers are localised to the same compartment rather than two compartments within 200 nm of one another higher resolution imaging methods are required. One option for this would be super resolution fluorescence microscopy, such as stimulated emission depletion (STED) microscopy, which can achieve a spatial resolution of 30-40 nm (Huang et al., 2009). This has the advantage of being able to use fluorescence markers for colocalisation analysis, which would enable easier quantitation, through colocalisation, of changes in the GLUT4 content of TGN, endosome membranes and GSVs following training, glucose administration or acute exercise. The alternative would be to use transmission electron microscopy (TEM), which can achieve a spatial resolution of 0.3-1 nm (Massover, 2011). In this case antibodies conjugated to colloidal gold particles of different diameters would be used to identify GLUT4 and TGN, endosomal or GSV markers (Hagiwara et al., 2010). These high resolution methods of course

require access to highly specialised equipment, which was not possible during the PhD studies presented in this thesis.

7.5.2. Suggestions for future applications of the newly-developed GLUT4 translocation assay

Future experiments need to investigate additional time points in studies similar to those presented in this thesis. Firstly, the early response to a hyperinsulinaemic-isoglycaemic clamp in LZR and to a hyperglycaemic glucose clamp in NGT should be investigated to determine whether, as suggested in this thesis, the GLUT4 translocation response is transient in these situations, similar to observations made during an OGTT in chapter 4 of this thesis. Secondly it would be worth investigating whether GLUT4 translocation can be detected in human skeletal muscle at 15 min following glucose feeding, as it is possible that the maximum GLUT4 translocation response occurs before the 30 min time point sampled in this thesis.

Another important application of this GLUT4 translocation assay in humans will be to compare increases in GLUT4 and dystrophin colocalisation, and if the methodological problems can be solved increases in GLUT4 T-tubule membrane content, in insulin sensitive, insulin resistant and T2D human populations, over a time course following glucose ingestion and during exercise. The number of possible time points comprising a time course is limited in a human study due to the invasive nature of a percutaneous muscle biopsy. The optimum time points are difficult to establish however suggestions would be at baseline and 15, 30 and 60 min following glucose feeding and in a separate cohort of matched participants at baseline and 15, 30 and 60 min into cycling exercise at 65 % VO_{2max}. Plasma membrane fractionation studies have suggested that insulin- but not contraction-mediated GLUT4 translocation would be reduced in T2D individuals (Zierath et al., 1996, Garvey et al., 1998, Kennedy et al., 1999). This now needs to be confirmed with the immunofluorescence microscopy method presented in this thesis. In an ideal scenario assessment of GLUT4 translocation would be

combined with assessment of leg glucose uptake and microvascular recruitment through the leg glucose balance technique (Baron et al., 1988) and contrast-enhanced ultrasound (CEU) (Clark, 2008, Sjoberg et al., 2011), respectively, to assess the contribution of the most important alternative mechanisms in the control of skeletal muscle glucose uptake. The CEU method to measure microvascular recruitment in response to insulin and exercise should be complemented with an immunofluorescence microscopy method used to measure eNOS Ser 1177 phosphorylation in the microvasculature (Cocks et al., 2012) at all time points at which muscle biopsy samples are collected. Taken together these data would provide valuable information on the relative role played by increases in GLUT4 PM content and microvascular recruitment in the increases in insulin- and contraction-mediated skeletal muscle glucose uptake at different time points after glucose feeding and following the onset of exercise.

Another area of interest to which a GLUT4 translocation assay could be applied is in the investigation of increases in insulin sensitivity that occur following an acute exercise bout. Once again membrane fractionation methods have suggested that insulin-mediated GLUT4 translocation to the PM is increased following a prior exercise bout (Hansen et al., 1998), however this again ought to be tested with the immunofluorescence microscopy method developed in this thesis. Similarly this immunofluorescence microscopy method could be used to further investigate the mechanisms behind the exercise training-induced increases in insulin sensitivity (Hughes et al., 1993, Dela et al., 1996, Cox et al., 1999, Babraj et al., 2009, Richards et al., 2010, Phillips et al., 1996, Daugaard et al., 2000, Burgomaster et al., 2007, Hood et al., 2011, Little et al., 2010). Firstly it should be investigated whether training induces increases in insulin- and contraction-mediated GLUT4 translocation, in addition to the increases in total GLUT4 content in human skeletal muscle in chapter 3. This could be assessed by comparing the increase in Pearson's correlation coefficient following glucose

feeding and exercise before and after a period of exercise training. Using the earlier suggestion to combine GLUT4 immunofluorescence staining with staining for TGN, endosomal and GSV markers for different pools of GLUT4, it may be possible to determine whether particular pools that increase their GLUT4 content following training are then preferentially depleted following glucose feeding or exercise to enhance the GLUT4 translocation response. This could help to further elucidate the mechanism behind the training-induced improvements in insulin sensitivity.

7.5.3. The importance of combining an assay for GLUT4 translocation with assessment of SNAP23 localisation

Combined staining of GLUT4 and SNAP23 at the PM, as was attempted in chapter 2, would enable assessment of whether regions of GLUT4 and SNAP23 staining heterogeneity at the PM are localised to the same region. If this were confirmed to be the case it would support the idea that GSV fusion with the PM occurs at specific PM domains. Chamberlain and Gould (2002) observed that the majority of SNAP23 was present in PM lipid rafts in 3T3-L1 adipocytes (Chamberlain and Gould, 2002). Lipid rafts are cholesterol and sphingolipid-enriched regions of the PM (Owen et al., 2012). Therefore in future studies it should be explored whether SNAP23 is also localised to lipid rafts domains in human skeletal muscle, implying that the lipid rafts would be the sections of the PM where preferential docking and fusion of GLUT4 occurs prior to subsequent diffusion of GLUT4 along the PM leading to the heterogeneous distribution seen in chapter 4 30 min after glucose feeding and the onset of cycling exercise. The lipid content of lipid raft domains may be vital for the successful docking and fusion of GLUT4 at the PM and would also bring GLUT4 into close proximity with the insulin signalling proteins Cbl and TC10 which reside in lipid rafts (Baumann et al., 2000, Chiang et al., 2001). Identification of individual lipid rafts through

immunofluorescence microscopy is challenging due to limitations in the markers available and the small size (10-200 nm) of the raft domains. However glycophosphatidylinositol (GPI)-anchored proteins have been used previously as lipid raft markers and super resolution microscopy methods discussed previously could be used to identify individual lipid raft domains and therefore assess colocalisation of GLUT4 and SNAP23 (Owen et al., 2012). In addition combination of GLUT4 and SNAP23 staining would allow further investigation of the SNARE highjacking hypothesis (Sollner, 2007) by determining whether increased skeletal muscle lipid content reduces SNAP23 content in the PM and inhibits the translocation of GLUT4 in the insulin stimulated state. This would add further to the limited evidence that reduced t-SNARE-PM abundance contributes to the impaired insulin action involved in the pathogenesis of T2D.

7.6. Final conclusions

The immunofluorescence method to assess GLUT4 localisation developed as part of this thesis has demonstrated that exercise training-induced increases in GLUT4 content are driven predominantly by increases in the number of large and area of small intracellular GLUT4 storage clusters. Furthermore insulin- and contraction-mediated GLUT4 translocation have been successfully visualised and quantified in human skeletal muscle for the first time. The data presented in this thesis further suggest that insulin-mediated GLUT4 translocation is transient and occurs following a similar temporal pattern to the peak elevation in plasma insulin concentration. In addition the evidence indicates that GLUT4 PM content is not always the determining factor for glucose uptake and other factors such as microvascular recruitment, intrinsic GLUT4 activation and HKII activity may play a role as well.

Further experiments are required to confirm that increases in translocation also occur in the first 30 min of hyperinsulinaemic-isoglycaemic clamp in LZR and 30 min after the start of a hyperglycaemic clamp in humans as suggested in chapters 5 and 6 (NGT group only). In future studies these methods should then be used to assess the fundamental mechanisms behind insulin- and contraction mediated glucose uptake and investigate the mechanisms underlying the development of skeletal muscle insulin resistance and T2D. Beyond that these methods will enable investigation into whether lifestyle and pharmaceutical interventions are able to rescue GLUT4 translocation and normalise glycaemic control. This can in turn inform medical professionals as to the optimal interventions and metabolic targets to combat the increasing prevalence of insulin resistance, metabolic syndrome and T2D worldwide thereby reducing the associated financial burden and mortality implications.

7.7. References

BABRAJ, J. A., VOLLAARD, N. B., KEAST, C., GUPPY, F. M., COTTRELL, G. & TIMMONS, J. A. 2009. Extremely short duration high intensity interval training substantially improves insulin action in young healthy males. *BMC Endocr Disord,* 9**,** 3.

BARON, A. D., BRECHTEL, G., WALLACE, P. & EDELMAN, S. V. 1988. Rates and tissue sites of non-insulin- and insulin-mediated glucose uptake in humans. *Am J Physiol,* 255**,** E769-74.

BAUMANN, C. A., RIBON, V., KANZAKI, M., THURMOND, D. C., MORA, S., SHIGEMATSU, S., BICKEL, P. E., PESSIN, J. E. & SALTIEL, A. R. 2000. CAP defines a second signalling pathway required for insulin-stimulated glucose transport. *Nature,* 407**,** 202-7.

BERGSTROM, J. 1975. Percutaneous needle biopsy of skeletal muscle in physiological and clinical research. *Scand J Clin Lab Invest,* 35**,** 609-16.

BREEN, L., PHILP, A., SHAW, C. S., JEUKENDRUP, A. E., BAAR, K. & TIPTON, K. D. 2011. Beneficial effects of resistance exercise on glycemic control are not further improved by protein ingestion. *PLoS One,* 6**,** e20613.

BURGOMASTER, K. A., CERMAK, N. M., PHILLIPS, S. M., BENTON, C. R., BONEN, A. & GIBALA, M. J. 2007. Divergent response of metabolite transport proteins in human skeletal muscle after sprint interval training and detraining. *Am J Physiol Regul Integr Comp Physiol,* 292**,** R1970-6.

CHAMBERLAIN, L. H. & GOULD, G. W. 2002. The vesicle- and target-SNARE proteins that mediate Glut4 vesicle fusion are localized in detergent-insoluble lipid rafts present on distinct intracellular membranes. *J Biol Chem,* 277**,** 49750-4.

CHIANG, S. H., BAUMANN, C. A., KANZAKI, M., THURMOND, D. C., WATSON, R. T., NEUDAUER, C. L., MACARA, I. G., PESSIN, J. E. & SALTIEL, A. R. 2001. Insulin-stimulated GLUT4 translocation requires the CAP-dependent activation of TC10. *Nature,* 410**,** 944-8.

CLARK, M. G. 2008. Impaired microvascular perfusion: a consequence of vascular dysfunction and a potential cause of insulin resistance in muscle. *Am J Physiol Endocrinol Metab,* 295**,** E732-50.

COCKS, M., SHEPHERD, S. O., SHAW, C. S., ACHTEN, J., COSTA, M. L. & WAGENMAKERS, A. J. 2012. Immunofluorescence microscopy to assess enzymes controlling nitric oxide availability and microvascular blood flow in muscle. *Microcirculation,* 19**,** 642-51.

COX, J. H., CORTRIGHT, R. N., DOHM, G. L. & HOUMARD, J. A. 1999. Effect of aging on response to exercise training in humans: skeletal muscle GLUT-4 and insulin sensitivity. *J Appl Physiol,* 86**,** 2019-25.

DAUGAARD, J. R., NIELSEN, J. N., KRISTIANSEN, S., ANDERSEN, J. L., HARGREAVES, M. & RICHTER, E. A. 2000. Fiber type-specific expression of GLUT4 in human skeletal muscle: influence of exercise training. *Diabetes,* 49**,** 1092-5.

DEFRONZO, R. A., GUNNARSSON, R., BJORKMAN, O., OLSSON, M. & WAHREN, J. 1985. Effects of insulin on peripheral and splanchnic glucose metabolism in noninsulin-dependent (type II) diabetes mellitus. *J Clin Invest,* 76**,** 149-55.

DELA, F., MIKINES, K. J., LARSEN, J. J. & GALBO, H. 1996. Training-induced enhancement of insulin action in human skeletal muscle: the influence of aging. *J Gerontol A Biol Sci Med Sci,* 51**,** B247-52.

FAZAKERLEY, D. J., HOLMAN, G. D., MARLEY, A., JAMES, D. E., STOCKLI, J. & COSTER, A. C. 2009a. Kinetic evidence for unique regulation of GLUT4 trafficking by insulin and AMP-activated protein kinase activators in L6 myotubes. *J Biol Chem,* 285**,** 1653-60.

FAZAKERLEY, D. J., LAWRENCE, S. P., LIZUNOV, V. A., CUSHMAN, S. W. & HOLMAN, G. D. 2009b. A common trafficking route for GLUT4 in cardiomyocytes

in response to insulin, contraction and energy-status signalling. *J Cell Sci,* 122**,** 727-34.

FERRANNINI, E., BJORKMAN, O., REICHARD, G. A., JR., PILO, A., OLSSON, M., WAHREN, J. & DEFRONZO, R. A. 1985. The disposal of an oral glucose load in healthy subjects. A quantitative study. *Diabetes,* 34**,** 580-8.

FOLEY, K., BOGUSLAVSKY, S. & KLIP, A. 2011. Endocytosis, recycling, and regulated exocytosis of glucose transporter 4. *Biochemistry,* 50**,** 3048-61.

FUEGER, P. T., BRACY, D. P., MALABANAN, C. M., PENCEK, R. R., GRANNER, D. K. & WASSERMAN, D. H. 2004. Hexokinase II overexpression improves exercise-stimulated but not insulin-stimulated muscle glucose uptake in high-fat-fed C57BL/6J mice. *Diabetes,* 53**,** 306-14.

FUEGER, P. T., LEE-YOUNG, R. S., SHEARER, J., BRACY, D. P., HEIKKINEN, S., LAAKSO, M., ROTTMAN, J. N. & WASSERMAN, D. H. 2007. Phosphorylation barriers to skeletal and cardiac muscle glucose uptakes in high-fat fed mice: studies in mice with a 50% reduction of hexokinase II. *Diabetes,* 56**,** 2476-84.

GARVEY, W. T., MAIANU, L., ZHU, J. H., BRECHTEL-HOOK, G., WALLACE, P. & BARON, A. D. 1998. Evidence for defects in the trafficking and translocation of GLUT4 glucose transporters in skeletal muscle as a cause of human insulin resistance. *J Clin Invest,* 101**,** 2377-86.

GUDBJORNSDOTTIR, S., SJOSTRAND, M., STRINDBERG, L., WAHREN, J. & LONNROTH, P. 2003. Direct measurements of the permeability surface area for insulin and glucose in human skeletal muscle. *J Clin Endocrinol Metab,* 88**,** 4559-64.

HAGIWARA, H., AOKI, T., SUZUKI, T. & TAKATA, K. 2010. Double-label immunoelectron microscopy for studying the colocalization of proteins in cultured cells. *Methods Mol Biol,* 657**,** 249-57.

HANSEN, P. A., NOLTE, L. A., CHEN, M. M. & HOLLOSZY, J. O. 1998. Increased GLUT-4 translocation mediates enhanced insulin sensitivity of muscle glucose transport after exercise. *J Appl Physiol,* 85**,** 1218-22.

HOOD, M. S., LITTLE, J. P., TARNOPOLSKY, M. A., MYSLIK, F. & GIBALA, M. J. 2011. Low-volume interval training improves muscle oxidative capacity in sedentary adults. *Med Sci Sports Exerc,* 43**,** 1849-56.

HUANG, B., BATES, M. & ZHUANG, X. 2009. Super-resolution fluorescence microscopy. *Annu Rev Biochem,* 78**,** 993-1016.

HUGHES, V. A., FIATARONE, M. A., FIELDING, R. A., KAHN, B. B., FERRARA, C. M., SHEPHERD, P., FISHER, E. C., WOLFE, R. R., ELAHI, D. & EVANS, W. J. 1993. Exercise increases muscle GLUT-4 levels and insulin action in subjects with impaired glucose tolerance. *Am J Physiol,* 264**,** E855-62.

IVY, J. L. 2004. Muscle insulin resistance amended with exercise training: role of GLUT4 expression. *Med Sci Sports Exerc,* 36**,** 1207-11.

KATZ, A., BROBERG, S., SAHLIN, K. & WAHREN, J. 1986. Leg glucose uptake during maximal dynamic exercise in humans. *Am J Physiol,* 251**,** E65-70.

KATZ, L. D., GLICKMAN, M. G., RAPOPORT, S., FERRANNINI, E. & DEFRONZO, R. A. 1983. Splanchnic and peripheral disposal of oral glucose in man. *Diabetes,* 32**,** 675-9.

KENNEDY, J. W., HIRSHMAN, M. F., GERVINO, E. V., OCEL, J. V., FORSE, R. A., HOENIG, S. J., ARONSON, D., GOODYEAR, L. J. & HORTON, E. S. 1999. Acute exercise induces GLUT4 translocation in skeletal muscle of normal human subjects and subjects with type 2 diabetes. *Diabetes,* 48**,** 1192-7.

LAAKSO, M., EDELMAN, S. V., BRECHTEL, G. & BARON, A. D. 1990. Decreased effect of insulin to stimulate skeletal muscle blood flow in obese man. A novel mechanism for insulin resistance. *J Clin Invest,* 85**,** 1844-52.

LAURITZEN, H. P., GALBO, H., BRANDAUER, J., GOODYEAR, L. J. & PLOUG, T. 2008. Large GLUT4 vesicles are stationary while locally and reversibly depleted during transient insulin stimulation of skeletal muscle of living mice: imaging analysis of GLUT4-enhanced green fluorescent protein vesicle dynamics. *Diabetes,* 57**,** 315-24.

LAURITZEN, H. P., GALBO, H., TOYODA, T. & GOODYEAR, L. J. 2010. Kinetics of contraction-induced GLUT4 translocation in skeletal muscle fibers from living mice. *Diabetes,* 59**,** 2134-44.

LAURITZEN, H. P., PLOUG, T., PRATS, C., TAVARE, J. M. & GALBO, H. 2006. Imaging of insulin signaling in skeletal muscle of living mice shows major role of T-tubules. *Diabetes,* 55**,** 1300-6.

LAURITZEN, H. P. & SCHERTZER, J. D. 2010. Measuring GLUT4 translocation in mature muscle fibers. *Am J Physiol Endocrinol Metab,* 299**,** E169-79.

LITTLE, J. P., SAFDAR, A., WILKIN, G. P., TARNOPOLSKY, M. A. & GIBALA, M. J. 2010. A practical model of low-volume high-intensity interval training induces mitochondrial biogenesis in human skeletal muscle: potential mechanisms. *J Physiol,* 588**,** 1011-22.

LIZUNOV, V. A., STENKULA, K. G., LISINSKI, I., GAVRILOVA, O., YVER, D. R., CHADT, A., AL-HASANI, H., ZIMMERBERG, J. & CUSHMAN, S. W. 2012. Insulin stimulates fusion, but not tethering, of GLUT4 vesicles in skeletal muscle of HA-GLUT4-GFP transgenic mice. *Am J Physiol Endocrinol Metab,* 302**,** E950-60.

MARTIN, I. K., KATZ, A. & WAHREN, J. 1995. Splanchnic and muscle metabolism during exercise in NIDDM patients. *Am J Physiol,* 269**,** E583-90.

MASSOVER, W. H. 2011. New and unconventional approaches for advancing resolution in biological transmission electron microscopy by improving macromolecular specimen preparation and preservation. *Micron,* 42**,** 141-51.

MICHELLE FURTADO, L., POON, V. & KLIP, A. 2003. GLUT4 activation: thoughts on possible mechanisms. *Acta Physiol Scand,* 178**,** 287-96.

MUECKLER, M. 1994. Facilitative glucose transporters. *Eur J Biochem,* 219**,** 713-25.

MURPHY, R. M., MOLLICA, J. P. & LAMB, G. D. 2009. Plasma membrane removal in rat skeletal muscle fibers reveals caveolin-3 hot-spots at the necks of transverse tubules. *Exp Cell Res,* 315**,** 1015-28.

OWEN, D. M., RENTERO, C., MAGENAU, A., ABU-SINIYEH, A. & GAUS, K. 2012. Quantitative imaging of membrane lipid order in cells and organisms. *Nat Protoc,* 7**,** 24-35.

PHILLIPS, S. M., HAN, X. X., GREEN, H. J. & BONEN, A. 1996. Increments in skeletal muscle GLUT-1 and GLUT-4 after endurance training in humans. *Am J Physiol,* 270**,** E456-62.

PLOUG, T., VAN DEURS, B., AI, H., CUSHMAN, S. W. & RALSTON, E. 1998. Analysis of GLUT4 distribution in whole skeletal muscle fibers: identification of distinct storage compartments that are recruited by insulin and muscle contractions. *J Cell Biol,* 142**,** 1429-46.

RICHARDS, J. C., JOHNSON, T. K., KUZMA, J. N., LONAC, M. C., SCHWEDER, M. M., VOYLES, W. F. & BELL, C. 2010. Short-term sprint interval training increases insulin sensitivity in healthy adults but does not affect the thermogenic response to beta-adrenergic stimulation. *J Physiol,* 588**,** 2961-72.

RODNICK, K. J., SLOT, J. W., STUDELSKA, D. R., HANPETER, D. E., ROBINSON, L. J., GEUZE, H. J. & JAMES, D. E. 1992. Immunocytochemical and biochemical studies of GLUT4 in rat skeletal muscle. *J Biol Chem,* 267**,** 6278-85.

SCHERTZER, J. D., ANTONESCU, C. N., BILAN, P. J., JAIN, S., HUANG, X., LIU, Z., BONEN, A. & KLIP, A. 2009. A transgenic mouse model to study glucose transporter 4myc regulation in skeletal muscle. *Endocrinology,* 150**,** 1935-40.

SJOBERG, K. A., RATTIGAN, S., HISCOCK, N., RICHTER, E. A. & KIENS, B. 2011. A new method to study changes in microvascular blood volume in muscle and adipose tissue: real-time imaging in humans and rat. *Am J Physiol Heart Circ Physiol,* 301**,** H450-8.

SOLLNER, T. H. 2007. Lipid droplets highjack SNAREs. *Nat Cell Biol,* 9**,** 1219-20.

STEINBERG, H. O., BRECHTEL, G., JOHNSON, A., FINEBERG, N. & BARON, A. D. 1994. Insulin-mediated skeletal muscle vasodilation is nitric oxide dependent. A novel action of insulin to increase nitric oxide release. *J Clin Invest,* 94**,** 1172-9.

STENKULA, K. G., LIZUNOV, V. A., CUSHMAN, S. W. & ZIMMERBERG, J. 2010. Insulin controls the spatial distribution of GLUT4 on the cell surface through regulation of its postfusion dispersal. *Cell Metab,* 12**,** 250-9.

SYLOW, L., JENSEN, T. E., KLEINERT, M., HOJLUND, K., KIENS, B., WOJTASZEWSKI, J., PRATS, C., SCHJERLING, P. & RICHTER, E. A. 2013. Rac1 Signaling Is Required for Insulin-Stimulated Glucose Uptake and Is Dysregulated in Insulin-Resistant Murine and Human Skeletal Muscle. *Diabetes,* 62**,** 1865-1875.

UTRIAINEN, T., MALMSTROM, R., MAKIMATTILA, S. & YKI-JARVINEN, H. 1995. Methodological aspects, dose-response characteristics and causes of interindividual variation in insulin stimulation of limb blood flow in normal subjects. *Diabetologia,* 38**,** 555-64.

VINCENT, M. A. & BARRETT, E. J. 2002. Insulin-induced capillary recruitment precedes changes in skeletal muscle glucose uptake. *Diabetes,* 51**,** A31-A31.

VINCENT, M. A., CLERK, L. H., LINDNER, J. R., KLIBANOV, A. L., CLARK, M. G., RATTIGAN, S. & BARRETT, E. J. 2004. Microvascular recruitment is an early insulin effect that regulates skeletal muscle glucose uptake in vivo. *Diabetes,* 53**,** 1418-1423.

WALLIS, M. G., WHEATLEY, C. M., RATTIGAN, S., BARRETT, E. J., CLARK, A. D. & CLARK, M. G. 2002. Insulin-mediated hemodynamic changes are impaired in muscle of Zucker obese rats. *Diabetes,* 51**,** 3492-8.

WANG, W., HANSEN, P. A., MARSHALL, B. A., HOLLOSZY, J. O. & MUECKLER, M. 1996. Insulin unmasks a COOH-terminal Glut4 epitope and increases glucose transport across T-tubules in skeletal muscle. *J Cell Biol,* 135**,** 415-30.

WASSERMAN, D. H., KANG, L., AYALA, J. E., FUEGER, P. T. & LEE-YOUNG, R. S. 2011. The physiological regulation of glucose flux into muscle in vivo. *J Exp Biol,* 214**,** 254-62.

YKI-JARVINEN, H. & UTRIAINEN, T. 1998. Insulin-induced vasodilatation: physiology or pharmacology? *Diabetologia,* 41**,** 369-79.

ZIERATH, J. R., HE, L., GUMA, A., ODEGOARD WAHLSTROM, E., KLIP, A. & WALLBERG-HENRIKSSON, H. 1996. Insulin action on glucose transport and plasma membrane GLUT4 content in skeletal muscle from patients with NIDDM. *Diabetologia,* 39**,** 1180-9.